The role of CD8 B-lymphocyte interactions in type 1 diabetes pathogenesis

Hanton, Emily

Awarding institution:
King's College London

THE ROLE OF CD8:B-LYMPHOCYTE INTERACTIONS IN TYPE 1 DIABETES PATHOGENESIS

BY

EMILY HANTON

A thesis submitted to King's College London for the degree of Doctor of Philosophy in Immunology

Department of Immunobiology

School of Immunology & Microbial Sciences

King's College London

March 2021

Abstract

Class I major histocompatibility complex (MHC-I) molecules on antigen presenting cells (APCs) present peptides derived from extracellular proteins to CD8 T cells (termed cross-presentation) to induce or maintain antigen-specific cytotoxic effector responses. This interaction may be important in autoimmune disorders such as type 1 diabetes (T1D), since self-reactive CD8 cytotoxic T cells are direct mediators of pancreatic β-cell damage. Little is known of the key APCs governing self-reactive CD8 T cell responses in the islets, however. Since recent evidence has highlighted B cell involvement in insulitic lesions in T1D, this study set out to test the hypothesis that B cells cross-present exogenous polypeptide to CD8 T cells and thus influence CD8 T cell effector responses in a way that could be relevant to β-cell destruction. During the thesis, development of an antigen delivery system (ADS) to target a selected antigenic polypeptide for uptake via the B cell receptor (BCR) led to the demonstration that co-culture of ADS-pulsed B cells with cognate antigen-specific CD8 T cell clones induced marked CD8 T cell degranulation, a marker of effector function following T cell activation. As a benchmark of cross-presentation potency, immature monocyte-derived dendritic cells were matured in the presence of the same polypeptide and comparable levels of degranulation were observed. Within B cell: CD8 T cell clone co-cultures, $CD20^+$ $CD8^+$ doublets were identified, suggesting a sustained interaction between CD8 T cells and B cells. Doublets were also detectable in the absence of cognate polypeptide; however functional T cell output and formation of a mature immunological synapse was only observed in the presence of cognate polypeptide. To further investigate the nature of this interaction between CD8 T cells and B cells, receptor-ligand pair expression between the two cells was studied by transcriptomic analysis. This revealed potential cell-cell communication pathways of signalling and adhesive capabilities. Finally, to provide an opportunity for analysis of these interactions in a tissue context, single B cells were isolated from the pancreatic islets of a T1D patient by laser capture microdissection, and their molecular phenotype studied. Thus, this project provides a novel insight into the role of B: CD8 lymphocyte interactions in the tissue pathobiology of T1D.

Acknowledgements

I would firstly like to thank my primary supervisor Prof. Mark Peakman for providing me with the opportunity to carry out this PhD in such an exciting area of research. I am grateful for his support, guidance, and expertise throughout my studies – the experience has been completely invaluable in shaping my career as a scientist. I owe special thanks to Prof. Timothy Tree, who provided supervision with no hesitation towards the end of my PhD and was always eager to offer insightful scientific feedback and helpful discussions. I also wish to thank my second supervisor Dr. Yuk-Fun Liu, for her input and support, and grateful thanks are due to my thesis committee: Prof. Malcolm Logan, Dr. Pierre Guermonprez and Prof. Jo Spencer for their useful suggestions.

To all my colleagues within the Tree and Peakman research groups, I wish to express my utmost appreciation for always providing both scientific and personal support throughout my research. In particular, I am grateful to have shared the PhD experience with James and Clara – thank you for all the insightful scientific discussions, for making me question the data and for all the support and laughter in the lab. I would also like to thank Dr. Martin Eichmann for enhancing my scientific training by providing stimulating feedback and discussion around my research, and for his continued mentorship throughout my studies. Additionally, I am grateful to Dr. Sefina Arif, Dr. Irma Pujol Autonell and Dr. Katrina Todd who were always happy to discuss experiments and provide advice. Thank you also to Dr. Yasmin Haque for her flow cytometry support and expertise, and to members of the BRC FlowCore at GSST for training on the Imagestream and guidance on experimental design.

A huge thank you to Yogesh Kamra, for sharing his vast molecular knowledge and expertise with me, for all the support and assistance with the molecular experiments, and for always being up for a pint in the Miller when experiments got tough. Additional thanks to the rest of the BRC Genomics group at GSST for their support in the molecular component of my thesis, in particular Dr. Shichina Kannambath for the bioinformatics analysis.

Many thanks to Prof. Francesco Dotta, Noemi Brusco and Dr. Guido Sebastiani for so openly and enthusiastically allowing me to visit their lab at the University of Siena and for their assistance with the LCM experiments which formed a central component to this thesis.

To my ‘wholesome’ friends: Kerina, Khairin, Lizzie and Macarena, I am so grateful to science for bringing us together and couldn’t have wished for better lab mates – your support, positivity and encouragement throughout my PhD was unparalleled, thank you for always believing in me.

My PhD experience would not have been the same without the friendship of my MRC-DTP ‘constants’, who could completely emphasise with the lows and highs of a PhD and who always provided encouragement and assurance. Additionally, thank you to Johanna, our coffee breaks and chats were a consistent support throughout my PhD.

To my flat mate, friend, and fellow PhD student Emma, thank you for keeping me sane throughout my PhD (particularly during the work-from-home stage of COVID-19!) and for always providing empathetic support and laughter. I am also indebted to my non-science friends who, despite probably having no clue as to what I was talking about, always provided words of encouragement and advice. I could not be more grateful for all the dinners, pub trips, gym classes, glasses of rosé drank, and PhD related rants listened too.

Finally, and most importantly, thank you to my parents, Robert and Sarah, and my sister, Laura. I am forever grateful for your constant and unwavering support, love, and encouragement throughout my PhD; it would never have been possible without you. Thank you for always making me laugh, for keeping me motivated and excited, and for making me believe I could do it. I dedicate this thesis to you.

Table of contents

Index of Figures

Index of Tables

Abbreviations

7AAD	7-aminoactinmycin D
ADS	Antigen delivery system
AID	Activation induced cytidine deaminase
AIRE	Autoimmune regulator
AMP	Amplification
ANOVA	Analysis of variance
APC	Antigen presenting cell
APC (FACs)	Allophycocyanin
APRIL	A proliferation inducing ligand
ATP	Adenosine triphosphate
BAFF	B cell activating factor
BCR	B cell receptor
BFA	Brefeldin A
BM	Bone marrow
BSA	Bovine serum albumin
BTK	Bruton tyrosine kinase
CD	Cluster of differentiation
CDC42	Cell division control protein 42
CDR1,2	Complementarity determining region
CLIP	Class II associated invariant chain peptide
CMV	Cytomegalovirus
CSR	Class switched recombination
CT	Cycle threshold
CTL	Cytotoxic T lymphocyte
DAPI	4'6-diamidino-2-phenylindole
DEG	Differential expression of genes
DEPC	Diethylpyrocarbonate
DM	Diabetes mellitus
DMSO	Dimethyl sulfoxide
DNA	Deoxyribonucleic acid
DZ	Dark zone
EBV	Epstein Barr virus
ECM	Extracellular matrix
EDTA	Ethylenediaminetetraacetic acid
EEA1	Early endosome antigen 1
ELISPOT	Enzyme linked immune absorbent spot
ER	Endoplasmic reticulum
ERAP	Endoplasmic reticulum aminopeptidases
ERK	Extracellular signal regulated kinase
EURODIAB	European diabetes
FACs	Fluorescence activated cell sorting

FAM	Fluorescein amidite
FBS	Fetal bovine serum
FDC	Follicular dendritic cells
FISH	Fluorescence in situ hybridisation
FITC	Fluorescein
FO	Follicular
FSC	Forward scatter
GAD	Glutamic acid decarboxylase
GADA	Glutamic acid decarboxylase antibodies
GEF	Guanine nucleotide exchange factor
GMCSF	Granulocyte macrophage colony stimulating factor
GP6	Glycoprotein VI platelet
HEL	Hen egg-white lysosome
HK	House keeping
HLA	Human leukocyte antigen
HPLC	High performance liquid chromatography
IA-2	Islet tyrosine phosphatase 2
IAA	Insulin autoantibodies
IAPP	Islet amyloid polypeptide
IBC	Insulin binding B cells
ICA	Islet cell antibody
IF	Immunofluorescence
IFN	Interferon
IGRP	Islet specific glucose 6 phosphatase catalytic subunit related protein
IL	Interleukin
INS	Insulin
IS	Immunological synapse
JNK	c-Jun N-terminal kinase
KLRG1	Killer cell lectin like receptor subfamily
LCM	Laser Capture Microdissection
LCM	Laser capture microdissection
LFQ	Label free quantitation
LN	Lymph node
LZ	Light zone
MAC	Magnetic activated cell sorting
MAPK	Mitogen activated protein kinase
MFI	Mean fluorescence intensity
MGB	Minor groove binder
MHC	Major histocompatibility complex
MPEC	Memory precursor effector cells
MPI	Mean pixel intensity
MW	Molecular weight
MWCO	Molecular weight cut off

MZ	Marginal zone
NK	Natural killer
NOD	Non-obese diabetic
nPOD	Network for pancreatic organ donors
NTC	No template control
OCT	Optimal cutting temperature
PAMP	Pathogen associated molecular patterns
PBMC	Peripheral blood mononuclear cells
PBS	Phosphate-buffered saline
PCA	Principle component analysis
PCR	Polymerase chain reaction
PD1	Programmed cell death protein 1
PE	Phycoerythrin
PERCP	Peridinin chlorophyll protein
PFA	Paraformaldehyde
PHA	Phytohemagglutinin P
PI3K	Phosphoinositide 30kinase
PIC	Physically interacting cells
PLC	Phospholipase c
PMA	Phorbol 12-myristate 13-acetate
PPI	Pre proinsulin
PTEN	Phosphatase and tensin homolog
RAG1/2	Recombination activating gene 1/2
RIN	RNA integrity number
RIP	Rat insulin II promoter
RNA	Ribonucleic acid
RPMI	Roswell park memorial institute
RS	Recombining sequence
RT	Reverse transcription
RT-PCR	Real Time - PCR
RTX	Rituximab
SEM	Standard error of the mean
SHM	Somatic hypermutation
SLEC	Short lived effector cells
SLO	Secondary lymphoid organs
SMCC	Succinimidyl 4-N-maleimidomethy cyclohexane 1
SNP	Single nucleotide polymorphism
SSC	Side scatter
T 1/2/3	Transitional 1/2/3
T1D	Type 1 diabetes
T2D	Type 2 diabetes
TAB	Tumour associated B cells
TACI	Transmembrane activator and CAML interactor

TAP1,2	Transporter associated with antigen processing 1,2
TCR	T cell receptor
TLR	Toll like receptor
TLS	Tertiary lymphoid cells
TNF	Tumour necrosis factor
TPM	Transcripts per million
ZNT8	Zinc transporter 8

1 INTRODUCTION

1.1 Type 1 Diabetes

Type 1 Diabetes (T1D) is a disorder characterised by the destruction of the insulin-producing β-cells in the pancreatic islets. A small minority of cases of T1D are due to an idiopathic failure of β-cells, however the majority of cases are caused by autoimmune mediated β-cell destruction. T1D contributes to a small percentage of the total cases of diabetes mellitus (DM) worldwide. The more prevalent contribution to DM is from Type 2 Diabetes, which is characterised by a resistance to the action of insulin and a progressive loss of β-cell insulin secretion. The defining feature between T1D and T2D is that in T1D the autoimmune-mediated destruction of the β-cells leads to an absolute insulin deficiency, rather than a relative loss. As a consequence, individuals with T1D clinically present with persistent hyperglycaemia. Criteria for diagnosis includes a fasting plasma glucose $\geq$ 126 mg/dL, 2 hour plasma glucose $\geq$ 200 mg/dL, hemoglobulin A1C (HbA1C) $\geq$ 6.5%, and a random plasma glucose $\geq$ 200 mg/dL (American Diabetes Association, 2020). Additionally, in the case of T1D, individuals display clear serological biomarkers. Over 90% of newly diagnosed individuals will carry detectable levels of antibodies that are specific for β-cell derived proteins including (but not limited to) insulin (IAA), insulinoma-associated antigen 2 (IA-2), glutamate decarboxylase (GAD), zinc transporter 8 (ZnT8) and islet cell antibodies (ICA) (to be discussed, Section 1.5.3).

1.2 Epidemiology

T1D is often considered a disease of childhood, with peaks in presentation occurring between 5-7 years of age, and at or near puberty (10-14 years of age) (Harjutsalo, Sjöberg and Tuomilehto, 2008). Children clinically present with common symptoms of polyuria, polydipsia, and weight loss, and around a third of individuals present with diabetic ketoacidosis. T1D does, however, present at any age, with some studies indicating that numbers of new cases are evenly distributed above and below the age of 30 (Thomas *et al.*, 2016).

The incidence and prevalence of T1D worldwide, as extracted from meta-analysis studies, is reported as 15 per 100,000 population and 9.5 per 100,000 people respectively (Mobasseri *et al.*, 2020). The incidence and prevalence of T1D has also been increasing worldwide for several decades, with overall annual increases estimated at about 2 -3% per year (Maahs *et al.*, 2010; Mayer-Davis *et al.*, 2017). Incidence can vary substantially between geographical locations and regions. T1D is most common in Finland (36.5 cases per 100,000 each year) and Sardinia (36.8 cases per 100,000 each year), and has the lowest incidence rates in China and Venezuela (<1 cases per 100,000 each year) (Karvonen *et al.*, 2000). In general, there is a higher incidence of T1D in Europe, or populations of European descent resulting in a global incidence pattern with a North and South hemisphere dichotomy (DIAMOND Project Group, 2006). Additionally, rates in Europe generally follow a north-south gradient (EURODIAB ACE Study Group, 2000).

Incidence of T1D also varies with seasonal changes and birth month. Specifically, diagnosis of T1D shows peaks in the autumn and winter, and troughs in the summer (Moltchanova *et al.*, 2009). Being born in the spring is associated with an increased likelihood of T1D (Kahn *et al.*, 2009). Both seasonality patterns are dependent on geographical location, with effects lost in more equatorial locations.

1.3 Aetiology: genetic and environmental factors

T1D arises from a complex interaction of genetic and environmental factors as evidenced by epidemiological studies. This concept is bolstered by population based twin studies and family studies, where T1D clusters within families, but does not present with a known mode of inheritance. Risk of T1D in a sibling is 15 times greater than a member of the general population (Spielman, Baker and Zmijewski, 1980) and concordance rates for monozygotic twins (MZ) has been estimated between 30 – 50% (Hyttinen *et al.*, 2003). Comparison of concordance rates between MZ twins and dizygotic twins (DZ) as the classic indicator of heritability, estimates as much as 70% of the variation of disease risk is attributed to genetic factors (Kaprio *et al.*, 1992; Kyvik, Green and Beck-Nielsen, 1995).

Of the multiple genes implicated in disease susceptibility, the most relevant are the human leukocyte antigen (HLA) complex on chromosome 6, with ~50% of familial

clustering attributable to variation in this region. HLA (also known as MHC in all vertebrates) is involved in the immune process of antigen presentation and therefore in the control of peripheral and central tolerance. The strongest association is with genes mapping to the HLA class II loci *HLA-DRB1* and *HLA-DQB1*. The highest risk haplotypes for T1D are *DR*B1*03:01-*DQA1**0501-*DQB1**0201 (DR3) and *DR*B1*04-*DQA1**0301-*DQB1**0302 (DR4) - at least one of the alleles is present in 95% of patients with T1D (Noble *et al.*, 1996). Conversely, the HLA-DQA1*0102, DQB1*0602 haplotype confers dominant protection to the disease (Pugliese *et al.*, 1995).

In addition to the class II region, several studies have also shown that HLA Class I genes are associated with T1D. HLA-A*2402 correlates with early disease onset, rapid disease progression, and total β-cell destruction (Nakanishi *et al.*, 1993, 1999; Fujisawa *et al.*, 1995). This association is expected given the role of HLA class I molecules in target cell recognition by CD8 cytotoxic T cells and therefore the rate of pancreatic β-cell destruction (Section 1.7).

Other non-HLA T1D susceptibility alleles have smaller effects on disease risk. These include single nucleotide polymorphisms (SNP) of the insulin gene (INS) (Bell, Horita and Karam, 1984). Additionally, a functional variant of the P*TPN22* gene is associated with T1D, as are polymorphisms in the *CTLA4* gene and SNPs in the IL2RA loci (Nisticò *et al.*, 1996; Bottini *et al.*, 2004; Qu *et al.*, 2009).

While concordance rates emphasise the importance of genetics in T1D, they also clearly demonstrate the influence of environmental factors. Viral infections have been postulated as a possible cause of T1D. Immunoreactivity towards the enteroviral VP1 protein is increased in the islets in young recent-onset type 1 diabetic individuals, compared to control subjects (Richardson *et al.*, 2009). Dietary factors also may contribute to risk, particularly in the case of perinatal and infant exposures (Frederiksen *et al.*, 2013). T1D risk is also increased in children born by Caesarean section, or a complicated delivery (Stene *et al.*, 2004; Cardwell *et al.*, 2008). Interestingly, these candidate environmental factors for T1D are related to the development and function of the human microbiome (Dominguez-Bello *et al.*, 2010). Evidence is emerging that dysbiosis of the gut microbiome also increases T1D predisposition (Zheng, Li and Zhou, 2018). Additionally, Vitamin D has been

examined as a protective factor for disease risk, due to its relevance in regulation of the immune system and metabolic pathways. This may reconcile the seasonality patterns in disease incidence, and the north-south hemisphere dichotomy. Studies have shown that children who received supplements of Vitamin D had a lower risk of T1D compared to those who were not supplemented (Zipitis and Akobeng, 2008).

1.4 Natural history of T1D

The initiation and progression of T1D is therefore influenced by both genetic and environmental factors. In 1984, George Eisenbarth proposed a model for T1D natural history, that is still widely accepted to this day (Eisenbarth, 1984). Specifically, the rate of immune-mediated β-cell destruction i.e. the β-cell mass, is plotted against age (Figure 1-1). Commencement of disease occurs with genetic susceptibility, which is then followed by a precipitating (environmental) trigger that initiates islet targeted autoimmunity. This process is marked by the development of peripheral islet-reactive autoantibodies (at least two), that portend the development of autoreactive T cells capable to mediate β-cell destruction. At this stage, insulin release remains normal - sustaining homeostatic glucose levels, however β-cell mass begins to decline. Eventually this leads to a progressive loss of insulin release, in turn causing dysglycemia and early metabolic alterations. β-cell loss continues to advance, until overt clinical diabetes presents, when over 80% of the β-cells have been destroyed. There is therefore a large delay from the onset of autoimmunity to the onset of T1D. In the final stage, rapid progression to complete loss of β-cell mass occurs, where no C-peptide is present.

While this model is widely accepted as the common disease progression, it is important to acknowledge that wide heterogeneity exists across individuals with T1D. This classical conception involves a near complete loss of β-cells and subsequently a failure to retain detectable C-peptide levels, however recent studies have identified a subset of T1D individuals with detectable peripheral c-peptide concentrations, indicative of (a level of) preserved β-cell function (Liu *et al.*, 2009; Wasserfall *et al.*, 2017). As will be discussed in detail in Section 1.5.4, this heterogeneity is reflected in histological analyses, where individuals diagnosed under the age of 7 display a near complete loss of β-cell function, while those diagnosed at

an older age (>13 years) retain a larger fraction of β-cell mass (Leete *et al.*, 2016). Additionally, heterogeneity exists in the time between initial appearance of autoantibodies and clinical onset. For example, latent autoimmune diabetes in the adult (LADA) is characterised by diabetes associated autoantibody positivity, but is distinguished from the 'classical' T1D model due to a much slower disease progression and a non-insulin requirement for at least six months from diagnosis (Hawa *et al.*, 2013). Therefore it is important to consider disease heterogeneity in a clinical setting; several immunotherapies that may appear ineffective for a wider patient population may be effective in a smaller subgroup of patients (Woittiez and Roep, 2015).

In view of the 'classical' model, and advancements in the identification of predictors of disease risk, many strategies have been proposed for disease prevention. Primary prevention (1) aims to prevent the onset of islet targeted autoimmunity in asymptomatic individuals that are at high genetic risk for T1D. Secondary and tertiary (2 and 3) prevention studies aim to preserve residual β cells, or sustain the remission, or 'honeymoon' phase. Individuals can be selected based on positivity for humoral biomarkers i.e. autoantibodies. These represent β-cell targeted autoimmunity, therefore outlining disease progression. Islet autoantibody positivity predates progression to disease by months (or in some cases years, i.e. LADA). This clearly highlights the rationale for early intervention studies.

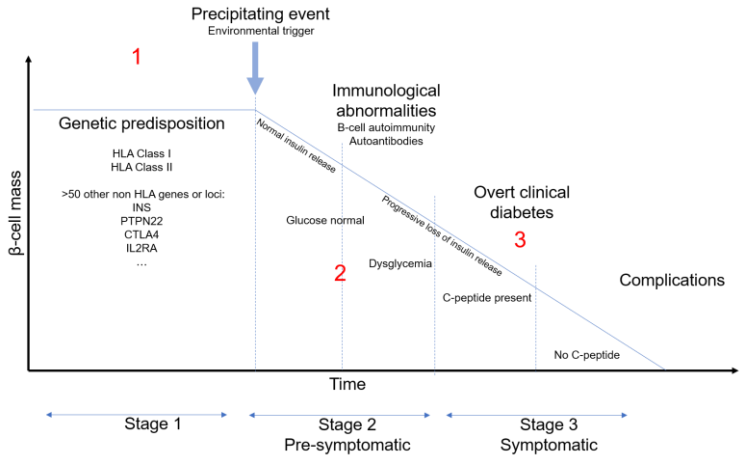

Figure 1-1 The natural history of Type 1 diabetes. Adapted from Eisenbarth *et al.*, 1984.

1.5 The immune phenotype of T1D

1.5.1 Immune pathways to β-cell destruction

Immune pathways involved in T1D pathogenesis are primarily mediated by autoreactive (β-cell specific) lymphocytes. During development, subsets of B and T cells generate diverse repertoires of cell surface receptors specific for antigenic epitopes, through recombination of V(D)J segments. Peripheral and central tolerance mechanisms exist to remove or neutralise any cells expressing reactivity for self-antigen (Theofilopoulos, Kono and Baccala, 2017). Central tolerance occurs in the thymus (T cells) or the bone marrow (B cells). Cells bearing high affinity receptors for antigen are clonally deleted or, in the context of B cells, self-reactive receptors are edited to generate an innocuous specificity. Peripheral tolerance mechanisms exist to restrain activation and expansion of self-reactive cells in the periphery, and induce tolerance through clonal deletion, or induction of anergy (Cambier *et al.*, 2007; Xing and Hogquist, 2012). The latter represents a hyporesponsive cell state, sustained by cognate antigen binding to the receptor, but a lack of co-stimulatory signals. Immunological ignorance is an additional mechanism that occurs when a T cell or B cell can co-exist with its cognate antigen, without being affected by it (Zinkernagel and Hengartner, 2001).

A widely accepted model of disease pathobiology has been constructed from animal and human studies where these autoreactive T cells directly mediate the destruction of the insulin producing β-cells (Roep, 2003). This process involves β cell proteins becoming visible to the immune system, through an undefined sequence of events (Roncarolo and Battaglia, 2007). Once exposed, β-cell proteins are endocytosed and processed by islet resident antigen presenting cells (APCs), such as macrophages and dendritic cells (Zirpel and Roep, 2021). The low-grade inflammation of the islets initially recruits these APCs. These cells than migrate to the local (pancreatic) draining lymph nodes, where they prime autoreactive naïve CD8 and CD4 T cells through antigen presentation on MHC class I or class II molecules respectively, resulting in T cell activation (to be discussed, Section 1.5.2). T cells are also endowed with the capacity to migrate to the pancreatic islets. Within the islets, events specific to the inflammatory tissue environment contribute to further

activation and restimulation of these T cells. Immune cell infiltration of the islets, or insulitis, represents the pathological landmark of T1D, and is the manifestation of the autoimmune attack against the β-cells (Section 1.5.4).

CD8 T cells can directly kill the β-cells through recognition of β-cell antigens presented by MHC class I molecules (Skowera *et al.*, 2008; Kronenberg *et al.*, 2012). Specifically, CD8 T cells release cytolytic granules and granzymes, and can also exert killing activity through Fas-FasL interactions (to be discussed, Section 1.6.2). CD4 T cells produce pro-inflammatory cytokines that promote tissue resident macrophages to produce reactive oxygen species, TNFα and IL-1β – further augmenting damage to the β-cells (Burrack, Martinov and Fife, 2017). Additionally, CD4 T cells aid and support the anti-islet CD8 T cell response by sustaining survival and enhancing proliferation and differentiation (Serr and Daniel, 2018).

1.5.2 Antigen presentation

Antigen presentation by APCs is therefore central to T cell activation and acquisition of effector functions critical to T1D pathogenesis.

MHC class I molecules report on intracellular events to CD8 T cells, presenting epitopes generated from endogenous sources. The MHC class I antigen presentation pathway is active in almost all nucleated cell types. This is necessary to display a sample of peptides derived from proteins synthesized in the cell at any given time. Thus, CD8 T cells are able to detect and destroy 'target' cells expressing viral proteins or tumour antigens, or in the context of autoimmunity – self proteins. In contrast, the MHC class II pathway is only active in 'professional' APCs. Peptides presented on MHC class II are derived from exogenous proteins, which can gain access to endosomal compartments. In this manner, CD4 T cells can respond to exogenous antigens that are internalized by the APCs through a variety of mechanisms: receptor mediated endocytosis, phagocytosis, and micropinocytosis.

1.5.2.1 Classical antigen processing and presentation pathways

In the context of MHC class I, intracellular antigens are firstly tagged for destruction by ubiquitylation. This results in processing and degradation by cytosolic multi-catalytic complexes, known as proteasomes, in order to generate antigen peptides (Groettrup, Kirk and Basler, 2010). The resulting peptides are translocated into the

lumen of the endoplasmic reticulum (ER) by transporters associated with antigen presentation (TAP1 and TAP2). Here, through a series of events involving components of the MHC class I peptide loading complex, the peptides intersect the MHC class I biosynthetic pathway. Peptides associate with nascent MHC class I heterodimers, generated in the ER from assembly of a polymorphic heavy chain, and a light chain: β_2-microglobulin. Importantly, prior to association with MHC class I molecules, longer polypeptides are trimmed to approximately 8-10 amino acids in length by ER aminopeptidases (ERAPs) (Serwold *et al.*, 2002). This allows binding of the peptide into the peptide-binding grove of the MHC molecule. The resulting trimeric complex then leaves the ER, is transported through the Golgi apparatus, and is presented at the cell surface (Figure 1-2B).

In contrast, exogenous antigens that are destined for presentation on MHC class II molecules firstly have to enter the endocytic pathway of the APC (Roche and Furuta, 2015). Such mechanisms include receptor-mediated endocytosis, micropinocytosis, phagocytosis, and autophagy. Internalised early endosomes fuse with late endosomal-lysosomal compartments, where MHC-CII-peptide complex formation occurs.

1.5.2.2 Antigen cross-presentation on MHC class I

Antigen cross-presentation presents an interesting link between the two classical antigen processing pathways. Here, exogenous antigens are presented by MHC CI molecules to CD8 T cells – a process that was first described by Bevan *et al*., in 1976, and is critical for the generation of CD8 T cell immune responses against exogenous proteins that do not infect APCs directly. In general consensus, two pathways of cross-presentation exist: TAP dependent (endosome to cytosol) and TAP independent (vacuolar pathway). In the latter, antigen processing and assembly with MHC CI molecules occurs directly in the endosomes and lysosomal compartments (Lawand *et al.*, 2016). Most studies, however, report cross-presentation via the TAP dependent pathway (Ackerman *et al.*, 2003; Guermonprez *et al.*, 2003). Here, exogenous antigen gains access to the cytosol and can enter the classical MHC CI processing pathway as a substrate for the proteasome (Rodriguez *et al.*, 1999).

A clear requirement for cross-presentation by MHC CI is that exogenous protein antigens gain access to the endocytic pathway, a necessity shared with successful antigen presentation by MHC-CII molecules to CD4 T cells. Pathways of antigen entry into the processing compartments of APCs for cross-presentation include receptor-mediated endocytosis, phagocytosis, and micropinocytosis (Figure 1-2A). Regardless of the route of antigen endocytosis, intra-endosomal antigen stability and delayed antigen degradation are critical in regulating cross-presentation (Embgenbroich and Burgdorf, 2018). This allows release of antigens into the cytosol for degradation by proteasomes into shorter peptides. These features are conducive with dendritic cells (DCs) being superior APCs: they express lower levels of lysosomal proteases, show a reduced velocity of endosome maturation, and can activate alkalization of endosomes in order to prevent pH dependent activation of proteases (Lennon-Duménil *et al.*, 2002; Trombetta *et al.*, 2003; Delamarre *et al.*, 2005).

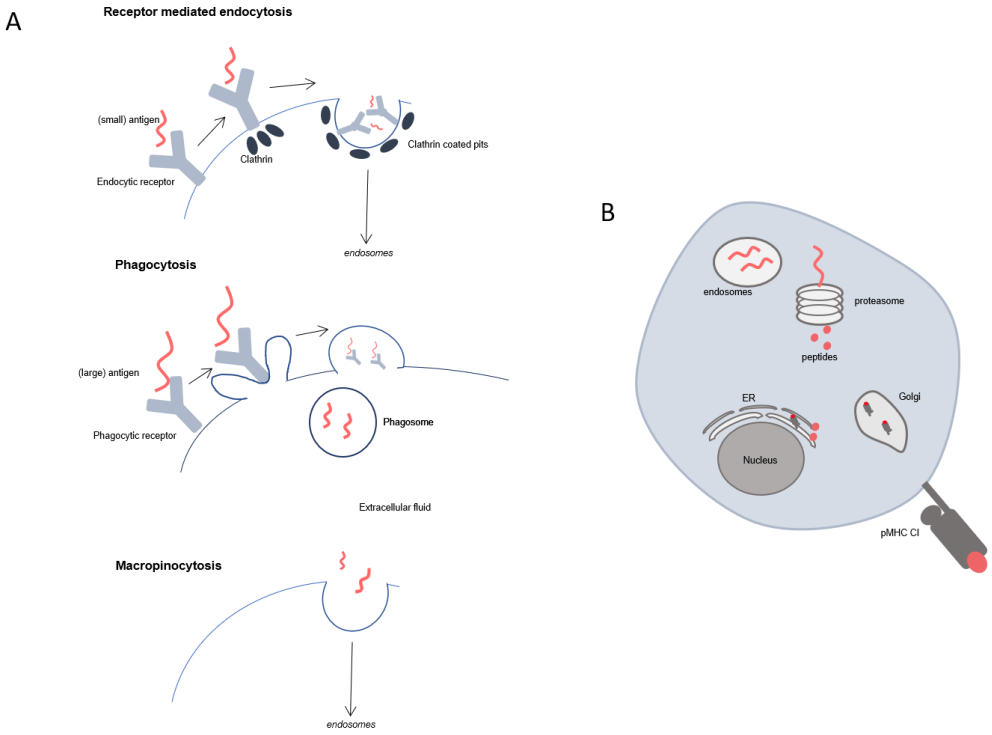

Figure 1-2 Pathways of antigen entry and the antigen cross-presentation pathway in APCs. A requirement for cross-presentation is uptake of antigen (A), release into the cytosol and access to the endocytic pathway for antigen processing by the proteosome and presentation on MHC class I molecules on the cell surface (B).

1.5.3 Serological biomarkers

Autoantibodies to islet cell antigens are known predictors of disease and have consistently been detected in the periphery of T1D individuals at clinical diagnosis (Bottazzo, Florin-Christensen and Doniach, 1974). The first autoantibodies detected, islet cell autoantibodies (ICAs), were loosely described as being organ specific and directed against cytoplasmic components of the islet cells (Bottazzo, Florin-Christensen and Doniach, 1974; Lendrum *et al.*, 1976). As research advanced, ICAs were found to represent autoimmunity to several different antigens, specifically single tissue antigens. These include autoantibodies against insulin (IAA), the protein tyrosine phosphatase-like insulinoma antigen IA-2, zinc transporter 8 (ZnT8) and glutamic acid decarboxylase 65-kilodalton isoform (GAD65) (Grubin *et al.*, 1994; Payton, Hawkes and Christie, 1995; Yu *et al.*, 2000; Wenzlau *et al.*, 2007). Primarily seen as a diagnostic biomarker, extensive work across multiple cohorts

have since revealed that presence of autoantibodies is a strong predictor of T1D, and risk is directly related to the magnitude and maturity of these autoantibody responses (Gardner *et al.*, 1999). This is relevant in the context of the natural history of T1D, where appearance of autoantibodies portend clinical diagnosis.

Both a younger age of seroconversion and positivity for multiple autoantibodies are considered major risk factors in developing T1D. For example, children who seroconvert (i.e. develop autoantibodies) before the age of two, are more prone to progression to T1D, and do so at a faster rate (Parikka *et al.*, 2012). Additionally, longitudinal studies revealed that progression to clinical T1D had occurred in ~70% of children who had multiple islet autoantibodies, compared to ~15% in children who had seroconverted with a single islet autoantibody (Ziegler *et al.*, 2013).

The order of appearance of autoantibodies for different islet specificities is related to the HLA-DR-DQ genotypes. IAA antibodies appear first in children of up to 6 years of age who carry the DR4-DQ8 haplotype, while GAD antibodies (GADA) present first in carriers of DR3-DQ2 (Krischer *et al.*, 2015; Endesfelder *et al.*, 2019). Interestingly, seroconversion for multiple autoantibody specificity following the appearance of the initial antibody was slower in the latter sample population, where GADA was the first ICA specificity. Disease risk is also associated with the titre of the antibody – highest risks are associated with high-titre IA2 and IAA, while GADA titre levels had no correlation with risk (Achenbach *et al.*, 2004; Steck *et al.*, 2015; Endesfelder *et al.*, 2019).

1.5.4 Pancreatic pathology: insulitis

Pancreatic histology remains the only true means of directly visualising β-cell destruction. Access to pancreatic tissue from T1D patients has been historically limited, however three pancreas biobanks specific to T1D - Exeter Archival Diabetes Biobank, UK (EADB), Diabetes Virus Detection Study (DiViD) and the Network for Pancreatic Organ Donors with Diabetes (nPOD), have been seminal in elucidating features of the insulitic lesion and islet inflammation.

The typical histological finding is insulitis (In't Veld, 2014a). Insulitis consists of an infiltrate of inflammatory cells targeting the islets (i.e. inflammatory lesion) that is associated with a loss of the β-cells. Islets from individuals without autoimmune

diabetes contain occasional immune infiltrates therefore the current consensus definition of insulitis is a threshold level of > 15 $CD45^+$ cells per islet, in a minimum of three islets (Campbell-Thompson *et al.*, 2013). A common observation is that the fraction of infiltrated lesions is usually low (<10% of islets profiled), contrasting the robust and consistent lesion that is observed in the NOD mouse, and suggesting a dynamic and asynchronous process of destruction (In't Veld, 2014a). Indeed, insulitis is preferentially observed in islets containing insulin-positive β-cells, however the same pancreas will also present with pseudo atrophic islets in which the inflammatory lesion is lost together with the β-cells; this is a critical criterion for the diagnosis of insulitis and supports the concept that insulitis represents an immunologically mediated destruction of the β-cells (Campbell-Thompson *et al.*, 2013).

Insulitis appears to be more prevalent in younger patients with a shorter duration of disease. Comparing between individuals under the age of 14, and individuals aged between 15 and 40 years, all with a disease duration of under 1 month, a meta-analysis revealed a 73% occurrence of insulitis in the younger group, compared to 29% of cases in the latter (In't Veld, 2011). Across disease durations this divergence remained, however each age group followed a similar pattern by which insulitis reduced significantly as disease duration increased; with minimal cases detected in individuals with disease duration of over 1 year (In't Veld, 2011; Campbell-Thompson *et al.*, 2016). Samples acquired from patients with a disease onset of under 14 years of age showed fewer islets with residual β-cells, supporting a more aggressive β-cell immune attack in young children (In't Veld, 2014b).

Organs from adult donors who were positive for autoantibodies against islet antigens, but who were not clinically presenting with overt disease (i.e. pre-diabetic) have also been analysed for insulitis (In't Veld *et al.*, 2007; Campbell-Thompson *et al.*, 2016). In one study, of 62 cases, only two cases showed islets with insulitis and this inflammatory lesion was present in 3 – 9% of the islets (In't Veld *et al.*, 2007). In these cases, donors were positive for three or more islet autoantibodies, while the majority of the remaining (non-insulitic) cases were only positive for one autoantibody. Similarly, in an additional study, insulitis was detected in two of five donors who presented with multiple autoantibodies but had not progressed to clinical

disease, with a similar frequency (1.4 – 6.4%) (Campbell-Thompson *et al.*, 2016). Insulitis therefore appears to be a rare phenomenon in autoantibody positive, non-diabetic individuals.

Investigations into the infiltrating cell types that compose the inflammatory lesion report heterogenous profiles. A common, historical pattern exists in that the infiltrate mainly consists of T cells, predominantly CD8 T cells (Hanninen *et al.*, 1992; Itoh *et al.*, 1993). A comprehensive study of 29 recent-onset patient samples stratified the composition of the inflammatory infiltrate based on the percentage of β-cells present in the islets (Willcox *et al.*, 2009). This allowed analysis of a temporal sequence of insulitis, extending from islets with a large insulin positive area and minimal immune infiltrate, to islets with pronounced inflammation and an evident loss of β-cells, to the final stage in which islets were devoid of both insulin positive β-cells and inflammatory infiltrate. At all stages of β-cell decline, CD8 T cells predominated the infiltrate, increasing in their relative number as insulin positivity decreased. At complete loss of insulin positivity, the number of CD8 T cells declined significantly. This profile was mirrored by each of the other major immune cell subtypes (CD4 T cells, CD20 B cells, and CD68 macrophages), although they were all present at lower numbers. Interestingly, CD20 B cells were the second most abundant population of cells, increasing as the percentage of insulin positivity decreased, before dramatically declining in number when insulin positivity was lost. These cells showed the largest proportionate increase, implicating their recruitment to the islets once the initial loss of β-cell mass has been established. Macrophages and CD4 T cells were present at a more constant number, independent of the level of insulin positivity, and deeper analysis of the CD4 T cell population revealed minimal detection of regulatory T cells within the islet infiltrate. NK cells were not detected as a major component of the insulitic lesion in this study. In contrast, a study by Dotta *et al.*, (2007) showed that in the insulitic lesions of patients with no apparent reduction of islet β-cells, the mononuclear cell infiltrate was composed mainly of CD94 positive NK cells. This was not seen in individuals with extensive β-cell loss. Interestingly, a key difference between the two patient groups was the presence of β-cell selective enterovirus infection in the former – implicating viral infection in the composition of the immune infiltrate, and providing a potential explanation for the conflicting reports on the presence of NK cells within the lesion.

Therefore, it is evident that the CD8 T cell is the likely candidate for β-cell killing that drives disease. CD8 T cells dominate the insulitic lesion of individuals with T1D, and this is a disease specific phenomena (Babon *et al.*, 2017). Additionally, β-cells upregulate HLA class I, indicative of an 'unmasking' of the islets that leads to an enhanced interaction between intra-islet CD8 T cells and the β-cells (Richardson *et al.*, 2016). This is supported by genetic studies in which HLA class I loci are associated with enhanced disease risk (Section 1.3). Of note, however, is that while islet hyperexpression of HLA class I is a defining feature of T1D, it is not a β-cell specific phenomenon, instead occurring in all islet endocrine cells (Richardson *et al.*, 2016). IFNα is thought to mediate upregulation of HLA class I, as well as contributing to the induction of inflammation and ER stress within the β-cells (Marroqui *et al.*, 2017). Interestingly, the expression and signalling of IFNα is known to be regulated by T1D genetic risk variants and viral infections associated with T1D i.e. enterovirus, presenting a clear link between genetic and environmental risk factors and disease pathogenesis.

1.6 CD8 T cell immunity

1.6.1 Priming of naïve CD8 T cells

During T cell development, successful recombination of a functional TCR and emergence from the thymus results in a resting naïve T cell. While this cell can migrate and traffic through the peripheral circulation and the secondary lymphoid organs (SLO – lymph nodes, spleen), it is unable to produce a response that would protect against antigen challenge. Activation into effector CD8 T cells occurs in the SLOs and involves coordinated interactions with APCs that cross-present cognate antigen in order to form an immunological synapse (Section 1.5.2.2). Stimulation of the naïve T cell with cognate antigen alone results in a hyperresponsive state i.e. anergy. In addition to TCR recognition of cognate peptide, priming therefore requires concomitant co-stimulatory signals (signal 2) and pro-inflammatory signalling pathways (signal 3) in order to induce clonal expansion and effective development of effector functions (Figure 1-3). A large effector T cell population is therefore generated in the SLOs; as few as 80 – 1200 naïve antigen specific CD8 T

cells expand by up to 50,000 fold following activation, before migrating to the site of infection (Butz and Bevan, 1998).

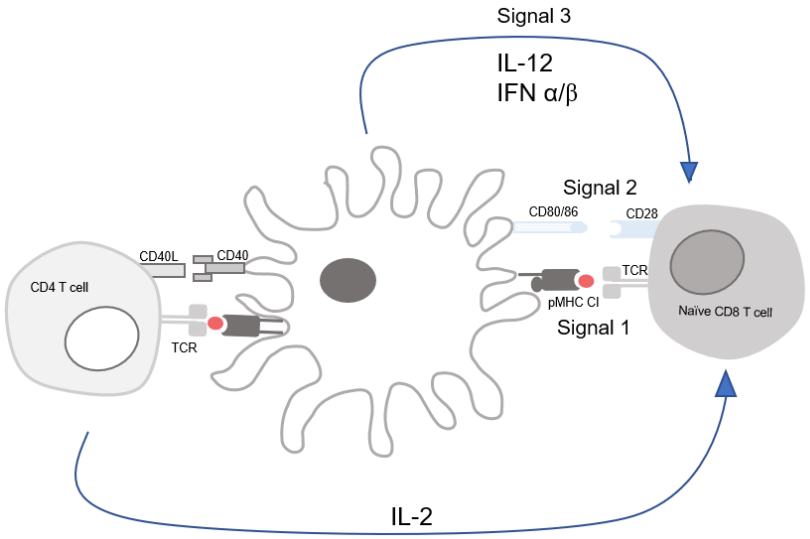

Figure 1-3 Priming and activation of a naïve CD8 T cell. Three signals are required for activation of a naïve CD8 T cell. Signal 1 consists of TCR signalling through recognition of pMHC class I. Interaction of APCs with CD4 T cells in a CD40-CD40L dependent manner result in upregulation of co-stimulatory molecules on the APC (licencing), which provide signal 2 to the CD8 T cell in the form of CD80/86 – CD28 signalling (other co-stimulatory markers include NKG2D, OX40 and 41-BB receptors), and IL-2. A third signal is provided through pro-inflammatory cytokines (IL-12 or IFNα/β).

1.6.2 CD8 T cell effector function

Activated effector CD8 T cells can eliminate pathogen either through cytokine secretion and/or cytolytic activity. CD8 T cells perform antigen specific lysis of infected cells by detecting cognate antigen presented by target cells in a peptide-HLA-class I complex. A TCR triggered immunological synapse is established, endowing the ability to kill the target cell. This occurs through the release of specialised lytic granules containing cytotoxic effector proteins, such as perforin and granzymes, that create pores in the lipid bilayer and destroy the integrity of the cell membrane (Smyth *et al.*, 1994). Additionally, the Fas-FasL signalling pathway is implicated in CD8 T cell mediated target cell apoptosis, whereby the ligation of Fas on the target cell results in the activation of caspases (Kägi *et al.*, 1994). CD8 T cells

also exert their effector function through the generation and release of pro-inflammatory cytokines – such as IFNγ, TNFα and TNFβ (Müllbacher *et al.*, 2002).

1.6.3 CD8 T cell memory

After CD8 T cells have mediated pathogen (antigen) clearance, the majority of the effector cells die via apoptosis i.e. the short-lived effector cells (SLECs, or terminal effector cells). A small subset survives from this effector response, the memory precursor effector cells (MPECs), which express high levels of IL-7α and CD27 (Obar and Lefrançois, 2010). These differentiate into memory CD8 T cells that circulate in the blood and lymphoid organs and are an essential component of long-lived T cell immunity.

Memory CD8 T cells exist as a heterogenous population, comprising subsets with distinct phenotypes and functions. Two subsets have been well characterised in research efforts - T effector memory (Tem), that preferentially track through the periphery and tissue sites and display rapid effector function upon antigen re-encounter, and T central memory (Tcm) populations which home to the SLOs and show increased proliferative capacity (Martin and Badovinac, 2018). Other subsets include T stem cell memory (Tscm) cells which are a rare memory population with a largely naïve phenotype but expression of CD95, and transitional memory (Ttm) cells and terminal effector (Tte) cells, which both have low proliferative and functional capacity (Gattinoni *et al.*, 2011). Notably, a third major CD8 memory population has emerged; resident memory T cells (Trm) (Gebhardt *et al.*, 2009). These cells permanently reside in peripheral tissues and therefore provide *in situ*, site specific protection upon antigen reencounter.

Importantly, diverging from their naïve and effector counterparts, memory cells have properties of ‘stemness’ which enables them with long term survival and plasticity in order to replenish the pool of effector cells upon secondary (or renewed) antigen challenge. Efforts have been made to elucidate the lineage relationships between naïve, effector and memory T cells, as well as between the distinct memory subsets. Evidence suggests that T cell memory differentiation follows a linear progression along a continuum of the major subsets (Naïve – Stem cell memory – Central memory – Transitional memory – Effector memory – Terminal effector) (Figure 1-4)

(Tomiyama, Matsuda and Takiguchi, 2002; Mahnke *et al.*, 2013). The differentiation path is graded from less to more differentiated with cells harbouring greater memory potential and longevity at one end, a more terminal effector phenotype at the other, and effector cells at intermediate differentiation states in between (Sallusto, Geginat and Lanzavecchia, 2004; Cui and Kaech, 2010; Mahnke *et al.*, 2013). At each stage of 'memory' the cell is quiescent, however following secondary encounter with cognate antigen, cells are re-stimulated and exert effector function to mediate a new immune response. This progressive model of differentiation therefore provides plasticity within the effector CD8 T cell lineage in which cells can transit between the different differentiation subsets. Signals that regulate fate decision are multiple, from signal strength at the priming stage, to epigenetic and transcriptional regulation, to pro-inflammatory cytokines and co-stimulatory signals (Mahnke *et al.*, 2013).

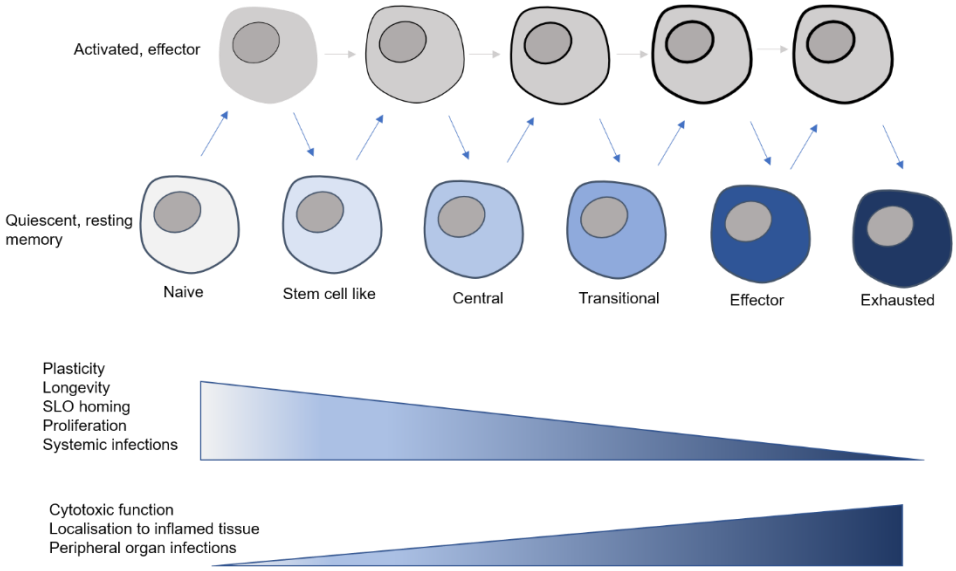

Figure 1-4 Progressive gradient model of CD8 T cell differentiation between memory cell subsets and effector cells. Figure adapted from Mahnke *et al.*, 2013.

1.6.4 CD8 T cell memory in autoimmunity

In the context of chronic inflammation i.e. autoimmunity, CD8 T cells are likely to encounter their cognate antigen multiple times, and undergo continuous rounds of antigen stimulation (Arif, Pujol-Autonell and Eichmann, 2020). Constant exposure to antigen leads to increased formation of memory effector subsets (Tem). This has

been documented in studies of chronic infection and immunisation where antigen persistence alters the lineage commitment pathway by precluding formation of Tcm cells and favouring Tem differentiation (Jabbari and Harty, 2006; Masopust *et al.*, 2006). In comparison to Tem, Tcm are much more slowly activated into effector cells in response to antigen (Tomiyama, Matsuda and Takiguchi, 2002). On the other hand, in response to antigen re-encounter, Tem rapidly differentiate into effector CD8 T cells, supporting their involvement in T cell mediated pathogenicity of autoimmunity. Constant antigen exposure additionally results in persistence of the Tem compartment, unlike in acute infection where cells decline over time (Devarajan and Chen, 2013) (Figure 1-5). Moreover, successive antigen encounter leads to changes in the transcriptomic signature of memory CD8 T cells, with each round of stimulation increasing the number of regulated genes (Wirth *et al.*, 2010). Therefore, repeated antigen experience is likely to result in a more transcriptionally diverse Tem population.

Taken together, these features account for the persistence of a CD8 T cell mediated autoimmune attack; whereby immunological memory represents a constant-remembrance of self-antigen.

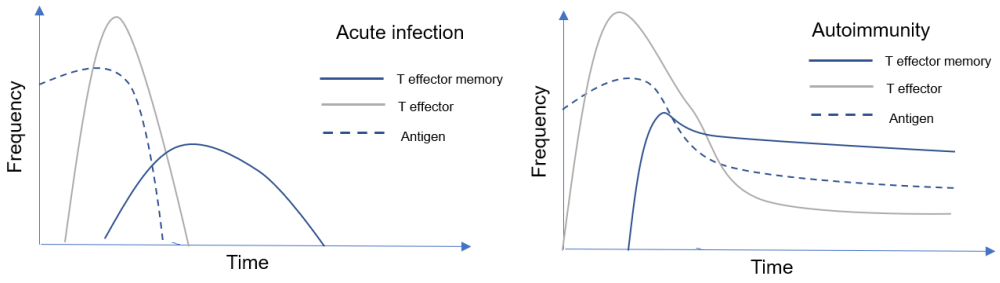

Figure 1-5 Dynamics of CD8 T cell memory and effector subsets in response to antigen in acute infection and autoimmunity. Figure adapted from Devarajan and Chen, 2013.

1.7 CD8 T cells in T1D

1.7.1 β-cell specific CD8 T cells in T1D

The importance of CD8 T cells in β-cell destruction led to extensive efforts into epitope discovery of antigenic targets that 1) exist within β-cells and 2) that are

recognised by CD8 T cells. The majority of epitopes that have been identified to date are primarily derived from β-cell antigens, most predominantly (pre-, pro-) insulin (Kimura *et al.*, 2001; Hassainya *et al.*, 2005; Pinkse *et al.*, 2005; Toma *et al.*, 2005; Skowera *et al.*, 2008). Other epitopes identified include those derived from additional β-cell proteins including GAD65 (Panina-bordignon *et al.*, 1995), IA-2 (Takahashi, Honeyman and Harrison, 2001), IAPP (Panagiotopoulos *et al.*, 2003) and IGRP (Takaki *et al.*, 2006).

Additionally, an evolving area of research considers the formation of neo-antigens; epitopes generated by various post-translational modifications of a DNA encoded antigen. In T1D, reports have highlighted the importance of enzymatic citrullination, disulfide modification and deamidation by tissue transglutaminase in the generation of both CD4 and CD8 T cell neoepitopes (Mannering *et al.*, 2005; van Lummel *et al.*, 2014; Marre *et al.*, 2018). Importantly, these mechanisms are thought to be triggered by ER stress within the β-cells, highlighting their pathogenic relevance (Marre *et al.*, 2018). Additionally, in the context of CD4 T cells, hybrid insulin peptides (HIPs) have been described – formed through covalent linking of peptides derived from pro-insulin with peptides derived from other β-cell specific proteins (Delong *et al.*, 2016; Baker *et al.*, 2019). For CD8 T cells, additional neoepitopes also include hybrid peptides, in addition to epitopes derived from defective ribosomal products or through alternative splicing (Kracht *et al.*, 2017; Gonzalez-Duque *et al.*, 2018).

1.7.1.1 Central effector pathway to β-cell destruction

To exemplify the potential of autoantigen specific CD8 T cells as the main effector pathway in β-cell destruction, studies aimed to demonstrate their 'killing' ability *in vitro.* Early studies using ELISPOT analysis demonstrated that stimulation of β-cell-specific CD8 T cells with cognate antigen led to an increase in expression of the cytolytic markers IFNγ and granzyme B, indicative of killing ability (Pinkse *et al.*, 2005). Extending this, co-culture of PPI_{15-24} specific CD8 T cell clones with human islet cells resulted in specific killing of β-cells in a cell-cell contact dependent manner (Skowera *et al.*, 2008). CD8 T cell clones specific for the HLA-A24 restricted epitope of the signal preproinsulin peptide also exhibited killing activity

towards surrogate β-cells *in vitro* and HLA-matched human islet cells (Kronenberg *et al.*, 2012).

Identification of β-cell specific CD8 T cells in the pancreatic islets of individuals with T1D further exemplifies their pathogenic contribution as the main effector pathway. *In situ* tetramer staining detected islet reactive CD8 T cells in insulitic lesions of T1D individuals (Coppieters *et al.*, 2012). In accordance, CD8 T cell lines grown from islet cells of individuals with T1D displayed autoreactivity against known islet peptide targets (Babon *et al.*, 2017). Importantly, the presence of islet-reactive CD8 T cells is specific to disease; comparisons between healthy controls and T1D individuals revealed an enrichment of $ZnT8_{186-194}$ specific CD8 T cells in the pancreatic tissue of the latter (Culina *et al.*, 2018). PPI_{15-24} specific CD8 T cells were found to also reside in the exocrine tissue of the pancreas (Bender *et al.*, 2020). The authors identified this phenomenon in healthy controls as well as autoantibody positive and T1D donors, suggesting their presence in the pancreas is the default state – increasing in frequency, and in proximity to the islets, with the advancement of T1D.

1.7.1.2 Frequencies in the periphery of T1D and healthy individuals

Whether the presence of β-cell specific CD8 T cells in the peripheral circulation is specific to disease, has however, been a source of debate over the years. Early reports presented evidence for an enrichment of these cells in T1D individuals. Frequencies of CD8 T cells against three major PPI peptides were significantly higher in T1D patients compared to controls (Luce *et al.*, 2011). Tetramer positive CD8 T cells reactive to the HLA-A24 restricted signal peptide PPI_{3-11} and the HLA-A2 restricted peptide PPI_{15-24} were significantly more frequent in recent-onset T1D patients (Skowera *et al.*, 2008; Kronenberg *et al.*, 2012). Frequencies of CD8 T cells specific for 6 islet autoantigens (InsB, IA-2, IGRP, PPI, GAD65, ppIAPP) were also significantly enhanced in T1D compared to healthy controls (Velthuis *et al.*, 2010).

More recently however, reports have consistently described similar frequencies of antigen specific CD8 T cells in the periphery between healthy and diabetic individuals: this is the currently accepted paradigm. Differences in the comparative frequencies have been attributed to alterations in the methodology for detection, ages

and stages of disease process, and T cell specificities studied. Across seven peptide specificities (PPI_{15-24}, $InsB_{10-18}$, $IGRP_{265-273}$, $IA\text{-}2_{797-805}$ and $GAD_{114-123}$), CD8 T cell frequencies were comparable between T1D patients and healthy controls (Skowera, Ladell, Mclaren, *et al.*, 2015). Similarly, CD8 T cells specific for IGRP were found to circulate at similar levels in age matched T1D and healthy donors, and HLA-B39 restricted CD8 T cells specific for the PPI_{15-24} peptide were identified in similar frequencies between T1D individuals and matched controls (Culina *et al.*, 2018; Yeo *et al.*, 2019). $ZnT8_{186-194}$ reactive CD8 T cells were also found to circulate at a comparable frequency between age-matched T1D and healthy donors (Culina *et al.*, 2018).

1.7.1.3 Disease specific phenotypes in peripheral circulation

This paradigm led to the hypothesis that disease-related differences in the self-reactive CD8 T cell population may mirror an antigen driven inflammatory process that does not present in quantitative terms.

β-cell specific CD8 T cells were found to be more differentiated in T1D patients, with a significantly lower frequency of naïve autoreactive CD8 T cells. In one study, autoreactive CD8 T cell populations were dominated by stem cell memory phenotypes and expressed higher frequencies of CD95 and the terminal differentiation marker CD57 as compared to healthy individuals, suggesting late stage antigen experience and memory status consistent with chronic antigen exposure (Skowera, Ladell, McLaren, *et al.*, 2015). Additionally, circulating islet specific CD8 T cells were enriched for memory phenotypes as compared to populations of polyclonal CD8 T cells from the same individual (Yeo *et al.*, 2019). Importantly, this enrichment was not observed in islet specific CD8 T cells of healthy controls, indicating acquisition of this phenotype is disease specific. Further studies supported these findings, with islet specific CD8 T cells enriched for effector memory phenotypes in patients as compared to healthy controls (Harms *et al.*, 2018; Ogura *et al.*, 2018; Yeo *et al.*, 2018). Interestingly, this phenotype appears to already be present in at-risk individuals i.e. those who have seroconverted (Harms *et al.*, 2018; Yeo *et al.*, 2018).

1.7.1.4 Relating effector subsets to β-cell function

An enriched effector memory phenotype in islet-specific CD8 T cells in T1D individuals presents the hypothesis that the properties of circulating effector T cells may determine disease initiation, progression, and severity. Disease correlation of circulating antigen-specific CD8 T cells is limited due to a lack of resolution of the relationship between tissue-infiltrating and circulating immune cells. Most studies presume a programmed recirculation of relevant islet-specific CD8 T cells between the blood and the islets, with little evidence to support this. Assessment of circulating islet-specific CD8 T cells in relation to β-cell function, however, allows some reconciliation of this confound.

Indeed, changes in effector memory islet specific CD8 T cells were found to track changes in β-cell function over time, in newly diagnosed patients who were followed longitudinally over 2 years (Yeo *et al.*, 2018). Effector memory cells expressed CD57 and spanned multiple β-cell specificities, with transcriptional profiling revealing enhanced cytotoxic potential and clonal expansion. An increase of these cells correlated with an increase in C-peptide retention, presenting a direct interplay between the β-cell and circulating islet-specific CD8 T cells. Authors speculated that increased β-cell function correlates with enhanced antigen availability to drive the antigen experienced CD8 T cell response, resulting in generation of effector memory cells with increased cytotoxic ability. In turn, this leads to increased CD8 T cell mediated β-cell killing upon antigen re-exposure in the islets, followed by a loss of antigen, and therefore waning of the cytotoxic CD8 T cell response. This correlation is in accordance with the aforementioned observations in the tissue that CD8 T cells are retained in insulin positive islets, but lost from those that are insulin deficient (Willcox *et al.*, 2009). Additionally, circulating islet reactive CD8 T cells with an activated memory phenotype correlated with rapid disease progression (i.e. increased β-cell destruction), while an exhausted memory phenotype was linked to slow progression of disease (Wiedeman *et al.*, 2020).

1.7.1.5 Differentiation and activation dynamics in the islets

Although these findings reconciled the relationship between circulating immune cells and tissue-infiltrating cells in T1D to some extent, the scarcity of human

pancreatic tissue samples limits data generation on the activation, differentiation, and re-stimulation dynamics of islet-specific CD8 T cells in tissue pathology.

In situ phenotyping of CD8 T cells in T1D insulitic lesions revealed that approximately 40% of CD8 T cells per islet had a tissue resident memory phenotype, determined by expression of CD69 and CD103. However, this study did not differentiate whether this feature was specific to islet reactive CD8 T cells or general to the polyclonal population. A later study focused on islet-specific CD8 T cells (PPI_{15-24}) in situ, and revealed a predominantly memory phenotype (Bender *et al.*, 2020).

In the NOD mouse, easy access to the pancreatic islets allows elucidation of the dynamics governing differentiation and (re)activation of CD8 T cells. Islet-specific CD8 T cells acquire effector function in the inflamed islets due to local restimulation events, with CD8 T cells expressing significantly higher levels of cytotoxic effector molecules compared to cells in the pancreatic lymph nodes (Graham *et al.*, 2011; Friedman *et al.*, 2014). This feature was independent of antigen presentation by the β-cell as conditional deletion of MHC CI from the β-cell had no impact on the acquisition of the cytotoxic phenotype. Therefore, it is likely that inflammatory mediators and cells within the islets govern the acquisition of this phenotype, such as proinflammatory cytokines and professional APCs. The latter was further exemplified by the activation of CD40 expressing cells leading to an increased CD8 T cell effector function and β-cell destruction (Graham *et al.*, 2011).

In addition to a gain of cytotoxic effector function in the islets, dynamics of memory differentiation have also been addressed. The effector-memory phenotype of islet-specific CD8 T cells was acquired in the islets of NOD mice, while priming of naïve T cells occurred in the pancreatic lymph node (Chee *et al.*, 2014). Differentiated cells emigrated from the islets to the periphery where they remained poised for rapid response to cognate antigen upon re-circulation to other islets. This is in concordance with the aforementioned study in human subjects study in which a dialogue between β-cell and effector memory CD8 T cells was observed (Yeo *et al.*, 2018).

Thus, this presents a model by which in the inflamed islet in T1D, the presence of high antigen concentrations, continued help from CD4 T cells, **activated antigen-**

presenting cells and high concentrations of pro-inflammatory cytokines synergize to mediate the differentiation and acquisition of cytotoxic functions of effector CD8 T cells. This restimulation at disease site therefore promotes and maintains the ongoing (self-perpetuating) autoimmune attack central to disease process. Interrogation of the cellular and molecular mechanisms governing CD8 T cell responses and effector function in the islets could therefore be critical for further elucidating pathogenesis and presenting targets for clinical intervention.

1.8 B cells in T1D

As discussed (Section 1.5.3), autoantibodies produced by B cells are critical in diagnosis of T1D and in stratification of disease risk, and B cells are detected as a major component in the inflammatory infiltrate in the islets of individuals with T1D. Thus, it is evident that B cells are involved in T1D pathogenesis, however their exact role is not well understood. Importantly, early studies ruled against their pathogenic role being attributed to antibody production. Removal of the B cells ability to secret immunoglobulins still resulted in disease development and progression in the NOD mouse model (Wong *et al.*, 2004).

Thus, it is apparent that a breach in B cell tolerance occurs in T1D, as evidenced by B cell production of autoantibodies. As autoantibodies are not directly implicated in pathogenesis, they may act as a proxy for autoreactive B cells of the same specificity, that are engaged in disease processes in an alternative manner

1.8.1 B cell immunity

1.8.1.1 Immunoglobulin structure

Antibodies, or immunoglobulins, are expressed by a B cell either on the cell surface to serve as an antigen receptor (B cell receptor – BCR) or are secreted as a soluble molecule (antibody). The typical structure of the immunoglobulin molecule is a Y-shape, comprised of two heavy and two light chains linked together by disulfide bonds (Figure 1-6). The N-terminus regions of the heavy and light chains form the antigen binding sites determining antigen specificity (Fab region); described as bivalency due to the two identical antigen binding sites. Five different isotypes of antibody exist – IgA, IgD, IgE, IgG and IgM, with each isotype defined by its own

class of heavy chain; α, δ, ε, γ and μ, respectively. Importantly, each isotype gives rise to distinct conformations in the C-terminus, or the heavy chain constant region (Fc region). Therefore, while different isotypes do not interfere with antigen specificity and binding, they impact the Fc-mediated effector function of the antibody. Early in B cell development, productively rearranged variable domains associate with the μ chain to express IgM, followed by IgD as a result of alternative splicing (naïve B cells). Later during development, in response to various extracellular cues, variable domains may associate with the other isotypes in a controlled process, known as isotype switching (to be discussed).

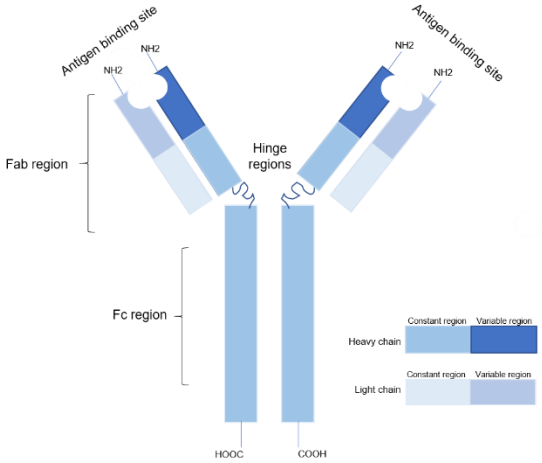

Figure 1-6 Structure of immunoglobulin.

1.8.1.2 B lymphocyte lineage subsets

B cells can be classified on ontogeny and anatomical location. Primarily, two principal classes exist in mice and humans consisting of B1 B lymphocytes and B2 B lymphocytes. These form part of the innate and adaptive immune system, respectively.

B1 cells are a self-renewing population of cells that develop in fetal life and persist beyond the neonatal period, populating pleural and peritoneal cavities and expressing high levels of CD5 and producing polyreactive IgM antibodies in a T cell independent manner (Montecino-Rodriguez and Dorshkind, 2012).

B2 cell maturation occurs in the bone marrow (BM), where common lymphoid progenitors (initiated from hematopoietic stem cells) commit to a specific B cell fate

and progressively undergo a process of gene recombination. This involves rearrangement of the segments V (variable), D (diverse) and J (joining) of the heavy chain and segments V and J of the light chain, in order to form membrane bound immunoglobulin (mIg) and generate wide diversity. This process is mediated by RAG1 and RAG2 proteins which cleave recombination signal sequences that flank the rearranging gene segments, and also relies on close interaction between developing B cells and BM stromal cells. The sequential steps of development of immature B cells in the BM are based on expression of certain surface markers, and are as follows (Figure 1-7): early pro-B (V-D joining, heavy chain), late pro-B (VD-J joining, heavy chain), large pre-B cell (heavy chain and surrogate light chain expressed at the surface i.e. a pre-BCR), small pre-B (light chain rearrangement) and immature B cells (rearranged BCR on the cell surface) (Hardy and Hayakawa, 2001). An important feature of gene recombination in the B cell development process is allelic exclusion, whereby each mature B cell will only express a single type of receptor i.e. monospecificity (Vettermann and Schlissel, 2010). Additionally, expression of the complete mIg enables the first tolerance checkpoint – receptor editing.

Immature B cells then emerge from the BM and home to the spleen, where they differentiate into transitional cells. Transitional B cells are coined to categorise early emigrants from the BM; in man they are the first to re-emerge after hematopoietic stem cell transplants or B cell depletion therapies (Marie-Cardine *et al.*, 2008; Mouquet *et al.*, 2008). Initially, transitional cells have high IgM surface expression but are negative for the surface markers IgD, CD21 and CD23. After entering the spleen follicles, transitional cells gain expression of these markers as well as the ability to recirculate. Transitional cells are responsive to apoptosis, therefore representing an important peripheral tolerance mechanism (Sater, Sandel and Monroe, 1998).

Transitional cells finally differentiate into fully (naïve) mature states: either as marginal zone B cells (MZB) or follicular B cells. Differences in the BCR signalling pathways, in combination with B cell activating factor (BAFF) signals, expression of transcription factors NOTCH2 and BTK and pathways mediating migration and retention, determine the commitment of B cells to one of the two fates.

Transitional cells develop into MZB in response to weak BCR signalling, NF-kB signals and NOTCH2 signalling (Moran *et al.*, 2007). MZB are retained in the spleen in the outer white pulp and constitutively express high levels of MHC class II and costimulatory molecules, resulting in antigen presentation activity to T follicular helper cells. MZB form the first line of defence against blood borne pathogens and elicit T cell independent immune responses by differentiating into short-lived plasma blasts.

In contrast, FO B cells, arise from transitional B cells in the spleen through a pathway dependent on tonic (or strong) BCR signals that initiate Bruton tyrosine kinase (BTK) signalling pathways, in addition to BAFF survival signals (Pillai and Cariappa, 2009; Almaden *et al.*, 2014). These cells are the conventional B cells of the adaptive immune response and recirculate through the peripheral circulation, populating various secondary lymphoid tissues. Upon encounter with cognate antigen, FO B cells can differentiate into plasma antibody secretory cells or memory B cells.

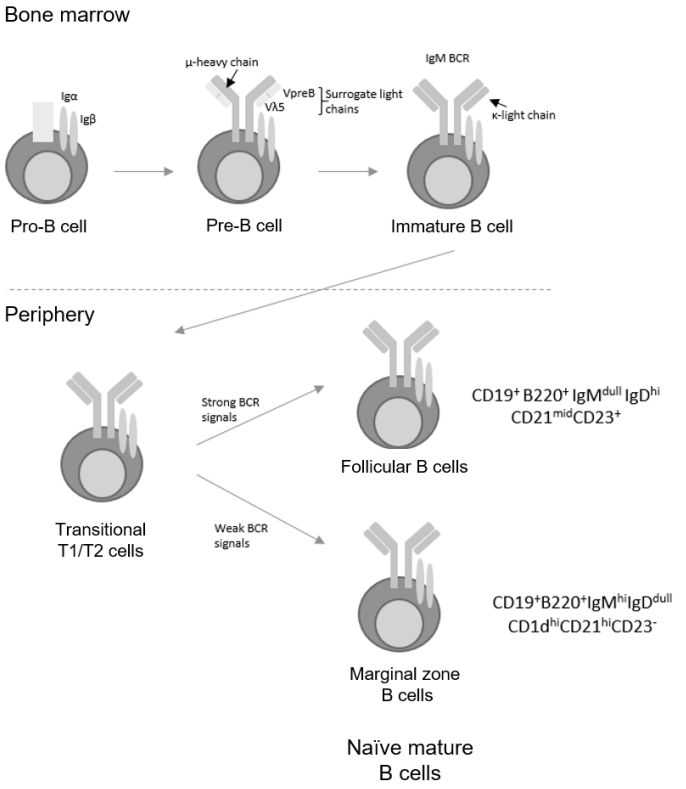

Figure 1-7 Stages of B cell development occurring in the bone marrow and the periphery, in order to generate mature naïve B cells.

1.8.1.3 Development and maintenance of plasma cells and memory B cells

B cell responses are categorized as T cell dependent and T cell independent. With T cell help, B cells are able to differentiate into long-lived memory B cells and plasma cells - a hallmark of humoral immunity. The antigen driven generation of long-lived plasma cells and memory B cells from the FO B cell compartment primarily occurs in the SLO, where lymphocytes are recruited from the bloodstream in response to chemotactic gradients (Ansel *et al.*, 2000). Generation occurs in two distinct phases in two distinct structures: B cell follicles and germinal centres (GC).

Phase 1 transpires in the B cell follicles, where cognate antigen recognition by the BCR results in antigen internalisation, processing, and presentation on MHC class II molecules. Chemokines CXCL13 and CCL19/21 then regulate the recirculation of antigen-activated B cells between the inner area and border of the B cell follicle (Allen *et al.*, 2004). The B cell follicle is adjacent to the T cell zone of the SLO, leading to establishment of stable B cell- T cell interactions (Stebegg *et al.*, 2018).

Here, B cells can present antigen to CD4 T cells and receive helper signals and co-stimulation from the T cells in return (Garside *et al.*, 1998; Okada *et al.*, 2005). This endows the B cells the ability to migrate to the outer follicles, where they undergo proliferation and differentiation either into short lived, extra follicular plasma (effector) cells, or GC-independent B cells. These attribute to the first wave of antibody responses to control early infection, but produce low affinity antibodies that are short lived (MacLennan *et al.*, 2003).

Alternatively, CD4 T cell activated B cells can return to the centre of the B cell follicle and undergo rapid proliferation to establish a GC. Once formed, clonal expansion of antigen specific B cells occurs (centroblasts) in the dark zone (DZ) of the GC, and cells upregulate activation-induced cytidine deaminase (AID) (Victora *et al.*, 2012). BCR diversification is established here through AID-regulated somatic hypermutation (SMH). AID regulates the introduction of single base pair substitutions (through conversion of cytosines to uracils by deamination) of antibody gene segments in the immunoglobulin variable region genes exon sequences (Stavnezer, Guikema and Schrader, 2008).

As the mutational process of SHM is random, mutated B cells require selection to ensure B cells bearing a BCR with 'improved' antigen binding ability are released into the periphery. To achieve this, B cell proliferation in the DZ reduces, and cells migrate along a CXCL13 gradient to the GC light zone (LZ) in order to undergo the process of affinity maturation (Bannard *et al.*, 2013). This occurs through the establishment of connections with follicular dendritic cells (FDCs), that provide survival factors and antigen presentation, and interactions with T follicular helper cells that provide selection and differentiation signals (Wang *et al.*, 2011).

Specifically, B cells compete for antigen on the FDCs, internalise it and present to T follicular helper cells. B cells are then selected on the basis of their increased avidity for cognate antigen. Higher affinity B cells bind and endocytose more antigen and therefore present peptide at a higher density, conferring an advantage in competing for Tfh help (CD40:CD40L), prolonging and intensifying the interaction and driving positive selection (Allen *et al.*, 2007). On the other hand, B cells producing unfavourable antibodies are rendered incapable of sufficient antigen uptake and undergo apoptosis at this stage (Mayer *et al.*, 2017). Following positive selection, B

cells will either be instructed to re-enter into the dark zone for further SMH and proliferation or exit the GC as memory cells or plasma cell precursors. Although not fully elucidated, GC fate is thought to be dependent on the intensity of the interaction with Tfh cells in the LZ. Long and strong interactions (as a result of high affinity B cells) result in differentiation of cells into plasma cell precursors that exit the GC as plasma cells, while low affinity B cells exit the GC as memory cells, or recycle back into the GC (Ise *et al.*, 2018; Palm and Henry, 2019).

B cell also undergo class switch recombination (CSR). This involves an intrachromosomal deletional rearrangement program within the Ig heavy chain constant region (i.e. the isotype), enabling the cell to switch the isotype of the antibody in order to adapt its effector functions, in addition to altering its tissue distribution (Manis, Tian and Alt, 2002).

Once generated, memory B cells will recirculate in the peripheral blood, colonise lymphoid organs including lymph nodes, spleens, and tonsils (i.e. antigen draining sites), as well as non-lymphoid organs including the lung, liver skin and gut. This positioning of cells within both lymphoid and non-lymphoid tissues confers a higher probability of encountering cognate antigen, and allows recirculation from the blood, to tissues, to sites of inflammation. In addition to a rapid secondary response through differentiation into plasma cells and production of antibodies, memory B cells also can act as very powerful antigen presenting cells.

1.8.1.4 B cells as antigen presenting cells

As previously discussed, APCs can internalise antigen by three means – phagocytosis, fluid phase pinocytosis and receptor mediated endocytosis (Section 1.5.2). In the context of B cell antigen presentation, the latter process is carried out by the BCR, allowing the cell to concentrate very small quantities of specific antigen. This is the major pathway of antigen uptake by B cells, where BCR affinity is directly proportional to the capability of the B cell to present soluble antigen to induce CD4 T cells responses.

To induce the same level of CD4 T cell proliferation, B cells with a low affinity for soluble antigen required a 10 times higher concentration as compared to B cells with a high affinity for the same antigen (Batista and Neuberger, 1998). The same study

solidified the importance of BCR-mediated endocytosis in antigen presentation, as when uptake was through (non-specific) fluid phase pinocytosis, a 5000 times higher concentration was required for the same level of T cell proliferation. Presentation of antigen internalised by the BCR is therefore favoured by the cells as opposed to passive uptake. Indeed, ligation of the BCR by antigen induces its internalisation and directs the BCR-antigen complexes through the endocytic pathway required for antigen presentation on MHC class II molecules (Siemasko *et al.*, 1999). Additionally, BCR signalling upregulates MHC class II expression by the cell, and induces changes in the late endosomes that favours appropriate loading of peptides onto MHC class II molecules, such as acidification (Siemasko *et al.*, 1998; Zimmermann *et al.*, 1999).

The antigen presenting function of B cells is also dependent on CD40-derived signals provided by Tfh cells. CD40-CD40L ligation results in an increase in the expression of co-stimulatory molecules such as MHC class I and II, CD86 and CD80, on the B cell surface – licencing the cell for effective APC function (Lee *et al.*, 2003). The role of Tfh-B cell interaction is important in recognising the dynamics of B cell antigen presentation in immune responses. It is likely that Tfh cells first have to be primed and activated by an alternative APC (i.e. DCs), before they can engage with B cells and induce the ability of the B cell to contribute as an APC. Therefore, while DCs may be critical for initiation (priming) of CD4 T cell responses, B cells may be more prevalent at a later, secondary stage.

The involvement of different APCs appears to be determined by the type and form of antigen. Indeed, in the context of autoimmunity, B cells are likely to be critical APCs for multiple reasons. For example, unlike DCs, the BCR cannot determine the origin of the antigen (whether it is self or foreign), and B cells are able to concentrate very small amounts of antigen (Batista and Neuberger, 1998). Finally, while DCs represent the most important APC during the initiation of an immune response, B cell antigen presentation may be important during the later phases of chronic immune reactions (to be discussed, Section 1.8.4.1).

1.8.2 Failure of B cell tolerance in T1D

The appearance of autoantibodies suggests that B cell tolerance to self has been breached in T1D individuals. Indeed, T1D subjects show an increase in the frequency of polyreactive clones in new emigrant (from the BM) and naïve B cell compartments, indicating defective central and peripheral tolerogenic checkpoint mechanisms respectively (Menard *et al.*, 2011). Additionally, recombining sequence (RS) rearrangement levels in circulating B cells were significantly lower in T1D donors in comparison to healthy control subjects. With RS rearrangement correlating to the level of antibody light chain receptor editing, these data support a failure of central tolerogenic checkpoints (Panigrahi *et al.*, 2008).

Recently, extensive efforts have focused on the integrity of anergy in individuals with T1D. Anergy is a fragile state of unresponsiveness maintained by the activation of negative regulatory pathways through continuous occupation of the BCR by cognate antigen. In healthy individuals, insulin binding B cells (IBCs, i.e. autoreactive cells) are contained in the anergic B cell compartment. In subjects with T1D, there was a significant loss in IBCs from this compartment, suggesting a reversal of anergy and release of autoreactive cells to the periphery to engage in disease (Smith *et al.*, 2015). Interestingly, prediabetic individuals and autoantibody-negative first-degree relatives (FDRs) showed a similar loss of anergic IBCs suggesting it is a primary event in disease pathogenesis, as opposed to a secondary by-product of the pro-inflammatory conditions induced in disease. In line with this notion i.e. that failure of anergy is of an intrinsic nature, investigations from the same group explored associations of certain risk allele genotypes with the loss of IBCs from the anergic compartment (Smith *et al.*, 2018). FDRs who carried the high-risk HLA Class II haplotypes showed lower IBC frequencies within the anergic compartment as compared to those carrying no-risk alleles, suggesting anergy is more readily reversed in these subjects.

1.8.3 Perturbations in circulating B cells in individuals with T1D

The contribution of various genetic factors to failure of B cell tolerance checkpoints in individuals with T1D, suggests that common, disease specific alterations in the B cell compartment may exist. A consistent disease relevant phenotype is yet to be

fully delineated, however perturbations in B cell subsets and phenotypes appear to exist in patients with T1D.

Increases in the frequencies of circulating transitional B cell subsets and marginal zone B cell subset have been identified in T1D patients, in comparison to healthy control subjects (Habib *et al.*, 2012; Deng *et al.*, 2016). Additionally, decreases in IL-10 producing B cells (B regulatory cells) have been described (Kleffel *et al.*, 2015; Wang *et al.*, 2020). In contrast, other detailed characterisations of the B cell compartment revealed no disease specific alterations in the frequencies of different subsets (Thompson *et al.*, 2014; Viisanen *et al.*, 2017). An interesting finding, however, was the identification of a disease specific enrichment in CXCR5+PD1+ICOS+ activated circulating T follicular helper (Tfh) cells (Viisanen *et al.*, 2017). Due to their ability to activate B cells, a pronounced increase in Tfh cells is likely to correlate with an immunopathological activation of B cells.

Disease specific enrichment of B cell phenotypes, as well as changes in subset frequencies, have also been reported. Extensive immunophenotypic analysis using flow cytometry revealed decreases in the frequencies of B cells expressing TACI (CD267) and FasR (CD95, cell death receptor) on various B cell subsets in T1D individuals as compared to healthy controls (Powell *et al.*, 2019; Hanna *et al.*, 2020). Reduced frequencies of CD95 expressing cells suggest circulating B cells in T1D subjects are less susceptible to apoptosis, therefore leading to an increase in frequencies of autoreactive B cells able to engage in disease. In concordance with this, slow progressors to disease (at risk individuals who, despite being positive for multiple autoantibodies, do not progress to T1D within 10 years) expressed higher levels of CD95 compared to newly diagnosed T1D subjects, particularly in response to polyclonal stimulation (Hanna *et al.*, 2020).

In addition to disease specific changes in CD95 expression, frequencies of CXCR3 and CD24 expressing B cells also appears to be disease linked. On circulating class-switched memory B cells, CXCR3 (chemokine receptor, trafficking) expression was reduced as compared to healthy controls, suggesting the CXCR3 B cells may have trafficked to the pancreas in T1D individuals to engage in disease (Powell *et al.*, 2018). Interestingly, CXCR3 expression is upregulated on memory B cells in response to IFNγ (Muehlinghaus *et al.*, 2005). Therefore, in the context of

inflammatory conditions i.e. autoimmunity, CXCR3 expression may increase on the B cells and drive their migration into inflammatory tissues, explaining the reduction of CXCR3 B cells from the periphery.

1.8.4 Pathogenic relevance of B cells in T1D

A loss of B cell tolerance is therefore prevalent in T1D individuals, allowing autoreactive B cells to escape into the periphery. This is reflected in the perturbations of circulating B cell phenotypes in T1D subjects compared to healthy controls, suggesting a disease specific phenotype in which B cells are localised to the site of antigen, and are less susceptible to death by apoptosis. Consequently, self-reactive B cells are available to engage in disease processes.

1.8.4.1 B cell depletion in NOD animal mouse models and significance of BCR specificity

Seminal studies in the 1990s highlighted the significance of B cells in disease pathogenesis in the NOD mouse animal model, with genetic ablation of B cells resulting in complete elimination of disease development (Serreze *et al.*, 1994; Akashi *et al.*, 1997). Short term treatment with an anti-CD20 monoclonal antibody also resulted in a decreased severity of insulitis and prevented diabetes development in the majority of mice (Xiu *et al.*, 2008).

To understand the role of B cells in the natural history of disease, conclusions can be drawn from studies where NOD mice were treated for B cell depletion at distinct time points, due to the well characterised disease progression in NOD mice. For example, treatment of mice at four weeks (little to no insulitis) and nine weeks (full insulitis) with an anti-CD20 antibody, showed a decrease in the overall incidence in disease in the latter subject group (Hu *et al.*, 2007). This suggests B cells are involved in the later pathogenic stages of disease i.e. in progression to overt clinical disease but not in the initiation (D. V Serreze *et al.*, 1996; Hu *et al.*, 2007; Fiorina *et al.*, 2008). In concordance, analysis of insulitis shows that B cells are undetectable in the early stages of insulitis but increase in numbers as insulitis proceeds and converts from benign to destructive, as ascertained by β-cell volume (Hanenberg *et al.*, 1989; Signore *et al.*, 1989; In't Veld, 2014a). Consistent with this, B cell deficient NOD mice develop a benign insulitis (D. V Serreze *et al.*, 1996). Additionally, in NOD

mice with established diabetes, B cell depletion results in restoration of normoglycemia, suggesting a continuous role for B cells in established disease (Hu *et al.*, 2007; Fiorina *et al.*, 2008).

While depletion studies resulted in global B cell deletion, later investigations revealed that antigen-specific B cells most likely formulate the majority of the B cell contribution to disease. Transgenes with different potentials for insulin binding were utilized in the NOD mouse model; with one producing a B cell repertoire in which 1-3% of circulating mature B cells were insulin specific (VH125), and another where B cells had a significantly reduced ability to bind insulin (VH128) (C Hulbert *et al.*, 2001). Here, skewing of the B cell repertoire towards insulin binding (VH125) promoted the development of diabetes in NOD mice, in comparison to mice expressing the VH128 transgene, who showed protection from disease development. In line with this, restriction of the B cell immunoglobulin repertoire to the disease irrelevant hen egg lysozyme (HEL) protein resulted in suppression of T1D in NOD mice (Silveira *et al.*, 2002).

The BCR is evidently critical for a pathogenic B cell function in NOD mice, implicating a role for B cell antigen presentation due to BCR mediated uptake of antigen, as opposed to passive uptake of intact antigens (Section 1.8.1.4). Indeed, specific deletion of MHC class II and class I from B cells leads to a reduction in disease prevalence and progression (Noorchashm *et al.*, 1999; Mariño *et al.*, 2012). Additionally, pancreas infiltrating B cells have elevated levels of both MHC molecules, as well as the co-stimulatory molecules B7-1 an B7-2 (Hussain and Delovitch, 2005).

Direct evidence to link BCR specificity and B cell activity arises from additional studies utilising B cells from the VH125 mouse model. Insulin binding B cells were more competent presenters of insulin antigen as compared to non-insulin binding B cells, in the context of CD4 T cell proliferation (Kendall *et al.*, 2013). B cells were also unable to generate T cell responses against the candidate autoantigen GAD when the B cell repertoire was skewed towards a pathologically irrelevant antigen (Silveira *et al.*, 2002). Therefore, it is likely that B cells serve as a preferential subset of diabetogenic APC in the NOD mouse, most likely due to the properties of the BCR that allow efficient and specific uptake of antigen, and presentation to antigen

specific CD4 T cells. The importance of MHC class II antigen presentation in the NOD mouse model has therefore been well established, while limited data has also eluded to a role of MHC class I antigen presentation (to be discussed).

Taken together, in the NOD mouse model, B cells play a continuous role in a later pathogenic stage of disease – mediating the progression from silent to overt disease. This is dependent on the expression of a (self) antigen specific BCR on the B cell, implicating an antigen-presenting mechanism of action.

1.8.4.2 B cell depletion in human T1D individuals

Data from a phase 2 clinical trial using Rituximab (RTX) to deplete CD20 B cells in T1D individuals, established the importance of B cells in human disease pathogenesis, building on the findings from NOD animal models. Recently diagnosed T1D patients (within 3 months) treated with RTX displayed a significantly higher absolute level of c-peptide at 3, 6 and 12 months post treatment, as compared to those treated with placebo (Pescovitz *et al.*, 2009). B cell depletion therefore results in a preservation of β-cell function, implicating the pathogenic role of B cells in β-cell destruction. At 30 months post treatment, however, c-peptide decline was comparable to those in the placebo control group (Pescovitz *et al.*, 2014). RTX treatment may therefore not fundamentally alter the underlying pathophysiology of disease. Indeed, frequencies of autoreactive antibodies expressed by single B cells before and after (52 weeks) treatment showed comparable levels, with those post treatment exhibiting features of newly generated clones (Chamberlain *et al.*, 2016). While RTX treatment results in a temporary dampening of pathogenic B cell mediated immune responses, it therefore fails to reset defective tolerogenic mechanisms. Repopulation of autoreactive B cells occurs, explaining the lack of therapeutic benefit seen at 30 months post treatment. Despite this, it is important to note the magnitude of the findings of these studies. For the first time in human subjects B cells are clearly implicated in the processes that lead to β-cell destruction.

1.8.4.3 B cells and β-cell destruction

Results from B cell depletion studies therefore implicate B cells in the immune processes that modulate β-cell destruction in the pancreatic islets. In support of this

is the observation that B cells are present in insulitis in NOD mice and are the second most abundant immune cell subset in the insulitic lesion in T1D patients (Section 1.5.4).

Studies utilising whole blood RNA sequencing further eluded to the B cell centric immune mechanisms leading to β-cell destruction. Patients presenting with a more rapid loss of insulin secretion, compared to those with a more 'steady' disease process, had a specific immunophenotype that was characterised by a high level of B cells (Dufort *et al.*, 2019). This finding was also confirmed at a protein level using flow cytometry. In concordance, a computational approach associated a peripheral B cell activation signature with an increased loss of insulin secretion in T1D (Speake *et al.*, 2019).

Evidently, the presence of B cells appears to be associated with more rapid loss of insulin secretion, and therefore a more aggressive destruction of β-cells. Analysis of the islet infiltrate in pancreatic tissue samples donated by T1D individuals, further elucidated the correlation between islet-infiltrating B cells and disease progression. A striking variation in the absolute numbers of CD20 B cells per islet across patients was observed, allowing stratification of two distinct patient groups based on the level of CD20 B cell infiltrate (Arif *et al.*, 2014). Changes in infiltrate composition was secondary to this distinction, with the CD20 high group displaying higher number of immune cells per islet (hyper immune), and the CD20 low group showing reduced levels of immune infiltration (pauci immune). It is therefore likely that distinct patterns of islet infiltration may represent different immunopathological processes that underlie T1D disease (endotypes).

Indeed, these differential insulitic profiles were later found to associate with the extent of β-cell destruction and the age at onset of T1D (Leete *et al.*, 2016). Age at diagnosis was predictive of the insulitic profile: diagnosis under 7 years of age was associated with the CD20 high profile, while diagnosis over 13 years of age displayed the CD20 low islet phenotype. Importantly, the former group retained a significantly lower proportion of insulin containing islets, suggesting a more aggressive destruction of β-cells and a more rapid disease progression.

Therefore, B cells clearly play an important accessory role in the destructive process as their presence exerts a profound influence on the extent of β-cell destruction. Indeed, the discovery of T1D endotypes based on CD20 islet infiltration resolved an observation of the Rituximab clinical trial, where RTX treatment was more effective in younger subjects (Pescovitz *et al.*, 2009). This is most likely due to an increased infiltration of CD20 B cells in the islets, increasing sensitivity to treatment.

1.8.5 B:CD8 T cell interactions in T1D

Data from animal and human studies therefore present a role for B cells in T1D disease pathogenesis, and this is summarised in Figure 1-8. Depletion of B cells, both in animal models (NOD mice) and individuals with newly onset disease, results in prevention of disease progression. This can be attributed to a preservation of β-cell function. B cells are likely to play an accessory role in the destructive process of the islets, a concept bolstered by the existence of a $CD20^{high}$ disease endotype, where high islet infiltration of CD20 B cells correlates directly with enhanced β-cell destruction.

As it is well established that CD8 T cells are responsible for β-cell destruction in disease, it seems pertinent to speculate a direct link between B cells and autoreactive CD8 T cells in the islets that promotes effector CD8 T cell pathways responsible for disease. As discussed, in insulitis, B cells are recruited in greatest numbers at the later stages once β cell decline is established, and B cell depletion post-insulitis results in restoration of normoglycemia in pre-clinical animal models (Section 1.8.4.1). This implicates B cells in a late pathogenic disease event, such as CD8 T cell mediated β-cell destruction. Additionally, analysis of the islet immune infiltrate presents the strongest islet residency relationship between CD8 T cells and B cells (Willcox *et al.*, 2009) . As β-cell death progresses, CD20 B cells increase in parallel with the influx of CD8 T cells and in nearly all cases CD20 B cells were only present when CD8 T cells were also present, consistent with a dynamic interplay between the two cells.

B cells therefore may be involved in the activation, expansion, or effector development of pathogenic CD8 T cells within the islets. As discussed, CD8 T cells

appear to acquire a cytotoxic effector function as a result of antigen-driven, disease specific events in the islet (Section 1.7.1.5).

Although limited, some understanding of the cellular and molecular interplay between B cells and CD8 T cells in the pancreatic islets has been revealed in various pre-clinical animal models of B cell depletion in diabetes. Anti-CD20 antibody treatment of transgenic NOD mice that expressed a human CD20 transgene on B cells mirrored previous depletion studies where onset of diabetes was significantly delayed (da Rosa *et al.*, 2018). Importantly, depletion of B cells in NOD mice of 6-8 weeks had a marked impact on T cells in the local islet infiltrate, resulting in a reduction in CD8 T cell activation and effector function, as determined by CD44 and IFNy expression, respectively. In line with this, in B cell deficient NOD mice and in NOD mice treated with the B cell depleting agent BCMA-Fc, the frequency of IGRP-reactive CD8 T cells in the pancreas, as well as the spleen and pLN, were reduced, implicating B cells in the proliferative expansion of self-reactive CD8 T cells (Mariño *et al.*, 2012). Similarly, intra-islet CD8 T cells were significantly reduced in B cell deficient mice of the transgenic inflammation-based NOD model of T1D, where TNFα expression is restricted to the islet and diabetes progression is independent of CD4 T cell involvement (Brodie *et al.*, 2008). Taken together, these data provide direct evidence that removal of B cells alters CD8 T cell activity in the islets, affording a mechanistic explanation for the delay in diabetes development upon B cell depletion.

The study by Brodie *et al.,* (2008) performed an elegant series of experiments to elucidate the intricate interactions between B cells and CD8 T cells in the inflamed target tissue that lead to destruction of the target cell. Using a unique inflammation driven NOD mouse model where TNFα expression was restricted to the islets, B cells were identified as playing a divergent role dependent on the environment in which they reside. While the frequency of islet specific CD8 T cells was significantly reduced in the islets upon B cell depletion, no significant changes in the proliferation, or the cytotoxic phenotype, of intra-islet CD8 T cells were observed. In the pLN however, B cell depletion resulted in a significant reduction in the frequency of proliferating islet specific CD8 T cells as well as the percentage of CD8 T cells expressing a cytotoxic phenotype. Therefore, in the islets, B cells provide

essential survival signals to CD8 T cells, as reflected by the increase in CD8 T cell apoptosis after B cell depletion. In the pLN, B cells are required for the proliferation and differentiation of primed CD8 T cells. The direct molecular mechanisms governing these functional interactions were not addressed in this study. Authors hypothesised that the CD8 T cell alterations in the pLN upon B cell depletion occurred as a secondary result of reduced B cell help to DCs, leading to dysfunctional antigen presentation to CD8 T cells by the latter. Indeed, this phenomena has been described in the context of DC-CD4 T cell interaction, upon depletion of B cells (Hu *et al.*, 2007).

The observation that B cell depletion had no impact on the acquisition of an effector function within the islets was surprising, specifically in the context of the aforementioned study by da Rosa *et al.,* (2017) where B cell depletion resulted in a reduction in the activation and effector function of CD8 T cells in the local islet infiltrate, and studies by Graham and colleagues, where stimulation of cytotoxic effector molecule expression occurs in the inflamed islets and not the pLN (Graham *et al.*, 2011). It is likely that this observation was a consequent of the inflammation-driven animal model used. TNFα is well established as a potent cytokine promoting DC function, therefore its excessive expression in the islet may empower islet residing DCs to provide the necessary signals to CD8 T cells, in the absence of B cells.

Further elucidation of the molecular mechanisms governing B:CD8 interactions *in vivo* was presented by Marino *et al*., (2012). Here, the standard NOD mouse model was utilised. Findings were consistent with the aforementioned study whereby while B cell depletion resulted in a reduction in the frequency of CD8 T cells in the islets, they were only required for the proliferative expansion of self-reactive CD8 T cells in the pLN. Authors focused experiments on the pLN events and aimed to elucidate the mechanism by which B cells governed CD8 T cell proliferation. B cells isolated from the NOD mouse (pLN and spleen) were able to cross present MHC class I peptide complexes to self-reactive CD8 T cells, with the resulting cognate B:CD8 interaction leading to proliferative expansion of CD8 T cells and development of a cytotoxic phenotype. Acquisition of antigen by B cells was dependent on BCR specificity i.e. the ability of B cells to capture exogenous antigen through specific

membrane bound Ig molecules, which resulted in targeting of antigen to the endosomes, and processing through the classical endogenous antigen processing pathway. *In vivo*, B cell cross-presenting function was central to diabetes development as selective removal of MHC class I exclusively from B cells prevented diabetes progression in the NOD mouse. Authors concluded that, in this model, B cell antigen cross-presentation to CD8 T cells drives expansion and effector development in the pLN, governing the subsequent CD8 T cell mediated β-cell destruction.

The reduction of intra-islet CD8 T cells upon B cell depletion was not directly addressed in this study, perhaps with the assumption that this was a by-product of the reduction of proliferation in the pLN. In the context of the Brodie *et al.*, (2008) findings, the reduction may also be due to a lack of survival signals provided by the B cells. An interesting extension would be to assess the activation and cytotoxic phenotype of the CD8 T cells in the islets in addition to the pLN, using IFNγ, Granzyme B and CD107α as markers. Despite no changes in the proliferative responses in the islets, B cells may represent an APC population central to the re-activation of CD8 T cells and acquisition of effector function in the islets, providing a mechanistic explanation for alterations in islet-residing CD8 T cell activity in the aforementioned recent study (da Rosa *et al.*, 2018) This concept is supported by the replete levels of CD80 and CD86 identified on islet infiltrating B cells (Hussain and Delovitch, 2005). Additionally, although molecular mechanisms were not directly addressed in the da Rosa *et al.*,(2018) study, the alteration in T cell phenotype and function remained after therapy completion and repopulation of B cells. Re-emerging B cells post depletion showed reduced expression of the co-stimulatory molecules CD80 and CD86. Reduced expression may therefore impair T cell activation due to a reduced ability of B cells to present antigen.

Shortcomings of the study by Marino *et al.*, (2012) do however implicate a significant gap in our understanding of B cell antigen cross presentation to CD8 T cells. Firstly, studies were focused on IGRP-specific CD8 T cell responses. IGRP is not a known target for autoantibodies in T1D and therefore does not provide evidence to link humoral immunity with disease mechanisms. Moreover, while data eluded to a cross-presenting function of the B cell, this was based on observations

that CD8 T cell proliferation was dependent on a functional (disease specific) BCR and an intact MHC class I molecule on the B cell. A direct link between B cell autoantigen presentation to pathogenic CD8 T cells was not evidenced.

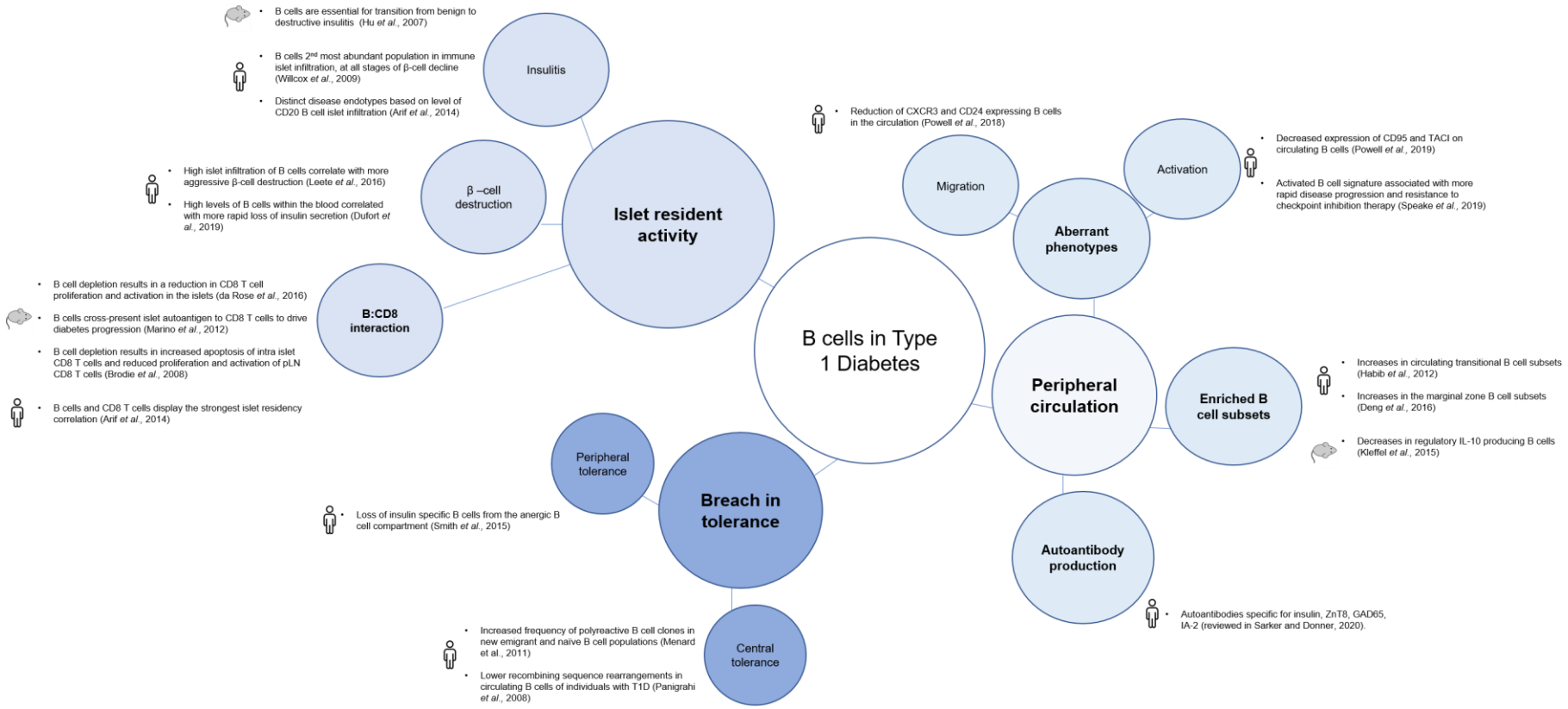

Figure 1-8 An overview of the relevance of B cells in Type 1 Diabetes.

1.9 Aims and significance of this thesis

The studies discussed above highlight the relevance of B cells in T1D pathogenesis. While the presence of islet specific autoantibodies is critical in determining disease risk, diagnosis, and progression, they have no clear involvement in β-cell destruction. Risk of T1D stratifies according to the number of specificities of autoantibody – as tolerance is lost to each β-cell antigen, the risk increases. The notion that such pivotal disease markers have no connection to disease mechanisms is paradoxical, particularly in the context of data highlighted above where B cell depletion correlates with therapeutic benefit. This therefore presents a model where autoantibodies are a proxy for autoreactive B cells, that are engaged in disease processes and disease progression in an alternative manner.

Elucidation of the immune pathways of disease progression can inform new therapeutic approaches for the treatment and prevention of clinical diabetes. As discussed above, a considerable body of evidence implicates CD8 T cells as the final effectors of β-cell death. Importantly, promotion of this effector function appears to be governed by events in the pancreatic islets, that are necessary for maintaining the ongoing autoimmune attack. This presents the cellular and molecular mechanisms governing pathogenic effector T cell function at the disease site as a critical node for therapeutic intervention. Intervention studies to maximise the preservation of β-cells are important therapeutic goals within the field as even low levels of endogenous insulin can improve disease complications and associated morbidity.

Data discussed throughout present a model where B cells are critical for disease progression – likely engaged in disease processes due to a relatively unexplored axis between autoreactive B cells (of islet specificity) and autoreactive CD8 T cells within the islets. B cell depletion studies in mice show a delay in disease onset and progression, with depletion post insulitis restoring glycaemic function and therefore implicating B cells in a late pathogenic disease event. In humans with T1D, treatment with RTX results in a preservation of β-cell function. Analysis of the immune cell composition of insulitis shows two distinct disease endotypes, existing as $CD20^{high}$ hyper-immune and $CD20^{lo}$ pauci-immune, with the former correlating

with a more aggressive β-cell destruction and disease progression. Importantly, further analysis of immune cell subpopulations identifies the strongest islet-residency relationship between CD8 T cells and B cells, supporting a direct interplay between the two cells in T1D.

The literature on cognate B:CD8 lymphocyte interactions and their biological and disease relevance is limited. As discussed, in the NOD mouse model, depletion of B cells both through antibody treatment (anti-CD20) and genetic ablation (transgenic models) has a profound impact on CD8 T cell populations in the islets and the pLN, reducing their frequency, activation status and cytotoxic phenotype. The mechanisms by which B cells govern these CD8 T cell responses in the NOD mouse model are eluded to, implicating B cell antigen cross-presentation and provision of survival signals. Further understanding of the mechanisms governing the interaction between B cells and CD8 T cells will elucidate potential pathways for therapeutic blockade. Therefore, this thesis aims to address the overarching hypothesis that a cognate and dynamic interaction occurs between CD8 T cells and B cells in the islets of individuals with T1D, driven by β cell autoantigen cross-presentation. This interaction is likely to be essential to the progression of disease from silent insulitis to overt disease. Moreover, this study will address the gap in understanding where, despite autoantibodies existing as a pivotal disease biomarker, they have no known connection to disease pathology.

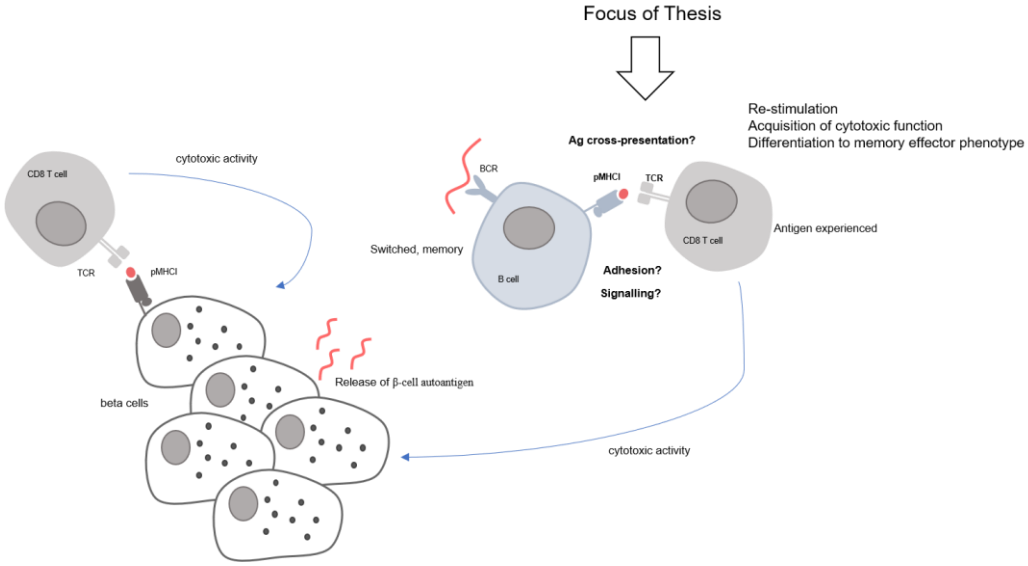

Figure 1-9 The potential role of B cells in Type 1 Diabetes, through interaction with CD8 T cells in the islets.

The aims of the study are shown below with experimental objectives established to address these aims indicated in bullet points:

1. **H: B cells acquire and internalise exogenous antigen through their surface BCR. This results in processing and presentation of peptide:HLA CI complexes to CD8 T cells, leading to their acquisition of an effector cytotoxic phenotype.**

   A: ***Provide in vitro proof of concept that a disease-relevant subset of human B cells can cross-present (model) antigen to CD8 T cells and induce CD8 T cell cytotoxic responses.***

   - Develop an antigen delivery system (ADS) to target antigen to the BCR for internalisation and antigen processing.
   - Assess the ability of ADS-pulsed B cells to cross-present antigen by measuring CD8 T cell cytotoxic responses.
   - Compare the cross-presentation potency between B cells and the professional APCs, dendritic cells.

2. **H: Pathways exist between B cells and CD8 T cells that are relevant to their interaction and subsequent CD8 T cell effector function.**

A: ***Investigate the key modalities involved in the interaction between B cells and CD8 T cells that may be relevant to B cell promotion of CD8 effector function.***

- Establish an *in vitro* experimental approach to detect interacting B cells and CD8 T cells.
- Assess the dependence of their interaction on B cell antigen cross-presentation.
- Use molecular analysis to identify ligand: receptor pairs (and therefore cell-cell communication) that exist between interacting B cells and CD8 T cells.

3. **H: B cells interact with CD8 T cells in the pancreas of T1D individuals.**
   A: ***Assess whether the interaction between B cells and CD8 T cells, driven by B cell antigen cross-presentation, is relevant in an in situ disease setting.***
   - Develop an immunofluorescence staining protocol to detect CD20 B cells in tissue sections, that is compatible with downstream molecular approaches.
   - Use laser capture microdissection to isolate single B cells from pancreatic tissue sections from individuals with T1D.
   - Perform single cell molecular processing of the captured B cells to determine their phenotype *in situ.*

2 Materials and Methods

2.1 Human Subjects

Two sources of blood donors were utilised in this study, depending on the downstream assays. For molecular workstreams, blood was obtained from healthy controls recruited in the "T cell studies in Type 1 diabetes" study at Guy's and St Thomas' Hospital and Bristol Royal Infirmary. This study was carried out with the approval of the UK National Research Ethics Service (REC reference 08/H0805/14) and informed consent was obtained from all participants. For all other assays, leucocyte cones were obtained from the NHS Blood and Transplant services (Non-Clinical Issue - Tooting, London, UK). Staining with an anti-HLA-A2 antibody (Dilution 1:100, clone: BB7.2, Biolegend) prior to use determined the HLA-A2 positivity of these blood donors.

2.2 Peripheral blood mononuclear cell (PBMC) isolation

PBMCs were isolated from fresh blood using density gradient centrifugation. Briefly, blood was diluted with 1x PBS (Gibco, Life Technologies, UK) at a 1:1 v/v ratio for fresh blood from healthy individuals, or 1:5 v/v for leucocyte cones. 30 ml of the diluted blood was layered onto 15 ml of lymphoprep (Stem Cell Technologies, UK) in a 50 ml falcon tube, and centrifuged for 30 minutes at 1000*g* with the brake off. The interphase layer was collected into 50 ml falcon tubes and washed in PBS at 300*g* for 10 minutes. The PBMC pellet was resuspended in PBS and centrifuged at 200*g* for 10 minutes. The cell pellet was again resuspended and counted using trypan blue. Cells were either cryopreserved for downstream assays or used fresh in assays.

2.3 Cell lines and antigen-specific CD8 T cell clones

K562-A2-CMV cells and TAP-deficient T2 cells were maintained in R10 medium: RPMI-1640 GlutaMAX (Thermo Fisher Scientific), 100 U/mL penicillin and 100 µg/mL streptomycin (penicillin-streptomycin 100X stock solution, Thermo Fisher Scientific) and 10% (v/v) heat-inactivated FCS (Sigma), at a density of 0.3–0.6 × 10^6 cells/mL. To heat-inactivate FCS, it was heated at 56°C for 30 minutes in a water bath with occasional shaking.

Antigen-specific CD8 T cell clones were obtained from Cardiff University, UK (Andrew Sewell and Garry Dalton laboratory) and stored in liquid nitrogen until use. The HLA-A2 restricted CD8 T cell clones obtained were specific for residues 495-503 of the CMV protein pp65 (the immunodominant sequence: NLVPMVATV), and were generated by members of the Sewell laboratory using the previously established protocol (Skowera *et al.*, 2008; Knight *et al.*, 2013).

When required in assays, CD8 T cell clones were expanded from cryopreservation using mixed feeder cells and PHA. Cells were thawed (Section 2.4) and cultured for 24 hours in 24-well plates at a density of 3-4 x 10^6 cells per well, in CD8 T cell clone media: R10 medium with the addition of 1x MEM non-essential amino acids (ThermoFisher), 1 mM sodium pyruvate (ThermoFisher), 10 mM HEPES buffer (ThermoFisher), 2 mM L-glutamine (ThermoFisher) and the cytokines, 25 ng/µl human IL-15 (Peprotech) and 20 IU/ml IL-2 (Proleukin from Prometheus). Cells were then harvested and counted, before being plated in a T25 flask at a density of 0.2-1 x 10^6 T cell clones per flask in 14 ml of CD8 T cell clone media. PBMC feeder cells were prepared from four subjects, two of which were HLA-A2 positive (HLA-matched), at equal volumes. PBMCs were irradiated at a dose of 3000cGy and washed once in CD8 T cell clone media (300*g*, 5 minutes). Feeders were resuspended at 15 x 10^6/ml in CD8 T cell clone media. A 15x concentration (15 ug/ml, therefore 1ug/ml final concentration) of phytohemagglutinin (PHA) (Alere Technologies) was added to the cells. 1 ml of the feeder/PHA mix was then added to each of the T25 flasks containing CD8 T cell clones (final flask volume = 15 ml). Flasks were placed in the incubator in an upright position at a 45° angle to allow cells to be in close contact and accumulate in the corner of the flask. After 4 days, half the media was removed and replaced with fresh CD8 T cell clone media, without disturbing the cell pellet. Cells were cultured for a further 2 days in the flasks before being harvested and counted, and placed in 24 well plates at a density of 3-4 x 10^6 cells per well in 2 ml of CD8 T cell clone media – now with 200 IU of IL2 rather than the initial 20IU. Every two days, 50% of the media was changed, and cells were split when media turned yellow. Cells were cultured up to 6 x 10^6 per well, so unnecessary splitting was avoided. CD8 T cell clones were expanded for a further two weeks, or until growth rate slowed and the clones displayed a rested

phenotype (round cells). CD8 T cell clones were either used directly in downstream assays or cryopreserved and stored in liquid nitrogen.

2.4 Cryopreservation and recovery of cryopreserved cells

Cells to be cryopreserved were centrifuged at 300*g* for 5 minutes. Cell pellets were resuspended in heat inactivated 90 % human AB serum (Sigma-Aldrich) and 10 % DMSO (Sigma-Aldrich) (v/v), by adding it drop wise to the cell pellet with gentle agitation. Cells were added to each 2 ml cryovial (Corning) in a total volume of 1 ml, placed in a CoolCell (BioCision, USA) and transferred to the -80°C freezer. For long term storage cells were transferred to liquid nitrogen stores.

Cells were recovered by thawing. Briefly, cells were swilled in a 37°C waterbath until ice was almost completely thawed. Cells were added to a 50 ml falcon and warm R10 media was added drop wise to the cells, before being centrifuged (300*g*, 5 minutes) and resuspended in the appropriate media at the recommended cell density.

2.5 Antigens and peptides

All peptides were obtained lyophilised and re-constituted in DMSO to a concentration of 2 mg/ml (Table 1). Peptides were purchased from Almac Sciences (Edinburgh, Scotland) or GL Biochem (Shanghai, China). Peptides were synthesised by Fmoc (9-fluorenylmethoxycarbonyl) solid-phase chemistry to more than 95% purity using mass spectrometry as well as reversed-phase high-performance liquid chromatography (RP-HPLC) to confirm identify and for purification of crude peptides. The amino acid sequence of each peptide is shown in Table 1. The 41-mer CMV pp65 peptide contains the HLA-A2 restricted immunodominant CMV pp65 (495-503) embedded centrally in the CMV sequence. The 41-mer peptides were synthesised with an added cysteine residue at the C-terminus and a biotin moiety at the N-terminus.

Peptide	MW (g/mol)	Amino acid sequence
41-mer CMV pp65	4730	Biotin-AVFTWPPWQAGILAR**NLVPMVATV**QGQNLKYQEFFWDAND**C**
40-mer CMV pp65	4620	Biotin-AVFTWPPWQAGILAR**NLVPMVATV**QGQNLKYQEFFWDAND
9-mer CMV	940	NLVPMVATV
13-mer DR4 binding	1504	IAFTSEHSHFSLK

Table 1 Peptides used throughout this study with their name, molecule weight and amino acid sequence.

2.6 Isolation of B cells from PBMCs

Class switched, memory B cells were isolated from cryopreserved PBMCs using a switched memory B cell isolation kit (Miltenyi Biotech), according to manufacturer's instructions. The number of starting PBMCs was calculated based on the assumption that ~1% of PBMCs were switched, memory B cells (i.e. if 600,000 B cells were required, 60 x 10^6 PBMCs were required to start). For the majority of experiments, donors were HLA-A2 positive, as determined by flow cytometry (Section 2.1). In experiments using HLA-A2 positive and HLA-A2 negative donors, B cells were isolated from both donor PBMCs in parallel.

PBMCs were centrifuged at 300*g* for 10 minutes, and the cell pellet was resuspended in 400 µl of MACs buffer (1x PBS, 0.5% BSA and 2mM EDTA) per 10^8 total cells. 100 µl of switched memory B cell biotin antibody cocktail was then added to the cell suspension and mixed well before incubation for 10 minutes in the refrigerator. Cells were then washed by adding 1 ml of MACs buffer per 10^8 cells and centrifuged at 300*g* for 10 minutes, 4°C. The supernatant was aspirated completely, and 800 µl of MACs buffer was added, along with 200 µl anti-biotin microbeads, per 10^8 cells. The cell suspension was mixed and incubated for 15 minutes in the refrigerator. Cells were washed by adding 5 ml of MACs buffer per 10^8 cells and centrifuged at 300*g* for 10 minutes, 4°C. Supernatant was removed and cells were resuspended in 500 µl of MACs buffer per 10^8 cells. LS columns (Miltenyi Biotech) were then placed in a magnetic field separator and prepared by rinsing with 3 ml of MACs buffer. The PBMC cell suspension was added to the column, and the flow through was collected (containing the unlabelled cells, representing the enriched switched memory B cell fraction). Columns were then washed 3 times with 3 ml of MACs buffer, and the flow through combined with the effluent. Unlabelled cells of interest were then centrifuged at 300*g* for 5 minutes and resuspended in MACs buffer. Cell numbers and viability were enumerated using trypan blue exclusion.

2.7 Class-switched memory B cell stimulation

Switched, memory B cells were plated in a 96-well round bottomed plate, at 0.15 x10^6 cells per well, in 100 µl of R10 media. Human MEGACD40L protein (Enzo

Life Sciences) was added to the cells and cultured for 24 hours. Initial stimulation experiments titrated the concentration for stimulation from 1000 ng/µl to 10 ng/µl (1000, 500, 100, 10). All future experiments used stimulated B cells with 500 ng/µl of MEGACD40L unless otherwise stated. In experiments comparing stimulated and unstimulated B cells, unstimulated B cells were cultured for 24 hours in the absence of MEGACD40L.

2.8 Generation of monocyte derived dendritic cells (MoDCs)

MoDCs were generated using a modified version of a previously published protocol (Dauer *et al.*, 2003). Cryopreserved PBMCs were thawed and counted using trypan blue. 10 x 10^6 PBMCs were added per well to a 6-well plate in 3 ml of warm R10 media. Cells were incubated for 90 minutes at 37°C, 5% CO_2, in order to allow monocytes to adhere to the plate. Following this incubation, media was gently removed with a stripette, taking care not to disturb the adherent cells. This formed the non-adherent fraction of cells. The well surface was then washed gently with 5ml of warm R10 media. This wash step was repeated two more times. The media was then replaced with 3 ml of fresh, warm R10 media and incubated for a further 60 minutes at 37°C, 5% CO_2. After this incubation, the wash steps were repeated as above.

To differentiate the monocytes, 2 ml of differentiation media: 1980 µl R10 media, 10 µl human GM-CSF (final concentration: 500 IU/ml, Peprotech) and 10 µl human IL-4 (final concentration: 500 IU/ml, Peprotech) was added to the adherent cells. Cells were incubated for 24 hours at 37°C, 5% CO_2. After the incubation, media was removed, and cells were washed twice with 2 ml of warm R10 media. 2 ml of maturation media containing proinflammatory cytokines: 1980 µl R10 media, 5 µl GM-CSF, 5 µl human PGE2, 5 µl human TNFα, 5 µl human IL1β (all final concentration: 500IU/ml, all Peprotech) was then added to the adherent cells, and incubated for a further 16 hours at 37°C, 5% CO_2. In experiments assessing antigen cross-presentation by the MoDCs, the 41-mer CMV pp65 was added to the maturation media at a concentration of 2.5 µg/ml and incubated with the cells for the 16-hour incubation period.

MoDCs were harvested from the plates for downstream assays after the final 16-hour incubation. To detach the cells from the plate, the media was carefully removed, and

the plate was placed on ice. 2 ml of ice-cold PBS was then added to each well and incubated for 5 minutes. A cell-scraper (Corning) was then used to detach the cells from the plate, and the media containing the cells was transferred to a 50 ml falcon tube. To ensure complete collection of cells, each well was washed twice more with 2 ml of PBS, and this residual media was added to the same 50 ml falcon. Harvested cells were washed in R10 twice (300*g*, 5 minutes), resuspended in R10 media and cell count and viability was enumerated by trypan blue.

2.9 Flow cytometry surface staining

To assess the phenotype of isolated and stimulated B cells and of MoDCs, flow cytometry was utilised. Cells were harvested into round bottomed polystyrene FACs tubes (BD, UK) and washed in at least 2 ml of FACs buffer (1x PBS supplemented with 4% heat-inactivated FCS) by centrifugation at 600*g* for 3 minutes. Of note, all wash steps were performed quickly and at 4°C to prevent antibody internalisation. The supernatant was decanted, and a master mix of fluorescently labelled antibodies was added to the residual buffer. Cells were stained for 30 minutes in the refrigerator in the dark, before being washed twice in 2 ml of FACs buffer by centrifugation at 600*g* for 3 minutes. Cells were then resuspended in the residual buffer and 1 µl of 7AAD (eBioscience) was added, before a 2-minute incubation at room temperature, in the dark. After a final wash in 2 ml of FACs buffer by centrifugation at 600*g* for 3 minutes, cells were resuspended in 200 µl ready for acquisition. Flow cytometry samples were acquired on a FACs Canto II (BD, UK) using FACS DIVA software. All flow cytometry data was analysed using FlowJo software v10.1 (TreeStar, USA). A full list of all antibodies used for B cell and MoDC phenotyping are shown in Table 2. Compensation controls were established when required by using UltraComp eBeads compensation beads (ThermoFisher) stained individually with each fluorochrome conjugated antibody.

Antibody	Flurophore	Dilution	Clone	Supplier
CD19	PE Cy7	1 in 100	HIB19	Biolegend
CD27	PE	1 in 100	M-T271	Biolegend
IgM	APC Cy7	1 in 100	MHM-88	Biolegend
IgD	FITC	1 in 100	1A6-2	Biolegend
CD14	V500	1 in 100	M5E2	Biolegend
DC-SIGN	V450	1 in 100	DCN46	Biolegend
CD11c	PERCP Cy5.5	1 in 50	N418	Biolegend
HLA-DR	FITC	1 in 100	G46-6	BD Biosciences
HLA-ABC	APC	1 in 100	G46-2.6	BD Biosciences
CD86	PE	1 in 100	2331	BD Biosciences
CD80	PE Cy7	1 in 100	2D10	Biolegend

Table 2: Antibodies used for phenotypic analysis of peripheral blood mononuclear cell populations by FACs. All antibodies were mouse monoclonal antibodies raised against human antigens.

2.10 Generation of antibody-polypeptide conjugates (ADS-conjugate)

Purified goat anti-human IgG (gamma chain) antibody was purchased at 1 mg/ml in PBS (Sigma). Prior to conjugation, the antibody was prepared in conjugate buffer (1x PBS, 2 mM EDTA). Anti-IgG antibody was treated with a molar excess of sulfosuccinimidyl 4-[N-maleimidomethyl]cyclohexane-1 carboxylate (10 mg/mL stock solution in double-distilled water; sulfo-SMCC from Thermo Fisher Scientific) crosslinker. The molar excess of crosslinker was based on protein concentration, and was consistently used at fifty-fold excess due to a protein concentration of ≤ 1 mg/ml. After 30 minutes incubation at room temperature, with moderate agitation using an orbital shaker, excess crosslinker (molecular weight: 436.37 g/mol) was removed using a desalting column, 7K MWCO Zeba Desalting columns (Thermo Fisher Scientific), equilibrated with conjugation buffer. The concentration of the sulfo-SMCC activated anti-human IgG antibody was then determined using NanoDrop spectrophotometer by measuring absorbance at 280 nm. Following this, the polypeptide (41-mer CMV pp65) was added to the antibody. Polypeptide was added to the antibody in a molar ratio corresponding to that desired for the final conjugate and consistent with the relative number of sulfhydryl and activated amines that exist on the two proteins. Specifically, polypeptide was added in conjugation buffer at a polypeptide/antibody ratio of 5:1 (molecular weight of polypeptide: 4.726 kDa, molecular weight of activated anti-IgG antibody: 150 kDa). Following 30 minutes further incubation with moderate agitation at room temperature, conjugates were aliquoted and stored at -20°C. When needed, conjugates were thawed and stored at 4°C.

2.11 Detection of the ADS antibody, and of the ADS-conjugate, on the B cell surface.

For all experiments, switched memory B cells stimulated with MEGACD40L were plated in 96-well v-bottomed plates, at a density of 0.1-0.15 x10^6 cells per well, per condition. Cells were washed once in ice-cold ADS buffer (PBS, (v/v) 2% heat inactivated FBS) through centrifugation at 600g for 3 minutes, 4°C.

For initial validation of the ability of the ADS antibody to detect B cell surface IgG expression, B cells were resuspended in 100 µl ice-cold ADS buffer containing the anti-human IgG ADS antibody at a final concentration of 2.5 µg/ml, or whole goat IgG (BioTechne, final concentration: 2.5 µg/ml) as an isotype control for non-specific binding, or ADS buffer alone. To determine the impact of activation and conjugation of the ADS antibody in detecting B cell surface IgG, B cells were also pulsed with the SMCC activated ADS antibody, polypeptide (41-mer CMV pp65) conjugated ADS antibody, or an alternative anti-human IgG antibody as a positive control (Enzo Life Sciences).

To determine the ability of the ADS to deliver the 41-mer CMV pp65 polypeptide to the cell surface, B cells were resuspended in 100 µl ice-cold ADS buffer containing the ADS-conjugate (at a final polypeptide concentration of 2.5 µg/ml), or the 41-mer CMV pp65 polypeptide alone, the 41-mer polypeptide and SMCC-activated ADS antibody together, or the SMCC-activated antibody alone. For each ADS component added alone i.e. the ADS antibody or the 41-mer polypeptide, it was added at the same concentration to its counterpart within the ADS-conjugate. This was the case for all experiments using the ADS components.

In all cases, cells were then incubated on ice for 30 minutes, before being washed three times in 200 µl ice-cold ADS buffer (600g for 3 minutes, 4°C). As the ADS antibody and the ADS-conjugate lacks a fluorescent label, a secondary staining step was required to detect cell surface expression/binding using flow cytometry. For the ADS antibody, a secondary rabbit anti-goat IgG (H+L) antibody conjugated to Alexa Fluor 488 was used (1:1000 dilution, Abcam), as the primary antibody was raised in goat. For the ADS-conjugate, as the aim was to determine CMV pp65 polypeptide on the B cell surface, an anti-biotin PE-conjugated antibody (1:200 dilution, Clone: 1D4-C5, Biolegend) was used, to detect the biotin moiety of the 41-mer CMV pp65.

In this step, washed cells were incubated on ice for 30 minutes with 100 µl ice-cold ADS buffer containing the secondary antibody before washing steps were repeated as above. Stained cells were then harvested into round bottomed polystyrene FACs tubes, in 200 µl of FACs buffer, and incubated with 7AAD as previously prior to acquisition on the FACs Canto II. To determine positive cells, a lymphocyte gate was established, followed by single cells, then live cells.

For experiments assessing internalisation of either the ADS antibody or the ADS-conjugate, after the primary incubation and subsequent washes B cells were harvested into 96-well round bottomed plates in 100 µl R10 media. Cells were then incubated at 37°C, 5 % CO_2 for the stated time points, before undergoing the same staining procedure with the secondary antibodies and flow cytometry acquisition.

2.12 Imaging flow cytometry to determine internalisation of the ADS antibody

To detect the ADS antibody on the B cell surface using imaging flow cytometry (Imagestream) the ADS antibody had to be conjugated to a fluorophore. To do this, the ADS antibody was pre-conjugated with APC using an APC conjugation kit (Abcam, ab201807) following the provided protocol.

B cells were plated in triplicate at 0.1 - 0.15 x 10^6/well in a 96-well v-bottomed plate. Cells were then incubated with the APC-conjugated ADS antibody for 30 minutes on ice. After incubation, B cells were washed three times by resuspension of cells in 200 µl of ADS buffer and centrifugation at 600*g* for 3 minutes at 4°C, as prior (Section 2.11). Similar to the flow cytometric analysis of ADS antibody internalisation (Section 2.11), B cells were then harvested in 200 µl of R10 and transferred to a 96-well round bottomed plate at 37°C, 5% CO_2. At specific time points, cells were harvested into sterile 1.5 ml Eppendorf tubes and placed on ice. At this point the triplicate wells for each time point were combined into one Eppendorf tube in order to achieve the cell numbers required for imaging flow cytometry. Samples were washed once with 1 ml of cold ADS buffer (600*g*, 3 minutes, 4°C). Cells were then resuspended in 100 µl of cold FACs buffer, containing 1 µl fluorescently labelled PE anti-human CD20 antibody (Clone: 2H7, Biolegend) and incubated on ice, in the dark for 30 minutes. This antibody was used as a positive control for surface staining, and to clearly segregate B cells from debris in the analysis. Cells were then washed twice with 1 ml of cold FACs buffer (600*g*, 3

minutes, 4°C), before being resuspended in 50 µl of FACs buffer and analysed on the ImageStream X MKII (Amnis-Luminex) imaging flow cytometer at 40X magnification. A minimum of 20,000 pre-gated cells were acquired per sample. Channel 1 detected the brightfield sample, and Channel 11 and 3 were used for APC and PE, respectively. Channel 6 was used to determine side scatter profiles. All other channels were turned off during sample acquisition and laser powers were set to maximum.

For data analysis, Amnis ® IDEAs version 6.2 (Luminex Corportation) was used. Single cells were selected based on area (size of cells in square microns) versus aspect ratio (ratio of minor axis divided by the major axis) of the brightfield cell images (Channel 1). From the single cell gate, cells in best focus are selected using gradient RMS (a measurement of the sharpness quality based on pixel values), followed by gating on the florescence positives through fluorescence intensity histograms of the channel containing the fluorochrome of interest. Firstly, CD20 B cells were selected, followed by the cells positive for the APC-conjugated ADS antibody (representing IgG-BCR population). An important feature of Imagestream is the detection of cells positive for the fluorochrome regardless of the cellular location; therefore, cells in this final gate will include ADS-antibody positive cells whether it is surface-bound or internalised. To assess internalisation, the built in Internalisation wizard feature of the IDEAs analysis software was applied to the CD20, IgG-BCR positve B cell gate. Briefly, this feature established an internalisation mask, created by eroding 4 pixels from the outer edge of the cell surface (determined by the CD20 staining), thereby excluding the cell membrane. An internalisation score was then computed by calculating the ratio of the intensity of the APC signal within the internalisation mask compared to the whole cell. Internalisation scores of zero contain cells with both surface bound and internalised signal, and the higher the score the greater the internalisation.

2.13 T2 assay

T2 cells were split the day prior to use to assure good quality. T2 cells were harvested and washed with 5 ml of R10 media, resuspended in 5 ml of R10 media and counted using trypan blue. Cells were then seeded in a 96-well round bottomed plate at a density of 0.1-0.15 x10^6/well in 100 µL of R10 containing either; the 41-

mer CMV pp65 polypeptide (unconjugated), the 9-mer CMV pp65 peptide, 14-mer irrelevant HLA-DR4 binding peptide, or DMSO. Three concentrations were established for each condition, representing a titration from 10 μg/ml to 2.5 μg/ml. Cells were incubated for 16 hours at 37°C, 5% CO_2. After the incubation, cells were harvested and transferred into 2 ml round-bottomed FACs tubes. Cells were washed once in 2ml of FACs buffer (600*g*, 3 minutes). Cells were then resuspended in 100 μl of FACs buffer containing 2 μl of APC anti-human HLA-ABC antibody (Clone: W6/32, Biolegend), and incubated on ice in the dark for 30 minutes. After incubation, samples were washed once in 2 ml of FACs buffer (600xg, 3 minutes) and resuspended in 100 μl of FACs buffer with 1 μl of 7AAD at room temperature for 2 minutes. A final wash was carried out with 2 ml of FACs buffer (600*g*, 3 minutes), and cells were resuspended in 200 μl of FACs buffer and acquired.

2.14 Delivery of antigen to B cells using the ADS

Switched, memory B cells stimulated with MEGACD40L were seeded at 0.1-0.15 x 10^6/well in 96-well v-bottomed plates. Cells were washed once in ADS buffer (600*g*, 3 minutes). Cells were resuspended in 100 μl ice-cold ADS buffer containing the ADS-conjugate at a concentration of 2.5 μg/ml for 30 minutes on ice. As controls, additional conditions were established where cells were pulsed either with SMCC-activated ADS antibody alone, unconjugated 41-mer CMV pp65 and SMCC-activated ADS antibody, or the 41-mer CMV pp65 alone. In some cases, a control was also established where B cells were pulsed with DMSO at an equal concentration to that in the ADS-conjugate. After 30 minutes, cells were centrifuged at 4°C for 3 minutes at 600*g*, before resuspension in 200 μl of ice-cold ADS buffer on ice. This wash step was repeated a further two times. B cells were then harvested in 200 μl warm R10 media into 96-well round bottomed plates and incubated at 37°C, 5% CO_2 for 16 hours.

2.15 CD107α T cell degranulation assay

CD8 T cell clones were prepared either directly from expansion cultures (Section 2.3) or from cryopreservation. Antigen presenting cells (ADS-conjugate pulsed B cells (Section 2.14), or antigen loaded MoDCs (Section 2.8) were counted using trypan blue before co-culture with antigen-specific CD8 T cell clones at a ratio of 1:1 (unless otherwise stated) in a 96-well round bottomed plate.

Prior to the co-culture, the required number of antigen-specific CD8 T cell clones were resuspended in warm R10 media and labelled with anti-human CD107α antibody (Dilution 1:200, Clone: H4A3, BD Biosciences) by incubation for 10 minutes at room temperature, in the dark. 100 µl of CD107α -labelled CD8 T cell clones containing the desired number to achieve the 1:1 ratio were then added to each APC containing well (200 µl final volume per well) and mixed by pipetting up and down.

As positive controls, antigen specific CD8 T cell clones were seeded at a density of 0.1 x 10^6 per well and either co-cultured with K562-A2-CMV cells at a 1:1 ratio or treated with PMA (50 ng/ml) and ionomycin (1 µg/ml). As a negative control, a condition was also included where antigen specific CD8 T cell clones were cultured alone.

Cells were co-cultured for 4 hours at 37°C, 5% CO_2. Following the co-culture, the plate containing the cells was centrifuged at 600*g* for 3 minutes. In the same plate, cells were then resuspended in 100 µl of FACs buffer containing fluorescently labelled antibodies: FITC-conjugated anti-human CD3 (Dilution: 1 in 50, Clone: 17A2, Biolegend) and PE-Cy7-cojugated anti-human CD8 (Dilution: 1 in 100, Clone: SK1, Biolegend). Cells were incubated in the dark, on ice for 30 minutes. Following this, cells were washed once in 200 µl FACs buffer (600*g*, 3 minutes) and resuspended in 100 µl of FACs buffer with 1ul of 7AAD, before incubation at room temperature for 2 minutes. A final wash was carried out in 200 µl FACs buffer (600*g*, 3 minutes). Cells were then resuspended in 200 µl of FACs buffer and transferred to 2 ml round-bottomed FACs tubes on ice. Samples were acquired on a FACs Canto II and compensated accordingly. Flow cytometry was performed by gating on live, single cells, followed by $CD3^+CD8^+$ T cells and the CD107α positive population was determined by setting a gate on the CD8 T cell alone condition (negative control). A minimum of 10,000 events for each condition were acquired from the live, single cell pre gate.

2.16 Establishment of a per cell index to compare cross-presentation potency of MoDCs and B cells

To establish a per cell index comparison of cross-presentation potency, antigen loaded MoDCs and ADS-conjugate pulsed B cells were counted using trypan blue.

Cells were then centrifuged at 600*g* for 3 minutes, and the pellet resuspended in 200 µl of R10. A two-fold dilution series of the cells was then established in a 96-well round bottomed plate. Briefly, 100 µl of R10 was added to 4 descending sequential wells, and the first well was left empty . To the first well, the 200 µl containing the cells was added, and mixed by pipetting up and down. 100 µl was then transferred from this well to the second well and mixed by pipetting. This was repeated until the final well (well 5), where 100 µl was discarded after mixing.

CD107α-labelled CD8 T cell clones were then added at a consistent concentration to each well. This cell concentration was determined by the number of APCs in the first well of the dilution series, where a ratio of 1:1 APC: CD8 clone was established. In this manner, in each descending well the ratio of APC: CD8 T cell clones increased – 1:2, 1:4, 1:8 and 1:16. The CD107α degranulation assay was then performed as before.

2.17 Identification of interacting B cells and CD8 T cell clone (B:CD8 doublets) in *in vitro* co-cultures.

To identify B:CD8 doublets using flow cytometry, B cells were pulsed with the ADS-conjugate as previously described (Section 2.14). In these experiments, a positive control was established where B cells were pulsed with the 9-mer CMV pp65 peptide, to allow direct binding to the MHC class I molecule of the B cell and recognition of peptide-MHC by the CD8 T cell clone. Briefly, switched, memory B cells stimulated with MEGACD40L were incubated for 16 hours at 37°C, 5% CO_2 in consistency with the ADS-conjugate pulsed B cells. Following this, B cells were centrifuged at 600*g* for 3 minutes, and resuspended in 100 µl of R10 containing 9-mer CMV pp65 peptide at a molar equivalent concentration to the 41-mer CMV pp65 within the ADS conjugate. B cells were incubated with peptide for 1 hour at 37°C, 5% CO_2 before being transferred to a 2 ml round-bottomed FACs tube. 2 ml of fresh, warm R10 media was then added to the FACs tube and washed once (600*g*, 3 minutes). This wash step was repeated. Peptide pulsed B cells were then harvested and counted using trypan blue. Additionally, a condition was established in these experiments where B cells were incubated with ADS buffer alone, during the 16-hour incubation.

Following establishment of these B cell conditions (ADS-conjugate pulsed, ADS buffer alone, 9-mer peptide pulsed), cells were co-cultured with antigen specific CD8 T cell clones and the CD107α assay performed as described. The only alteration to the protocol was the addition of a PE-conjugated anti-CD20 antibody to the master mix (Dilution: 1 in 100, Clone: 2H7, BD Biosciences) to allow detection of the B cells by flow cytometry. To identify B:CD8 doublets, a lymphocyte gate was established, followed by a doublet gate. Within the doublet gate, live cells were identified, followed by $CD3^+CD8^+$ cells before a gate was established for $CD8^+CD20^+$ positive doublets.

2.18 Blocking of B cell surface HLA-A2 using the BB7.2 antibody

To determine the relevance of cognate HLA to the B:CD8 doublet formation, HLA-A2 was blocked on the surface of the B cell. To do this, B cells (ADS-conjugate pulsed, ADS buffer alone, peptide pulsed) were treated with an HLA-A2 blocking antibody (Clone: BB7.2, Biolegend). Just prior to co-culture with CD8 T cell clones to begin the CD107α degranulation assay, 10 µg/ul of BB7.2 was added to the B cells, in 100 µl of R10, and incubated for 1 hour at 37°C, 5% CO_2. The antibody was not removed before co-culture with CD8 T cell clones.

2.19 Imaging flow cytometry of B:CD8 doublets

To visualise B:CD8 doublets using Imagestream, a very similar experimental approach was used to that to detect doublets using flow cytometry (Section 2.17). Two B cell conditions were established in triplicate in 96-well round bottomed plates: 9-mer peptide pulsed B cells and B cells alone. Briefly, B cells were then cultured with antigen-specific CD8 T cell clones at a 1:1 ratio, for 4 hours at 37°C, 5% CO_2, as previously described. For Imagestream experiments, CD8 T cell clones were not stained with CD107α as this was beyond the scope of the research question. After co-culture, cells were harvested into sterile 1.5 ml Eppendorf tubes and placed on ice. At this point the triplicate wells for each condition were combined into one Eppendorf tube in order to achieve the cell numbers required for imaging flow cytometry. Samples were washed once with 1 ml of cold ADS buffer (600*g*, 3 minutes, 4°C). Cells were then resuspended in 100 µl of cold FACs buffer, containing a fluorescently labelled anti-human CD20 antibody, an anti-human CD8 antibody and an anti-human CD3 antibody (same antibodies and concentrations as

used in flow cytometry, Section 2.17). Cells were incubated on ice, in the dark for 30 minutes. Cells were then washed twice with 1 ml of cold FACs buffer (600g, 3 minutes, 4°C), and resuspended in a final volume of 70 µl FACs buffer. Just prior to acquisition of the samples on the Imagestream, 1.75 µl DAPI (ThermoFisher) was added to each sample, at a final concentration of 0.25 µg/ml. and analysed on the ImageStream X MKII (Amnis-Luminex) imaging flow cytometer at 40X magnification. A minimum of 20,000 pre-gated cells were acquired per sample. Channel 1 detected the brightfield sample, and Channels 2, 3 and 6 were used for FITC (CD3), PE (CD20), PE-Cy7 (CD8), respectively. Channel 7 was used to detect the DAPI (live/dead) signal. Channel 12 was used to determine side scatter profiles. All other channels were turned off during sample acquisition and laser powers were set to maximum.

For data analysis, Amnis ® IDEAs version 6.2 (Luminex Corporation) was used. To detect B:CD8 doublets, a similar gating strategy was used to that in flow cytometry. Cells in best focus were first selected using gradient RMS, before doublets were selected based on the area versus aspect ratio. Live cells (DAPI negative) were then selected, followed by CD3+CD8+ doublets before a final gate was established on CD20+CD8+ doublets. Events within this gate were then directly visualised.

For analysis of CD3 concentration at the interface between CD8 T cell clones and B cells, an interface mask was generated between the CD8 T cell and B cell. To do this morphology masks were first generated for the T cell and B cell using CD8 and CD20 staining, respectively. An interface mask (of 3 pixels) was then applied by setting the T cell morphology mask as the cell of interest and the B cell morphology mask as the conjugate. Thereafter, protein accumulation was calculated as the ratio between the mean pixel intensity (MPI) of CD3 within the interface mask and the MPI of CD3 within the T cell morphology mask.

2.20 RNA extraction

Fresh blood was obtained from healthy (HLA-A2 positive) individuals. PBMCs were isolated for initial optimisation experiments as before. For B cell analysis, the switched, memory B cell population was isolated from PBMCs as previously described (Section 2.6).

Prior to RNA extraction, cells were harvested into RNAase free, sterile 1.5 ml Eppendorf tubes (ThermoFisher), and washed with 1 ml of nuclease-free water (600*g*, 3 minutes). This washing step was repeated to ensure complete removal of residual media. Supernatant was then completely removed by aspiration before resuspension in 350 µl of RLT buffer (Qiagen). Samples were vortexed to ensure homogenisation. RNA was then extracted using the RNeasy Micro Kit (Qiagen), according to manufacturers protocol. Briefly, 1 volume of 70% ethanol was added to the homogenised lysate and mixed well by pipetting. Up to 700 µl of the sample was then transferred to an Rneasy MinElute spin column in a 2 ml collection tube, and centrifuged for 15 seconds at 8000*g*. The flow through was then discarded, 350 µl of buffer RW1 added to the spin column, and the centrifugation step repeated. DNase I stock solution combined with buffer RDD was added onto the spin column directly onto the membrane and incubated at room temperature for 15 minutes. 350 µl of buffer RW1 was then added again to the spin column, and the centrifugation step repeated. Following this, 500 µl of RPE buffer was added to the spin column, and centrifuged again, followed by an addition of 500 µl of 80% ethanol to the spin column. The column was then centrifuged at 8000*g* for 2 minutes, in order to wash the membrane. An additional centrifugation step was then carried out in a new collection tube, for 5 minutes at 8000*g*. Finally, the spin column was placed in a new collection tube, and 14 µl of RNase-free water was added directly to the spin column membrane. The tube was then centrifuged for 1 minute at 8000*g* to elute the RNA. This step was repeated to ensure complete elution of RNA, resulting in a final volume of 28 µl. RNA was stored at -80 °C until required.

Extracted RNA was assessed for integrity and concentration using the Agilent 2100 Bioanalyser (Agilent Technologies) and Qubit fluorometer (ThermoFisher), respectively. For assessment of RNA integrity number (RIN), the Agilent RNA 6000 Nano kit (Agilent Technologies) was used according to manufacturer's instruction. For quantification, the Qubit RNA HS Assay Kit (ThermoFisher) was used according to the manufacturers protocol. RNA was stored at -80°C until use.

2.21 RNA sequencing

Library preparation and RNA sequencing was performed by the BRC Genomics Platform in the NIHR Guy's and St Thomas Research centre. Library preparation

was performed by Mr. Yogesh Kamra and bioinformatics analysis was performed by Dr. Shichina Kannambath. The SureSelect Strand-Specific RNA library preparation system (Agilent Technologies) was used in order to prepare mRNA sequencing libraries from total RNA samples. Briefly, poly-A RNA was purified from the total RNA samples using microparticles containing oligo(dt), and chemically fragmented to a size appropriate for RNA sequencing library preparation. First strand cDNA was then synthesized using the first strand master mix and purified using AMPure XP beads (Beckman Coulter). Second strand cDNA was then synthesised using a dUTP second strand marking method to allow strand specific RNA sequencing and the ends of the cDNA fragments were repaired before the purification step using AMPure XP beads was repeated. dA tailing master mix was then added to the purified, end-repaired cDNA sample, in order to dA-tail the 3' ends of the cDNA. Adaptor ligation of the dA-tailed cDNA was then carried out, before the adaptor ligated DNA was purified with the AMPure XP beads, and then amplified in a three primer PCR that included the required indexing primer. The amplification cycle number was determined based on the initial concentration of the RNA sample. Once amplified, a final purification step was carried out and the quality of the library determined using the 2100 Bioanalyser DNA 1000 assay (Agilent Technologies) according to manufacturer's instructions. Samples were then prepared for multiplexing, before preceding to cluster amplification using the Illumina paired-end cluster generation kit (Illumina), according to the manufacturers instructions. Libraries were sequenced on HiSeq 2500 (Illumina) for 100 paired end cycles in rapid mode.

Bioinformatics analysis was performed by Dr. Shichina Kannambath. The quality of the sequencing reads was examined using the stand alone tool FastQC (v0.11.4) (BaseSpace Labs), with a Phred score of >35 indicating accurate base calling. Raw sequencing reads (100-nt, paired-end) were trimmed using Trimgalore (v0.4.4) to remove adapters and short reads, and any traces of ribosomal DNA and mitochondrial DNA were removed using Bowtie2 (v2.2.5). Reads were then aligned to the human reference genome GRCh38 using STAR (v2.5.3a) (Dobin *et al.*, 2013) with the two-pass mapping multi-sample setting. Mapping and alignment quality were then examined using FastQC. Any duplicate reads were removed using the MarkDuplicates function of the Picard tools (v2.17.11). Aligned reads were then

annotated and the number of genes detected using the HTseq v0.11.0 with GENCODE v32. Differential expression analysis was performed using the DESeq2 package in R. The first step of this analysis package was count normalisation, which is required to make accurate comparisons of gene expression. Raw counts were normalised and expressed as a transcript per million (TPM) value i.e. the number of transcripts you would see for a given gene if you were to sequence 1 million full length transcripts. This normalisation method accounts for the sequencing depth of the experiment and the gene length. Samples were explored using unsupervised methods in R, and sample clustering was based on principle component analysis, tSNE and hierarchical clustering. DEG with a fold change >=2 and FDR<-0.05 were used for pathway enrichment and gene ontology analysis on the DAVID bioinformatics platform v6.8, where ontologies and pathways with adjusted p<0.05 were considered significant.

To confirm the cell population within each sample, the CIBERSORT algorithm was used. This is a gene-based deconvolution algorithm that infers 22 human immune cells types and uses 547 cell specific marker genes in order to calculate the scores for each of the immune cell types within the sample. For each sample, the standardised processed RNA-seq full dataset of gene expression (TPM) values was uploaded to the CIBERSORT website (https://cibersort.standford.edu/index.php).

2.22 Identification of ligand: receptor pairs in RNA sequencing data

To identify potential cell-cell interactions and calculate interaction scores, data analysis was carried out by myself using Excel. Firstly, a list of ligand: receptor pairs was generated from the Ramilowski *et al*., (2015) study, resulting in a total of 2556 ligand: receptor pairs. TPM values from the RNA-seq analysis were then extracted for each gene of each ligand: receptor pair. Directionality was considered in both directions, i.e. expression of the ligand on the B cell and receptor on the CD8 T cell, and expression of the ligand on the CD8 T cell and the receptor on the B cell. Each CD8 T cell clone was sequenced in technical triplicate, and therefore TPM values for each clone were averaged across the technical triplicates at this stage. All ligand: receptor pairs were then filtered by setting a TPM threshold of > 1. Ligand: receptor pairs were only carried forward if the TPM value for both the ligand and receptor gene was >1. Ligand: receptor pair interaction scores were then calculated. For each

ligand: receptor pair within the filtered list, interaction scores were calculated between each donor and each T cell clone, as the product of the ligand expression and the receptor expression. The average interaction score was then calculated across the B cell donors and CD8 T cell clones. In this manner, the standard error of the mean of each interaction could also be calculated. An example of the data analysis pipeline for each ligand: receptor pair is shown in Figure 2-1.

To infer the pathways in which the identified ligand: receptor pairs were involved in, the pathways common tool was used (https://www.pathwaycommons.org). This is a web interface designed for disseminating biological pathway and interaction data. A list of the genes observed in the ligand: receptor pairs was uploaded into the database, and pathways that contained these genes were identified. The number of genes involved in each pathway was also recorded.

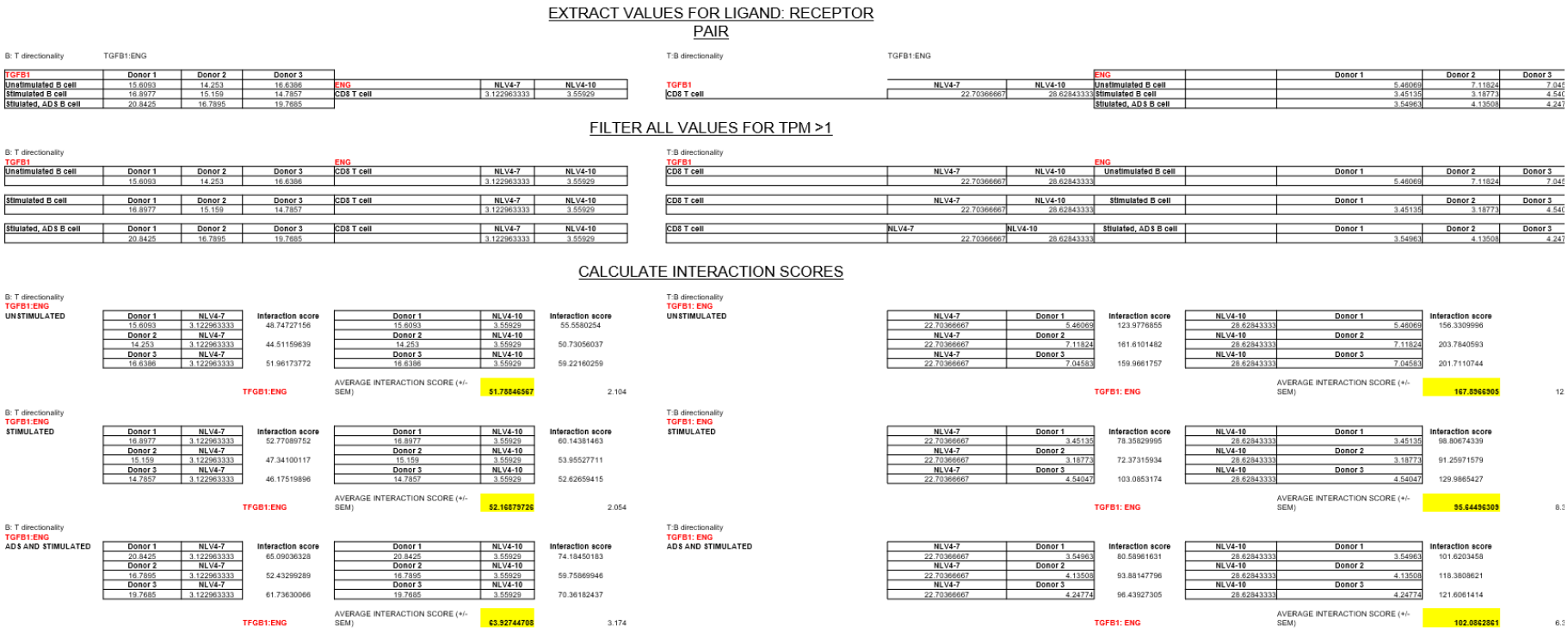

Figure 2-1 Data analysis pipeline for calculating ligand: receptor pair interaction scores, using TGFB1:ENG as an example ligand: receptor pair.

TPM values were extracted from the RNA-seq data set and analysed in Microsoft Excel to determine ligand: receptor pairs expressed between B cells and CD8 T cell clones. Data was filtered for a TPM value of >1, and interaction scores were first calculated between individual donors and each T cell clone (6 results), before the mean average interaction score was calculated. B: T directionality = ligand expressed on B cell, receptor expressed on T cell, T: B directionality = ligand expressed on T cell, receptor expressed on B cells.

2.23 cDNA synthesis from bulk cell populations

cDNA was synthesised from either bulk populations of PBMCs, or bulk populations of switched, memory B cells. Firstly, RNA was extracted as previously described (Section 2.20). Total RNA was converted to cDNA using the high-capacity cDNA reverse transcription kit (ThermoFisher Scientific) according to manufacturers instructions. Briefly, a reverse transcriptase master mix was prepared from RT buffer, dNTP mix, random primers, reverse transcriptase, RNase inhibitor and nuclease-free water. Master mix was then added to each RNA sample and loaded onto the thermal cycler. Reverse transcription was performed using the following cycle – 10 minutes at 25°C, 120 minutes at 37°C and 5 minutes at 85°C, and synthesised cDNA was stored at -20°C until required.

2.24 TaqMan primer validation

TaqMan gene expression assays (Applied Biosystems, ThermoFisher) were used for quantitative real-time PCR (qPCR) analysis of gene expression. Assays consisted of a pair of unlabelled PCR primers and a TaqMan probe with a dye label (FAM) on the 5' end and a minor groove binder (MGB) and non-fluorescent quencher on the 3' end. To validate and determine the efficiency of the chosen TaqMan probes, a standard curve for each gene expression assay was generated. Gene expression assays used are identified in Table 3. The standard curve was established by testing five concentrations of cDNA (synthesised from the same RNA isolated from bulk PBMCs, Section 2.20) with a dilution factor of 1:10. Samples were diluted in nuclease-free water and prepared in sterile PCR tubes. Each serial dilution was then used in separate real time reactions, in the QuantStudio 5 real-time PCR system (50°C for 2 minutes, 95°C for 10 minutes, and 40 cycles of 95°C for 5 seconds and 60°C for 1 minute). Specifically, using a 384-well reaction plate, 1 µl of the TaqMan gene expression assay of interest was added to 10 µl of gene expression master mix, 5 µl of nuclease free water and 4 µl of the cDNA template, with a final volume of 20ul per well. In a base-10 semi-logarithmic graph, the threshold cycle versus the dilution factor was plotted in excel, and the data was fit to a straight line. The correlation coefficient for the line was calculated, as was the slope of the curve to determine efficiency of the reaction.

Assay ID	Gene	Amplicon Length
Hs00998133_m1	TGFB1	57
Hs07290747_g1	TNFSF13	66
Hs00187058_m1	TNFRSF14	76
Hs04188773_g1	LTA	81
Hs00222859_m1	CXCL16	62
Hs00189032_m1	CALR	95
Hs00233566_m1	CD79A	75
Hs01047410_g1	CD19	57
Hs01060665_g1	ACTB	63
Hs00923996_m1	ENG	64
Hs01122445_g1	YWHAZ	62

Table 3 List of TaqMan gene expression assays utilised in this study. Assays consisted of a pair of unlabelled PCR primers and a TaqMan probe with a dye label (FAM) on the 5' end and a minor groove binder (MGB) and non-fluorescent quencher on the 3' end.

2.25 Tissue specimen collection and processing

Tissue specimens were obtained from the INNODIA network EUnPOD biobank collection. Sample and donor information are shown in Table 4.

Case ID	Donor Type	Tissue Type	Age	Gender	Ethnicity	HLA
010316	Non-diabetic Control	Pancreatic lymph node	57	F	Caucasian	**HLA:A*02**; B*35,B*41; C*15, C*17; DRB1*01, DRB1*16, DQB1*05
060217	Type 1 Diabetic	Pancreata (Region block: TAIL_01A)	39	F	Caucasian	**HLA:A*01,02**; B*08,B*50; C*07, C*12; DRB1*03, DQRB1*17, DQB1*02

Table 4 Donor information for tissue samples obtained from the EUnPOD biobank and used in this study.

Information on the disease characteristics of the T1D donor was also obtained from the EUnPOD INNODIA biobank. Specifically, the donor had a disease duration of 21 years at the time of death and was seropositive (as detected by ELISA) for GAD65 autoantibodies, but seronegative for IA-2 and ZnT8 antibodies. Previous immunofluorescence studies on the tissue sample detected the presence of residual β-cells (insulin containing islets).

2.26 Tissue specimen freezing

Tissue specimens were prepared and frozen at the University of Siena by members of the Francesco Dotta laboratory, as previously described (Culina *et al.*, 2018; Fignani *et al.*, 2020; Nigi *et al.*, 2020). Specimens were frozen directly after dissection to achieve optimal RNA preservation. For the pancreata samples, the pancreas was divided into three main regions (head, body and tail) followed by serial transverse sections, and tissues intended for frozen blocks were trimmed to no larger than 1.5 x 1.5 cm. Pancreatic lymph node tissue blocks were prepared by firstly dissecting the PLN in the peripancreatic fat, before removing any fat or connective tissue and incising the capsule if required. For both types of tissue preparation was completed within 2 hours in order to maintain RNA integrity. To freeze the tissue, dry ice was prepared in an appropriate container, and isopentane was poured into the container until the level of isopentane was just above the layer of dry ice. A thin layer of the embedding medium OCT (ThermoScientific) was placed on the bottom of a cryomold, and the tissue specimen segment was then placed in the desired orientation on the layer of OCT in the cryomold. Additional OCT was then added until the specimen was completely covered and the cryomold filled. The cryomold containing the specimen was then carefully placed into the cooled isopentane, allowing the OCT to completely solidify. Specimens were stored at -70°C until use.

2.27 Tissue sectioning and slide preparation

Tissue slides were prepared at the University of Siena, with assistance from Noemi Brusco. Frozen tissue specimens were sections using a cryostat (Leica Biosystems). The cryostat was precooled for 1 hour prior to use, and a new disposable microtome blade was installed into the cryostat. The cutting thickness was set to 7 μm. The cryomold containing the specimen was transferred to the cryostat and equilibrated to the temperature of the cryostat for a minimum of 10 minutes. The specimen was then

mounted to the specimen holder using OCT, and cryosections of 7 μm were cut. Sections were then mounted in the centre of a microscope slide (VWR), at room temperature. The slide was placed immediately on dry ice, and a thin layer of OCT added to the surface of the specimen prior to storing at -70C.

2.28 Immunofluorescence of tissue sections

Fixing solution was prepared by mixing acetone (VWR) and ethanol (VWR) at a 1:1 v/v ratio and stored at 4°C for at least 20 minutes so it was cold for use. Tissue sections were removed from the -80C and immediately placed into the fixing solution for 2 minutes. The sections were then placed in a damp chamber and washed twice in PBS for 2 minutes each at room temperature. Circles were then drawn around the section using a Dako Cytopen (VWR), before being blocked with 5% BSA in PBS for 3 minutes at room temperature in a damp chamber. All further incubations were performed in the damp chamber at room temperature unless otherwise stated. Residual liquid was removed, and primary antibodies were added in a solution of 5% BSA, rat monoclonal anti-human CD8 (Dilution: 1 in 25, Clone: YTC182.20, Abcam) mouse monoclonal anti-human CD20 (Dilution : 1 in 50, Clone: L26, Dako). Slides were incubated for 5 minutes and washed twice with PBS at room temperature. Residual liquid was then removed, and a secondary antibody solution added of PBS, AF488-conjugated goat anti-rat IgG (Dilution: 1:250, Invitrogen,), and AF594-cojugated goat anti-mouse IgG (Dilution: 1:250, Invitrogen). Slides were incubated for 5 minutes, before washing the slides once in PBS at room temperature for two minutes. DAPI stain (1:3000 in PBS) was then added to the section and incubated for 1 minute. Residual liquid was removed and the slides were mounted by adding 1 drop of Dako mounting medium to the section. A coverslip was placed over each slide and the mounting medium left to dry in the fridge. Slides were either stored at 4°C or visualised on a fluorescence microscope.

For the staining procedure prior to laser capture microdissection, the same protocol was followed with minor modifications to allow compatibility with tissue dehydration and B cell detection. The primary antibody solution consisted only of the mouse monoclonal anti-human CD20 antibody in 5 % BSA PBS solution, and the secondary antibody solution was made up in PBS containing Cy2-conjugated

goat anti-mouse IgG antibody (Dilution: 1 in 50, Jackson Immunoresearch). The DAPI staining step was omitted.

2.29 Laser capture microdissection of single B cells and cell lysis

Dehydration of tissue sections was carried out immediately after the immunofluorescence staining protocol was complete. The following solutions were prepared beforehand; 70 % ethanol (v/v in DEPC treated H_20), 95 % ethanol (v/v in DEPC treated H20), 100 % ethanol, 100% xylene. Slides were first placed into 70 % ethanol for 30 seconds, transferred to 95 % ethanol for 30 seconds, transferred to 100 % ethanol for 30 seconds, and finally transferred to the Xylene solution for 5 minutes. Slides were left to air dry for 5 minutes. Slides were then visualised on the immunofluorescence microscope to confirm successfully staining, before immediately proceeding with the LCM. This was conducted on the Arcturus Pixcell II laser capture microdissection. The surface of the microscope was first cleaned with RnaseZap, and the CapSure cap holder was loaded with HS LCM caps and aligned to ensure proper positioning of the cap in relation to the capture zone. The laser beam was focussed to obtain a bright, well defined spot and the spot size selected as 7.5 μm. LCM was then performed using the blue colour filter and the 40x objective; under microscopic visualisation to locate the CD20 positive B cell fluorescence. The microdissection session was performed in under 1 hour to preserve the RNA from degradation. Once the cell was captured onto the cap, it was connected directly to a 0.5 ml microcentrifuge tube containing the lysis buffer. Lysis buffer was composed of 9 μl of single cell lysis solution and 1 μl of single cell DNase I (ThermoFisher). The tube was inverted so that the extraction buffer came in contact with the microdissected cell on the cap service. The cell was then incubated with the lysis buffer for 30 minutes at 42°C. 2 μl of stop solution was then added to the lysed cells and incubated for 2 minutes at room temperature. Lysed cells were then placed directly on ice, before storage at -80°C.

2.30 Fluorescence activated cell sorting (FACs) of single B cells

To perform single cell sorting, 10,000 MEGACD40L-stimulated B cells were harvested into sterile polypropylene FACs tubes, in 100 μl of FACs buffer, containing 1 μl of 7AAD. Cells were incubated at room temperature in the dark for 2 minutes. Cells were then washed by adding 2 ml of FACs buffer to the tube and

being centrifuged for 3 minutes at 600g. This wash step was repeated, and cells were then resuspended in 300 µl ice-cold PBS. Single live cells were sorted on the FACs ARIA (BD UK) by Yasmin Haque, into 96-well V-bottomed plates. Plates were prepared prior to the single cell sort, where 9 µl of single cell lysis solution and 1 µl of single cell DNase I (Single Cell-to-CT q RT-PCR kit, ThermoFisher) was added to each well. After the single cells were sorted into the wells, plates were incubated at 42°C for 30 minutes, and 2 µl of stop solution was added to each well and incubated at room temperature for 2 minutes. Plates were stored at -80°C until required.

2.31 Single cell qPCR

Single cell qPCR was performed using the Single Cell-to-CT q RT-PCR kit (ThermoFisher) and TaqMan gene expression assays specific for the target genes (Table 3), following the manufacturers guidelines unless otherwise stated. cDNA synthesis was performed by reverse transcription in a thermal cycler (25°C for 10 min, 42°C for 60 min, 85°C for 5 min). Taqman gene expression assays for all the targets of interest were then mixed with pre-amplification reagents based on the kit instructions (95°C for 10 min, 4 cycles of 95°C for 15 secs, 60°C for 4 min, and 60°C for 4 min). Pre-amplified products were then used for the RT-PCR reaction in the QuantStudio 5 real-time PCR system (50°C for 2 minutes, 95°C for 10minutes, and 40 cycles of 95°C for 5 seconds and 60°C for 1 minute). Specifically, using a 384-well reaction plate, 1 µl of the TaqMan gene expression assay of interest was added to 10 µl of gene expression master mix, 5 µl of nuclease free water and 4 µl of the preamplified product (diluted 1:20 with TE buffer), with a final volume of 20ul per well. For each gene, each sample was plated in duplicate. Results were analysed using an automatic baseline and a threshold set to 0.2. Amplification plots were reviewed and outliers removed if necessary. Ct values were taken as the level of expression of target genes. At each stage of the protocol, negative and positive controls were included. For cDNA synthesis, to confirm successful RT and no contamination, a no template (negative) control (NTC) was established where nuclease free water replaced the lysed cell. A positive control used RNA extracted as previously described (Section 2.20) from 100,000 B cells, that was diluted 1 in 200 in nuclease-free water, therefore equating to RNA from ~500 B cells. For the pre-

amplification stage, cDNA was synthesised as previously described (Section 2.23), from 100,000 cells. cDNA was diluted 1 in 200 and added into the pre-amplification stage. A NTC was also included here to control for contamination. Finally, a NTC was included when loading the RT-PCR 385-well plate to again control for contamination.

2.32 Data analysis

For all *in vitro* experiments, data was analysed, and graphs devised, using GraphPad Prism 8. Data is expressed as the mean average ± SEM, unless otherwise stated. In instances where at least three independent experiments were performed, data was tested for significance using the appropriate statistical test as indicated. A Shapiro-Wilk test was used to assess the normal distribution of data. For pairwise comparisons, unpaired or paired two-tailed student T tests were used. For multiple comparisons, a one-way ANOVA with Tukey's post hoc test or Dunnett's post hoc, or two-way ANOVA with Sidak's post hoc test, were used. An F-test was used to test for unequal variances, and where significant, a Welch's correction was applied to the statistical test. In each graph, individual experiments are represented by the same colour data point across the conditions in order to show the nature of the data within the experiment. In primary cell experiments, an independent blood donor was used for each individual experiment.

3 ANTIGEN CROSS-PRESENTATION BY B CELLS

3.1 Background

In the pre-clinical NOD mouse model B cell depletion reduces the frequencies of circulating and islet-infiltrating CD8 T cells, as well as resulting in a reduction in CD8 T cell activation and cytotoxic effector function (Hu *et al.*, 2007; Brodie *et al.*, 2008; Mariño *et al.*, 2009, 2012; Da Rosa *et al.*, 2018). Additionally, B cell depletion in NOD mice with established diabetes restores normoglycemia, and B cell depletion post-insulitis reduces the overall incidence of disease (Hu *et al.*, 2007; Fiorina *et al.*, 2008). Together, these observations suggest B cells are involved in a late pathogenic event in disease, most likely through regulation of CD8 T cell mediated β-cell destruction. Indeed, infiltration of CD20 B cells into the inflamed islet of T1D individuals occurs in parallel with CD8 T cell influx, suggesting a dynamic interplay between the two cells (Willcox *et al.*, 2009; Arif *et al.*, 2014). A higher infiltrate of CD20 cells is also associated with a more aggressive disease endotype characterised by a more rapid destruction of β-cells (Leete *et al.*, 2016).

Generation of CD8 T cell effector activity *in vivo* requires activation and stimulation by so called 'professional' antigen presenting cells (APCs). APCs acquire and internalise exogenous antigens and present them as peptide-HLA-I complexes for TCR recognition, in a process known as antigen cross-presentation. Following establishment of inflammation in the islets of the pancreatic tissue, CD8 T cell mediated β-cell destruction appears to be self-sustaining, at least in pre-clinical models, occurring in the absence of the pancreatic lymph node (pLN) and spleen (Gagnerault *et al.*, 2002). Until recently, autoreactive effector T cells in peripheral tissues were viewed as having predetermined effector function, that did not require restimulation by professional APCs (Friedman *et al.*, 2014). However, it has become evident that restimulation of antigen specific CD8 T cells in peripheral tissues is required for optimal cytotoxic function. Not only is this consistent with the concept that β-cell destruction is self-perpetuating after disease initiation, pre-clinical studies have also shown that CD8 T cells acquire their cytotoxic function within the islets, and this is independent of antigen presentation by the β-cells and significantly reduced upon depletion of CD40 expressing cells (Graham *et al.*, 2011). Interrogation of the cells promoting CD8 T cell effector function at the disease site in

order to promote and maintain the ongoing disease process may therefore present insights into critical nodes for therapeutic intervention.

Early evidence suggests that antigen cross-presentation to CD8 T cells by B cells may be relevant to disease pathogenesis in NOD mice, with the observation that disease was dependent on expression of MHC class I molecules on the B cells (Mariño *et al.*, 2012). Historically, dendritic cells (DCs) have been well established as the predominant professional cross-presenting cells, through endocytic and phagocytic intracellular pathways (Jung *et al.*, 2002). Studies into antigen cross-presentation by B cells, in comparison, is still a somewhat undefined field. Seminal studies in the 1990's assessed the relevance of the antigen-specific BCR in processing exogenous antigen through the MHC CI pathway (Ke and Kapp, 1996). Here, BCR-mediated uptake of antigen resulted in a significant induction of cognate CD8 T cell responses, a finding that was lost when antigen-specificity of the B cell was irrelevant. Linking BCR specificity and antigen presentation, extensions of these studies targeting antigen-specific surface immunoglobulin molecules (i.e. the BCR) for antigen delivery conferred B cell efficiency as APCs in the context of MHC CII (Silveira *et al.*, 2002). B cells acquiring exogenous antigen non-specifically are unable to induce CD8 T cell proliferation (Robson, Donachie and Mowat, 2008). Relevant to the current research question, in NOD mouse models, BCR antigen specificity is critical to the expansion of self-reactive CD8 T cells (Mariño *et al.*, 2012). This is presumably due to receptor-mediated endocytosis and targeting of the antigen to the MHC CI processing pathway.

de Wit *et al.,* (2010) targeted uptake of *Salmonella* through the IgM-BCR of B cells isolated from peripheral blood and showed specific induction of CD8 T cell cytotoxic responses, suggesting antigen cross-presentation. However, whether this was a B-cell centric mechanism or a *Salmonella* bacteria specific mechanism i.e. cytosol delivery of antigens by the type three secretion system or survival in the unique salmonella-containing vacuole organelle, remains unclear.

The hypothesis to test in this study is that, in the islets, a cognate B: CD8 T cell interaction driven by B cell cross-presentation of islet autoantigen promotes CD8 T cell mediated β-cell destruction. To address this hypothesis, this chapter aims to provide evidence for a 'proof of principle' of this pathogenic mechanism, using a

disease relevant subset of human B cells. Firstly, I will develop an antigen delivery system (ADS) in order to model antigen-specific B cells *in vitro*, targeting the BCR due to its pertinence for efficient APC function. I will then use this system to characterise and assess the ability of B cells to cross-present polypeptide to CD8 T cells and induce cytotoxic responses. Finally, I will compare B cell cross-presentation potency to monocyte-derived dendritic cells generated *in vitro.*

3.2 Isolation and activation of B cells from PBMCs

3.2.1 Isolation and characterisation of a B cell subset from PBMCs

To investigate the ability of B cells to cross-present antigen, I selected the class-switched, memory B cell population due to its association with T1D and generation of CD8 T cell immunity. In tumour immunology, memory CD20 B cells in the tumour infiltrating lymphocyte population correlates with enhanced, tumour specific CD8 T cell responses (Helmink *et al.*, 2020). Moreover, antibodies isolated from T1D patients are IgG positive, and human IgG memory B cells have long since been reported to be associated with autoreactivity (Achenbach *et al.*, 2004; Tiller *et al.*, 2007). Finally, as the hypothesis to address is that B cells cross-present antigen to CD8 T cells in the pancreas, this necessitates that they have already matured and differentiated into memory cells in secondary lymphoid organs before migrating to the site of inflammation (Section 1.8.1.3).

Magnetic bead isolation was used to purify the switched, memory B cell population from PBMCs, by depleting cells expressing undesired markers (see Materials and Methods). The isolated B cell subset showed a significant enrichment for CD19 cells as compared to the whole PBMC population (88.1 $\pm$ 5.69 % vs. 15.73 $\pm$ 5.65 %, p = 0.0036); indicating this isolation protocol resulted in the selection of a cell population of high B cell purity (Figure 3-1A). Importantly, within the whole PBMC population, the frequency of CD19 B cells was consistent with reported values in the literature – validating the use of these antibodies. Of note, the purity of the isolated B cell population was not consistently checked after each B cell isolation in experiments throughout this thesis. However, Figure 3-1A indicates the robustness of the isolation, and additionally provided a bench mark frequency of B cells within the PBMC population that was used to determine the success of each B cell isolation.

To assess whether isolated B cells displayed a phenotype consistent with isotype switching, expression of IgM and IgD was analysed using flow cytometry. As expected, CD19 B cells within the whole PBMC population segregated into various subsets based on their IgM and IgD expression (Figure 3-1B). In contrast, isolated B cells showed a significant enrichment of a class switched phenotype, with 85.77 $\pm$ 3.2 % of cells staining negative for IgM and IgD as compared to 9.237 $\pm$ 0.41 % of B cells within the whole PBMC population (p=0.002).

CD27 is a marker of memory on B cells (Tangye *et al.*, 1998), and I used this marker to identify the memory B cell population in the phenotypic analysis. The majority of the isolated B cells expressed CD27 (80.17 $\pm$ 2.74 %), while the frequency of B cells that were CD27 positive within the whole PBMC population was significantly lower (34.17 $\pm$ 5.32 %, $p = 0.017$), and in line with literature that reports up to 40% of peripheral B cells express CD27 (Klein, Rajewsky and Küppers, 1998) (Figure 3-1C). Of note, B cells were negatively selected based on lack of IgM and IgD expression and not on expression of memory markers. CD27 negative class switched B cells have been reported (Fecteau, Côté and Néron, 2006), explaining the CD27 negative cells within the isolated B cell population.

These results show that B cells can be isolated from PBMCs with a high CD19 B cell purity, and that these CD19 B cells are enriched for a switched, memory phenotype as shown by the expression of CD27 and lack of surface IgM and IgD.

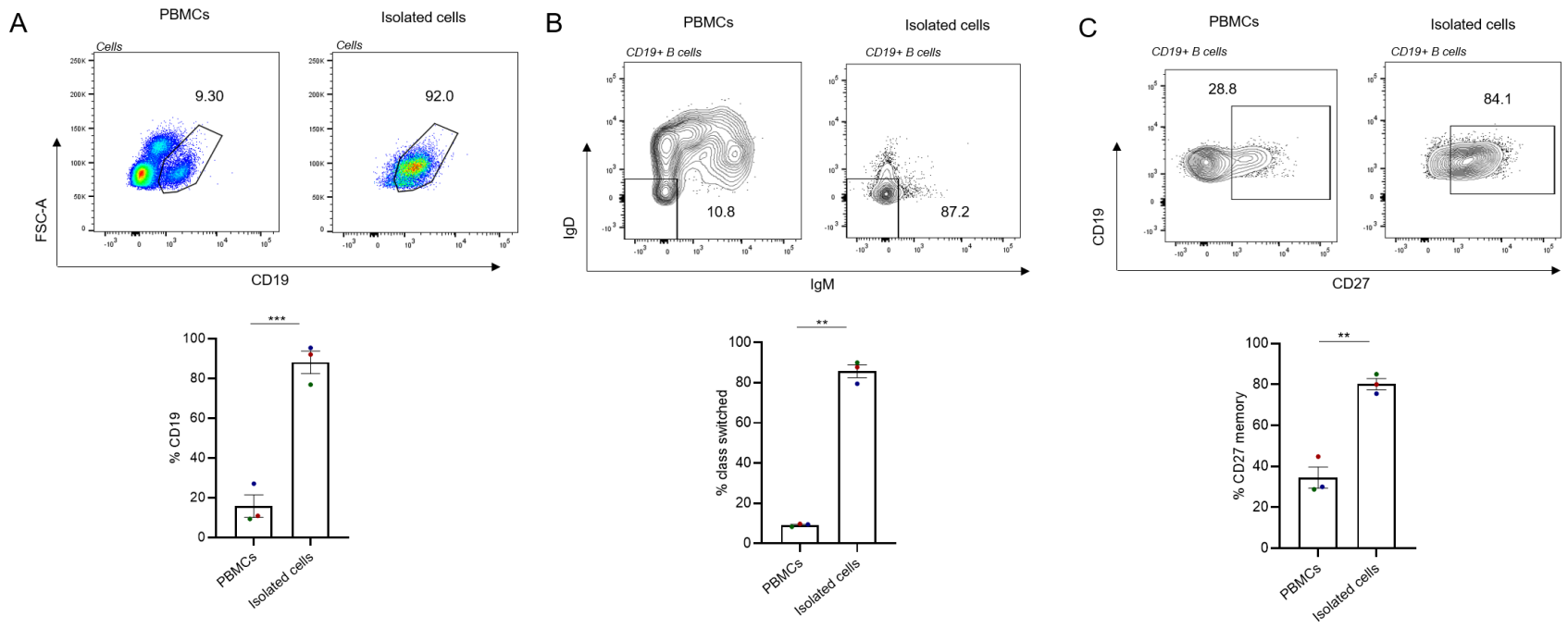

Figure 3-1 Isolated B cells from PBMCs display a class-switched, memory B cell phenotype.

B cells were isolated from PBMCs using a depletion magnetic isolation kit and their phenotype was characterised by flow cytometry and compared to that of B cells present in the whole PBMC population. Cells were stained for CD19 to assess the purity of B cells isolated (A), and these B cells were then stained for IgM and IgD to identify a class switched phenotype (B) and CD27 as a memory marker (C). Flow cytometry plots are representative of all three experiments and graphical data is expressed as the % population from parent of three independent experiments (mean $\pm$ SEM). Data were tested for significance using an unpaired students T test where *<0.05, **<0.01, ***<0.001. Individual experiments are matched by colour of the data points.

3.2.2 Stimulation of switched, memory B cells through a CD40-dependent mechanism

Previous studies have demonstrated that the function of B cells as APCs is dependent on their activation (Kakiuchi *et al.,* 1983). This is due to an upregulation of co-stimulatory molecules that provide a secondary signal to the T cell, therefore bypassing induction of T cell peripheral tolerance. Stimulation of B cells occurs in either a T cell independent mechanism, such as through TLR9 upon recognition of CpG, or a T cell dependent mechanism which involves CD40 engagement on B cells. Both mechanisms can be mimicked *in vitro*, however T cell dependent activation of B cells is biologically relevant in the context of autoimmunity.

To mimic T cell dependent activation, B cells were cultured with MEGACD40L - an oligomer that mimics *in vivo* membrane assisted CD40L aggregation and stimulation by binding to cell surface CD40. To investigate whether this resulted in activation of the B cells, flow cytometry was used to detect expression of CD80, CD86, HLA classes I and II (Figure 3-2). Culture of B cells with MEGACD40L consistently resulted in CD80 and CD86 upregulation as compared to unstimulated cells, and this occurred in a concentration dependent manner (Figure 3-2A). CD86 showed the greatest magnitude of upregulation, increasing by an average fold change of 5.81 ($\pm$ 1.94) at the highest concentration of 1000 ng/ml. A similar trend was identified for HLA CI and CII (Figure 3-2B) – the fold change in MFI increased in a concentration dependent manner. Unlike CD80 and CD86, unstimulated B cells were positive for both HLA molecules, and so the magnitude of CD40L-induced upregulation was lower, particularly for HLA class I. Thus, these results suggest that B cells activated by MEGACD40L display a phenotype consistent with activation and therefore potential APC function.

A secondary aim of this experiment was to identify the optimal concentration of MEGACD40L to stimulate B cells in future experiments – taking into consideration the induction of sufficient expression and cost-efficiency of the reagent. 500 ng/ml of MEGACD40L was selected as it induced considerable upregulation of the markers as assessed by the fold change in MFI for each marker; 2.5 $\pm$ 0.35 (CD80), 5.5 $\pm$ 1.6 (CD86), 1.43 $\pm$ 0.2 (HLA Class I) and 2.5 $\pm$ 0.82 (HLA Class II) (Figure 3-2). Although the top concentration of 1000 ng/ml showed a pattern of inducing the

highest upregulation of costimulatory markers and HLA class molecules, this response was comparable to 500 ng/ml.

Overall, data from section 3.2 has characterised a robust protocol for isolating switched-memory B cells from PBMCs and optimised an efficient method of activation to stimulate the cells in a CD40L-dependent manner. Throughout the rest of the chapter the B cells referred to in experiments are switched-memory B cells that have been stimulated for 24 hours with 500 ng/ml of MEGACD40L.

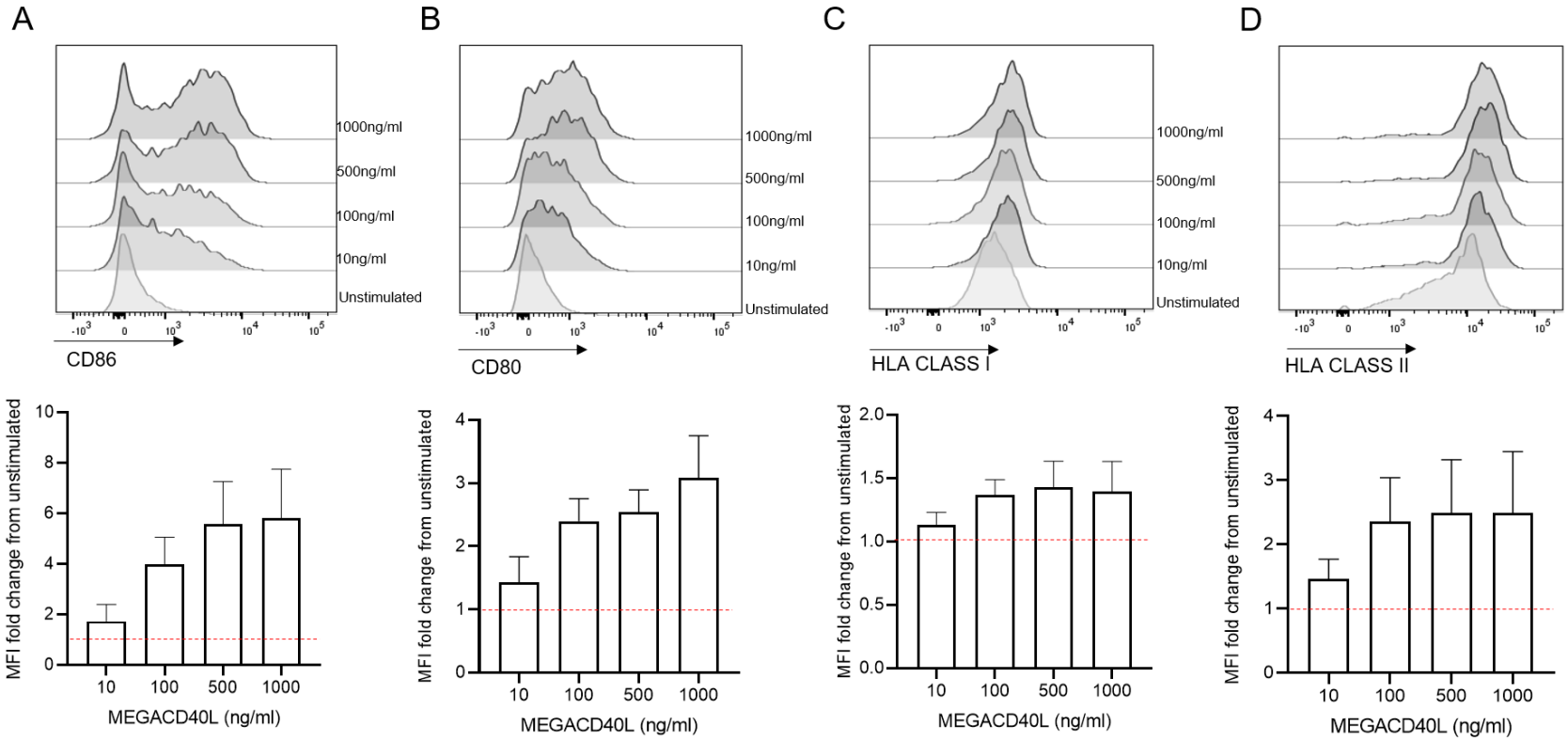

Figure 3-2 Stimulation of B cells with MEGACD40L upregulates the costimulatory markers CD80 and CD86, and HLA molecules class I and II.
B cells were stimulated with increasing concentrations of MEGACD40L for 24 hours, and the surface expression of CD80 and CD86 (A) and HLA CI and HLA CII (B) were assessed by flow cytometry. Flow cytometry plots are representative of all three experiments and graphical data is expressed as the fold change in MFI of the marker from unstimulated B cells of three independent experiments (mean ± SEM). A fold change higher than one is indicated by the red dotted line. Data was tested for significance using one-way ANOVA with Tukey's post hoc comparisons.

3.3 Generation and optimisation of an antigen delivery system (ADS)

3.3.1 ADS design and rationale

To assess the ability of B cells to cross-present antigen to T cells and induce T cell responses, it was necessary to devise an ADS in which delivery of the polypeptide of interest could be specifically targeted to the BCR for uptake and internalisation. Proof of principle studies focussed on the use of a 41-mer viral cytomegalovirus (CMV) polypeptide centrally containing the immunodominant epitope ($CMV_{495\text{-}503}$), which displays high affinity for HLA-A2 and is able to elicit a specific CD8 T cell response (Wills *et al.*, 1996). Extensive analysis has characterized efficacious proteasomal-dependent generation of this epitope from the whole CMVpp65 antigen and elongated epitope precursors (polypeptides) (Urban *et al.*, 2012), and the availability of CD8 T cell clones specific for the immunodominant epitope validate its use.

An additional C-terminal sulfhydryl group (-SH) was added to the sequence to allow covalent conjugation to amine (-NH) containing proteins. This permitted the conjugation of the peptide to a BCR-specific antibody using a heterobifunctional cross linker (sulfo-SMCC). An antibody specific to human IgG γ-chain (ADS antibody) was used (Figure 3-3).

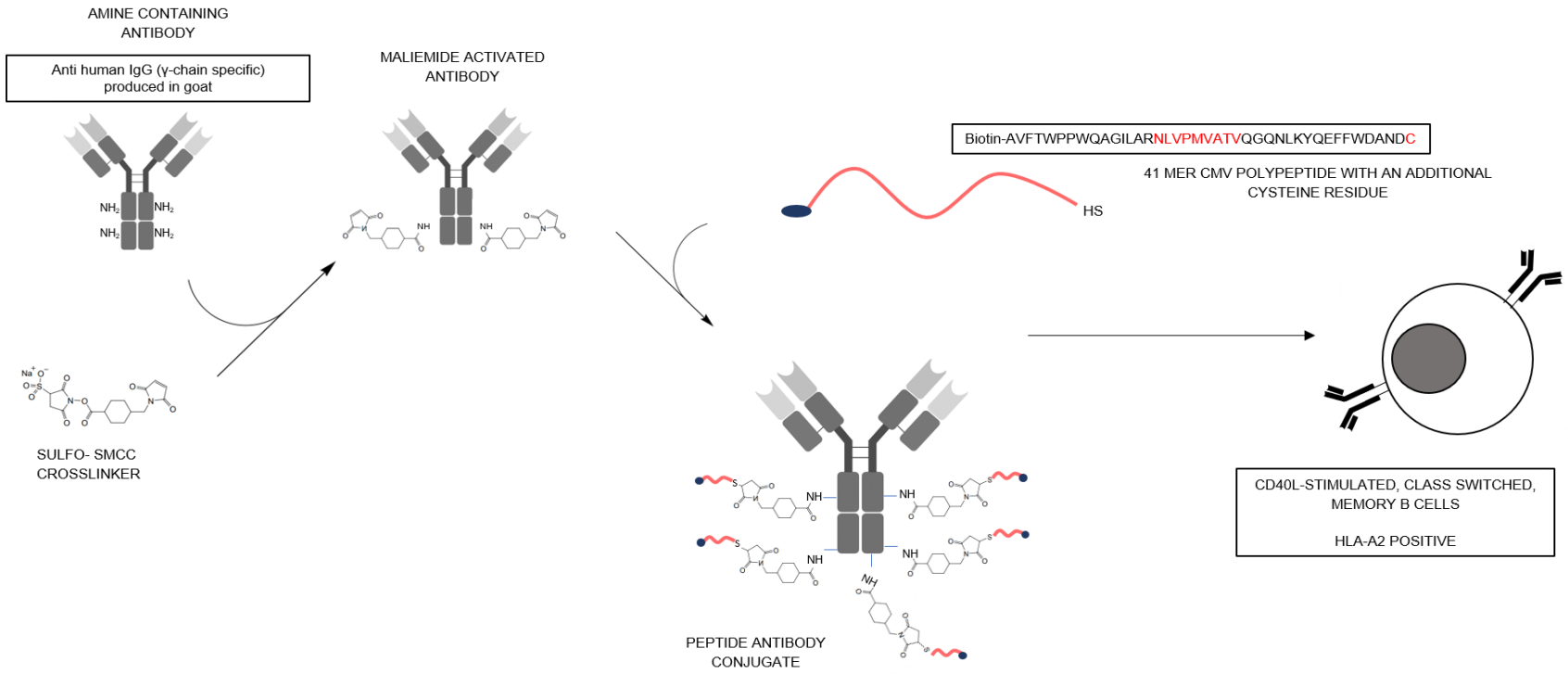

Figure 3-3 Construction of the antigen delivery system.

To achieve targeted delivery of the polypeptide to the BCR of the B cells, an antibody specific to human IgG was conjugated to a 41-mer polypeptide from the viral protein CMV, using sulfo-SMCC as a crosslinker. This crosslinker is first reacted with the antibody to produce a maleimide activated antibody through targeting of the amine groups (NH2) to form amine bonds. Excess non-reacted crosslinker is then removed through column separation, and the maleimide activated antibody is reacted with the 40mer polypeptide through the cysteine sulfhydryl group at the c-terminus of the sequence, at a molar ratio of 5:1 polypeptide to antibody. Once conjugated, B cells (~150,000/well) are pulsed with the conjugate on ice in a v-bottomed plate for 30 minutes to allow binding of the antibody to cell surface IgG, before being washed three times in PBS 2% FCS to remove any non-bound conjugate.

3.3.2 Optimisation of the ADS antibody

3.3.2.1 Use of surface bound IgG (IgG-BCR) for B cell targeting

As the ADS antibody was specific for human IgG, B cells were stained with an anti-IgG antibody and analysed by flow cytometry to determine surface IgG expression. Across three independent experiments, the average frequency of B cells with surface expression of an IgG-BCR was 60% (Figure 3-4A). This is in line with reports that state that the ratio of IgA-BCR and IgG-BCR B cells within a switched B cell population is around 1:1.5, inferring that the remaining B cells express an IgA-BCR (Seifert and Küppers, 2016). Thus, the presence of a large population of B cells with an IgG-BCR supports the use of the ADS antibody for polypeptide delivery.

3.3.2.2 Detection of IgG-BCR B cells with the ADS antibody

Next, I aimed to validate that the ADS antibody could specifically bind to the IgG-BCR. Cells were pulsed with the ADS antibody on ice for 30 minutes, before being stained with a FITC-conjugated secondary antibody specific for goat IgG. As the ADS antibody was raised in goat, this would allow flow cytometric detection of the surface-bound ADS antibody (Figure 3-4B).

The antibody was efficient in detecting the majority of IgG-BCR B cells as the frequency of FITC positive cells was comparable to data seen in Figure 3.4A; 56.7 $\pm$ 3.81 % as compared to 60.3 % (Figure 3-4C). To further confirm the specificity of the ADS antibody, an isotype control was used (whole goat IgG). This showed low frequencies of positive cells (8.075 $\pm$ 3.32 %) indicating little non-specific binding of the ADS antibody, for example through Fc receptors.

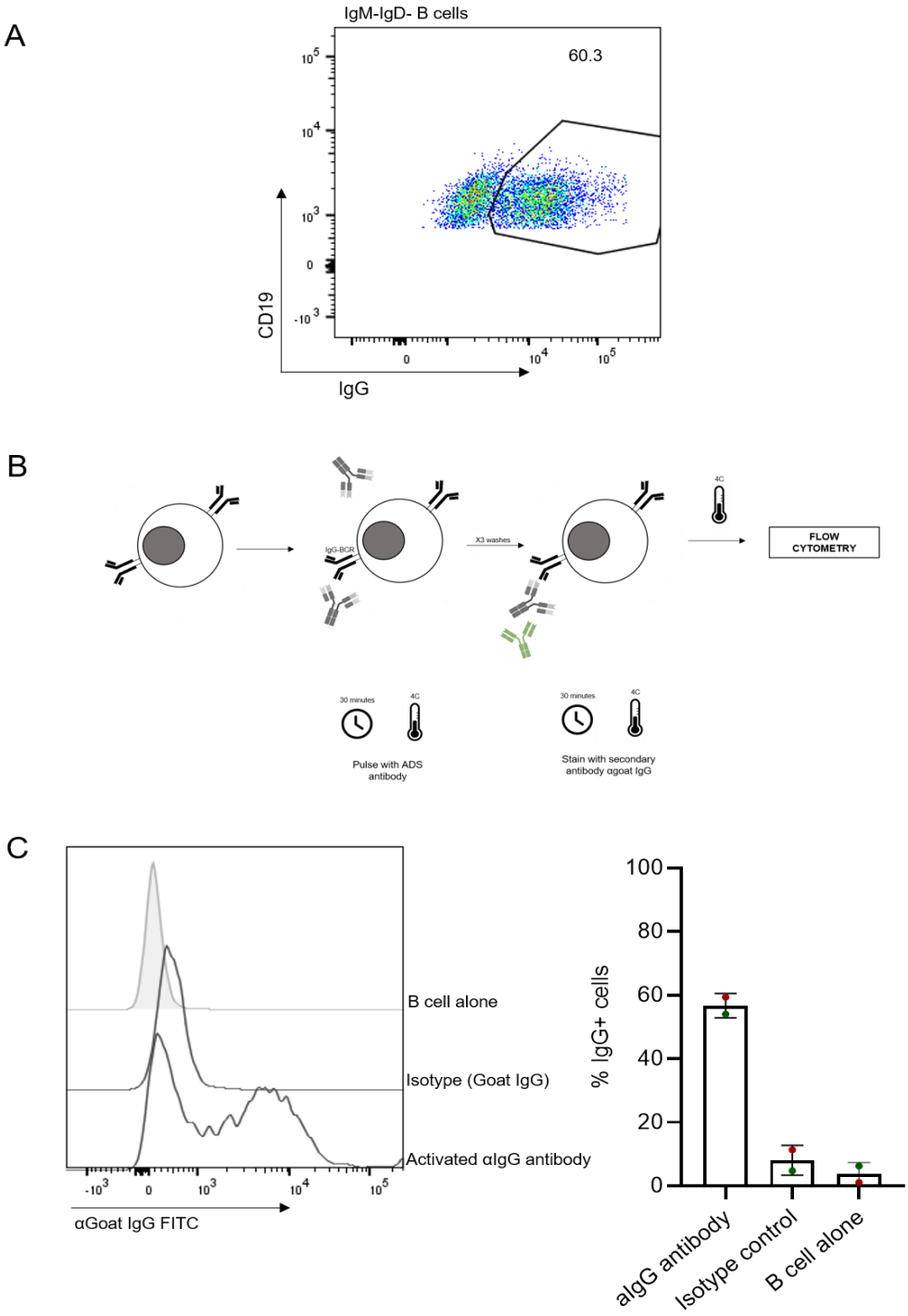

Figure 3-4 The ADS antibody detects the majority of IgG positive B cells, and shows minimal non-specific binding to B cells.

Class switched, memory B cells isolated from PBMCs were stained with an anti-IgG flow cytometry antibody to determine the (%) frequency of IgG positive B cells within the B cell population (A). To detect binding of the ADS antibody, and of its isotype, a secondary antibody specific for goat IgG conjugated to FITC was used (B,C). FACs plots are representative of three (A) or two (B) independent experiments, and bar charts represent the (%) frequency population from parent (mean ± SD). Individual experiments are matched by colour of the data points.

3.3.2.3 Effect of activation and conjugation of the ADS antibody on its detection of IgG-BCR B cells

ADS construction involved two modifications to the ADS antibody, activation with the crosslinker and conjugation to the polypeptide. To ensure this did not impact binding of the ADS antibody to the IgG-BCR, the frequency (%) of cells detected by the ADS antibody in its different forms was compared. Antibody concentration was standardised across the conditions through measurement by Nanodrop. Using a FITC-conjugated secondary antibody specific for goat IgG (Figure 3-4B), data showed no significant difference in the frequency of FITC positive cells between the non-activated antibody, the activated antibody and the conjugated antibody (Figure 3-5). Results were comparable to a previously validated anti-IgG antibody which served as a comparative control. Thus, activation and conjugation of the ADS antibody did not affect its binding to IgG-BCR B cells, confirming its utility in the ADS for polypeptide delivery to B cells through the BCR.

Although there were no significant differences between the conditions, a trend towards a slight reduction in cell surface binding upon activation and conjugation of the antibody was observed. Unexpectedly an average of 81 $\pm$ 3.8% cells cultured with the non-activated ADS antibody were positive for FITC (frequency of IgG positive cells) – higher than the previously defined number of IgG-BCR B cells within a population (~60%) (Figure 3-5). Antibody activation requires reaction of amine groups with the crosslinker, and a high proportion of these amine groups will be located on the Fc portion of the antibody. Therefore, the higher frequency of cells showing surface binding of the non-activated antibody may be due to the low-level non-specific binding through Fc receptors: amine group activation by the crosslinker may reduce the ability of the Fc region to bind Fc receptors.

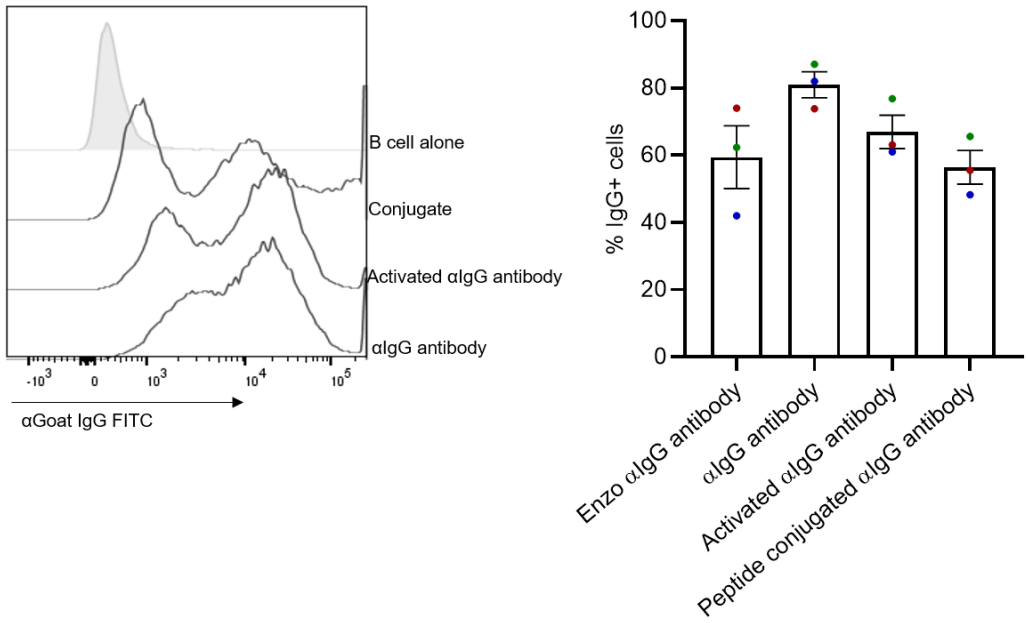

Figure 3-5 Activation and conjugation of the ADS antibody has a minimal effect on its binding to IgG positive B cells.

To determine the effect of activation of the ADS antibody with the crosslinker and conjugation to the polypeptide, a secondary antibody specific for goat IgG conjugated to FITC was used to assess the level of surface binding of the ADS antibody, and compared to another antibody specific to human IgG (A). Flow cytometry histograms are representative of three independent experiments, and bar charts represent the (%) frequency of FITC (IgG) positive cells (mean ± SEM). Data was tested for significance using a one way ANOVA with Tukey's multiple comparison post hoc test. Individual experiments are matched by colour of the data points.

3.3.2.4 Internalisation of the ADS antibody by the B cells

To allow processing of the polypeptide and peptide presentation, the ADS must be internalised by the B cell. Flow cytometry was used to assess the level of ADS antibody on the cell surface as measured by the mean fluorescence intensity (MFI) of the secondary (FITC-conjugated) antibody (Figure 3-6A). After 30 minutes, a reduction in the MFI suggested a decrease of ADS antibody on the cell surface. MFI continued to decrease at 1 and 2 hours, albeit at a slower rate (Figure 3-6B). These data therefore showed a rapid loss of cell surface signal of the ADS antibody; conducive with literature that shows rapid BCR internalisation upon stimulation of Ig receptors.

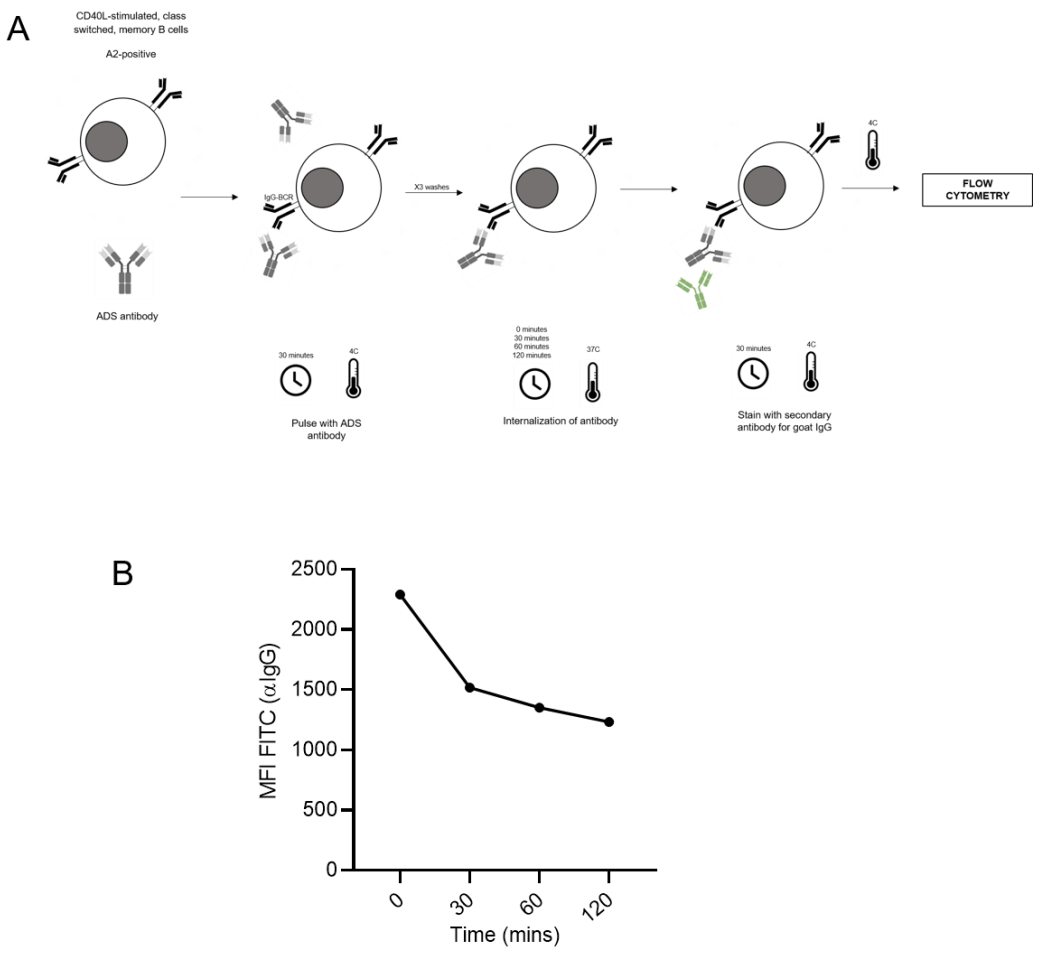

Figure 3-6 Reduction of ADS surface expression over time.
To assess the internalisation of the ADS antibody, pulsed cells were incubated over a time course at 37°C and the level of surface bound antibody assessed by the signal of the secondary antibody specific for goat IgG conjugated to FITC (A) Line graph represents one individual experiment (B).

Next, I addressed the reason for the loss of cell surface ADS using Imagestream. In line with the flow cytometry experiment, B cells were pulsed with an APC-conjugated ADS antibody and incubated for 0 minutes, 30 minutes or 1 hour at 37°C (Figure 3-7).

Flow cytometry data suggested a loss of surface bound ADS antibody upon incubation at 37°C, perhaps indicating internalisation. Immediately after pulsing with ADS antibody (0 minutes), it was observed by Imagestream that a high proportion of these cells presented with a uniform staining pattern around the cell surface. This was consistent with signal localisation at the plasma membrane and an internalisation ratio between 0-1 (Figure 3-7B). As there is some degree of overlap between the intracellular and extracellular signal, the average mean internalisation

score for this condition was 1.04 (Figure 3-7B). In contrast, it was observed that most cells incubated at 37°C did not display this uniform staining pattern, instead showing increased internalisation (Figure 3-7B). This was reflected in the mean average internalisation score of 1.69 and 1.70 for 30 minutes and 60 minutes, respectively (Figure 3-7A). Consistent with flow cytometry data, internalisation appeared to be rapid, with a steep increase in the level of internalisation after just 30 minutes at 37°C. Thus, this data suggests that the reduction of ADS antibody signal from the cell surface at incubation of 37°C is due to internalisation of the antibody. This property is necessary for the ADS to permit processing of the polypeptide and presentation of the peptide.

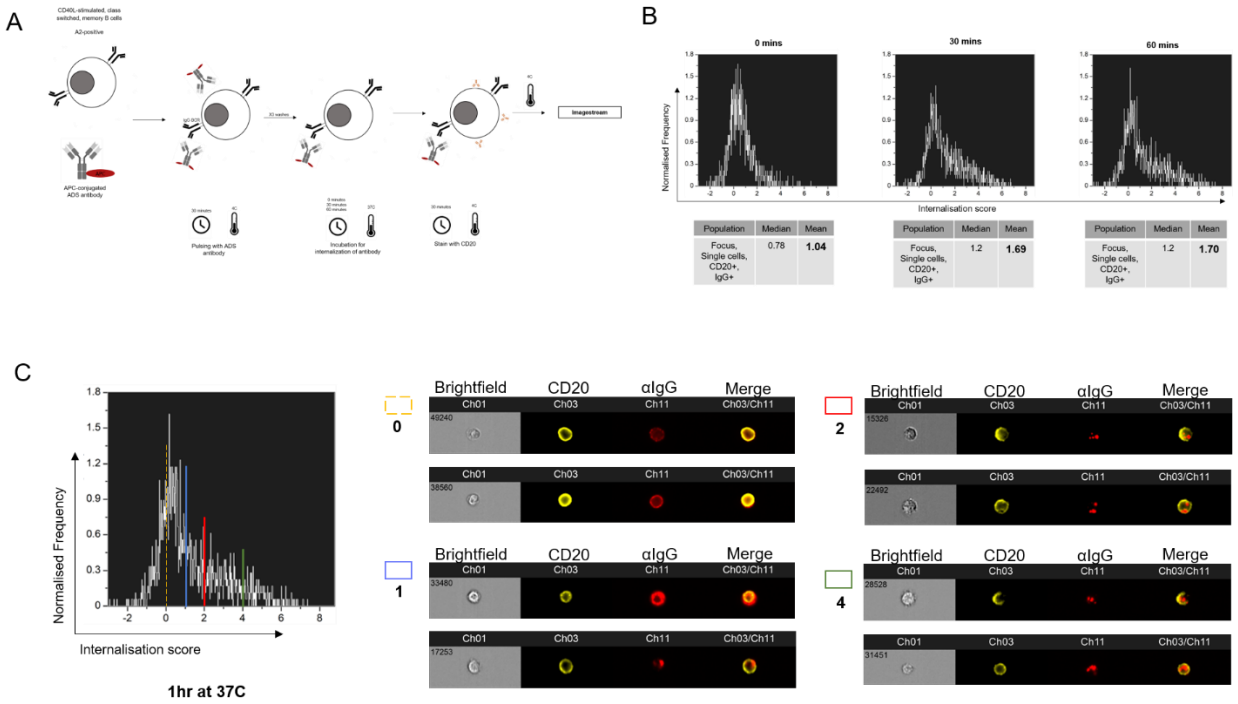

Figure 3-7 B cells internalise the ADS.

The ADS antibody was conjugated to an APC fluorophore, and B cells were pulsed with this antibody before being incubated at 37°C for 30 minutes, 1 hour or 2 hours. Cells were then stained with CD20 and analysed using Imagestream (A). To determine internalisation of the antibody, the internalisation wizard in the Imagestream IDEAS software was applied. Using an 'erosion' mask of 4 pixels from the CD20 B cell mask, the internalisation score of the antibody for the cells was determined as the ratio of intensity of the antibody within the cell as compared to the whole cell. Mean and median internalization scores were calculated for cells at each time point (B). Representative images of cells with an internalization score of 0, 1, 2 and 4 were shown for cells pulsed and then cultured for 1 hour at 37°C (C). Data is representative of one independent experiment.

3.3.3 Optimisation of the ADS-conjugate

3.3.3.1 41-mer CMV polypeptide delivery via the ADS antibody

Data had demonstrated that the ADS antibody binds to the IgG-BCR of B cells and is internalised. To test functional antigen processing, the next step was to conjugate ADS antibody to 41-mer CMV polypeptide and determine whether this ADS-conjugate would result in polypeptide delivery to the B cell.

Initial experiments to infer surface delivery of polypeptide utilised the biotin moiety on the N-terminus of the 41-mer CMV polypeptide with a fluorescent anti-biotin antibody. At equimolar concentrations, B cells were pulsed on ice for 30 minutes with the ADS-conjugate, the 41-mer CMV polypeptide alone, or the ADS antibody and 41-mer CMV polypeptide together, but unconjugated. Cells were stained with the anti-biotin antibody and analysed using flow cytometry to determine the cell surface level of polypeptide (Figure 3-8A). B cells pulsed with ADS-conjugate showed a population of cells positive for biotin, confirming surface polypeptide (Figure 3-8B). This population was comparable to the staining pattern seen with the ADS antibody alone (Figure 3-4C). Thus, ADS-conjugate is able to deliver polypeptide to the cell surface of the IgG-BCR positive B cells. For both conditions in which cells were pulsed with either the 41-mer CMV polypeptide alone, or the ADS antibody and 41-mer CMV polypeptide alone in unconjugated form, no biotin was detected on the cell surface of the cells (Figure 3-8B). This suggested no non-specific binding of the ADS-conjugate. Taken together, these results demonstrate that the ADS-conjugate delivers polypeptide to the B cells in an IgG-BCR dependent mechanism. Thus, this addresses the aim to target polypeptide delivery through the BCR for antigen processing and presentation.

3.3.3.2 Internalisation of the ADS-conjugate

Experiments had shown the ADS antibody was internalised. The next aim was to determine if the ADS-conjugate was also internalised by the B cells. B cells were pulsed with the ADS-conjugate, as well as the two control conditions (as above), and incubated at 37°C for 2 hours, 4 hours and 6 hours. Cells were then stained with anti-biotin antibody to detect cell surface polypeptide (Figure 3-8B). Similar to the FITC signal to detect the ADS antibody, the biotin signal decreased as the incubation

time increased. There was a significant reduction in the biotin signal after 6 hours of incubation as compared to immediately after pulsing, with the MFI at 0 hours being 7705 $\pm$ 2521 compared to 1876 $\pm$ 505.5. As expected, the biotin signal in the two control conditions remained as background, with no significant change over time (Figure 3-8B). Thus, the data imply that the reduction of biotin signal from the cell surface is consistent with ADS-conjugate internalisation. This could not be confirmed by Imagestream due to technical obstacles such as the lack of a fluorescence-tagged polypeptide and the need to permeabilise the cells to detect intracellular biotin-tagged polypeptide.

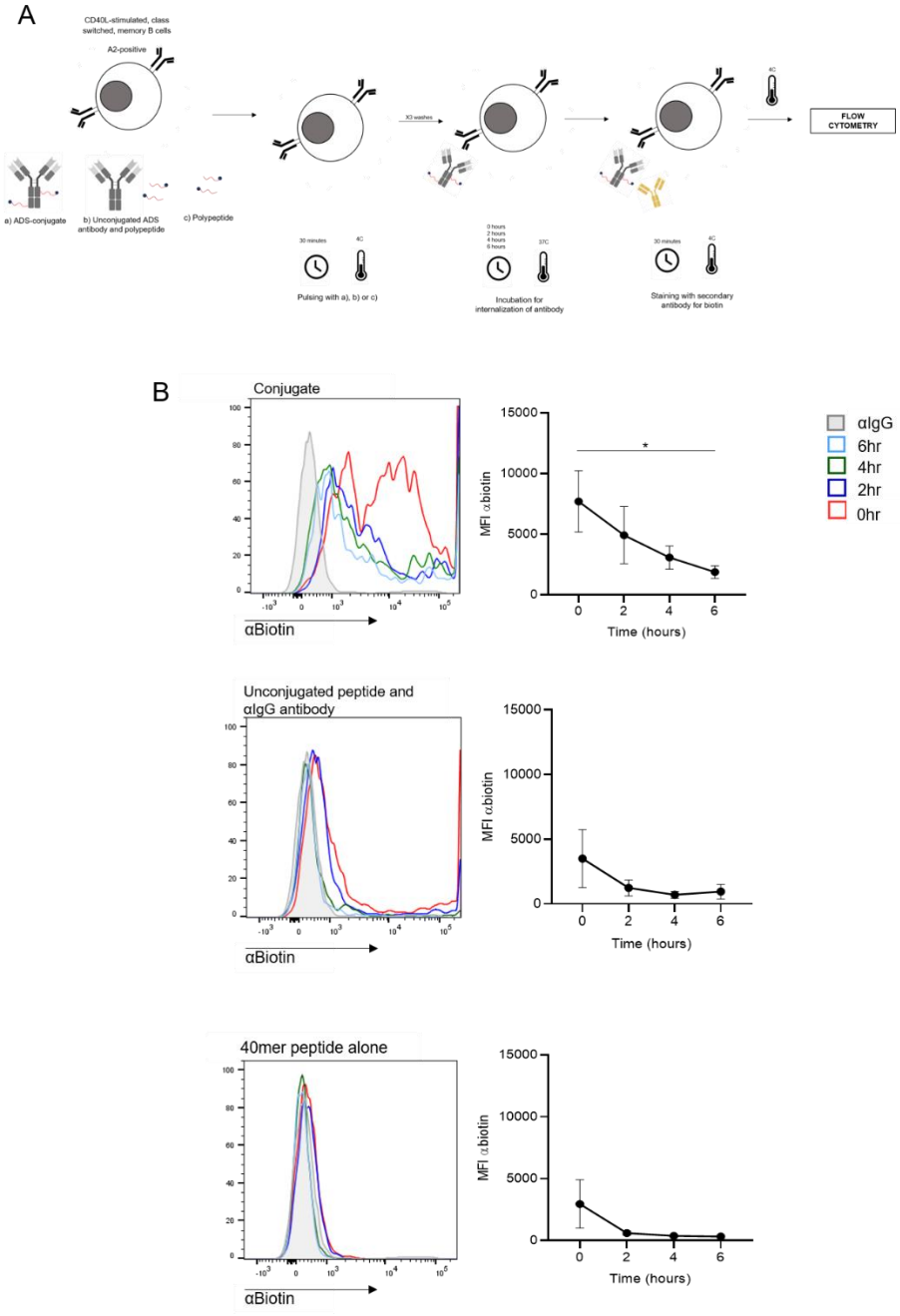

Figure 3-8 The ADS-conjugate is lost from the cell surface of B cells over time.
A flow cytometry antibody specific for biotin was used to detect the level of polypeptide on the B cell surface when B cells were either pulsed with the ADS-conjugate, the 41-mer polypeptide alone or the ADS antibody and 41-mer polypeptide in unconjugated form (A).The level of cell surface polypeptide for each condition was assessed over a time course of incubation periods at 37°C (B) and the MFI of the biotin signal calculated (C). Flow cytometry plots are representative of three independent experiments, and graphical data presents the average MFI of biotin signal from the parent population of three independent experiments (mean $\pm$ SEM) and were tested for significance using a one way ANOVA with Tukeys multiple comparison test where *<0.05.

3.3.3.3 HLA binding kinetics of the 41-mer CMV polypeptide

B cells pulsed with the 41-mer CMV polypeptide alone showed no biotin signal on the cell surface. This ruled out the possibility that the polypeptide was binding to the HLA class I molecule in a non-specific manner and undergoing extracellular processing – an important criterion for the ADS in which the aim is to deliver peptide to the cell through the BCR. To confirm the 41-mer CMV polypeptide could not bind directly to the HLA-A2 molecule on the B cell surface, a TAP deficient cell line (T2) was used.

TAP deficiency results in the inability of cells to transport peptide into the ER for loading onto HLA class I molecules. This leads to an accumulation of empty HLA class I molecules in the ER, Golgi apparatus and at the cell surface. As association with peptide sufficiently increases the stability of the HLA class I molecules on the cell surface, empty molecules are endocytosed rapidly – T2 cells exhibit an 80% reduction of surface HLA-A2 (Schweitzer *et al.*, 2000). Binding of peptides, however, result in stabilisation of HLA-A2 and detection using flow cytometry. Therefore, this cell line is useful to study binding kinetics of HLA-A2 restricted epitopes.

As a positive control, cells were pulsed with the 9-mer CMV peptide that is the central immunodominant sequence of the 41-mer CMV polypeptide, and a known high binder of HLA-A2. This short peptide resulted in detectable HLA-class I expression in a concentration dependent manner. A 1.74 ($\pm$ 0.09) fold change of HLA class I MFI was detected after pulsing with 10 μg/ml of peptide, as compared to T2 cells pulsed with DMSO (Figure 3-9). Although not significant, these data indicate that the 9-mer peptide binds HLA-A2 and stabilises its expression on the cell surface. Pulsing of the T2 cells with an HLA class II DR4 binding 12-mer peptide showed, as expected, no stabilisation of the HLA class I molecule. Importantly, addition of the 41-mer CMV polypeptide to the T2 cells showed no change in HLA class I expression, with the MFI fold change remaining close to 1 at 0.99 ($\pm$ 0.02) at the top peptide concentration of 10 μg/ml. Thus, these data suggest that the 41-mer CMV polypeptide cannot bind directly to the HLA-A2 molecule. An important caveat to note in this experiment is the molar inequality between the 9-mer

peptide and the 41-mer polypeptide. Overall, data from section 3.3 provides evidence for the development of a robust ADS, which specifically targets polypeptide to the BCR, and results in its internalisation.

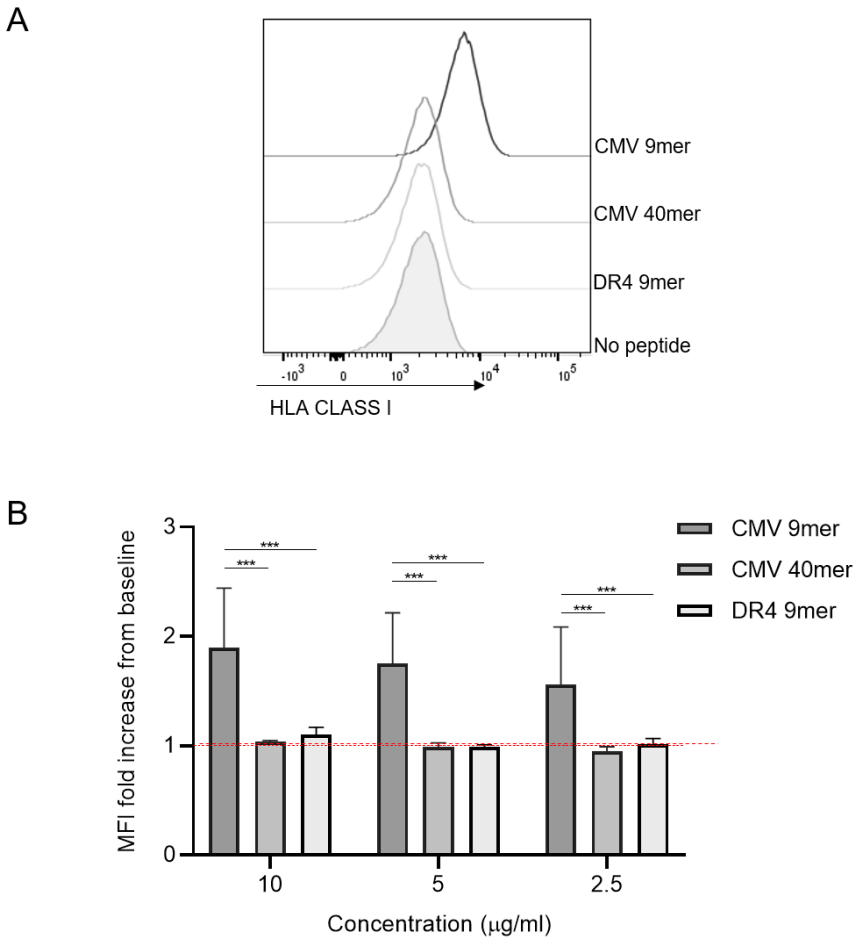

Figure 3-9 41-mer CMV polypeptide does not bind directly to the HLA class I (A2) molecule on the cell surface of the B cell.

To assess the binding kinetics of the 41-mer CMV polypeptide, T2 cells, which contain empty HLA-A2 molecules on the cell surface that are stably expressed once bound to short peptide, were pulsed with different concentrations of the 41-mer CMV polypeptide, the 9-mer CMV HLA A2-binding peptide and a HLA DR4-binding 12-mer peptide. The level of HLA class I expression was detected via flow cytometry and compared across conditions. Flow cytometry plots are representative of the results of three independent experiments, and graphical data is presented as the MFI fold increase of HLA class I as compared to T2 cells pulsed with no peptide. Data were tested for significance within each concentration using a one way ANOVA with Tukeys multiple comparison test where ***<0.005.

3.4 Assessment of cross-presentation of CMV polypeptide by B cells

3.4.1 ADS-conjugate pulsed B cells activate CD8 T cells

Optimisation of the ADS showed that the ADS antibody was able to specifically bind to the IgG-BCR of B cells and be internalised by the cell. Conjugation of ADS antibody to 41-mer CMV polypeptide resulted in IgG-specific delivery of polypeptide to the cell surface. Loss of polypeptide signal after incubation at 37°C was consistent with internalisation of the ADS-conjugate. Therefore, the next logical step in the experimental approach was to determine whether the ADS-conjugate pulsed B cells were able induce cytotoxic T cell responses – reflecting B cell processing of the polypeptide and cross-presentation of the immunodominant epitope on the HLA-A2 molecule of the B cell.

For these studies, I used a HLA-A2 restricted CD8 T cell clone specific for residues 495-503 of CMV protein pp65 (Knight *et al.*, 2015). Throughout the series of experiments presented in this chapter, although the same T cell clone was used, it is important to note the clone underwent multiple expansions thereby inherent variability is expected. The extent of this variability was assessed with the inclusion of specific controls, as discussed later.

T cell activation by B cell cross-presentation was assessed by flow cytometry to detect CD8 T cell surface expression of CD107α. This is a T cell degranulation marker and its expression correlates with cytotoxic effector function following antigen specific T cell activation and stimulation. A gating strategy was established based on the negative control, containing T cell clones alone, and the positive control in which T cell clones were cultured with K562 cells transduced to express both HLA-A2 and the CMV protein. The CD107α positive gate was established based on the negative population of cells in the T cell alone condition, and the positive population within the K562-A2-CMV co-culture (Figure 3-10).

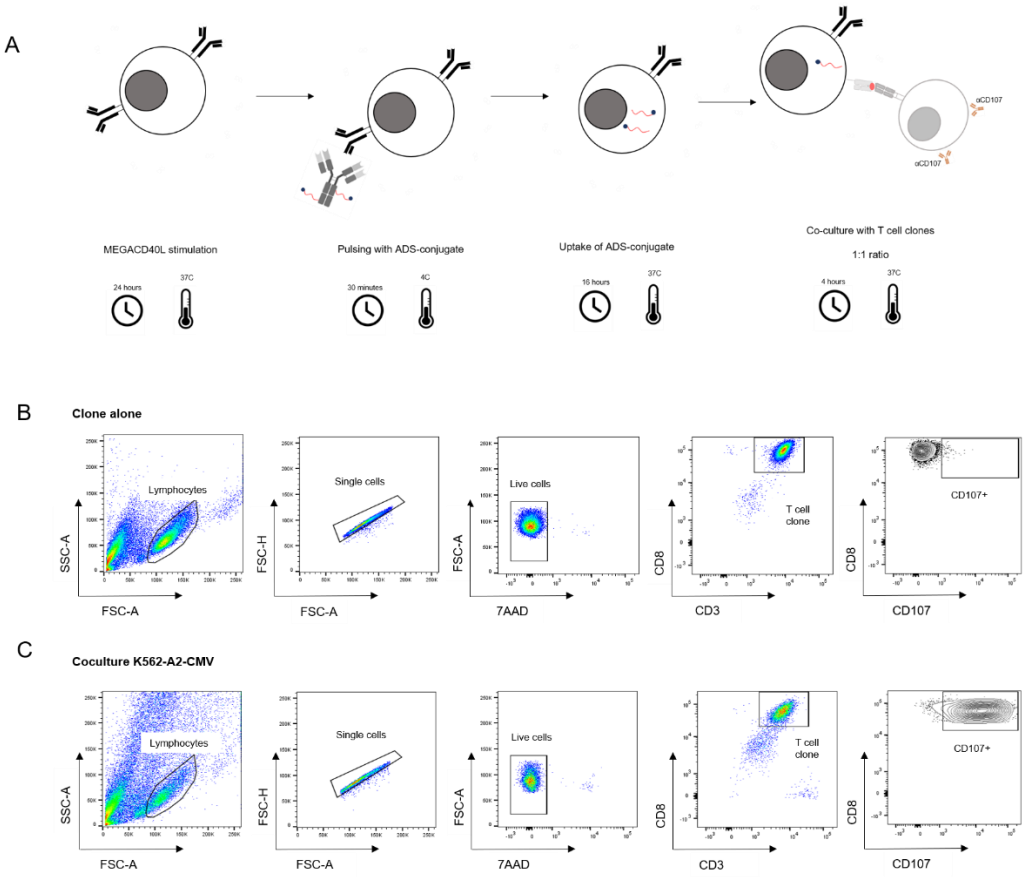

Figure 3-10 Experimental strategy to assess induction of T cell responses by B cells (A) and gating strategy used to identify CD107α expression (B,C).

Upon co-culture with ADS-conjugate pulsed B cells, a significant proportion of CD8 T cell expressed CD107α (48.5 ± 12 %) as compared to all other conditions controlling for the ADS (Figure 3-11), suggesting antigen specific T cell activation and degranulation. This is strong evidence that the CMV $pp65_{495\text{-}503}$ epitope was 1) generated from B cell intracellular processing of polypeptide in the ADS-conjugate, and 2) cross-presented on HLA class I molecules. Importantly, B cells pulsed with activated ADS antibody alone, or with the 41-mer CMV polypeptide alone, did not induce CD107α expression on T cells (1.8 ± 1% and 3.7 ± 0.9%, respectively). This indicates that internalisation and processing of the 41-mer polypeptide are required for a T cell response. Moreover, the activated ADS antibody does not have a direct stimulatory effect on the CD8 T cell clones. Individually, the components of the ADS-conjugate do not result in induction of CD8 T cell responses. Acquisition of a T cell cytotoxic phenotype is dependent on conjugation of polypeptide to the ADS

antibody, presumably due to targeted delivery of polypeptide to the BCR for processing and epitope generation.

To further elucidate the necessity of conjugation and thereby BCR targeted delivery, rather than just the presence of both ADS components, B cells were pulsed with activated ADS antibody and 41-mer CMV polypeptide in unconjugated form. Data showed induction of CD107α expression on some CD8 T cell clones (17 ± 13.5%), however the frequency of positive cells was significantly lower than co-cultures with ADS-conjugate pulsed B cells (Figure 3-11). It is likely this slight induction of T cell degranulation is due to some spontaneous conjugation of the two components.

Taken together, these data show that B cells can induce CD8 T cell responses, as measured by T cell degranulation. Acquisition of CD8 T cell cytotoxic function is dependent on targeted delivery of polypeptide to the BCR. BCR mediated uptake of polypeptide presumably allows processing and generation of epitopes for cross-presentation to CD8 T cells. This concept was bolstered by the comparable response of T cell activation between the co-culture of ADS-conjugate pulsed B cells and the co-culture of K562-A2-CMV cells. The latter induced T cell degranulation in 67 ± 15.04% of the CD8 T cell population (Figure 3-11). K562 cells transduced with HLA-A2 and CMV antigen will endogenously express CMV and process and present through the classical HLA class I, endogenous pathway (Section 1.5.2). Data therefore suggests access of exogenous polypeptide (through the ADS-conjugate) to the HLA class I processing pathway in the B cells.

As seen in Figure 3.12A and B, while the trend in responses across conditions remained consistent, an obvious observation is the variability - each experiment is represented by a different colour data point. As each experiment used different donor B cells, one explanation is inherent-donor variability. This may be due to different frequencies of IgG-BCR positive B cells, impacting the number of B cells targeted by the ADS-conjugate. However, variability remains within the co-cultures of T cell clones with the K562-A2-CMV cell line. Therefore, variability arises from the T cell clone. This is likely to be due to differences in the length of time in culture or the round of expansion. The ‘responsiveness’ of the clone in each experiment was assessed by the frequency of T cells degranulating in the K562-A2-CMV coculture. Normalisation of the data set as a whole to account for this variation could be

achieved by presenting data as a percentage of the K562-A2-CMV co-culture response. However, as the use of the clone was consistent within each independent experiment, the presentation of matched data helps to account for this variance.

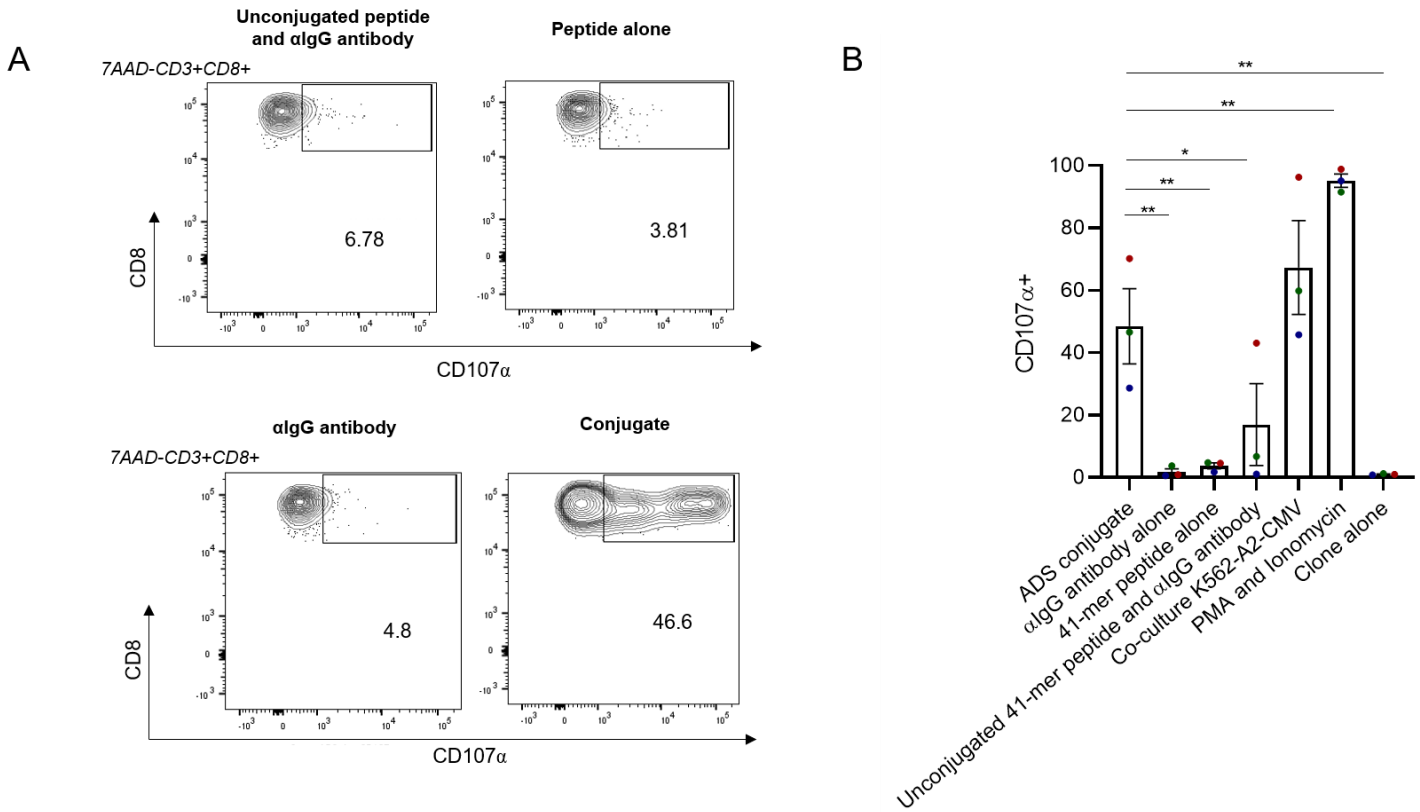

Figure 3-11 B cells pulsed with the ADS-conjugate induce T cell effector activity as measured by CD107α expression.

Flow cytometry plots are representative of three independent experiments, and graphical data presents the average frequency (%) of CD107α positive cells from the parent population for each condition (mean ± SEM) and were tested for significance using a one-way ANOVA with Dunnett's multiple comparison test to compare all conditions to the ADS-conjugate, where *<0.05, **<0.01. Individual experiments are matched by colour of the data points.

3.4.2 HLA-restriction of presented epitopes by ADS-conjugate pulsed B cells

To assess whether the CD8 T cell response was restricted to presentation of peptide in context of HLA-A2, B cells were isolated from HLA-A2 positive and HLA-A2 negative donors, pulsed with the ADS-conjugate and co-cultured with CD8 T cell clones. As a comparator to consider peptide independent, B cell mediated activation of T cells, B cells were also pulsed with a DMSO control. Consistent with the previous findings, co-cultures of CD8 T cell clones with HLA-A2 positive B cells pulsed with the ADS-conjugate, induced significant T cell degranulation. In contrast, there was no induction of CD107α expression when HLA-A2 negative B cells were used (Figure 3-12). B cells treated with DMSO showed no induction of T cell responses, independent of HLA-A2 expression. These data indicate that the T cell response to ADS-conjugate pulsed B cells is both HLA-restricted and peptide-restricted and provides further evidence for B cell processing of the 41-mer polypeptide for presentation on cognate HLA class I.

Overall, data from Section 3.4 has shown that BCR-mediated delivery of the 41-mer polypeptide by the ADS-conjugate results in significant, antigen-specific activation of the CMV specific CD8 T cell clone. I*n vitro,* B cells can process polypeptide, and cross-present epitopes to CD8 T cells to induce their cytotoxic effector responses. This is proof of principle that B cells can cross present exogenous antigen, and validates their potential role in T1D pathogenesis.

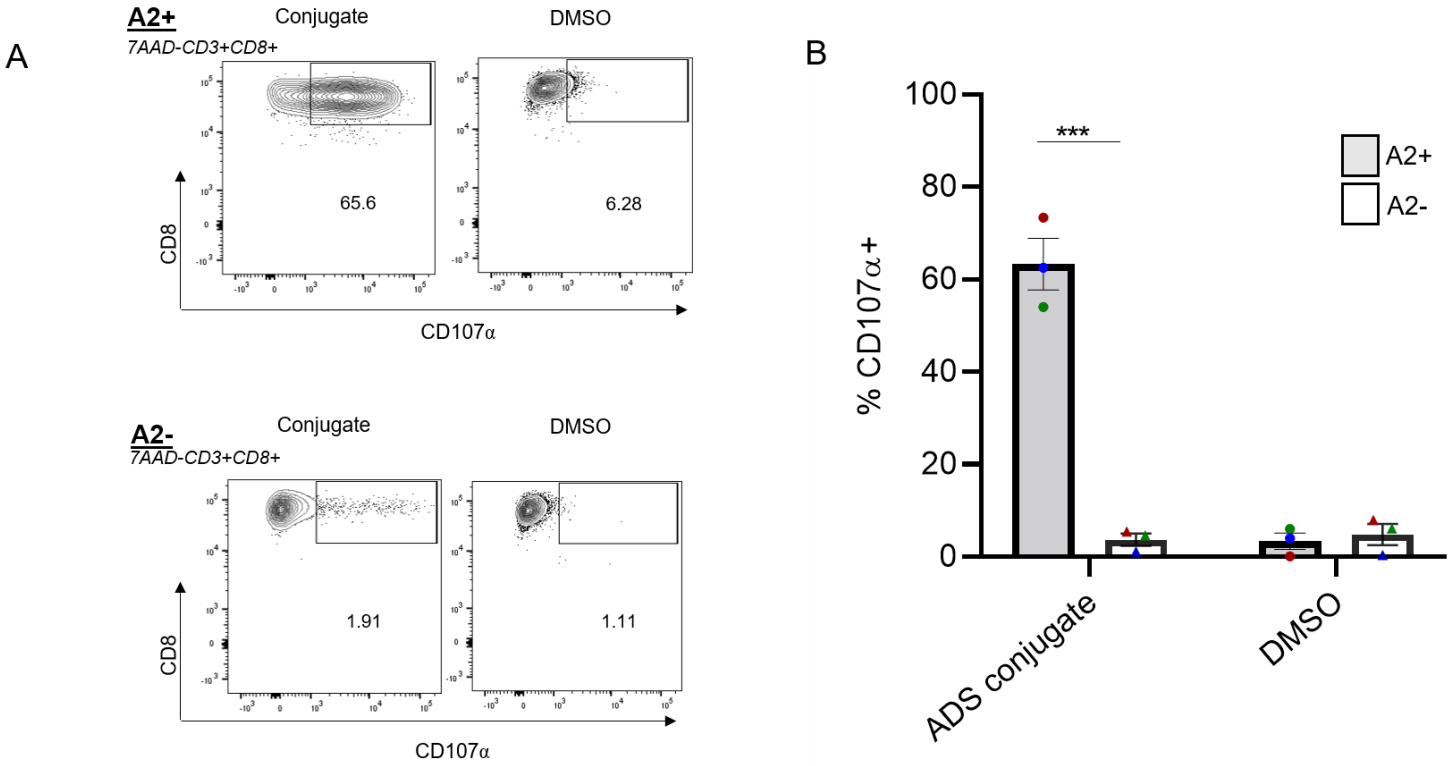

Figure 3-12 CD107α expression on CD8 T cell clones induced by ADS-conjugate pulsed B cells is dependent on B cell expression of HLA-A2. HLA-A2 positive and HLA-A2 negative B cells were pulsed with the ADS-conjugate or DMSO control and co-cultured with CMV-specific CD8 T cell clones. T cell activation was assessed as the frequency of CD3+CD8+ T cell clones expressing CD107α on and compared across conditions (A,B). Flow cytometry plots are representative of three independent experiments, and graphical data presents the average % of CD107 positive cells from the parent population for each condition (mean ± SEM) and were tested for significance using a using a two way ANOVA with Sidaks multiple comparison test, where ***<0.001.Significance shown is between A2 positive and A2 negative cells in each culture condition. Individual experiments are matched by colour of the data points.

3.5 Comparison of cross-presentation potency of ADS-conjugate pulsed B cells and dendritic cells

3.5.1 Generation of activated, mature dendritic cells

3.5.1.1 Differentiation of monocyte-derived dendritic cells from PBMCs

A previously published protocol which had reported 'fast' generation of cross-presenting DCs was modified for use in these experiments (Dauer *et al.*, 2003). Highlighted in Figure 3-13A, PBMCs were plated in 6-well plates and incubated at 37°C to allow adherence of certain cells. As assessed by flow cytometry, this method resulted in an enrichment of monocytes as compared to the whole PBMC population, or the non-adherent fraction (Figure 3-13). Monocytes were then cultured with GM-CSF and IL-4, and their phenotype assessed by flow cytometry.

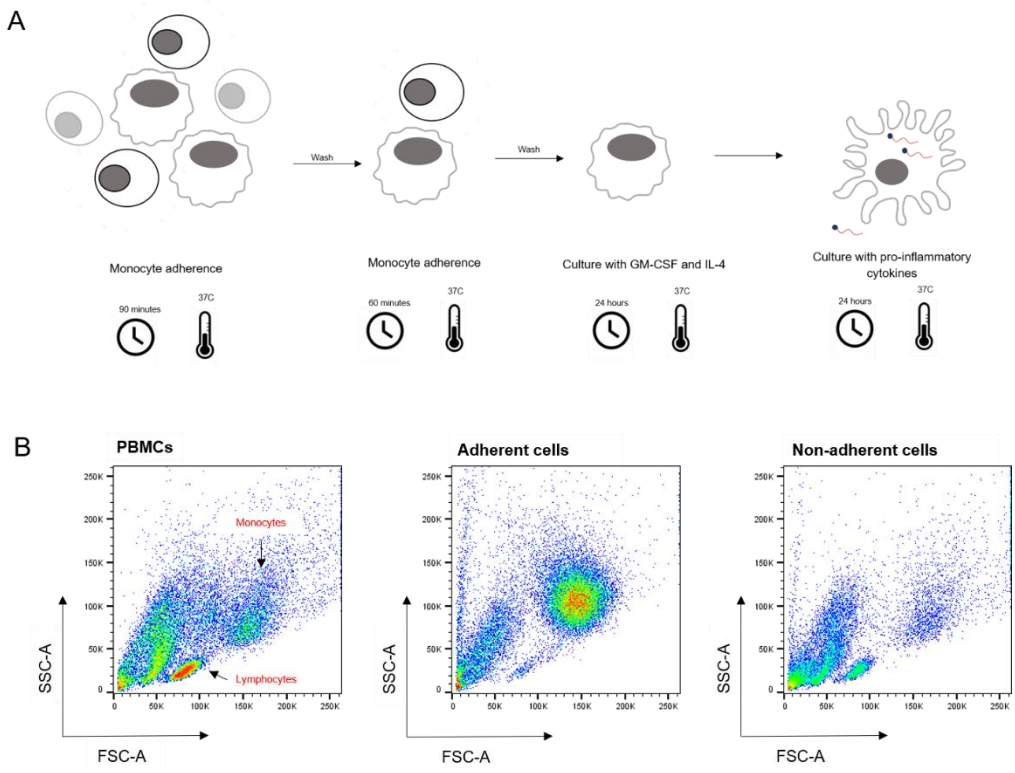

Figure 3-13 Experimental strategy for generating mature, activated dendritic cells (A), through an enrichment of monocytes (B).

Culture with GM-CSF and IL-4 resulted in downregulation of the monocyte marker CD14 (Figure 3-14A). This was demonstrated by both a significant loss of CD14 positive events and a significant reduction in CD14 MFI as compared to cells cultured with no cytokines, where a high proportion of cells were CD14 positive. Interestingly, the loss of CD14 expression on cells appeared to be transient, with two populations of cells identified via flow cytometry indicating low CD14 expression and mid CD14 expression. Thus, culture of adherent monocytes with GM-CSF and IL-4 results in their loss of a monocytic phenotype, consistent with differentiation.

To determine the cells had differentiated into DCs, DC-SIGN expression, a c-lectin receptor expressed on the surface of DCs, was assessed by flow cytometry (Figure 3-14B). Adherent monocytes cultured with no cytokines showed negligent DC-SIGN expression. However, culture with GM-CSF and IL4 showed significant induction of DC-SIGN expression, as reflected in both the frequency (%) of positive events and the DC-SIGN MFI. Therefore, treatment of adherent cells with differentiation cytokines results in significant upregulation of DC-SIGN expression.

Taken together, these data demonstrate the utility of the adherence method in generating DCs; adherent monocytes cultured with GM-CSF and IL-4 acquire a DC phenotype as determined by significant downregulation of the monocyte marker CD14 and upregulation of the DC specific marker DC-SIGN.

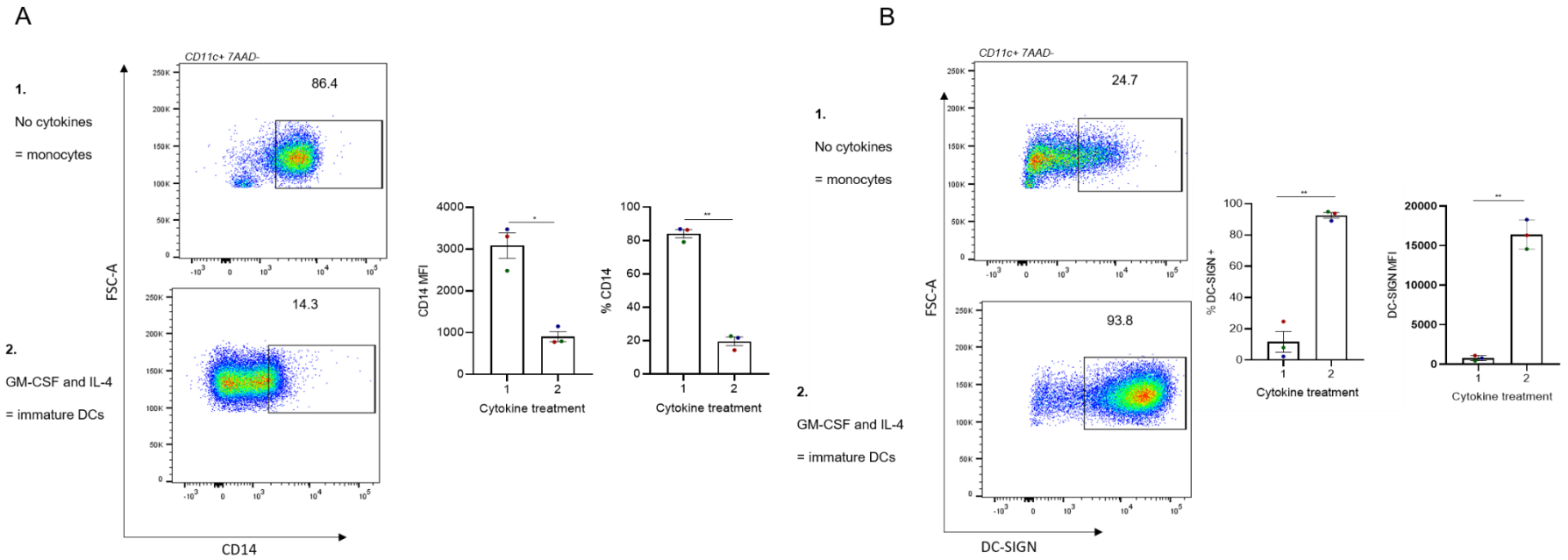

Figure 3-14 : Monocyte-derived dendritic cells (MoDCs) can be differentiated from adherent monocytes and display a DC-associated phenotype.
To generate MoDCs, adherent monocytes from PBMCs were cultured with differentiation cytokines (A, B). The phenotype of MoDCs was assessed by flow cytometry to determine expression of CD14 (C) and of DC-SIGN (D), comparing cells treated with differentiation cytokines and no cytokines. Flow cytometry plots are representative of three independent experiments, and graphical data is presents the % frequency of positive cells, or the MFI of the marker within the parent population of three independent experiments (mean $\pm$ SEM) and were tested for significance using paired student T tests where *<0.05, **<0.01. Individual experiments are matched by colour of the data points.

3.5.1.2 Activation and stimulation of monocyte-derived dendritic cells

To generate antigen cross-presenting DCs, literature reports a mature, activated phenotype. This included expression of HLA class molecules and co-stimulatory molecules (Dauer *et al.*, 2003). To induce DC maturation, differentiated cells were cultured with pro-inflammatory cytokines IL1β, TNFα and PGE2, in addition to GM-CSF and IL4. Flow cytometry compared expression of activation markers between adherent monocytes cultured with no cytokines (Condition 1), with the differentiation cytokines (Condition 2), or differentiation and maturation cytokines (Condition 3) (Figure 3-15).

In comparison to condition 1, expression of HLA class II, CD80 and CD86 was upregulated with the addition of cytokines in both conditions. Differentiation cytokines alone were enough to induce significant upregulation of HLA CII and CD86, with the secondary culture with maturation cytokines increasing this expression, significantly for the former. Induction of CD80 was entirely dependent on the secondary culture with maturation cytokines. Expression was minimal in cells cultured with no cytokines or differentiation cytokines alone, however culture with maturation cytokines induced significant expression. An unexpected observation in this experiment is the significant downregulation of HLA CI with addition of GM-CSF and IL-4, that then returns to a comparable level of expression with the addition of pro-inflammatory cytokines.

Thus, DCs differentiated from monocytes and cultured with GM-CSF, IL4, IL1β, TNFα and PGE display an activated, mature phenotype as evidenced by high expression of HLA class I, class II, CD80 and CD86. This phenotype is consistent with DC cross-presentation of antigen.

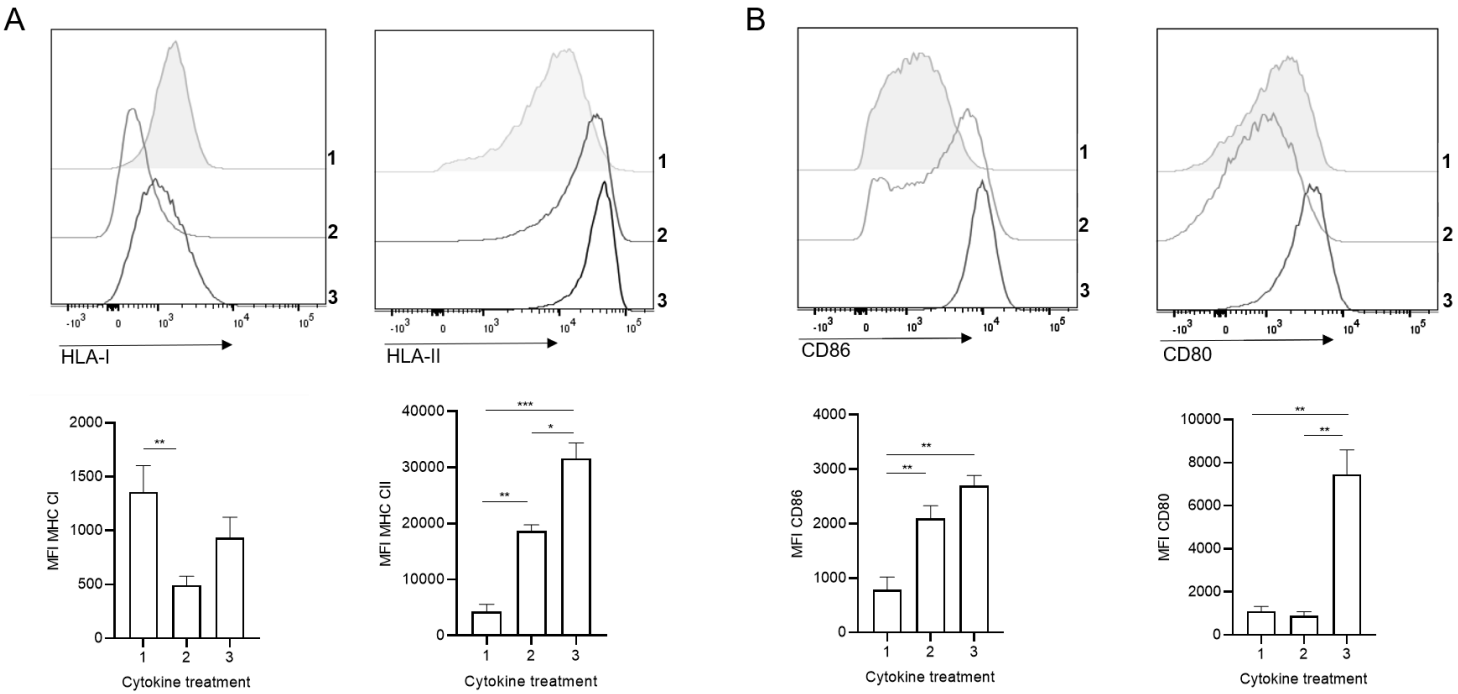

Figure 3-15 Monocyte derived DCs display an activated, mature phenotype after treatment with pro-inflammatory cytokines.

To generate MoDCs with an activated phenotype, monocytes were first differentiated in the presence of GM-CSF and IL-4, before being treated with the maturation cytokines IL1β, TNFα and PGE2. Their phenotype was assessed using flow cytometry to determine expression of HLA class molecules (A) and the costimulatory molecules CD80 and CD86 (B). Flow cytometry plots are representative of three independent experiments, and graphical data presents MFI of the marker within the parent population of three independent experiments (mean ± SEM) and were tested for significance using one-way ANOVA with Tukeys multiple comparison test where * $p<0.05$, **<0.01, ***<0.001.

3.5.2 Co-cultures of peptide loaded APCs and CD8 T cell clones

With the generation of activated, mature MoDCs, I was able to compare the cross-presentation potency between B cells and MoDCs to assess their ability to induce T cell responses (Figure 3-16). For peptide delivery to MoDCs, the 41-mer CMV polypeptide was added to the cells for the entirety of the 16 hour maturation phase. Peptide loaded APCs were co-cultured with CMV-specific CD8 T cell clones, with an increasing ratio of APCs to effector cells.

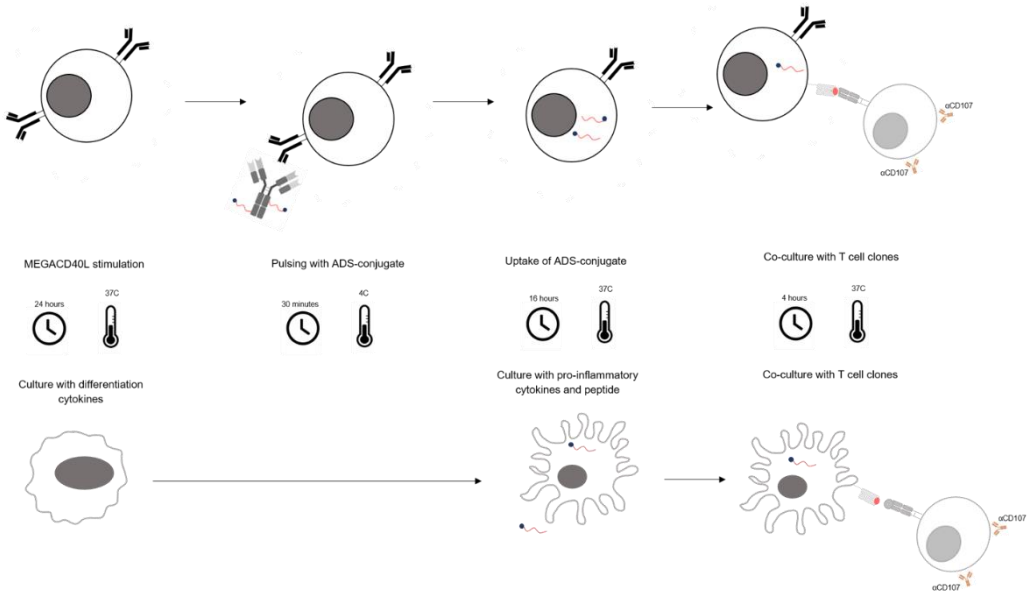

Figure 3-16 Experimental strategy for direct comparison of cross-presentation by ADS-conjugate pulsed B cells and MoDCs.

In line with previous experiments, induction of T cell responses was assessed by first setting gates on the positive (K562-A2-CMV) and negative (T cell clone alone) controls (Figure 3-10B,C). As seen in Figure 3-17A, B at a 1:1 ratio of APC to T cell clone, DCs and B cells showed a similar induction of T cell degranulation with an average of 49.5 $\pm$ 4.78% and 63.7 $\pm$ 3.3% CD107α positive T cell clones, respectively. As expected, for both APC subsets this level of induction decreased as the number of APCs in culture reduced. Data indicated a trend towards DCs inducing a higher response of T cell activation as compared to B cells at each ratio, however tests for significance between DCs and B cells showed no difference.

Taken together, data from this section show that both ADS-conjugate pulsed B cells, and peptide loaded DCs, are capable of inducing T cell cytotoxic responses and do so in a comparable manner. Thus, in this experimental setting, B cells can process and cross-present polypeptide at a similar ability to dendritic cells.

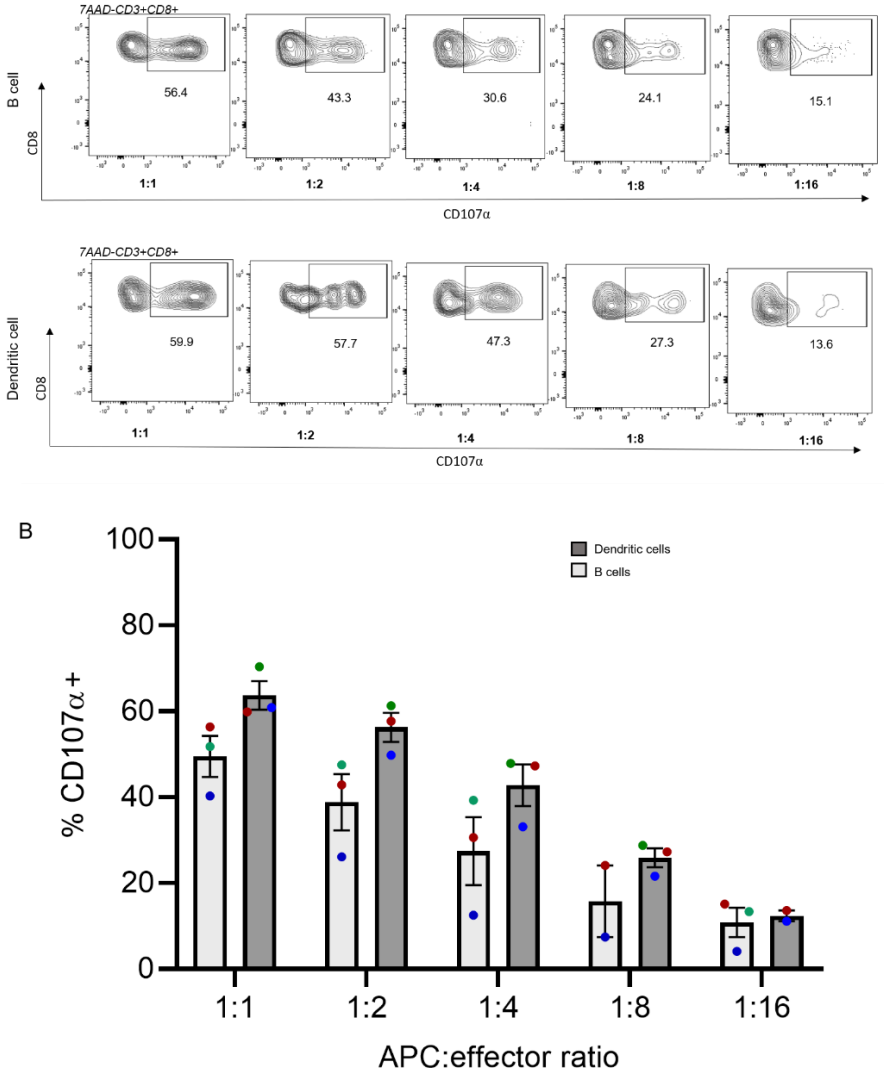

Figure 3-17 B cells induce a comparable amount of T cell degranulation as compared to MoDCs.

To compare the cross-presentation potency of B cells with DCs, both APCs were loaded with peptide and co-cultured with T cells at an increasing ratio of APC: effector cells and flow cytometry was used to measure the expression of CD107α as a marker of T cell degranulation. Flow cytometry plots are representative of data seen across three independent experiments and graphical data is presented as the % of CD107+ cells within the CD8+CD3+ T cell population of three independent experiments (mean + SEM) and were tested for significance using a two way ANOVA with Sidak's multiple comparison test. Significance was tested between DCs and B cells at each APC:effector ratio. Individual experiments are matched by colour of the data points.

3.6 Discussion

In this chapter, evidence has been presented to show that B cells can cross-present antigen to CD8 T cells, inducing cytotoxic T cell responses. Experiments support the development of an ADS that specifically delivers a 41-mer CMV polypeptide to the IgG-BCR of switched, memory B cells that have been activated in a CD40L-CD40 dependent manner. Subsequent co-culture of these cells with antigen-specific CD8 T cell clones results in expression of CD107α, a marker of effector function following stimulation. Importantly, this response appears to occur in a BCR-specific, HLA-restricted manner, and is comparable to that induced by the 'professional' antigen presenting cells - DCs. Thus, these findings suggest that B cells can mediate induction of CD8 T cell effector responses due to cross-presentation of exogenous antigen.

This is an important finding since it provides proof of principal evidence for the mechanistic role of B cells in T1D pathogenesis. B cell antigen cross-presentation and induction of CD8 T cell effector responses supports a disease model in which B cells could acquire autoantigen in the islets and cross-present to antigen-experienced CD8 T cells. This could then result in CD8 T cell stimulation and acquisition of a cytotoxic phenotype that is critical for β-cell destruction. The ability of B cells to cross-present antigen provides mechanistic reconciliation for the arrest of progression to a destructive insulitis seen in B-cell deficient NOD mice, and the significant reduction of intra-islet CD8 T cells seen in the absence of B cells (Brodie *et al.*, 2008; Mariño *et al.*, 2012). Importantly, it may provide a mechanistic explanation for the reduction of β-cell destruction seen in T1D patients treated with Rituximab, and presents a mechanism of action for the aggressive phenotype and accelerated loss of insulin-containing islets in T1D individuals with a CD20 high infiltrate phenotype (Pescovitz *et al.*, 2009; Leete *et al.*, 2016).

B cells exhibit antigen-specific immunoglobulin molecules on their cell surface that form the B cell receptor (BCR). This feature confers highly efficient, specific uptake of antigen, even at very low concentrations (Batista and Neuberger, 1998). Moreover, it is a critical property for B cell mediated induction of T cell stimulation, likely due to receptor mediated internalisation and delivery of antigen to the appropriate intracellular compartments for processing. Studies indicate that non-

antigen specific B cells lack the ability to induce T cell activation, or can only do so in the presence of very high antigen concentrations (Song *et al.,* 1995). Indeed, the importance of an antigen-specific BCR is also relevant to the role of B cells in T1D. Skewing of the receptor specificity reduces disease initiation and progression in the NOD mouse model (Mariño *et al.*, 2012; Packard *et al.*, 2016). To assess the ability of B cells to cross-present antigen, it was therefore critical to develop an ADS to model specific antigen uptake by the BCR *in vitro.* The amount of B cells that specifically recognise an antigen *in vivo* is relatively low; animal studies allow circumvention of this due to the availability of transgenic models. For example, the mouse strain MD4 carries rearranged heavy and light chain transgenes encoding HEL-specificity and was used by Robson *et al.*, (2008) to study B cell antigen presentation.

Previous *in vitro* studies using human cells have exploited properties of the BCR - using antibodies specific for certain immunoglobulin isotypes. This mimics an antigen-specific BCR and subsequently induces receptor mediated endocytosis and antigen delivery to the required intracellular compartments for antigen processing and presentation. Stevens and Peakman (1998) developed an ADS in which antigen delivery was achieved with three sequential components: i) a biotinylated antibody specific for human IgG, ii) an avidin molecule, and iii) a biotinylated antigen of interest. The current ADS extrapolated from this, conjugating an anti-IgG antibody to a 41-mer CMV polypeptide. Results presented in this chapter demonstrated specific delivery of polypeptide via the IgG-BCR of B cells. Stevens and Peakman postulated that a large amount of uptake in their experiments was mediated by the biotinylated antibody binding to additional endocytic surface receptors i.e. Fc receptors. This was due to the detection of biotinylated antigen on a larger frequency of the cell population that did not correlate with the expected proportion of IgG positive cells. In the present case, the population of cells positive for the ADS antibody mirrored the frequency of cells expressing an IgG-BCR in both the phenotyping studies and as reported in the literature (Seifert and Küppers, 2016). Additionally, an isotype control of the ADS antibody showed minimal surface binding. To definitively rule out Fc engagement of the ADS-conjugate, the ADS-antibody could have been replaced with a F(ab)’2 antibody structure. However, this

may have had technical implications on the conjugation process due to a reduction in the available amine groups.

The importance of BCR-mediated delivery of antigen is reflected in the current study, in experiments of CD8 T cell responses. Conjugation of the 41-mer polypeptide to the ADS antibody was necessary for significant induction of a cytotoxic CD8 T cell phenotype (CD107α expression). This data provides a clear indication that BCR-mediated uptake of exogenous antigen is necessary for induction of CD8 T cell responses. This is in line with the aforementioned studies that report enhancement of CD8 T cell responses induced by antigen-specific B cells in comparison to non-specific antigen uptake (Robson, Donachie and Mowat, 2008; de Wit *et al.*, 2010; Mariño *et al.*, 2012; Boldison *et al.*, 2019).

An interesting extension of the current findings would have been to directly measure the efficiency of the ADS as compared to passive, non-specific uptake of polypeptide over the 16-hour incubation. What concentration of polypeptide is needed to achieve the same level of CD8 T cell activation as that seen with the ADS? For example, in the context of CD4 T cell induction, an elegant study by Batista and Neuberger compared BCR-mediated uptake of soluble antigen with fluid phase pinocytosis. The authors found that to achieve the same level of T cell activation, a 5000 times greater concentration of antigen was required in the context of non-specific uptake (Batista and Neuberger, 1998).

Co-culture of CD8 T cells with ADS-conjugate pulsed B cells resulted in T cell expression of CD107α, a marker of T cell effector function following activation. This is consistent with B cell processing of the polypeptide and presentation of epitopes in the context of HLA Class I. Experiments using B cells isolated from HLA-A2 positive and negative donors supported this, as the TCR of the CD8 T cell clone was specific for the HLA-A2 restricted immunodominant CMVpp65 epitope.

Literature has extensively demonstrated that B cells possess the cell surface molecules necessary for functional interaction with CD8 T cells (i.e. co-stimulatory molecules and MHC class molecules) as well as the intracellular machinery required for processing of intracellular antigen through the classical HLA class I pathway. For example, exogenous loading of B cells with short (9-mer) HLA class-I binding

peptides have induced robust cognate CD8 T cell effector responses, presumably through direct binding of the peptide to surface HLA class I molecules (Schultze *et al.*, 1997). Additionally, RNA-transfection of B cells with an mRNA encoding the antigen of interest (providing an intracellular source) has been shown to induce functional, cognate CD8 T cell responses (Coughlin *et al.*, 2004).

Studies into B cell cross-presentation of exogenous antigen, however, are not so well defined. Seminal studies in the 1990s showed that BCR-mediated uptake of soluble protein antigen by murine B cells could prime CD8 T cells *in vitro* (Ke and Kapp, 1996). Building on this, naïve antigen-specific B cells purified from the B cell transgenic HEL-specific MD4 mouse model were incubated with their cognate antigen and co-cultured with HEL-specific CD8 T cells (Robson, Donachie and Mowat, 2008). Here, CD8 T cell proliferation was significantly induced, and at a much higher level than when CD8 T cells were co-cultured with (non-specific) B cells isolated from wild-type mice. Significant to a T1D research context, B cells were necessary for the post-insulitic expansion of self-reactive CD8 T cells and acquisition of T cell effector function in NOD mice. Selective removal of surface MHC class I molecules from the B cells resulted in disease protection. This was characterised by the inability of NOD mice to convert from silent insulitis to overt disease; solidifying the importance of B cell presentation of peptide MHC CI complexes to self-reactive CD8 T cells (Mariño *et al.*, 2012). The novel finding that switched-memory human B cells stimulated in a CD40 dependent manner can induce antigen-specific CD8 T cell effector responses, extend these previous studies. Data presented in this chapter clearly demonstrate antigen cross-presentation by a disease relevant subset of B cells.

In the current study, T cell degranulation (CD107α expression) was used as a surrogate readout for acquisition of effector function following activation i.e. cytotoxicity, as is well documented in the literature (Knight *et al.*, 2015). *In vivo* the primary effector outcome of CD8 T cell activation is their ability to kill target cells. This occurs through Fas-FasL interactions, or through perforin-granzyme-mediated activation of apoptosis, for which T cell degranulation is a prerequisite (Section 1.6.2). Therefore, testing for the induction of target cell death (i.e. the antigen presenting B cell) following antigen cross presentation within the co-culture system

would further bolster the conclusion that B cells are cross presenting antigen to induce CD8 T cell cytotoxic responses. For example, de Wit *et al*., (2010), who showed that B cells were able to induce CD8 T cell IFNγ production and CD107α expression through antigen cross presentation, also found that the activated CD8 T cells were cytotoxic as they could specifically kill the *Salmonella*-infected B cells. Specific lysis of the B cells was measured by ^{51}Cr release.

Internalisation of the ADS antibody and the loss of cell surface polypeptide over time in my experiments was consistent with intracellular processing of the antigen. T2 cells showed no stabilisation of HLA class I complexes with the addition of 'free' 41-mer CMV polypeptide, suggesting no extracellular processing. What this study failed to address, however, was the intracellular route used by the B cell for polypeptide processing. Induction of CD8 T cell responses allow speculation that the BCR-mediated uptake of antigen in the *in vitro* setting results in receptor mediated endocytosis and polypeptide targeting to the classical MHC class I processing pathway (Ke and Kapp, 1996). Broadly, this includes proteasomal degradation of proteins, transport of resultant peptides into the ER and loading onto MHC CI molecules. Indeed, Marino *et al.,* (2012) identified rapid co-localisation of fluorescently labelled insulin antigen with EEA1-positive endosomes in NOD B cells, indicating targeting of antigen to early endosomes. These distinct endosomal compartments are associated with antigen protection, as the high pH is critical for protection against rapid lysosomal degradation (Gondre-Lewis, Moquin and Drake, 2001). In line with this, another study using EBV-transformed B cell lines loaded with CMVpoly protein showed strong colocalization of antigen with EEA1, but no relocation to late endosomes or lysosomes (Dasari *et al.*, 2016).

Marino *et al.,* (2012) showed that addition of proteasome inhibitors prior to B cell pulsing with insulin reduced CD8 T cell activation, as did the addition of BFA to inhibit protein transport into the ER. Authors therefore concluded that B cell cross-presentation to CD8 T cells involved key components of the endogenous MHC CI-restricted pathway, and that antigen was processed in a proteasome, TAP-dependent manner. In line with this pathway, CD8 T cell responses induced after delivery of antigen in immune-stimulating complexes to antigen-specific murine B cells, were significantly decreased with the individual addition of chloroquine, lactacystin or

brefeldin A (Robson, Donachie and Mowat, 2008). Endosomal acidification, proteasomal processing and ER protein transport, respectively, were therefore found to be central components to B cell presentation of MHC CI/peptide complexes. In human B cells in which uptake of *Salmonella* was mediated through the BCR, antigen presentation was also shown to be proteasome dependent. Whether this was due to specific properties of *Salmonella* such as antigen translocation from the unique *Salmonella*-containing vacuole is unclear (de Wit *et al.*, 2010). Interestingly, one study reported loading of T cell epitopes onto MHC CI within the autophagosomal compartment due to TAP-independence in B cells (Dasari *et al.*, 2016). The use of lymphoblastoid cell lines in this study do not necessarily model BCR-mediated uptake of antigen. This may reconcile the dependence on the autophagosomal pathway, as B cell antigen processing and presentation through the classical MHC class I pathway is a function of BCR mediated endocytosis (Ke and Kapp, 1996). Therefore, it can be speculated through previous evidence, that in this experimental setting B cells are targeting antigen through the classical MHC class I processing route. Additional data to test this hypothesis could have been generated by using inhibitors that would compromise the classical pathway of antigen transport. Interestingly, reports have also shown that IFNα enhances cross-presentation in human dendritic cells due to induction of a preferential ability to prevent early degradation of the internalised antigen, and through enhanced routing of antigen to the MHC class I processing pathway (Spadaro *et al.*, 2012). Addition of IFNα into the co-cultures and assessment of CD8 T cell degranulation would further elude to the pathway of B cell cross presentation.

To further clarify the role B cells may play in T1D pathogenesis, the ability of B cells to cross-present antigen to that of DCs was compared. As aforementioned, DCs are considered the most relevant APC in governing CD8 cytotoxic responses. This is evidenced by their possession of intracellular machinery required for antigen processing and presentation (Jung *et al.*, 2002). Therefore, it was necessary to show B cells have a comparable efficiency if they are to be important in disease pathogenesis. To generate DCs, a previously published protocol was modified (Dauer *et al.*, 2003). In line with results presented in this chapter, authors showed that the differentiation and maturation of DCs from monocytes resulted in a mature

DC immunophenotype ($CD80^+$ $CD86^+$ MHC CII^+). Importantly, these cells carried the ability to activate T cells after addition of antigen.

Generation of MoDCs allowed a direct comparison to activated B cells with regard to cross-presentation ability. A comparable induction of CD107α expression was identified between the DCs and B cells at increasing ratios of APC: T cell. No significant differences were seen between the two APC subsets, providing evidence that B cells have an alike ability to cross-present antigen to DCs. A similar study in animal models devised experiments to compare antigen presentation between antigen-specific CD40-L activated B cells and DCs. In concordance, no significant differences were identified between responses induced with DCs to those induced by CD40L-activated B cells (Ahmadi *et al.*, 2008). T cell populations used, however, were isolated based on their CD3 positivity. Induction of CD4 and CD8 T cell responses was not differentiated. Instead, the authors extrapolated evidence from experiments comparing DCs and B cells pulsed directly with HLA class I binding peptides.

Although not significant, at all ratios, it was observed that B cells showed a trend towards decreased induction of CD8 T cell effector responses as compared to DCs. It can be speculated that this is not due to the ability to cross-present antigen. Instead, it can be attributed to the expected differences in expression levels of HLA CI and co-stimulatory molecules that correlate with the surface area of the cell. For example, DCs are larger and would therefore express more HLA CI and co-stimulatory molecules. Additionally, the efficiency with which the antigen-specific B cells induce responses may be underestimated due to the nature of the ADS only targeting a proportion of the B cell population (IgG-BCR, ~60%). This therefore presents the need for an extension of these studies to enhance the accuracy of a direct cell-cell comparison, such as standardisation for cell size and/or surface expression of HLA and co-stimulatory molecules.

It is important to note that cross-presentation by DCs and B cells may not be a mutually exclusive event in T1D pathogenesis - each APC is likely to operate in spatially and timely distinct areas. Indeed, de Wit *et al.*,(2010) showed that in the context of *Salmonella*, antigen-specific B cells were unable to induce significant proliferation of naïve CD8 T cells but were superior in activating memory CD8 T

cell populations as compared to DCs. DCs, on the other hand, were optimal activators of naïve CD8 T cells. B cell depletion from NOD mice has consistently been reported to prevent progression to an overt disease, but not affect the initial development of insulitis in the islets i.e. the priming stage. This suggests B cells are engaged in a late pathogenic event that is important in disease acceleration, as opposed to disease initiation (D. V. Serreze *et al.*, 1996; Akashi *et al.*, 1997).

Taken together, this allows speculation of a model in which DCs may be important in the initial activation and priming of naïve CD8 T cells, while B cells are necessary for the (re)stimulation of antigen experienced CD8 T cells and acquisition of effector function in the islets – driving β-cell destruction. Indeed, in pre-clinical NOD mouse models, this phenomenon has been reported to occur specifically in the islets. Initial contact with antigen and activation of IGRP-specific CD8 T cells occurred in the pLN, however differentiation into a stable effector memory phenotype was only seen in the islets (Chee *et al.*, 2014). Autoreactive CD8 T cells in the islets also exhibited higher expression of cytotoxic effector molecules (Graham *et al.*, 2011). Authors showed that this resulted from a stimulation event in the islet that was independent of antigen presentation by the β-cell itself. Interestingly, activation of CD40-expressing cells enhanced this increase in CD8 T cell cytotoxic function further, and heightened β-cell destruction. Therefore, in NOD mice, cytotoxic function becomes complete in the islet, likely due to cognate stimulation from APC i.e. B cell cross-presentation of islet autoantigen. This in is line with studies of circulating antigen specific CD8 T cells in cohorts of T1D individuals. Effector memory phenotypes correlate with β-cell function, suggesting antigen driven acquisition of this phenotype in the islets, due to tissue specific inflammatory responses (Yeo *et al.*, 2018).

Questions remain in this model, however. My data shows DCs are as capable of inducing CD8 T cell effector function as B cells. Additionally, DCs have been detected in the islets of T1D individuals (Rosmalen *et al.*, 2000) – what would lead to favourable antigen presentation by B cells? It is most likely that in the context of autoimmunity, which is not encapsulated within this study, the preferential role of B cells as APC lies in the favourable properties conferred by the antigen-specific BCR.

The BCR allows uptake of very low concentrations and/or limiting concentrations of antigen, such is often the case in tissue specific autoimmunity.

As eluded to, a limitation of my study is that while I provide evidence of antigen cross-presentation by B cells to induce CD8 T cell responses, it is in the context of a high affinity viral epitope. I do not provide evidence that this is operative with epitopes of low-medium affinity, such as the characterised CD8-restricted self-epitopes in T1D pathogenesis. A generalisation of the relationship between peptide affinity and immunogenicity in the context of MHC class I is a positive correlation. High affinity peptides display invariable immunogenicity as opposed to those of low-medium affinity (Sette *et al.*, 1994). However, anti-insulin specific B cells pulsed with insulin antigen showed induction of CD69 and IFNγ expression on CD8 T cells upon co-culture (Mariño *et al.*, 2012; Boldison *et al.*, 2019). This indicates that B cells are able to process and present lower affinity autoantigens (insulin) that induce effector T cell responses.

Interestingly, it has been reported that the affinity of the epitope for MHC class I can determine the helper requirement for the APC to induce productive CD8 T cell activity. This presents in the form of APC interaction with CD4 'helper' T cells in a CD40-CD40L dependent manner (Franco *et al.*, 2000). Peptides that bind to the relevant MHC class I restriction element with high affinity *in vivo* do not require T cell help to induce and sustain CD8 T cell activity. Antigens with low affinity require a source of help to induce productive effector T cell responses. As shown in this chapter, CD40-CD40L activation of the B cells results in an upregulation of co-stimulatory molecules. B cells in the islets of NOD mice have replete surface expression of CD80 and CD86 (Hussain and Delovitch, 2005). Expression is increased at onset of diabetes and is higher in insulin-specific B cells as compared to non-specific cells (Mariño *et al.*, 2012; Boldison *et al.*, 2019). This suggests that autoantigen-specific B cells in the islets have been provided with 'help' by CD4 T helper cells. Perhaps it is this property that allows the B cells to compensate for low-medium (HLA class I) affinity of autoantigens and still induce functional CD8 T cell responses. Indeed, in the context of *Salmonella*, CD4 T cell help was critical for the induction of CD8 T cell responses by antigen-specific B cells (de Wit *et al.*, 2010). A development of my studies would therefore be to first assess the ability of B cells to

cross-present T1D-relevant autoantigen, using autoantigen-derived polypeptides in the ADS and CD8 T cell clones specific for their cognate autoantigen. Secondly, the dependence on T cell help could be determined by comparing induction of T cell responses by CD40L-stimulated and unstimulated B cells.

Extending this notion, an additional consideration of the current study is the use of a singular stimulation signal (CD40-CD40L ligation). *In vivo* it is unlikely that B cell stimulation occurs as a single signal. If T cell help is required for cross presentation of low affinity autoantigens, cytokines such as IL21 and IL4 secreted by the T cells are also likely to cooperate with CD40 signals to endow optimal B cell stimulation and operative antigen presentation (Franke *et al.*, 2020). Inclusion of these cytokines in the co-cultures may more accurately encompass B cell stimulation that occurs *in vivo.*

Additionally, the avidity of the TCR interaction with the HLA-peptide complex should also be considered when speculating on B cell cross-presentation of disease specific autoantigens. In comparison with virus-specific CD8 T cells, CD8 T cells specific for the islet autoantigen PPI displayed significantly lower killing capacity of target cells (Knight *et al.*, 2013). Authors suggested a cell extrinsic explanation for this reduction in effector function: the TCR of the PPI-specific CD8 T cell clone has known ultra-low affinity for cognate peptide-HLA, while the TCR of the virus-specific CD8 T cell clone displays high affinity for its cognate HLA-peptide complex. This results in a lower avidity interaction between the PPI-specific CD8 T cell and its target cell, likely reducing signalling by peptide-HLA ligands and therefore limiting the effector functions of the cell. In relation to the current study in which a virus-specific CD8 T cell clone is used, it is necessary to keep in mind the resultant high avidity interaction that is unlikely to be the case *in vivo* in the case of disease relevant autoantigens. This bolsters the experimental extension to use autoantigen-derived polypeptides in the ADS.

Concluding remarks

In summary, work presented in this chapter demonstrates the development of a robust antigen delivery system to mimic antigen-specific B cells *in vitro*. Conjugation of a 41-mer viral polypeptide to an anti-IgG antibody results in targeted

delivery to the BCR of class-switched, memory B cells activated in CD40-CD40L dependent mechanism. Evidence presented supported internalisation of the ADS complex for polypeptide processing. Using a CD8 T cell clone specific for the immunodominant epitope central to the viral polypeptide, a series of experiments showed that ADS-pulsed B cells were able to induce degranulation of the T cell clone – supporting cross-presentation of exogenous antigen by the B cell. Importantly, this induction was specific for the ADS, as ADS components alone showed little to no response, and the CD8 response was HLA-restricted. Generation of monocyte-derived dendritic cells allowed a direct comparison of the cross-presentation potency with B cells, and experiments showed comparable responses.

Overall, although in the context of a high affinity viral epitope, data presented in this chapter demonstrate that B cells can cross-present antigen in order to induce CD8 cytotoxic activity; a mechanistic concept that may be central to their role in β-cell destruction and progression of T1D.

4 CHARACTERISATION OF THE INTERACTION BETWEEN B CELLS AND CD8 T CELLS

4.1 Background

In the previous chapter I established an antigen delivery system to assess cross-presentation of antigen by B cells. This utilised an anti-IgG antibody to efficiently deliver a 41-mer polypeptide to the BCR of primary human B cells for processing and antigen cross-presentation.

Data provided proof of principle that B cells can cross-present exogenous antigen for recognition by CD8 T cells, resulting in the acquisition of CD8 T cell effector function. This process may be involved in sustaining the self-perpetuating nature of CD8 T cell mediated β-cell destruction in the pancreatic islets (in pre-clinical models) after initiation of the autoimmune response (Friedman *et al.*, 2014). In addition to antigen presentation, further qualitative and quantitative parameters of the APC-CD8 T cell interaction are known to modulate CD8 T cell fate and effector state (Curtsinger *et al.*, 1999). These include co-stimulatory molecules and adhesion molecules, as well as inflammatory related effector molecules such as cytokines and chemokines, and inhibitory co-receptors including PD-1 and CTLA-4. Therefore, pathways of additional capacities may occur between B cells and CD8 T cells that are important for optimal activation of effector CD8 T cells in the inflamed tissue. Interrogating the molecular cross talk that governs the effector state of autoreactive CD8 T cells in T1D could elucidate potential nodes of therapeutic intervention.

Thus, the main aim of this chapter was to characterise the interaction between B cells (as an APC) and CD8 T cells, using the previously established *in vitro* ADS and co-culture system. The hypothesis of the study is that molecular cross-talk exists between the two cells that is relevant to their interaction. This cross-talk may synergise with the signals from B cell cross-presentation in order to induce or optimise effective CD8 T cell cytotoxic function. Specifically, this study aims to 1) develop a methodology to identify interacting B cells and CD8 T cells in *in vitro* co-cultures and 2) determine key factors that contribute to their interaction.

Additionally, a transcriptomic approach will be used to dissect molecular cell-cell communication pathways between B cells and CD8 T cells through identification of ligand: receptor pairs.

4.2 Identification of B:CD8 doublets interacting CD8 T cells and B cells in co-cultures of ADS-conjugate pulsed B cells and CD8 T cell clones

4.2.1 Gating strategy to identify doublets

To elucidate the interaction between cross-presenting B cells and CD8 T cells, I sought to identify interacting cells within the co-cultures of ADS-conjugate pulsed B cells and antigen-specific CD8 T cell clones.

The gating strategy in Figure 4-1A was used to identify cell doublets by analysing CD20 and CD8 expression. In comparison to single cells, doublets exhibit a higher FSC/SSC distribution and the first lymphocyte gate was extended to include this, whilst still excluding debris. A 'doublet' gate was established in an FSC-A vs FSC-H plot, where doublets were detected due to higher FSC-A values in comparison to the 'singlet' gate. Living cells were selected before gating on $CD3^{+}CD8^{+}$ doublets. From this parent population, the $CD20^{+}CD8^{+}$ doublets were detected as simultaneously expressing CD20 and CD8. A large population of $CD20^{+}CD8^{+}$ doublets were identified in co-cultures of ADS-pulsed B cells and CD8 T cell clones (Figure 4-1A). Back gating of the $CD20^{+}CD8^{+}$ doublet cell population showed no overlap with the single B cell population or single CD8 T cell population (Figure 4-1B). Flow cytometry parameters were therefore able to segregate CD8 T cells and B cells in a doublet versus those not in a doublet. These data suggest $CD20^{+}CD8^{+}$ doublets may represent a stable interaction between T cells and ADS-conjugate pulsed B cells.

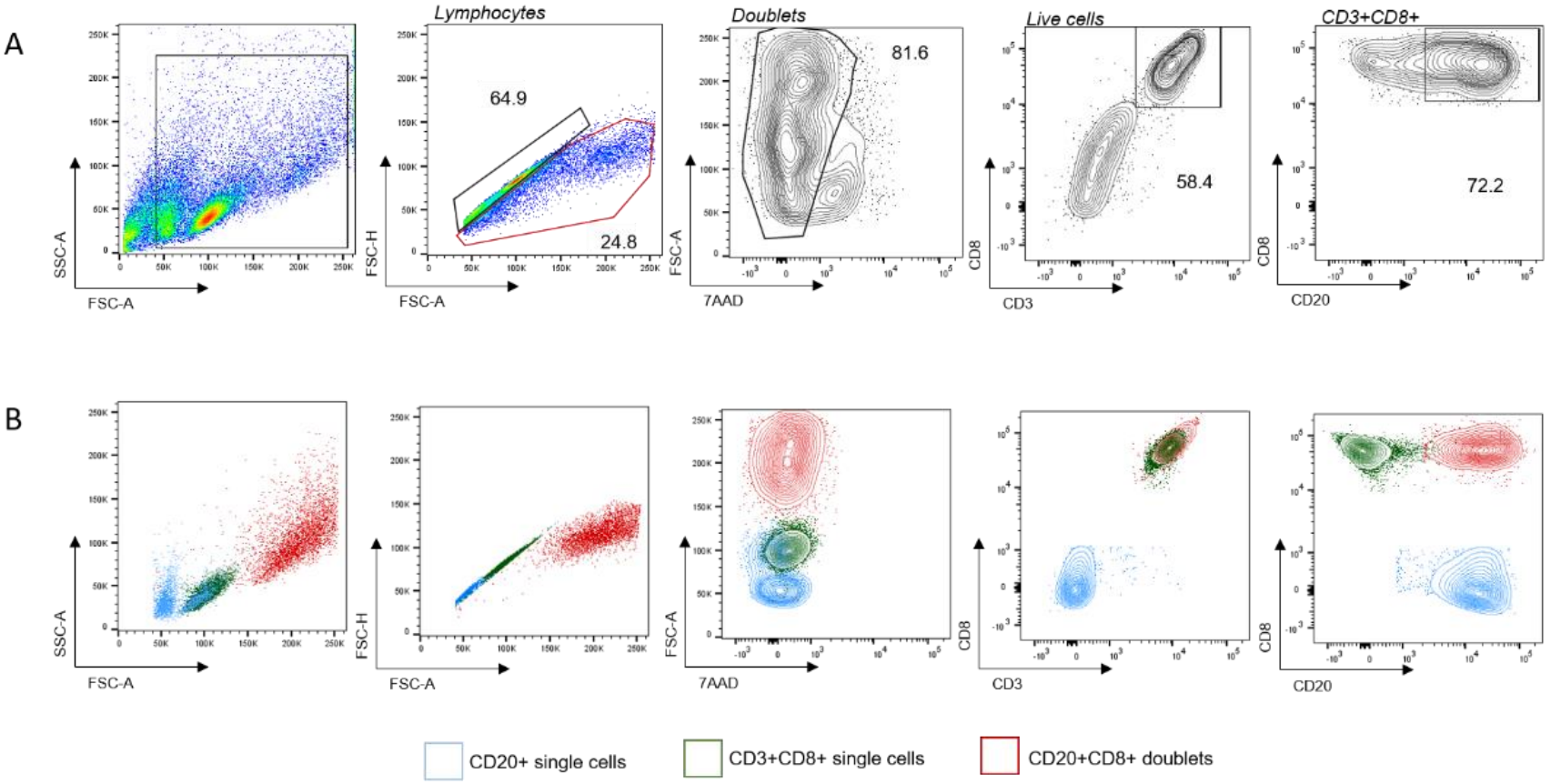

Figure 4-1 CD20^{+}CD8^{+} cell doublets are identified in co-cultures of ADS-pulsed B cells and CD8 T cell clones and are a distinct population.
Gating strategy to identify cell doublets and confirm their segregation from single cell populations using back gating (A, B). B cells were pulsed with ADS-conjugate and cultured for 16 hours prior to co-culture with antigen-specific CD8 T cell clones. Doublets were identified as a population with higher FSC/SSC in the doublet zone of FSC-A/FSC-H (gate in red in panel A, population in red in panel B), showing dual expression of CD8 and CD20.

4.2.2 Visualisation of doublets in co-cultures using imaging flow cytometry

To provide stronger evidence for the presence of doublets within the co-cultures, imaging flow cytometry (Amnis Imagestream) was utilised to visualise the $CD20^{+}CD8^{+}$ doublets directly. Using the same experimental approach, and a similar gating strategy, a $CD20^{+}CD8^{+}$ doublet gate was established (Figure 4-2A, R4). $CD20^{+}CD8^{+}$ doublets were clearly identified as a CD20 B cell in very close association (Brightfield) with a $CD3^{+}CD8^{+}$ T cell (Figure 4-2B).

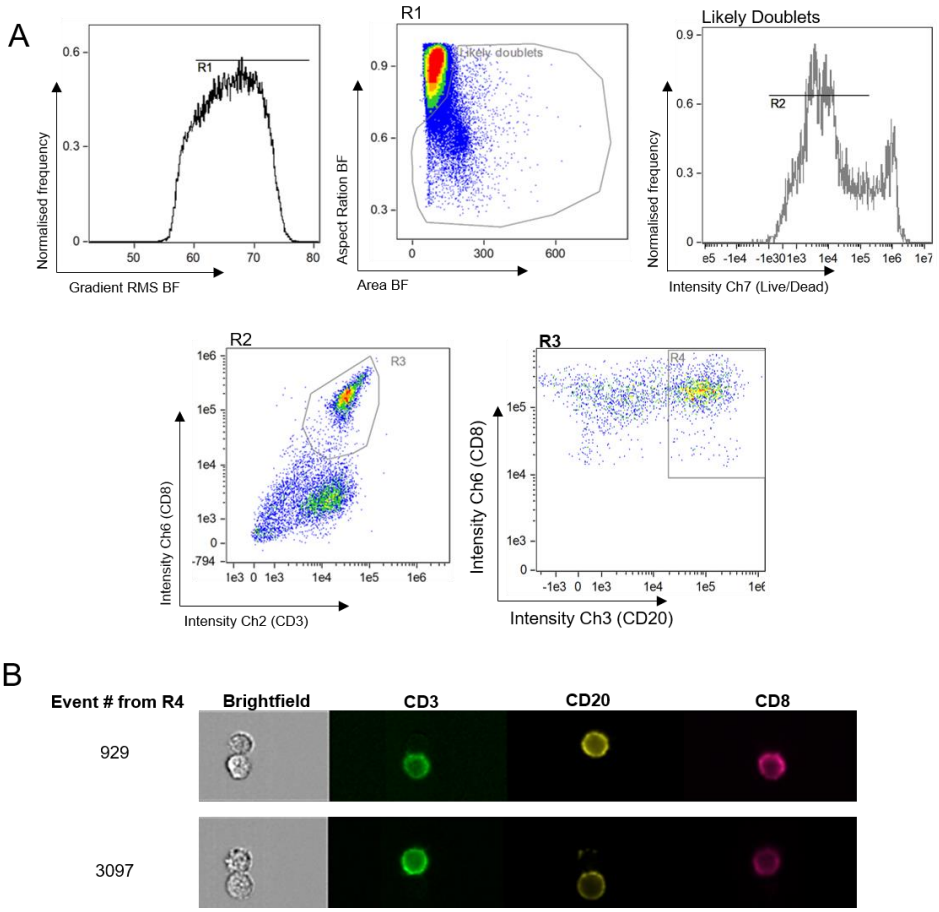

Figure 4-2 $CD20^{+}CD8^{+}$ cell doublets can be visualised using Imagestream.
Cell doublets were identified by Imagestream using a gating strategy similar to that used in flow cytometry (A) in order to visualize $CD20^{+}CD8^{+}$ cell doublets (B). Cell images are individual events representative of all events detected in the R4 population.

These findings support the flow cytometry data and the concept that the $CD20^{+}CD8^{+}$ cell doublets consist of B cells interacting with CD8 T cells (herein referred to as B:CD8 doublets). Additionally, clear brightfield identification of two distinct cells within the doublet gate rejects the possibility that they are occurring due to trogocytosis or are artefacts of the flow cytometry staining and processing i.e. nonspecific binding or debris.

4.3 Characterisation of B:CD8 doublets in *in vitro* co-cultures

4.3.1 Impact of B cell presentation of cognate peptide on doublet formation

In addition to data from Chapter 1, detection of B:CD8 doublets in co-cultures of ADS-conjugate pulsed B cells and CD8 T cells suggested that doublets were forming due to B cell cross-presentation of antigen. To test this hypothesis, I sought to investigate the role of antigen cross-presentation by the B cell on B:CD8 doublet formation. B cells were either pulsed with the ADS-conjugate to allow antigen delivery through the BCR or pulsed with conjugate buffer alone. As a positive control, cells were pulsed with the cognate target of the CD8 T cell clone (9-mer CMVpp65 peptide) to allow direct binding to the HLA class I molecules. B cells were co-cultured for four hours with CMV-specific CD8 T cell clones (Figure 4-3), and the gating strategy applied to identify the B:CD8 doublets (Figure 4-1A).

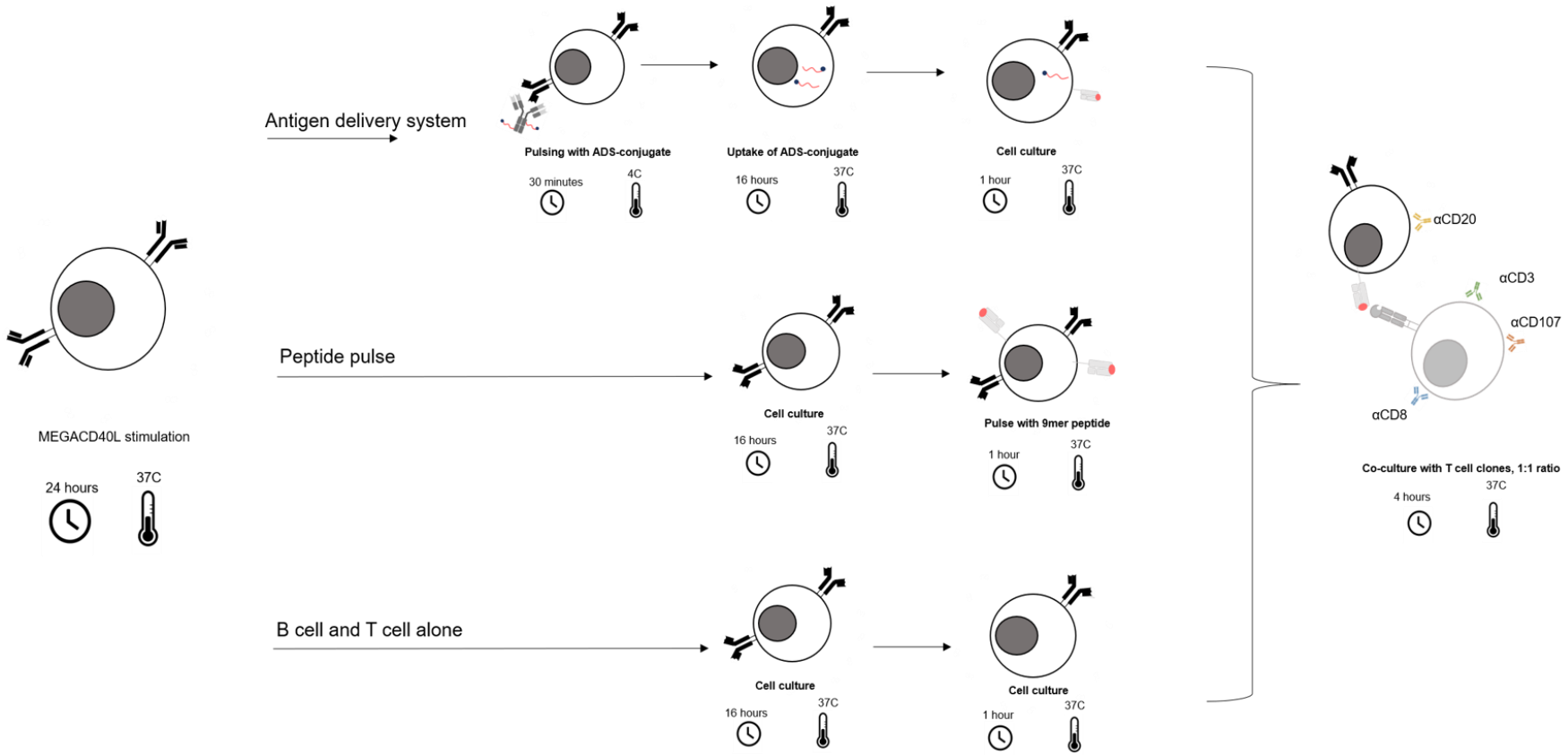

Figure 4-3 Experimental strategy to characterise B:CD8 doublets *in vitro.*

B cells were either pulsed with the CMV ADS-conjugate, with the 9-mer CMV pp65 or with no peptide before co-culture for 4 hours with CD107α-labelled CMV-specific CD8 T cell clones.

As expected, doublets were identified in conditions where peptide was present. No significant differences in the frequency of doublets depending on how peptide was presented by the HLA class I molecule (i.e. via presentation of endocytosed antigen or via presentation of pulsed peptide) was found.

The frequency of B:CD8 doublets within the $CD3^{+}CD8^{+}$ parent gate was 73.83 % $\pm$ 1.63 for ADS-conjugate pulsed B cells, and 84.1 % $\pm$ 3.13 for 9-mer CMVpp65$^{(495-503)}$ peptide pulsed B cells (Figure 4-4A). Surprisingly, a B:CD8 doublet population (72.10 % $\pm$ 7.1%) was observed within co-cultures of B cells and CD8 T cell clones in which no peptide was present on the B cell (Figure 4-4A). There were no statistically significant differences in the frequency (%) of B:CD8 doublets across all conditions (Figure 4-4B).

These data suggest that B:CD8 doublets form independently of the presence of peptide on the B cell and may represent a stable interaction between B cells and CD8 T cells. Additionally, delivering antigen through the BCR (ADS-conjugate) resulted in no significant differences in the frequency of B:CD8 doublets. Therefore, their formation is not dependent on changes that occur to the B cell upon treatment with the ADS-conjugate, such as stimulation of the BCR or antigen processing.

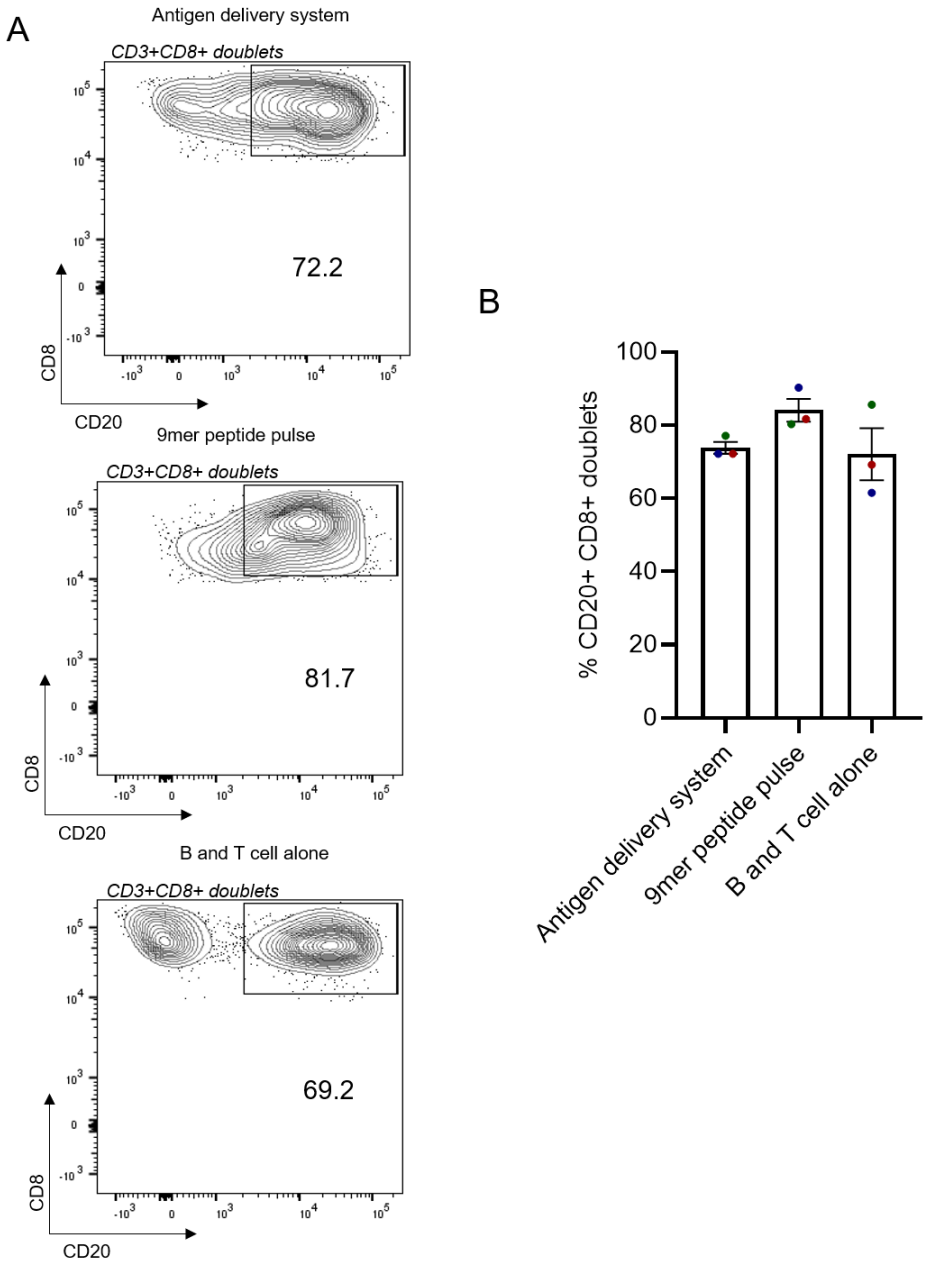

Figure 4-4 B:CD8 cell doublets are present in co-cultures of B cells and CD8 T cell clones, independent of the presence of peptide on the B cell surface.

B cells were either pulsed with the CMV ADS-conjugate, with the immunodominant 9mer CMV peptide sequence or with no peptide before co-culture for 4 hours with CMV-specific CD8 T cell clones (A) for detection of B:CD8 cell doublets (B). Flow cytometry plots are representative of three independent donors and graphical data presents the average frequency (%) of B:CD8 cell doublets from the parent population of each condition (mean ± SEM) and were tested for significance using a one-way ANOVA with Tukeys multiple comparison post-hoc test. Individual experiments are matched by colour of the data points.

4.3.2 Functional analysis of B:CD8 doublets

4.3.2.1 Formation of a mature immunological synapse between B cells and CD8 T cells

While doublets form in the absence of peptide, functional T cell activation only occurs with HLA-peptide presentation (Chapter 3). This prompted me to investigate the functional relevance of B cell antigen presentation within the B:CD8 doublet. T cell activation occurs via the formation of an immunological synapse (Dustin, 2014). Using imaging flow cytometry, the immunological synapse between an APC and a T cell can be visualised, and therefore the formation of a 'mature' immune synapse required for downstream T cell function can be assessed. B cells were either pulsed with the 9-mer CMV pp65 peptide for direct binding to the HLA class I molecule, or with DMSO as a negative control, before the 4 hour co-culture with CMV-specific CD8 T cell clones. Using the gating strategy previously specified (Figure 4-2A), B:CD8 doublets were identified in each condition. For immunological synapse analysis, an interface mask was generated using the T cell and B cell morphology masks (CD8 and CD20 staining, respectively) (Figure 4-5A), that identified pixels within the contact zone between the two cells (Figure 4-5B,C). The mean pixel intensity (MPI) of CD3 within the interface mask divided by the MPI of CD3 in the T cell morphology mask was then used to generate a value representative of CD3 accumulation at the interface - a formal marker of a mature, functional immunological synapse (Krummel *et al.*, 2000). The presence of peptide on the B cell resulted in clear concentration of CD3 at the immunological synapse, as indicated by the mean and median CD3 accumulation values (6.3 and 5.99, respectively), and the distinct staining pattern at the interface of the two cells (Figure 4-5C). In comparison, without peptide the immune synapse did not form. CD3 staining on the T cell remained uniform around the perimeter of the cell, as shown by the CD3 accumulation at the immunological synapse values being close to 1 (Figure 4-5D). Thus, antigen presentation of peptide by the B cell is required for the formation of a mature immunological synapse between the interacting B cells and CD8 T cells, i.e. the B:CD8 doublet.

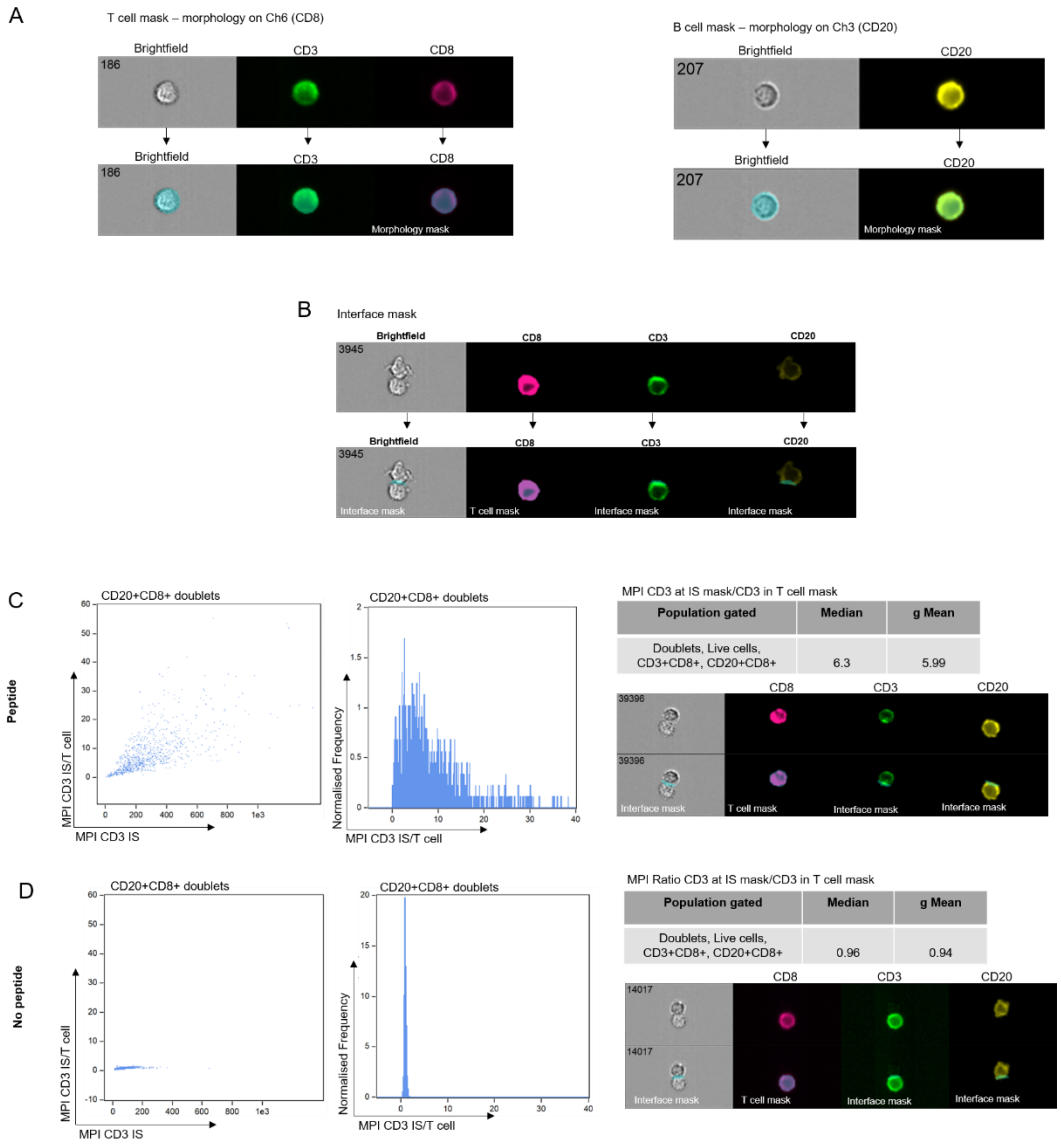

Figure 4-5 The presence of peptide on the cell surface of the B cell results in CD3 enrichment at the interface of the B:CD8 doublet

B cells were pulsed with either the 9-mer CMV pp65 or DMSO control and co-cultured with CD8 T cell clones. To determine CD3 accumulation at the interface of the doublet, morphology masks were first established for CD8 T cells and CD20 B cells (blue) (A) and an immunological synapse (IS) mask (blue) was then computed by using the interface mask function (3 pixels) to establish the interface between the T cell morphology mask (cell of interest) and the B cell morphology mask (conjugate) (B). CD3 accumulation within the IS was then calculated (median and geometric mean) by calculating the mean pixel intensity of CD3 within the IS mask divided by the mean pixel intensity of CD3 in the T cell morphology mask in cells pulsed with (C) and without (D) peptide. Images are representative of events detected by Imagestream.

4.3.2.2 Induction of cytotoxic CD8 T cell responses within doublets

Antigen presentation by B cells resulted in CD3 accumulation at the interface of the B:CD8 doublet, indicative of a mature immune synapse that is required to induce a T cell responses. I next investigated whether this would result in functional activation of CD8 T cells within the B:CD8 doublets.

The frequency (%) of B:CD8 doublets positive for CD107α, a marker of effector function following T cell activation, was significantly higher when antigen (cross-) presentation by the B cell was occurring, as opposed to when no peptide was present (74.5 % ± 1.8, 14.4 % ± 4.7, respectively). Nearly all B:CD8 doublets stained positive for CD107α after B cells were pulsed with the 9-mer CMVpp65 (97.6 % ± 0.8), and a high proportion stained positive when antigen was delivered via the ADS-conjugate (74.5 % ± 1.8). In contrast, in co-cultures of B and CD8 T cells alone (without peptide), only a few B:CD8 doublets were positive for CD107α (14.4 % ± 4.7) (Figure 4-6).

Taken together, these data show that B:CD8 doublets form in the *in vitro* co-cultures, suggesting a biological interaction. Interestingly, these occur independently of antigen (cross-)presentation by the B cell. However, formation of a mature immune synapse within the B:CD8 doublet and subsequent cytotoxic activity requires peptide presentation. This indicates that other biological factors, besides antigen presentation and recognition of cognate peptide, may be relevant for the observed interaction.

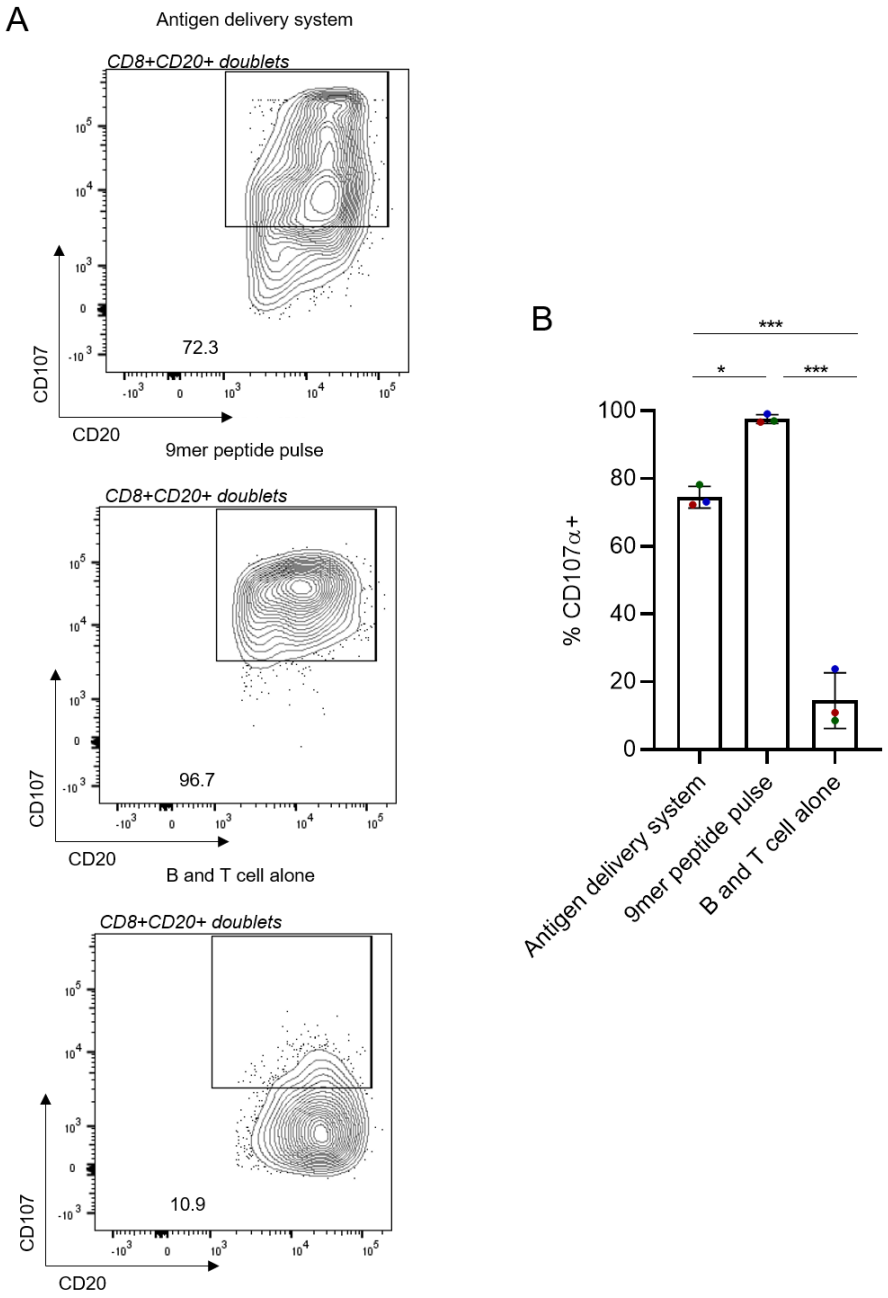

Figure 4-6 B:CD8 doublets express CD107α when B cells are pulsed with the ADS-conjugate, or the 9-mer CMV pp65 peptide but not when B cells and CD8 T cell clones are co-cultured alone.

B cells were either pulsed with the CMV ADS-conjugate, with the 9-mer CMV pp65 or with no peptide before co-culture for 4 hours with CMV-specific CD8 T cell clones in the presence of anti-CD107α for detection of CD107α positive B:CD8 cell doublets (B). Flow cytometry plots are representative of three independent donors and graphical data presents the average frequency (%) of CD107α+ positive cell doublets from the parent population (B:CD8 doublets) of each condition (mean ± SEM), and were tested for significance using a one-way ANOVA with Tukeys multiple comparison post-hoc test where ** <0.01, ***<0.001. Individual experiments are matched by colour of the data points.

4.3.3 Impact of HLA class I molecules on B:CD8 doublet formation

Interactions between cognate HLA molecules and T cell receptors have been reported to occur in a peptide independent manner- a biological phenomenon that mediates TCR scanning of a diverse milieu of peptides presented by MHC molecules in order to recognise a cognate peptide (Wu *et al.*, 2002). I wanted to address whether interaction between the cognate HLA class I molecule (i.e. HLA-A2 as the CD8 T cell clone is restricted towards an HLA-A2 restricted epitope) and the TCR of the CD8 T cell clone was pertinent to the formation of the B:CD8 doublets.

B cells were isolated from HLA-A2 positive or negative donors and the same experimental approach was used as previously (Figure 4-3). Co-cultures of HLA-A2 positive B cells with CD8 T cell clones resulted in the same level of B:CD8 doublet formation as seen previously, across all conditions (Figure 4-7A). Interestingly, the absence of HLA-A2 on the B cell resulted in a significant reduction in B:CD8 doublet formation (Figure 4-7B). This appeared to be entirely dependent on B cell surface expression of HLA-A2 and not the presence of peptide, as the extent of the reduction in doublet formation was consistent across all conditions. B cells pulsed with ADS-conjugate exhibited a 3.2-fold decrease in doublet formation when B cells were HLA-A2 negative (73.8 % $\pm$ 1.63 to 22.5 % $\pm$ 0.64). Similarly, when B cells were co-cultured with CD8 T cell clones alone, a 3.4-fold decrease was seen in the formation of doublets in the absence of HLA-A2 (72.1 % $\pm$ 7.1 to 21.4 % $\pm$ 4.4) (Figure 4-7C). To some extent, the presence of cognate HLA on the surface of the B cells therefore appears to mediate the formation of B:CD8 doublets.

To further understand the importance of cognate HLA molecules to the formation of B:CD8 doublets, a second experimental approach was utilized. A monoclonal antibody directed against HLA-A2 (BB7.2) was used to block the HLA-A2 molecule on the surface of the B cell. Specifically, the antibody binds to an epitope at the c-terminus of the alpha-2 helix within the HLA-A2 molecule and has been reported to exhibit blocking activity in terms of TCR recognition of peptide-HLA complexes. B cells were incubated with 10 μg/ml of BB7.2 for 1 hour at 37°C just prior to co-culture with the CD8 T cell clones.

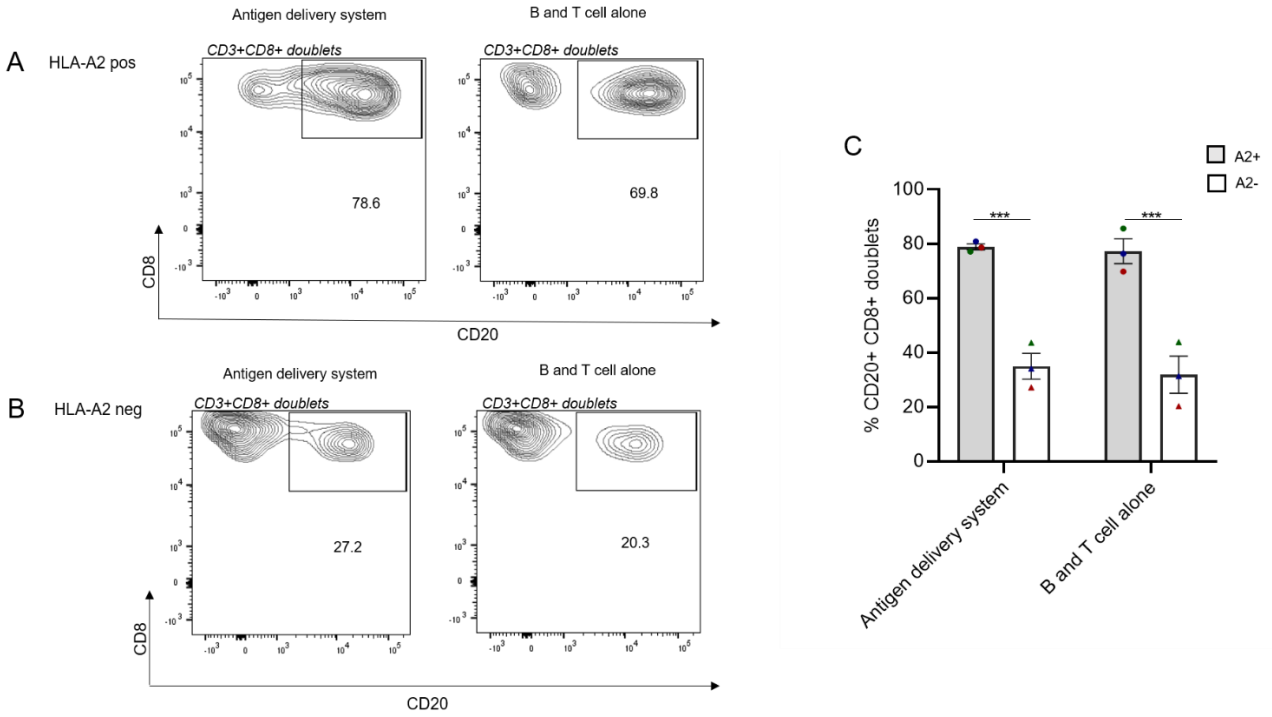

Figure 4-7 B:CD8 doublets are significantly reduced across all conditions when B cells are HLA-A2^{-} as compared to HLA-A2^{+} B cells.

HLA-A2 positive and HLA-A2 negative B cells were pulsed with the ADS-conjugate, 9-mer CMV pp65 or no peptide and co-cultured with CMV-specific CD8 T cell clones. The frequency of B:CD8 doublets was assessed and compared across all conditions. Flow cytometry plots are representative of three independent experiments, and graphical data presents the average frequency (%) of B:CD8 doublets from the parent population (CD3+CD8+ T cells) for each condition (mean $\pm$ SEM) and were tested for significance using a using two way ANOVA with Sidaks multiple comparison test, where ***<0.001. Significance displayed is between A2 positive and A2 negative cells within each co-culture condition. Individual experiments are matched by colour of the data points, and symbols indicate HLA-A2 positive (circle) or HLA-A2 negative (triangle) donors.

As indicated in Figure 4-8, blocking of B cells with the BB7.2 antibody resulted in a significant reduction in the formation of B:CD8 doublets, in comparison to conditions in which the B cell was blocked with the isotype control antibody (54.6 % $\pm$ 3.8, 37 % $\pm$ 3.2, respectively). Again, the level of reduction appeared to be consistent across all conditions, implying it was occurring independently of the presence of peptide on the B cell. Interestingly, while the reduction was still significant, in comparison to experiments in which B cells were completely deficient of HLA-A2 (Figure 4-7), the extent of the disruption of the B:CD8 doublets was much lower. For example, ADS-pulsed B cells treated with BB7.2 antibody showed a 1.45-fold reduction in doublet formation in comparison to the isotype control treated cells, while in the HLA-A2 deficient cells, the fold change was 3.2 in comparison to HLA-A2 positive cells (Figure 4-8).

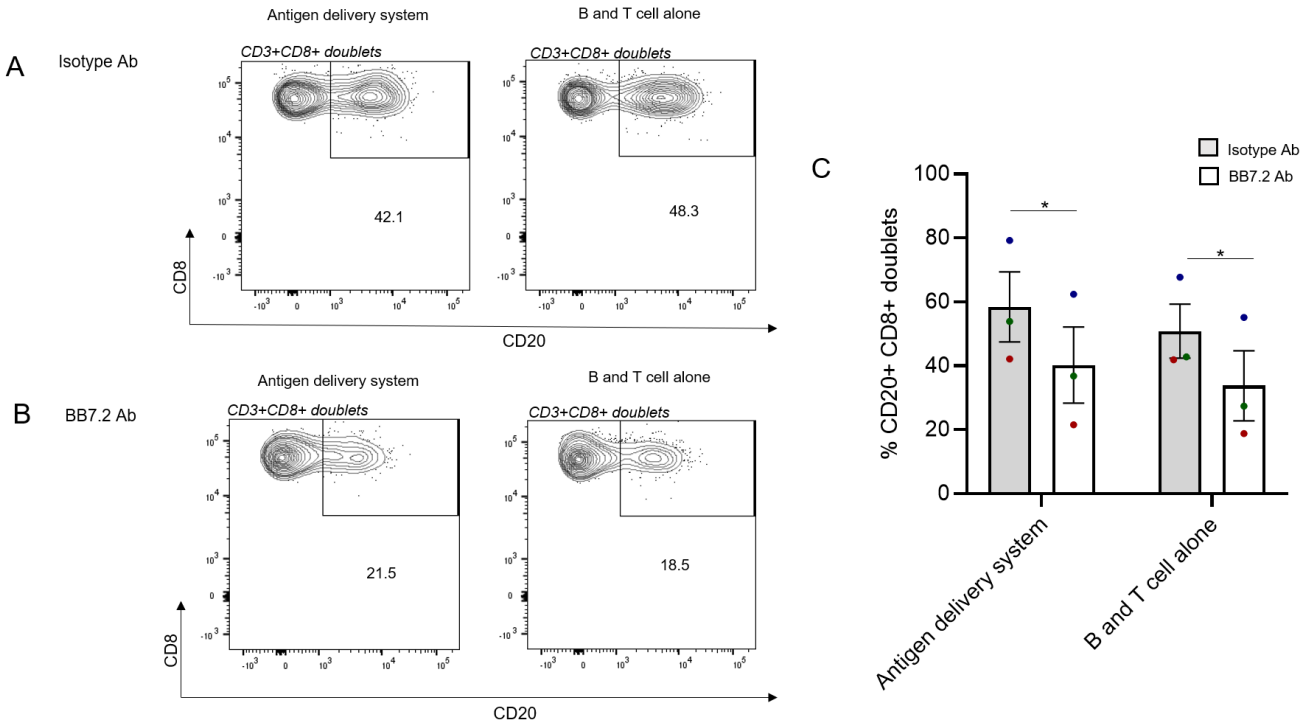

Figure 4-8 B:CD8 doublets are significantly reduced across all conditions when B cells are treated with BB7.2 antibody to block HLA Class I as compared to B cells treated with an antibody isotype control.

B cells were pulsed with the ADS-conjugate, short 9-mer peptide or no peptide. Prior to the co-culture with CMV-specific CD8 T cell clones, B cells were incubated with BB7.2 antibody, or its isotype control. The frequency of B:CD8 doublets was assessed and compared across all conditions. Flow cytometry plots are representative of three independent experiments, and graphical data presents the average frequency (%) of B:CD8 doublets from the parent population for each condition (mean $\pm$ SEM) and were tested for significance using a using a two way ANOVA with Sidaks multiple comparison test, where *<0.05. Significance displayed is between isotype-treated and antibody-treated cells within each co-culture condition. Individual experiments are matched by colour of the data points.

4.3.4 Effect of B cell stimulation with MEGACD40L on doublet formation

I next aimed to determine the impact of B cell stimulation to B:CD8 doublet formation. As discussed in Chapter 3, B cells were stimulated and activated with MEGACD40L, to mimic T cell dependent help. Stimulation of B cells may govern the formation of stable interactions with CD8 T cells due to changes induced by CD40L-CD40 signalling that are conducive to cell-cell interaction. To identify the role of B cell stimulation, B cells were either stimulated for 24 hours with MEGACD40L, or left unstimulated. Cells were then pulsed with the ADS-conjugate or 9-mer CMVpp65, and co-cultured with CD8 T cell clones. Stimulation of B cells had a significant impact on the presence of B:CD8 doublets (Figure 4-9). B:CD8 doublet formation with stimulated B cells was comparable to the levels seen in prior experiments, and consistent across all conditions. Unstimulated B cells resulted in a decrease in the presence of B:CD8 doublets; with a fold reduction of 1.8, 1.68 and 1.67, across the ADS-conjugate, peptide and B and T cell clone alone conditions respectively (Figure 4-9A). Therefore, to some level, B cell stimulation is relevant to the formation of B:CD8 doublets.

Taken together, these data show that the presence of B:CD8 doublets is governed by various biological factors; primarily the presence of cognate HLA on the B cell, and the stimulation status of the B cell. Importantly, these data elucidate the mechanisms by which stable interactions form between CD8 T cells and B cells. Further, they support the notion that the B:CD8 doublets are not a result of random association of cells. The ability to modulate their formation *in vitro*, bolsters the concept that the B:CD8 doublets represent a stable, biological interaction occurring between the B cells and CD8 T cells.

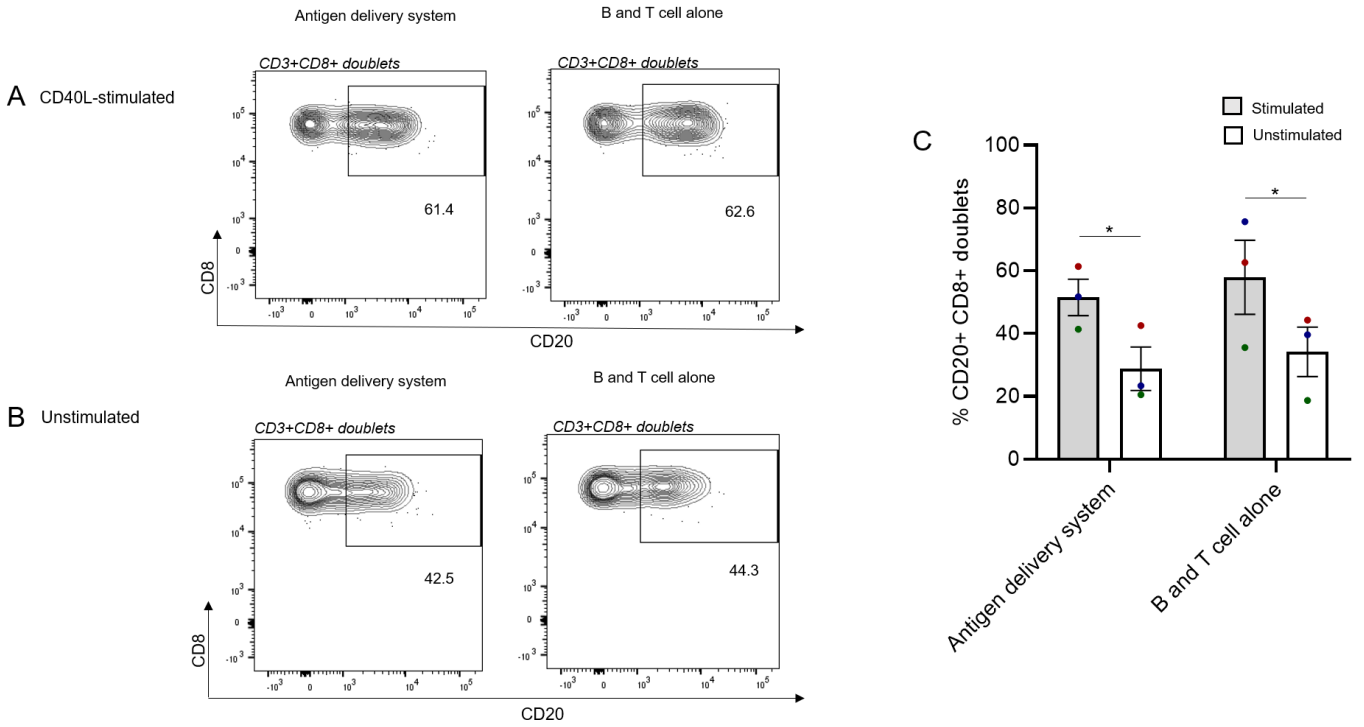

Figure 4-9 : B:CD8 doublets are significantly reduced across all conditions when B cells are not stimulated in comparison to when B cells are stimulated with MEGACD40L.

B cells were cultured for 24hrs with or without MEGACD40L, prior to pulsing with the ADS-conjugate, short 9-mer peptide or no peptide, followed by co-culture with CMV-specific CD8 T cell clones. The frequency of B:CD8 doublets was assessed and compared across all conditions. Flow cytometry plots are representative of three independent experiments, and graphical data presents the average frequency (%) of B:CD8 doublets from the parent population for each condition (mean $\pm$ SEM) and were tested for significance using a using a two way ANOVA with Sidaks multiple comparison test, where *<0.05. Significance displayed is between stimulated and unstimulated cells within each co-culture condition. Individual experiments are matched by colour of the data points.

4.4 Transcriptome analysis of B cells and CD8 T cells

4.4.1 Experimental strategy and sample quality control

4.4.1.1 Experimental justification and design

To further understand the interaction between B cells and CD8 T cells, experiments were focused to a molecular level by adopting a bulk-RNA sequencing (RNA-seq) experimental approach (Figure 4-10). The aim of this approach was two-fold.

Firstly, data indicated that stimulation of B cells had an impact on their stable interaction with CD8 T cell clones, due to the increase in B:CD8 doublet formation (Figure 4-9). It seemed pertinent to identify gene expression signatures induced during B cell stimulation, that may be relevant to their enhanced interaction with CD8 T cells. Additionally, as antigen delivery through the BCR did not appear to impact doublet formation, it was considered important to see if this was reflected in the gene expression signature of B cells pulsed with the ADS-conjugate. Therefore RNA was isolated from B cells under three distinct conditions; i) B cells that were stimulated with MEGACD40L for 24 hours, ii) B cells that were left unstimulated for 24 hours, and iii) B cells that were stimulated for 24 hours with MEGACD40L prior to pulsing with the ADS-conjugate, and incubated at 37°C for 16 hours to allow antigen processing. Blood from three independent healthy donors was used, and B cells were isolated via negative magnetic isolation as described previously from fresh PBMCs.

Secondly, data suggested that B cells were forming stable interactions with CD8 T cells, independent of antigen presentation by the B cell. It can therefore be speculated that this interaction may be representative of additional cell-cell communication between the two cells, that may be relevant to B cell governing of CD8 T cell responses and biological output *in vivo*. As cell-cell communication often arises due to interactions between ligands and their corresponding receptors, I aimed to identify ligand-receptor pairs between the two cells. RNA-seq of two independent CMV-specific CD8 T cell clones used in the *in vitro* experiments, in addition to RNA-seq of B cells as outlined above, allowed detection of ligand-receptor pairs at a transcriptomic level.

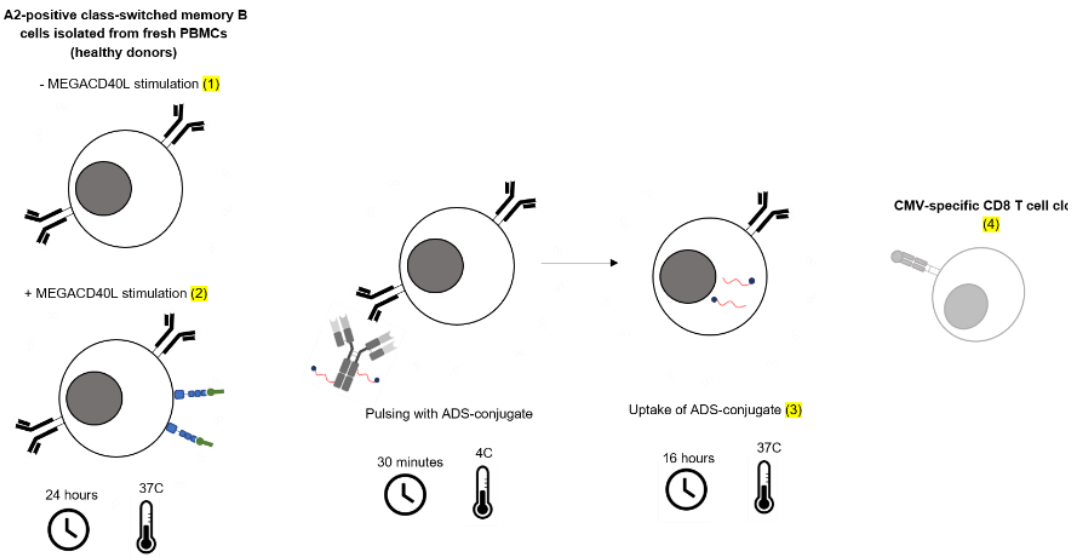

Figure 4-10 : Experimental strategy for RNA-seq experiment
RNA was extracted from three B cell conditions (n=3 donors): B cells incubated for 24 hours without (1) or with (2) MEGACD40L, from B cells incubated with MEGACD40L for 24hrs followed by pulsing with the ADS-conjugate and incubation for 16 hours to allow antigen processing. RNA was extracted in technical triplicate from two different CMV-specific CD8 T cell clones (4).

4.4.1.2 RNA concentration and integrity of samples

Initial optimisation experiments were carried out to ensure efficient isolation of RNA from PBMCs, both in terms of concentration and integrity. A concentration of ~50 ng of RNA was required for optimal library generation and downstream RNA sequencing. It was necessary to determine the expected RNA yield in order to obtain a large enough blood sample from healthy donors. Using PBMCs thawed from cryopreserved samples, RNA was extracted from increasing numbers of PBMCs with concentration and RNA integrity number (RIN) analysed using Qubit and bioanalyzer respectively. As shown in Figure 4-11A, the RIN remained high across all cell numbers. Above 500,000 cells, the concentration of RNA was calculated at between 0.56-0.6 pg per cell, however at the lower cell concentrations of 250,000 and 100,000 the concentration per cell was calculated at 0.32 ng and 0.16 ng, respectively. Based on these data, it was necessary to acquire enough blood volume from healthy donors that would result in an isolation of at least 350,000 B cells per

condition. As indicated in Figure 4-11B and C, isolation of sufficient concentrations of RNA was achieved across the B cell conditions. Importantly, the RIN scores for all samples were >9, and visualization showed minimal degradation i.e. high signal intensity of the two ribosomal bands, and no elevated baseline indicative of increases in shorter fragments.

A

Number of PBMCs	Concentration (ng)	RIN
10,000,000	5682	9.5
5,000,000	3416	10
1,000,000	594	9.9
500,000	292	9.8
250,000	81	9.7
100,000	16.1	9.9

B

		Cell number	Concentration (ng)	RIN Score
Donor 1	Unstimulated	700,000	437	10
	Stimulated	570,000	215	9.9
	ADS-pulsed	570,000	451	10
Donor 2	Unstimulated	500,000	178	10
	Stimulated	400,000	203	10
	ADS-pulsed	400,000	409	10
Donor 3	Stimulated	225,000	79	9.4
	Unstimulated	225,000	93	9.8
	ADS-pulsed	225,000	166	9.9

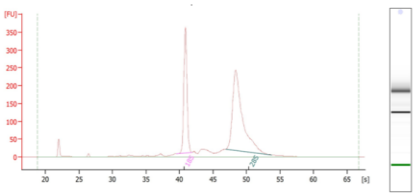

C

		Cell number	Concentration (ng)	RIN Score
Clone 1	1	500,000	382	10
	2	500,000	282	10
	3	500,000	339	10
Clone 2	1	500,000	737	10
	2	500,000	686	10
	3	500,000	647	10

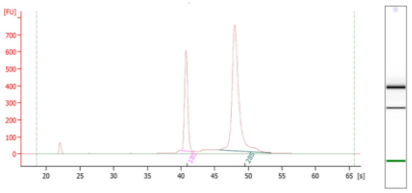

Figure 4-11 High quality and sufficient concentrations of RNA was extracted from all RNA-seq samples.

RNA was extracted from an increasing number of PBMCs in order to determine the optimal number of cells required to achieve at least 50 ng of RNA (A). RNA was extracted from three B cell conditions across three independent donors (B) and in technical triplicate from two independent CMV CD8+ T cell clones (C). RNA concentration for each sample was measured by Qubit and RNA integrity number (RIN) calculated using bioanalyzer.

4.4.1.3 Post sequencing quality control and cell type identification

RNA sequencing was performed on all samples as described in detail in the methods. All samples showed good sequencing coverage, at over 30 million reads per sample. Reads were successfully aligned to the human genome hg38 (alignment rate of 96% uniquely aligned reads), and over 14,000 genes were identified per sample – indicating a rich transcriptome for each. Principle component analysis showed clear segregation of the CD8 T cell samples from the B cell samples, indicating distinct gene expression profiles between the two cell subtypes (Figure 4-12A).

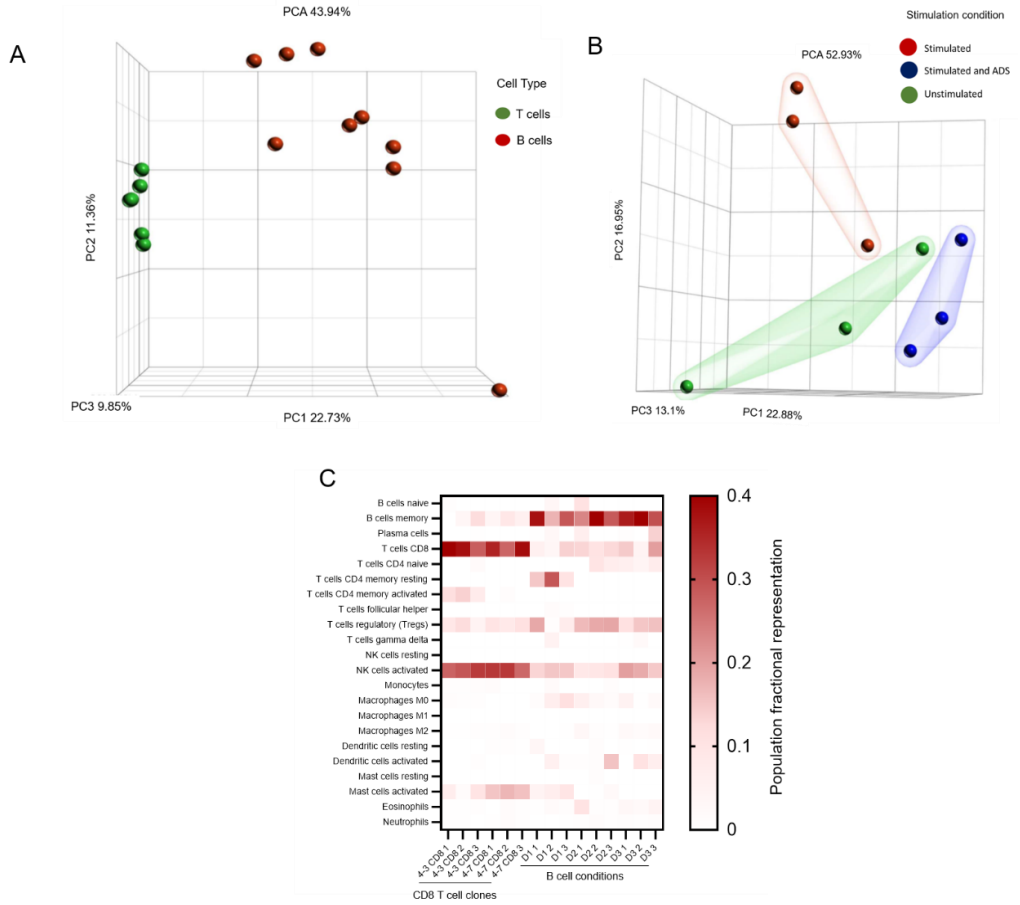

Figure 4-12 : T cell samples and B cell samples formed distinct clusters in unsupervised principle component analysis and show distinct and expected cell type identities as determined by CIBERSORT

Unsupervised principle component analysis was used to visualize clustering similarity of T cell and B cell samples (A), and of stimulated, stimulated and ADS, and unstimulated B cell conditions (B). The cell identity of each sample was determined as the fractional representation of 22 immune cell populations using CIBERSORT (C). PCA plots were generated by Shichina Kannambath, BRC Genomics GSST.

To confirm that the cell populations in each sample were as expected, CIBERSORT (Cell type identification by estimating relative subsets of RNA transcripts) was used. This is an open access algorithm that enables estimation of cell type abundances from bulk tissue transcriptomes. By using the known expression profiles of 22 purified immune cell populations, the algorithm calculates the proportions of each of these populations in each sample. Figure 4-12C shows the relative proportions of each immune cell population in each of the experimental samples. Results are presented as a heatmap, where the darker the red the higher the proportion of that immune cell subset in that sample. Transcriptomes from the CD8 T cell clone samples were enriched for the 'T cell CD8' population. Interestingly, the samples were also enriched for the 'NK cells activated' population. It is widely reported that NK cells and CD8 T cells share a similar gene expression signature (Cursons *et al.*, 2019). For the B cell samples, enrichment was seen in the 'B cells memory' population, confirming that the cells in these samples are memory B cells. Therefore, these analyses confirmed the expected cell type identities of each sample.

4.4.2 Assessment of the effect of stimulation and delivery of antigen through the BCR on B cell gene expression profiles

4.4.2.1 Principle component analysis of B cell conditions

Principle component analysis of the different B cell conditions showed that each condition formed a distinct cluster, with unstimulated B cells clustering together, stimulated B cells clustering together, and stimulated B cells pulsed with ADS-conjugate also forming a distinct cluster (Figure 4-12B). This data suggested that stimulation of B cells induced significantly distinct gene expression signatures, as did delivery of antigen through the BCR of the B cell.

4.4.2.2 Differential gene expression profiles between unstimulated and stimulated B cells

To understand the gene expression signatures driving the clustering, and identify those that may be relevant to the enhanced interaction between activated B cells and CD8 T cells (Figure 4-9), differential gene expression analysis was performed (FDR <0.05, fold change >2). Comparison of the unstimulated and stimulated B cells found differential expression of 132 genes, 77 of which were upregulated and 53 of

which were downregulated, as shown in the Volcano plot in Figure 4-13A, with the top 5% differentially expressed genes (DEG) indicated. Gene ontology enrichment was also performed to identify the significantly enriched molecular functions to provide mechanistic insight into the gene lists of DEGs (Figure 4-13B) .

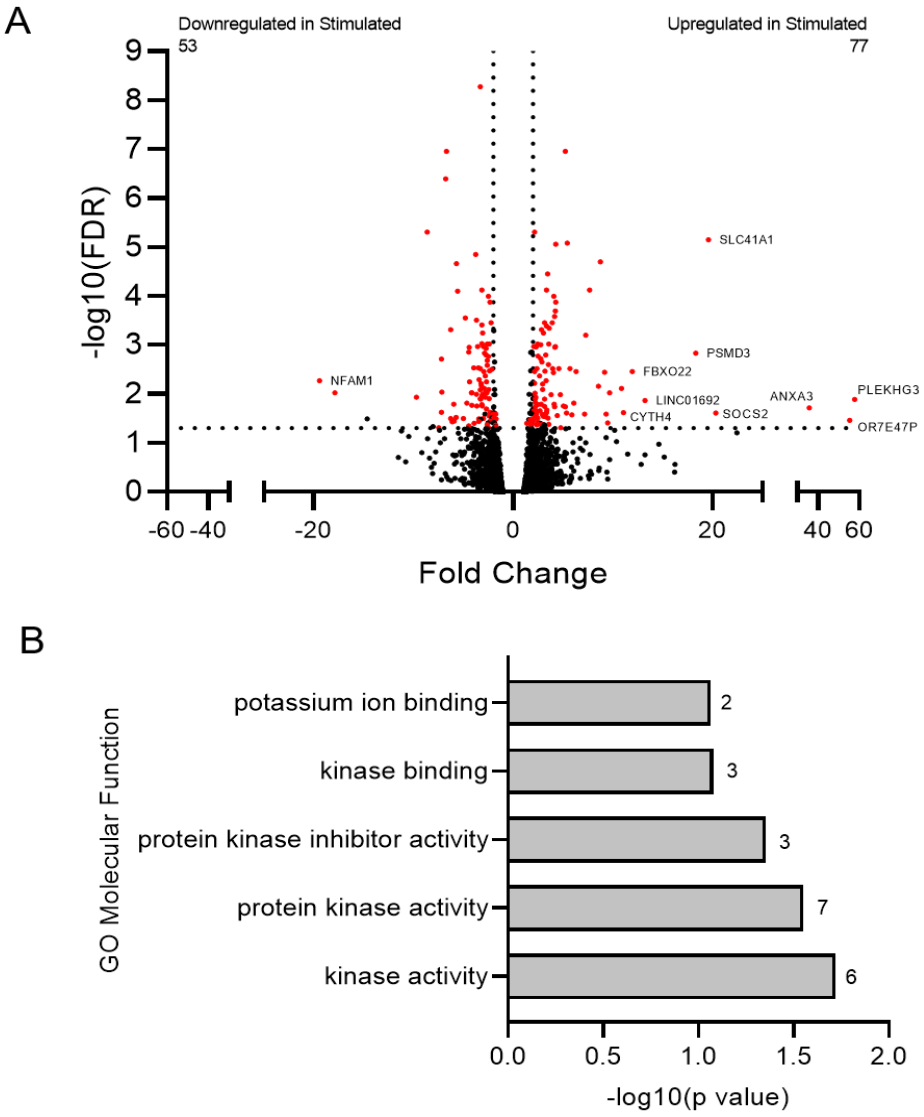

Figure 4-13 : Gene expression profiles indicate enrichment of genes and molecular function associated with activation of kinase pathways and actin cytoskeleton remodelling upon stimulation of B cells with MEGACD40L

RNA was extracted from unstimulated and stimulated B cells, and RNA sequencing performed using HiSeq Illumina platform performed. Differential expression analysis was performed with the DESeq2 package in R, and all upregulated and downregulated genes are shown in Volcano plots where horizontal dashed line, FDR <0.05; vertical dashed line, log2(fold change) = 2 to assess significant differentially expressed genes (red), with the top 5% labelled. Gene ontology enrichment analysis was performed using the R package clusterProfiler, to identify significantly enriched gene ontology terms (molecular function) represented within differentially expressed genes (number of genes involved at side of bar), when adjusted p values <0.05 (B).

The tumour necrosis factor receptor (TNFR) superfamily molecule CD40, while lacking intrinsic tyrosine kinase activity, when ligated with its cognate ligand CD40L, is known to signal to the cell and induce kinase activation. Indeed, the data were in line with this biological outcome, as the gene ontology analysis revealed significant enrichment of kinase pathway induction within the genes differentially expressed between stimulated and unstimulated B cells. These included kinase binding, protein kinase inhibitor activity, protein kinase activity and kinase activity.

Ligation of membrane bound CD40 therefore appears to trigger intracellular signalling through kinase pathway induction, which in turn mediates downstream gene expression. This is reflected in the 132 differentially expressed genes (DEGs) identified in the stimulated B cells as highlighted in Figure 4-13A, in which the top 5% differentially expressed genes are indicated. The most highly upregulated gene upon stimulation of B cells with MEGACD40L was *PLEKHG3* (57.6 fold, 1.30E-04), or pleckstrin homology and RhoGEF domain containing G3 – a PI3K regulated Rho guanine nucleotide exchange factor (RhoGEF) for Rac1 and Cdc42, that is involved in actin polymerization, cell polarization and integrin stabilization (Nguyen *et al.*, 2016). *ANXA3* was significantly upregulated (35.79 fold, 1.92E-02) upon stimulation, and encodes a member of the annexin family involved in calcium signalling and direct interactions with actin (Wu *et al.*, 2013). *CYTH4* (cytohesion4) was also significantly upregulated, encoding a member of the PSCD family of proteins that also contains a pleckstrin homology domain and functions as a guanine-nucleotide exchange protein involved in the activation of proteins involved in vesicle formation.

Stimulation of B cells with MEGACD40L therefore resulted in significant changes to the transcriptome of the cells. Primarily, as expected with CD40-CD40L ligation, this included the induction of kinase pathways, and upregulation of genes relevant to B cell polarity, actin cytoskeleton remodelling and vesicle formation. These biological processes may be relevant to the formation of stable B:CD8 cell interactions in vitro, and the increased formation of doublets seen upon B cell stimulation.

4.4.2.3 Differential gene expression profiles between stimulated B cells and stimulated, ADS pulsed B cells

Gene expression signatures were also compared between stimulated B cells, and stimulated B cells that were pulsed with ADS-conjugate and incubated for 16 hours to allow antigen processing and presentation. Of note, a caveat of the experimental strategy was the absence of a condition in which B cells were stimulated, and then incubated for a further 16 hours in the absence of the ADS-conjugate. This prevented a direct comparison of gene expression signatures between these two samples, as some changes in gene expression may be attributed to increased incubation times.

However, comparison of stimulated B cells, and stimulated, ADS-pulsed B cells found differential expression of 742 genes; 181 were upregulated and 561 were downregulated, as shown in the Volcano plot in Figure 4-14A, with the top 5% DEGs indicated. Gene ontology enrichment analysis showed enrichment of various molecular functions (Figure 4-14B). Protein binding was the most significantly enriched function, involving the highest number of DEGs (372), and other pathways included peptide binding, ATP binding and protein-C terminus binding. This differential gene expression profile observed with the addition of ADS-conjugate to the B cells is consistent with antigen processing and presentation by the cell. This is in line with the in vitro data, in which delivery of antigen through the BCR via the ADS-conjugate had no impact on doublet formation (Section 4.3.1).

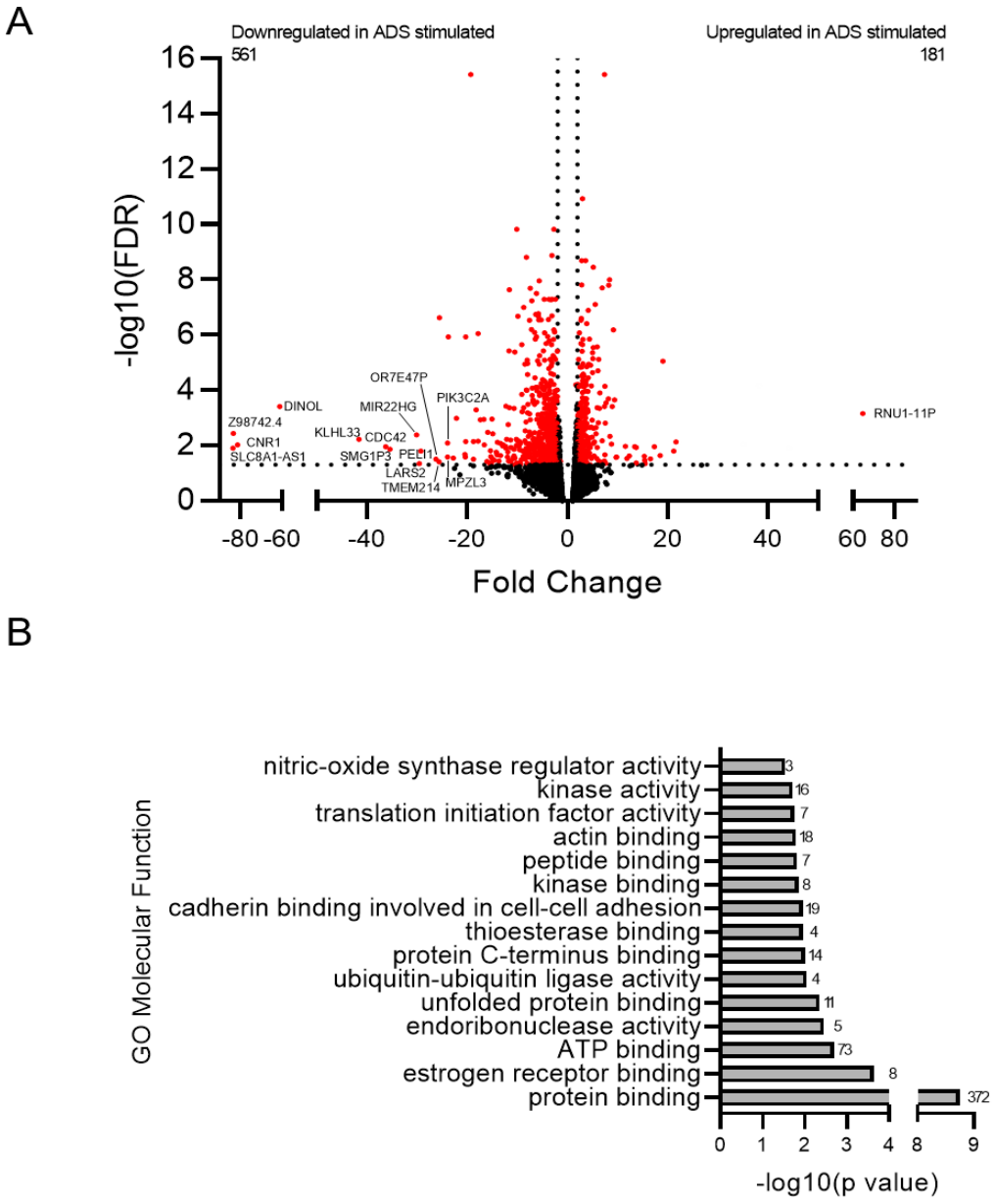

Figure 4-14 Gene expression profiles indicate enrichment of genes and molecular function associated with protein binding and processing upon delivery of antigen using the ADS

RNA was extracted from stimulated B cells, and stimulated B cells pulsed with ADS-conjugate and incubated for 16 hours to allow antigen internalisation and processing, and RNA sequencing using HiSeq Illumina platform performed. Differential expression analysis was performed with the DESeq2 package in R, and all upregulated and downregulated genes are shown in Volcano plots where horizontal dashed line, FDR <0.05; vertical dashed line, log2(fold change) = 2 to assess significant differentially expressed genes (red). Gene ontology enrichment analysis was performed using the R package clusterProfiler, to identify significantly enriched gene ontology terms (molecular function) represented within differentially expressed genes (number of genes involved at side of bar), when adjusted p values <0.05 (B).

4.4.3 Identification of cell-cell communication pathways mediated by ligand: receptor interactions between cell types

4.4.3.1 Analysis pipeline

Since the mRNA expression levels of ligands and their receptors could reflect the cell-cell communication, I aimed to identify ligand: receptor pairs expressed between B cells and CD8 T cells (see Materials and Methods). Firstly, ligand: receptor pairs were identified from a previously published interaction database (Ramilowski *et al.*, 2015). This list contained 2,422 interactions, 1,894 'reference' pairs which were supported with primary literature, and 528 'putative' pairs without literature support. Transcript per million (TPM) values were then extracted for every ligand and receptor within each interaction pair from the RNA-seq gene expression data, with a TPM threshold of 1 for both ligand and receptor expression. In this manner, ligand: receptor pairs were detected where the ligand was expressed on one cell type, and the corresponding receptor on the other cell type. Directionality of the interaction was determined by the ligand expressing cell. B:T directionality expressed the ligand on the B cell and its receptor on the T cell, while T:B directionality expressed the ligand on the T cells and its receptor on the B cell.

4.4.3.2 Identification of ligand: receptor pairs between B cells and CD8 T cells

For each ligand: receptor pair detected between the B cells and CD8 T cells, an interaction score was assigned to determine the 'strength' of the interaction. Pairs were scored by calculating the product of the ligand expression and the receptor expression (TPM) values (Kumar *et al.*, 2018). Figure 4-15 shows the ligand: receptor pairs detected between B cells and CD8 T cells. Heatmaps represent the interaction score for each detected ligand: receptor pair (Figure 4-15A), where each column represents the B cell condition (1 = Unstimulated, 2 = Stimulated, 3 = Stimulated and ADS-pulsed). Pairs were also displayed in ranks (Figure 4-15B); with the top 20% and bottom 20% for each B cell condition, in order to account for differences in the experimental conditions of each that may impact the gene expression values i.e. condition 3 being incubated for 16 hours longer than condition 2.

Observationally, the ligand: receptor pairs identified were consistent across the B cell conditions. Despite some differences in the interaction scores for each pair in each condition, when ranked according to the highest and lowest scoring ligand: receptor pairs, similar stratification was observed i.e. *TNFSF13:TNFRSF14* was in the highest expressing group (top 20%) across all B cell conditions. Although lacking formal statistical analysis, this suggests that the expression of ligand: receptor pairs between the B cells and CD8 T cells exists in a default state and is not impacted by B cell stimulation or antigen processing and presentation.

Of the ligand: receptor pairs detected, a large proportion of the ligands on the B cells were identified as a member of the cytokine/chemokine family (10 out of 23 ligands present within ligand: receptor pairs), suggesting an enrichment of these signalling pathways. The highest scoring interaction was between members of the TNF superfamily, *TNSFS13:TNFRSF14*. *TNFSF13* encodes APRIL (a proliferating inducing ligand), which is involved in inducing proliferation (Hahne *et al.*, 1998). Ligation of the receptor TNFRSF14 on T cells is involved in activation of NFκB pathways and promotion of cell survival and proliferation (Steinberg, Cheung and Ware, 2011). Additionally, other cytokine mediated interactions included *LTA* (which encodes lymphotoxin A) and *TNFRSF14*, *TNFSF13* and the gene that encodes the cell death receptor *FAS*, and *TGFB1* and *ENG* (endoglin). The chemokine *CXCL16*, and its cognate receptor, *CXCR6* also showed a high interaction score across all B cell conditions.

In addition to cytokine/chemokine mediated interactions, interactions related to the extracellular matrix (ECM) were also observed, conducive with mediation of cell-cell adhesion and interaction stability. These may be relevant to the previous findings, in which B:CD8 interactions were occurring in a manner independent of pHLA-TCR interaction. For example, the integrin-binding glycoprotein fibronectin (*FN1*) was the most common ligand detected in the B cells (involved in three ligand: receptor pairs) and was identified in a ligand: receptor pair with the integrin adhesion receptor gene *ITGB7*. Additionally, an interaction between the intercellular adhesion molecule 3 gene (*ICAM3*) and *ITGB2*, a subunit of LFA-1 which is central to T cell adhesion to APC, was identified (Dustin, 2002).

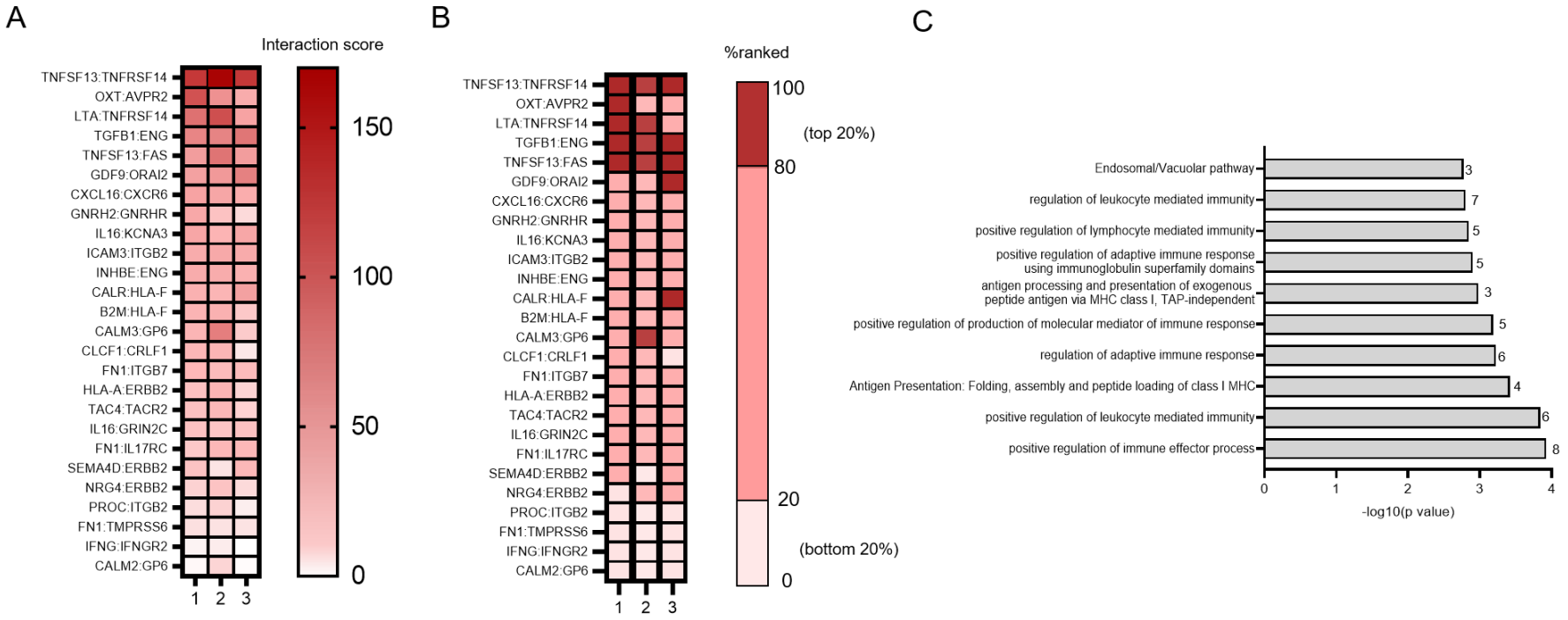

Figure 4-15 Ligand: receptor pairs are identified between B cells and CD8 T cell clones at a gene expression level.

Interaction scores for receptor: ligand pairs were calculated as a product of the expression of the ligand on the B cell and the expression of the receptor on the CD8 T cell clone, where expression was quantified as a transcript per million (TPM) value, with a threshold of >1 TPM for each gene. Heatmaps show the mean average interaction score in each B cell condition (A), and the percentiles of the top and bottom scoring pairs across B cell conditions (B). Condition 1 = Unstimulated B cells and CD8 T cell clones, Condition 2 = Stimulated B cells and CD8 T cell clones, Condition 3 = ADS-conjugate pulsed B cells and CD8 T cell clones. Pathway enrichment analysis was performed on all the detected ligands and receptors using the Pathways common tool (C).

In line with ECM involvement, the glycoprotein collagen receptor (*GP6*) expressed on the CD8 T cells, was detected as interacting with two calmodulin proteins, *CALM2* and *CALM3*. Interestingly, interactions were also detected involving MHC molecules. Again, this was an observation particularly pertinent due to the identification that the interaction between B cells and CD8 T cells in my experiments could be disrupted by the removal and/or blocking of cognate class I molecules. An interaction was detected between the membrane-bound molecules *HLA-A* (ligand) and *ERBB2*, or *HER2* (receptor); the latter of which is a tyrosine kinase receptor.

Potential interactions between B cells and CD8 T cells were therefore inferred from the gene expression data, that may reflect cell-cell communication. Specifically, ligand: receptor pairs appeared to be enriched in cytokine and chemokine signalling, as well as involving ligand and receptors central to the ECM and integrin families, and to antigen presentation machinery i.e. MHC class I.

In line with these observations, the Pathways Common tool was used to carry out pathway enrichment analysis of all the genes involved in the 26 ligand: receptor pairs identified (Figure 4-15B). The most enriched pathway, involving the most genes, was 'positive regulation of immune effector processes.' Other positive regulation pathways were also enriched, such as of leukocyte mediated immunity and production of molecular mediators of immune responses. Additionally, in line with the involvement of MHC class I molecules, enriched pathways included antigen presentation. Taken together, these interactions therefore present evidence that B cells may govern CD8 T cell responses through direct cell-cell interaction (juxtacrine), and through secretion of molecules detected by corresponding receptors on the CD8 T cell (paracrine).

CD8 T cell regulation of B cells may also be relevant to their interaction in addition to the primary research focus on B cells governing CD8 T cell responses through cell-cell communication. Using the same approach, I analysed ligand: receptor pairs between the CD8 T cells and B cells, where the ligand is expressed on the T cell (T:B, ligand: receptor). Fewer ligand: receptor pairs were identified as compared to ligand expression on the B cell, with 17 pairs observed, and once again pairs appeared to be consistently expressed regardless of the B cell condition (Figure 4-16). Pairs were primarily part of the cytokine/chemokine family, with *TNFSF13*

interacting with *TNFRSF14* and its cognate receptor *TNFRSF13B* or *TACI*, a predominantly B cell restricted receptor central to B cell homeostasis. The interaction with the highest score was *TGFB1:ENG*, and other cytokine mediated interactions included *LTA:TNFRSF14* and *CLCF1:CRLF1*. Pairs were also identified involving integrins and ECM components, for example the two integrin receptors *ITGB7* and *ITGB2* on the B cells were found to interact with the cell adhesion molecules *MADCAM1* and *ICAM3* expressed on the CD8 T cells, respectively. Interestingly, three interactions were identified between *ERBB2* expressed on the B cell – with *HLA-A, NRG4* and *HSP90B1* on the CD8 T cell.

Pathway enrichment analysis identified the most significantly enriched pathway as 'TNFs binding their physiological receptors', and other pathways included those identified in B:T cell interactions (Figure 4-16B), such as 'positive regulation of leukocyte mediated immunity' and 'molecular mediators of immune responses'. Interestingly, the pathway 'integrin cell surface interactions' was significantly enriched, suggesting T cells may be more relevant in mediating cell adhesion with B cells.

These data suggest that cell-cell communication also occurs between CD8 T cells and B cells, in which the ligand is expressed on the T cell. Similar to where B cells were the 'senders' and CD8 T cells the 'receivers', the identified ligand: receptor pairs suggest cross-talk mediates effector functions of the B cells, in response to cytokines, as well as cell adhesion and interaction through membrane bound ligands and receptors.

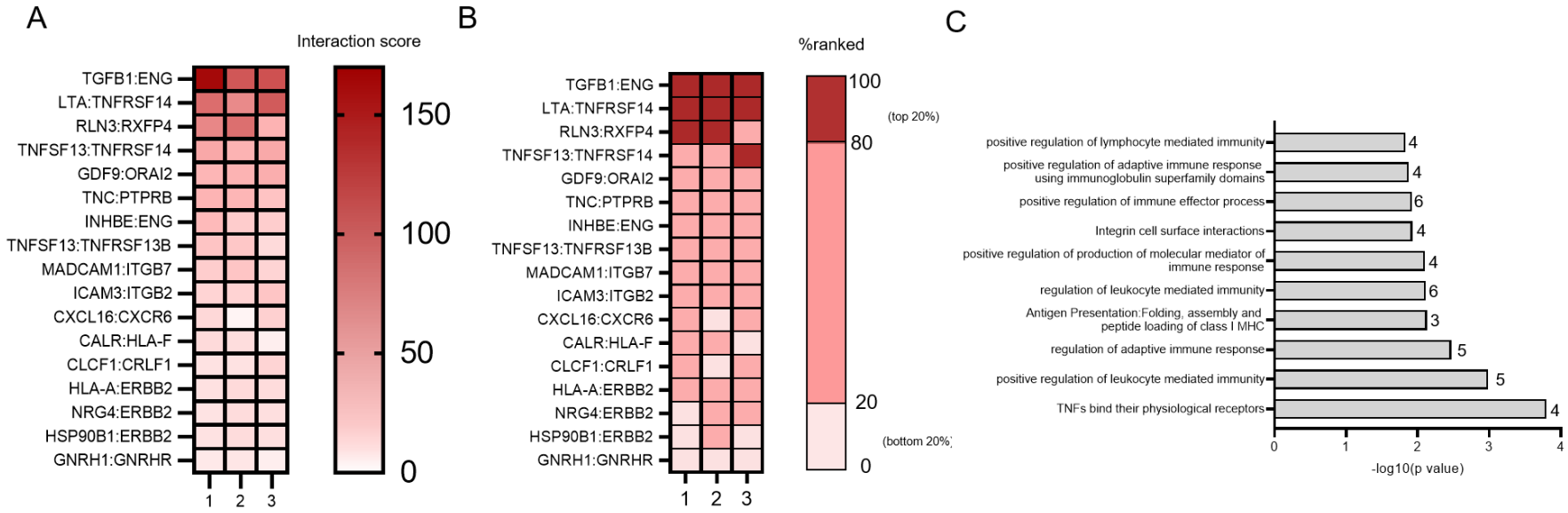

Figure 4-16 Ligand: receptor pairs are identified between CD8 T cell clones and B cells at a gene expression level

Interaction scores for ligand: receptor pairs were calculated as a product of the expression of the ligand on the CD8 T cell clone and the expression of the receptor on the B cell , where expression was quantified as a transcript per million (TPM) value, with a threshold of >1 TPM for each gene. Heatmaps show the mean average interaction score in each B cell condition (A), and the percentiles of the top and bottom scoring pairs across B cell conditions (B). Condition 1 = Unstimulated B cells and CD8 T cell clones, Condition 2 = Stimulated B cells and CD8 T cell clones, Condition 3 = ADS-conjugate pulsed B cells and CD8 T cell clones. Pathway enrichment analysis was performed on all the detected ligands and receptors using the Pathways common tool (C).

An obvious observation was the similarity in ligand: receptor pairs identified across analyses. Indeed, of the ligand: receptor pairs identified, 12 (of 17 in T cell ligand analyses, and of 26 of B cell ligand analyses) were expressed commonly on both B cells and CD8 T cells. For example, the ligand: receptor pair *TNFSF13:TNFRSF14* was detected in both analyses, meaning that *TNFSF13* was expressed by both the B cell and CD8 T cell, as was the receptor. This indicates that the ligands and receptors in the observed pairs are not necessarily cell-type restricted and may be commonly expressed and shared across cells of the same lineage – a phenomenon widely described in immune cells (Ramilowski *et al.*, 2015). However, dominant directionality of the interaction could be inferred by the interaction scores, as shown in Figure 4-17. Here, average scores are presented between the stimulated, ADS-conjugate pulsed B cells and CD8 T cells, of the 12 shared ligand: receptor pairs.

For the majority of shared ligand: receptor pairs, the interaction score was higher when the ligand was expressed on the B cell (B:T, ligand: receptor), in line with the concept that B cells are governing CD8 T cell responses through cell-cell communication. Exceptions included *TGFB1:ENG* and *LTA:TNFRSF14*, where interaction scores were higher when the ligand was expressed on the T cell (T:B, ligand: receptor). Therefore, despite some ligand and receptor expression not showing cell type specificity, the more pertinent direction can be inferred from the interaction scores. Additionally, it is important to note that this shared expression pattern highlights the potential presence of autocrine signalling networks within each cell subset, due to the expression of both the ligand and the corresponding receptor of a pair on the same cell.

Taken together, transcriptome analysis presents a network of cell-cell communication that may exist between B cells and CD8 T cells. The predominance of ligand: receptor pairs involved in cytokine/chemokine signalling, ECM and antigen presentation machinery implicate adhesive and signalling capacities. These may be relevant to B cell governing of CD8 T cell responses through cell-cell interaction and mediation of the quality of effector responses.

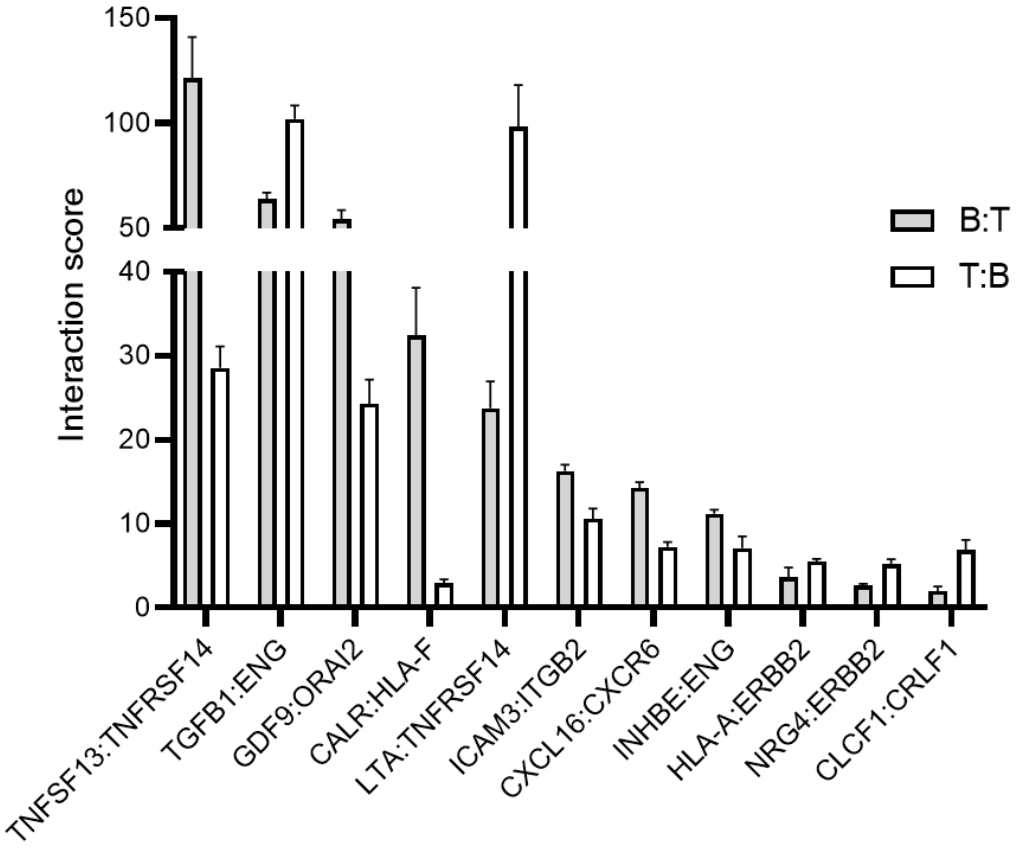

Figure 4-17 Interaction scores for ligand: receptor pairs expressed in both directions inferred the most relevant directionality of the interaction

Interaction scores were calculated for the 12 ligand: receptor pairs that were detected on both the B cells and the T cells. B:T – expression score is calculated as the product of the ligand expression on the B cell, and the receptor expression on the CD8 T cell. T:B - expression score is calculated as the product of the ligand expression on the CD8 T cell, and the receptor expression on the B cell. Data represents the average interaction score between the ADS-conjugate pulsed B cells and CD8 T cell clones $\pm$ SEM.

4.5 Discussion

Data in this chapter further characterised the interaction between B cells and CD8 T cells. Specifically, evidence supports an antigen-independent interaction between B cells with CD8 T cells that may represent pathways of signalling and adhesive capabilities. Dissemination of these antigen-independent modalities suggested novel mechanisms by which B cells may govern CD8 T cell responses. This further elucidates the potential role of B cells in mediating CD8 T cell effector function that is central to β-cell destruction in T1D pathogenesis.

A stable interaction occurs between B cells and CD8 T cells in the *in vitro* co-cultures, as detected by the presence of B:CD8 doublets using (imaging) flow cytometry. These interactions occurred in an antigen independent manner. Frequencies of B:CD8 doublets were consistent across co-culture conditions with and without antigen delivery and cross-presentation by the B cell. Antigen presentation was, however, required for the formation of a mature IS and induction of cytotoxic T cell responses. This suggested the interaction detected between B cells and CD8 T cells represented cross-talk that was mediated by non-antigen specific modalities. Stimulation of the B cell in a CD40 dependent manner had a positive impact on the formation of the B:CD8 interaction. Transcriptome analysis revealed that, upon stimulation, an enrichment of kinase pathway signalling, and differential expression of genes involved in actin cytoskeleton remodelling, vesicle formation and ECM modulation, occurred. Removal of the cognate HLA molecule on the B cell resulted in a reduction in B:CD8 doublet formation, suggesting presence of cognate HLA may contribute to the interaction. Ligand: receptor pairs were identified at a transcriptomic level between the B cells and CD8 T cell clones, and were enriched for cytokine and chemokine signalling, ECM and integrin interactions, and antigen processing and presentation machinery.

The serendipitous observation of a doublet cell population expressing both CD20 and CD8 within my co-cultures, led to the discovery that $CD20^{+}CD8^{+}$ double positive cells existed within the ‘doublet’ gate, and that these cells were CD20 B cells tightly associated with CD8 T cells. Studies on ‘doublet’ cells within flow cytometric analyses have been somewhat limited, with doublets often excluded upon

analysis as artefacts of the experimental procedure, or a random association of cells, with little biological significance. To the contrary, data presented in this chapter provides evidence that doublets may represent a biological interaction between two cell subsets. Disruption of doublet formation by removal of cognate HLA molecules from the B cell provided evidence against their formation being due to a staining artefact such as non-specific antibody binding to the Fc receptors. Formation of doublets was promoted upon CD40L-stimulation of the B cell - if doublets were occurring due to random close association of cells, stimulation would not impact their frequency. Finally, visualization of the doublets using imaging flow cytometry provided evidence to reject the possibility that trogocytosis, or the exchange of extracellular material i.e. CD20 cell membrane fragments on the CD8 T cells, was accounting for their presence. Doublets were clearly visualized as two distinct cells - a CD20 B cell and a CD8 T cell.

The detection of B:CD8 doublets in co-cultures, and their robustness as a stable, biological interaction, therefore led to the hypothesis that they were interacting cells due to antigen cross-presentation by the B cell. Previous reports have evaluated APC: T cell conjugates using similar experimental approaches as this study. Dubbed 'doublet technology', one study found that tumour reactive cytotoxic T cells could be identified and isolated based on their ability to form stable interactions with target cells. Double positive cells were identified via flow cytometry as a similar population to that presented in this chapter; showing higher FSC/SSC distribution and appearing in the doublet zone of FSH-H/FSC-A plot (García-Guerrero *et al.*, 2018). Here, the frequency of cell couplets was enhanced when antigen was presented by the APC, and T cells within the doublets showed significantly higher effector function. Based on these data it could be hypothesised that the B:CD8 doublets identified in the *in vitro* co-cultures of the present study were a result of B cell antigen cross-presentation to the CD8 T cell.

Surprisingly, in both the flow cytometry and imaging flow cytometry data presented in this chapter, the occurrence of B:CD8 doublets was independent of antigen presentation by the B cell, therefore providing evidence against the interaction forming solely due to antigen specific modalities. Historical data has shown that human CD8 T cell clones are susceptible to antigen-independent interaction with

target cells, due to the observation of conjugates forming between CD8 T cell clones and antigen-negative targets (Shaw *et al.*, 1986; Shaw and Luce, 1987). Authors showed that these conjugates formed with the same speed, frequency and strength as conjugates occurring with antigen specific target cells.

In T1D, B cell activation has been associated with increased rate of disease progression (Speake *et al.*, 2019). Additionally, a cellular phenotype associated with resistance to immune checkpoint blockade treatment (Abatacept) was characterised by an increase in activated B cells in the periphery (Linsley *et al.*, 2019). Activation and stimulation of B cells therefore appears to be relevant to B cell function in disease. Interestingly, stimulation of B cells in a CD40-dependent manner increased the frequency of B:CD8 doublets in my *in vitro* co-cultures, independently of presence of antigen on the B cell. This suggested that CD40-mediated B cell stimulation was enhancing the antigen independent interaction between B cells and CD8 T cells. This finding provides a potential mechanistic explanation for the relevance of B cell activation to T1D disease severity. Activated B cells may increasingly interact with CD8 T cells and modulate their effector function, leading to augmented β-cell destruction.

Gene expression signatures induced upon B cell stimulation that may be relevant to this enhanced frequency of B:CD8 doublet formation were identified through transcriptomics analysis. Literature shows that pathways induced in response to CD40 ligation in B cells include: NFκB pathway, the mitogen activated proteins kinases (MAPKs: ERK1 and ERK2, and JNK1 and JNK2), the stress responsive p38 kinase pathway, and the phosphatidylinositol 3-kinase (PI3K) and phospholipase C (PLC) pathways (Berberich, Shu and Clark, 1994; Ren *et al.*, 1994; Berberich *et al.*, 1996; Li *et al.*, 1996; Sutherland *et al.*, 1996). Indeed, pathway enrichment analysis identified kinase pathways (kinase activity, protein kinase activity, protein kinase inhibitor activity, kinase binding) as the most significantly enriched molecular processes within the DEGs of the stimulated B cells in my study.

The gene with the largest fold increase in expression upon B cell stimulation was *PLEKHG3*, which encodes the pleckstrin homology domain and Rho-GEF domain containing protein G3. Its protein expression is regulated by PI3K, and it acts as a RhoGEF for Rac1 and CDC42. In one study, PLEKHG3 was found to be important

in the regulation of cell polarity and motility, due to its ability to directly bind F-actin filaments, and its involvement in a positive feedback loop with actin filaments and Rac1/cdc42 (Nguyen *et al.*, 2016). Despite being in a fibroblast cell line, this supports the theory that stimulation of B cells induces actin cytoskeleton remodelling and cell polarity. Importantly, these processes are implicated in the activation of integrins (Lub *et al.*, 1997). The relevance of this to the enhanced interaction of the B cell with the CD8 T cell is seen in studies of antigen-independent interactions of CD8 T cell clones with target cells, whereby pathways of integrin dependent adhesion were critical to conjugate formation i.e. LFA-1, CD2 (Shaw *et al.*, 1986; Shaw and Luce, 1987; Voss *et al.*, 2009).

Interestingly, in T1D individuals, peripheral blood B cells exhibited reduced levels of PTEN (a negative regulator of PI3K signalling) leading to excessive and aberrant PI3K signalling (Smith *et al.*, 2018). In the VH125.NOD mouse model, correcting of this failed PI3K pathway regulation using a PI3K inhibitor led to a sufficient delay in development of autoimmunity (Franks, Getahun and Cambier, 2019). While the authors concluded this was due to inhibition of autoreactive B cell participation in autoimmunity due to restoration of appropriate anergy, data in the present study alludes to additional pathogenic mechanisms for PI3K signalling in the B cell. For example, CD40 mediated induction of kinase pathways leading to integrin activation and enhanced interaction with CD8 T cells.

With this concept in mind, it should be noted that no integrin encoding genes were detected in the differential gene expression analysis, and few ligand-receptor pairs involving integrins were observed in the cell-cell communication analysis. Activation of integrins into a high affinity/ high avidity state occurs in response to induction of intracellular signalling pathways through immunoreceptor stimulation. This occurs at a protein level, therefore there would be little change at the gene expression level due to qualitative changes as opposed to quantitative changes in integrin mRNA. Moreover, as previously discussed, B cells were stimulated with CD40L alone in the absence of pro-inflammatory cytokines to provide a ‘third’ signal. This does not fully encapsulate the inflammatory milieu likely to occur in disease, and as cytokines are well characterised to induce integrin gene expression through signalling cascades (i.e. STAT3 phosphorylation) this may reconcile the

lack of differential integrin gene expression. Experimental strategies to validate the notion that CD40-mediated induction of kinase pathways resulted in activation of integrins relevant to increased interaction with CD8 T cells could be applied. The protein expression levels of integrins in their active conformation could be compared between stimulated and unstimulated B cells, using flow cytometry antibodies specific for this conformation.

In addition to B cell stimulation, the presence of cognate HLA on the B cell significantly influenced the frequency of B:CD8 doublets. This was intriguing as data had shown that the interaction was occurring in an antigen independent manner, presumably not involving peptide-HLA interaction with TCR. However, the presence of cognate HLA was necessary to the interaction in conditions both with and without peptide. This suggests it may be mediating cell-cell interaction through non-peptide domains of the molecule. Indeed, structural and functional analysis of pMHC-TCR interactions in the literature indicate an inherent TCR reactivity with the MHC molecule, dictated by sets of conserved contacts. With the knowledge that T cells are required to probe and 'scan' a diverse milieu of peptides presented by MHC molecules in order to recognise a cognate peptide and generate efficient T cell responses, Wu *et al.,* (2002), undertook a seminal study to elucidate the physical basis of this scanning process. The authors presented a model by which MHC molecules guided the docking of the TCR, though interactions between the TCR germline CDR1 and 2 regions and the MHC alpha helices. This structural observation has now been reported in > 20 published structures for TCR-MHC.

From this seminal study, a two-step mechanism is presented (Wu *et al.,* 2002). Initial TCR-MHC interactions, aided by minor contributions from TCR-peptide contacts, guide the TCR to its ligand. In the case of cognate antigen recognition, peptide contacts with the TCR then stabilise the interaction and trigger T cell activation. MHC restriction therefore acts as a gatekeeper that promotes peptide scanning, providing an intrinsic bias to recruit the TCR regardless of the antigenic peptide identity. Thus, the contribution of HLA-A2 on the B cell to the formation of B:CD8 interactions may be due to interactions between the CDR1 and CDR2 of the CD8 clone TCR and the HLA-A2 molecule.

With the notion that it is the peptide contact that attributes the stability of the interaction, this theory could be bolstered by comparing the stability of the interaction with and without antigen cross-presentation by the B cell though *in vitro* disruption techniques such as vigorous pipetting or mild sonication (Burel *et al.*, 2019). Experiments using the HLA-A2 blocking antibody BB7.2 supported this theory, as while blocking showed a reduction in the formation of B:CD8 doublets, it was to a much lower extent than experiments in which B cells were HLA-A2 negative. The antibody exhibits blocking activity specifically at the alpha-2 domain of the HLA molecule, a domain that binds the peptide and would therefore block TCR recognition of the peptide. If the main contribution of HLA-A2 on the B cell is due to interaction with CDR1 and 2 of the TCR, it would be expected that this blocking experiment would have had a lower impact on doublet formation.

Data presented in this chapter show that B cells and CD8 T cells appear to interact in a manner that is just as efficient between antigen negative i.e. no (cross-)presentation of antigen by the B cell, and antigen positive conditions. This raised the question as to the biological relevance of this interaction. It can be speculated that it is important in one of two ways. Firstly, a key difference between those B:CD8 doublets in which antigen was present and those without was the functional outcome. The presence of antigen resulted in the formation of a mature immunological synapse as measured by CD3 accumulation at the cell-cell contact interface. In addition, this correlated with T cell effector function, due to the expression of CD107α on the B:CD8 doublets. Therefore, antigen independent pathways relevant to the interaction may precede or occur concurrently with antigen recognition and represent adhesive and signalling capabilities that optimise the CD8 T cell effector response. On the other hand, the interaction may represent a B cell helper role, by which in the absence of antigen signals are provided that 'help' the CD8 T cell i.e. survival or differentiation.

A CD8 T cell helper role for B cells was identified in a study by Deola *et al.*, (2008), describing a novel interaction between B cells and activated CD8 T cells that was independent of antigen presentation. The authors used the well characterised HLA-A2 restricted Flu (M1: 58-66) specific CD8 T cell clone and found distinctive coupling with CD19 B cells in cultures during *in vitro* sensitization. Further dissection of the dynamics of this coupling, in which sorted CD8 T cell clones were

cultured for 16 hours with freshly isolated CD19 cells loaded with no peptide, cognate peptide, or irrelevant peptide, revealed that it was occurring independently of B cell antigen presentation. These experiments mirrored the conclusions drawn from my data.

Additionally, in line with my findings, coupling in the absence of antigen did not induce CD8 T cell cytotoxic activity. CD8 T cell – B cell coupling did, however, promote survival and proliferation of CD8 T cells. Interestingly, the use of a trans-well system identified that both direct cell-to-cell contact, and paracrine cytokine release were relevant to B cell mediation of CD8 T cell survival and proliferation. Therefore, while my study did not address this directly, the interaction between B cells and CD8 T cells may represent B cell governance of CD8 T cell survival and proliferation in the absence of antigen presentation.

Deola *et al.,* (2008) aimed to characterise the molecular mechanism by which B cells were promoting CD8 T cell survival and proliferation. CD70 was universally expressed by the CD8 T cell, while its ligand CD27 was expressed on the B cell. Blocking of this interaction resulted in complete abrogation of the survival advantage provided by coupling with the B cell. The present study did not reveal this ligand: receptor pair in the analyses, however this is likely due to analysis of protein expression in the Deola *et al.,* study versus gene expression analysis in my experiments. Importantly however, it highlights the functional relevance of antigen independent ligand: receptor pairs in B: CD8 interactions, inferring a potential 'helper' role for the B cell.

With the identification of B cell antigen independent pathways that may serve to govern CD8 T cell functions, the relevance of this *in vivo* settings should be examined. A limitation of both the present study and the study by Deola *et al*., was the controlled system of *in vitro* co-cultures – *in vivo* how likely would it be that CD8 T cells would encounter and interact with non-antigen specific B cells? Deola *et al.,* discussed as to whether it occurred as a result of disturbed immune reactivity. In diabetes, in which the islets are sites of autoimmune inflammation, this phenomenon may therefore occur. Indeed, this was the case in an inflammation-based NOD model of T1D (RIP TNFα-NOD), in which constitutive expression of TNFα is restricted to the islet (therefore generating a highly pro-inflammatory

environment) (Green, Eynon and Flaveirti, 1998). B cell deficient mice showed a significant reduction in the frequency of intra-islet CD8 T cells, however the activation status of CD8 T cells was unchanged (Brodie *et al.*, 2008). The authors found that the frequency of CD8 T cells undergoing apoptosis was significantly higher in the islets of B cell deficient mice– indicating that B cells provide a vital survival signal to intra-islet CD8 T cells. Therefore, in situations of tissue-specific inflammation, B cells are able to interact with CD8 T cells in an antigen independent manner to enhance their survival. This provides *in situ* evidence for the B cell 'helper' role described by Deola *et al.,* (2006), and a disease relevant attribute to the antigen independent interaction (and ligand: receptor pairs) detected in the present study.

On the other hand, when speculating on the relevance of antigen independent pathways between B cells and CD8 T cells to the pathogenesis of T1D, it is important to consider the dependence on BCR specificity for B cell pathogenic function. Studies show that skewing of the B cell receptor specificity to an irrelevant antigen i.e. HEL, significantly delayed T1D development in NOD mice, while NOD mice harbouring a B cell population with an increased potential to bind insulin promotes the development of diabetes (Hulbert *et al.*, 2001; Brodie *et al.*, 2008). Therefore, in addition to our observations that B cells are able to cross-present antigen to CD8 T cells to induce cytotoxic function (Chapter 3), it is likely that the antigen independent interaction seen between B cells and CD8 T cells either precedes or occurs concurrently with antigen recognition, in order to mediate and promote the CD8 T cell effector response.

As aforementioned, B cell stimulation in a CD40-dependent manner increased the frequency of B:CD8 doublet formation, potentially due to activation of kinase pathways that in turn lead to integrin activation central to cell-to-cell adhesion. In the context of CD8 T cell effector responses, antigen independent adhesion may precede the TCR-MHC interaction, in order to ensure that T cells can be triggered by cognate antigen, specifically that of low concentrations on the APC. Historical data has shown that adhesive pathways occurring between a T cell and an APC contribute to maintaining a broad area of close proximity between the two cells, allowing diffusion to then bring together the TCR-pMHC complex (Shaw and Luce, 1987).

Further dissemination of these adhesive pathways showed that the integrin CD2, played a role in positioning the T cell membrane at a distance suitable for recognition of peptide-MHC (Wang *et al.*, 1999). Importantly, redistribution of these adhesive molecules resulted in pre-arrangement of the activation machinery required for subsequent antigen recognition, such as the TCR complex, lipid microdomains and associated signalling molecules (i.e. contribution to formation of mature immune synapse) (Tibaldi, Salgia and Reinherz, 2002). Therefore, antigen independent B:CD8 doublets seen in this chapter may represent a 'pre-synapse', that precedes cognate antigen recognition but prepares the T cell for effective, and optimal, antigen recognition and activation. An interesting extension of my experiments to directly address this would be to analyse the longevity of the interactions, comparing those with antigen presentation by the B cell to those without. In contrast to antigen specific interactions, which last for prolonged periods of times, those without antigen involvement would be significantly more transient.

Additionally, the B:CD8 doublets may represent antigen independent signalling pathways that occur concurrently with antigen recognition in order to mediate and optimise the CD8 T cell response. It is well established that in addition to TCR pMHC recognition (signal 1), effective CD8 immunity requires an additional two signals; co-stimulatory signals (signal 2) and pro-inflammatory signals (signal 3) (Curtsinger *et al.*, 1999). These signals synergize with TCR cell signalling, impacting T cell activation, differentiation, effector function and survival. Data presented in this chapter supports this theory. Of the ligand: receptor pairs observed between the B cells and the CD8 T cells, many were members of the cytokine or chemokine families, indicating signalling capabilities. Additionally, pathway enrichment analysis revealed positive regulation of immune responses as the most highly enriched function. Ligand: receptor pairs detected therefore may represent molecular mechanisms by which B cells can modulate CD8 T cell function. Bolstering this concept, is the expression of some of the same B cell ligands *in situ*, on tumour associated B cells (TABs) from melanoma patients, such as *TGFB1, LTA, TNFRSF14* (Griss *et al.*, 2019) . Importantly, the authors found that these TABs were essential for sustaining tumour inflammation, in particular anti-tumour CD8 T cell responses, and their presence correlated strongly with overall patient survival due to effective tumour destruction.

Analyses to identify ligand: receptor pairs were pertinent in addressing our research question and revealed novel cell-cell communication between B cells and CD8 T cells that, as discussed, may be relevant to their interaction in disease. Foundational work by Ramilowski *et al.,* (2015) catalogued all known ligand: receptor pairs, and this provided a database by which the cell-cell communication network could be assessed. Indeed, various studies in a wide array of research fields utilised this database for similar cellular cross-talk analyses, validating my approach (Kumar *et al.*, 2018; Yuan *et al.*, 2019).

However, it is important to consider the limitations of this analysis. Other published databases such as CellPhone DB, utilise a similar repository of ligands, receptors and their interactions but account for the subunit architecture of both the ligands and receptors (Efremova *et al.,* 2020). This is an important consideration in order to represent heteromeric complexes accurately i.e. where ligand: receptor interactions involve multiple subunits such as the receptor for IL1B consisting of the subunits IL1RAP and IL1R1. Interestingly, one-third of the ligand: receptor pairs within the CellPhone database were identified as having a multi-subunit stoichiometry, particularly protein families such as those of the cytokine and chemokine family. This emphasises the relevance to my analyses in which cytokine mediated interactions dominated those detected.

In addition, it is important to highlight that conclusions on cell-cell communication are drawn based on the assumption that mRNA expression values of the ligand: receptor pairs correlate with effective translation of these transcripts into a functional protein. Analysis of the proteome and transcriptome of cells isolated from a tumour microenvironment showed a high correlation of mRNA and protein abundance – where Spearman correlation coefficients between the TPM values for mRNA expression, and LFQ intensity values for protein expression were calculated (Worzfeld *et al.,* 2018). Without proteomics data on the relevant cell subtypes, transcriptomics data is therefore the best alternative, and defendable as indicated by literature showing good correlation between mRNA and protein levels. To support this correlation, an extension of our experiments would have been to validate the expression of the ligands and receptors at a protein level on the surface of the B cells and CD8 T cells, using flow cytometry or western blot analysis.

This study did not directly address the functional impact of ligand: receptor pairs to CD8 T cell function, and it is important to highlight that the pairs identified were between B cells and CD8 T cell *prior* to their interaction. To address the former, an experimental strategy would have been to identify expression of ligand: receptor pairs at a protein level, and then utilise commercial antibodies with blocking activity targeted to one component of the ligand pair (Deola *et al.*, 2008). To assess the impact on CD8 T cell function, the ability of the T cells to generate effective cytotoxic responses (i.e. CD107α degranulation assay) in the presence and absence of blocking antibodies could be compared. Additionally, the impact on CD8 T cell survival could be compared between conditions, using a combinational flow cytometry approach with staining antibodies for 7AAD and annexin IV – this would allow determination of cells in different stages of cell death (i.e. early apoptosis, late apoptosis, necrosis) (Brodie *et al.*, 2008). Moreover, to determine whether any of the ligand: receptor pairs identified were involved in juxtracrine signalling (direct cell-to-cell adhesion), assessment of the frequency of B:CD8 doublets between blocking conditions could be compared.

While these experiments would help segregate the functional relevance of the antigen independent interaction of B cells with CD8 T cells, it is important to note that using this approach would require considerable optimization to ensure that upon blocking the ligand: receptors interaction *in vitro*, complete inhibition of the interaction was achieved i.e. by targeting the region of interaction on the molecule. Additionally, the 'blocking' reagent should have no capacity to induce signalling pathways within the target cell. To achieve this it would be necessary to understand the binding kinetics and structural interaction of each ligand: receptor pair. The identification of ligand: receptor pairs therefore provides potential guidance and reference for future experimental design beyond the scope of this study.

Finally, an interesting experimental extension to address the hierarchy of factors relevant to the B:CD8 doublet formation (CD40L stimulation, cognate HLA expression and ligand: receptor pairs of adhesive capacity) would be to perform combination experiments using both CD40L stimulation and the HLA-A2 blocking antibody (BB7.2) and assess the frequency of B:CD8 doublets. For example, the frequency of doublets present in experiments with the BB7.2 antibody and without

the CD40L stimulation may elude to the contribution of the ligand: receptor pairs to doublet formation.

Concluding remarks

In summary, data presented in this chapter characterise the interaction between B cells and CD8 T cells. B:CD8 doublets were observed in an antigen-independent manner, and key modalities contributing to their formation were identified. Antigen-independent pathways with potential signalling and adhesive capacities were observed between the B cell and the CD8 T cell. Overall, although in a controlled *in vitro* setting, data demonstrate that B cells may govern CD8 T cell responses through adhesion and signalling pathways. This governance may be critical for efficient cytotoxic CD8 T cell responses that mediate β-cell destruction central to T1D pathogenesis and present a critical node for clinical intervention.

5 ANALYSIS OF B CELLS IN THE PANCREAS OF A T1D INDIVIDUAL

5.1 Background to the chapter

The central hypothesis of this thesis is that B cells interact with CD8 T cells in the pancreatic islets of individuals with T1D, in a manner that promotes the β-cell directed cytotoxicity of the CD8 T cells. The previous two chapters have presented data to elucidate the mechanisms by which B cells may interact with CD8 T cells in order to promote effector function. My i*n vitro* studies have revealed that 1) B cells can cross-present antigen to CD8 T cells, to induce their cytotoxic responses, and 2) have identified cell-cell communication pathways that may be relevant to B cell governing of CD8 T cell function. In this *in vitro* setting, data highlights the functional relevance of B:CD8 T cell interactions to β-cell destruction.

While central to elucidating the mechanisms and functional relevance of B:CD8 cell interactions, a limitation of the data is the *in vitro* experimental system that uses peripheral B cells from healthy controls, and antigen specific CD8 T cell clones. To recapitulate interactions relevant to disease, it is necessary to analyse the cells within the inflammatory tissue microenvironment. Therefore, the overarching aim of this final data chapter was to develop and optimise an experimental approach which would provide preliminary data to validate the relevance of B cells and their interaction with CD8 T cells *in situ* i.e. in the pancreatic tissue of an individual with T1D. Building on the transcriptomic data from Chapter 2, I hypothesise that if the ligand: receptor pairs are relevant to B cell governing of CD8 T cell responses in tissue pathology, B cells in the pancreas will express these ligands and/or receptors. To address this, I will establish an experimental system by which single B cells can be identified and isolated from tissue sections in order to perform downstream molecular analysis.

Laser capture microdissection (LCM), allows isolation of individual cells of interest, under direct microscopic (immunofluorescence – IF) visualisation and subsequent molecular profiling (Espina *et al.*, 2006). Therefore, the present study aimed to identify single B cells in the pancreatic tissue and use LCM to isolate these for gene expression analysis. To analyse expression of ligand: receptor pairs on the tissue-residing B cells, RNA-seq analyses (Chapter 2) will be extended in order to probe

for top expressing ligand: receptor pairs between B cells and CD8 T cells. I then aim to establish an experimental system to assess single cell gene expression, in order to determine the molecular profile of the LCM-B cells and ascertain the relevance of B cell governance of CD8 T cell responses *in situ.*

5.2 Optimisation of a fast staining protocol to detect CD20 B cells and CD8 T cells in lymph node tissue sections

Optimal cutting temperature (OCT) solution embedded pancreatic lymph node sections from control (non-diabetic) individuals (obtained from the EUnPOD INNODIA biobank, see section 2.25), were stained for CD20 B cells and CD8 T cells using IF. Briefly, this method utilised an indirect staining approach. A primary antibody specific for the target (CD20 or CD8) was followed by a secondary antibody conjugated to a fluorophore. As the aim of this chapter was to perform molecular analysis on LCM cells, it was pertinent that the staining protocol to identify cells for LCM was rapid in order to preserve RNA integrity. A previously established protocol (University of Siena, Dotta laboratory) took 4 hours to complete, as indicated in Figure 5-1A. Using this protocol, CD20 B cells and CD8 T cells were clearly identified in the lymph node tissue sections (Figure 5-1B). Of note, images were taken using a confocal microscope to clearly display the level of staining for the purpose of this thesis, however throughout the optimisation steps a standard IF microscope was sufficient to visually compare staining of B cells and CD8 T cells. To establish a 'fast' staining protocol, adjustments were made to each step of the original protocol by sequentially reducing the incubation times, and efficient staining confirmed following each adjustment (data not shown). To summarise, the air dry step was removed, the length of the fixation step reduced to two minutes, all wash steps reduced by one cycle and cut from five minutes per wash to three minutes, and staining incubations with the primary antibody and secondary antibody were reduced from one hour to five minutes. This resulted in a fast stain procedure time of 25 minutes, that provided a comparable staining profile for the CD20 B cells and CD8 T cells (Figure 5-1B). Thus, data supported the use of the fast staining protocol to detect B cells and CD8 T cells in pancreatic lymph node tissue sections, for subsequent LCM.

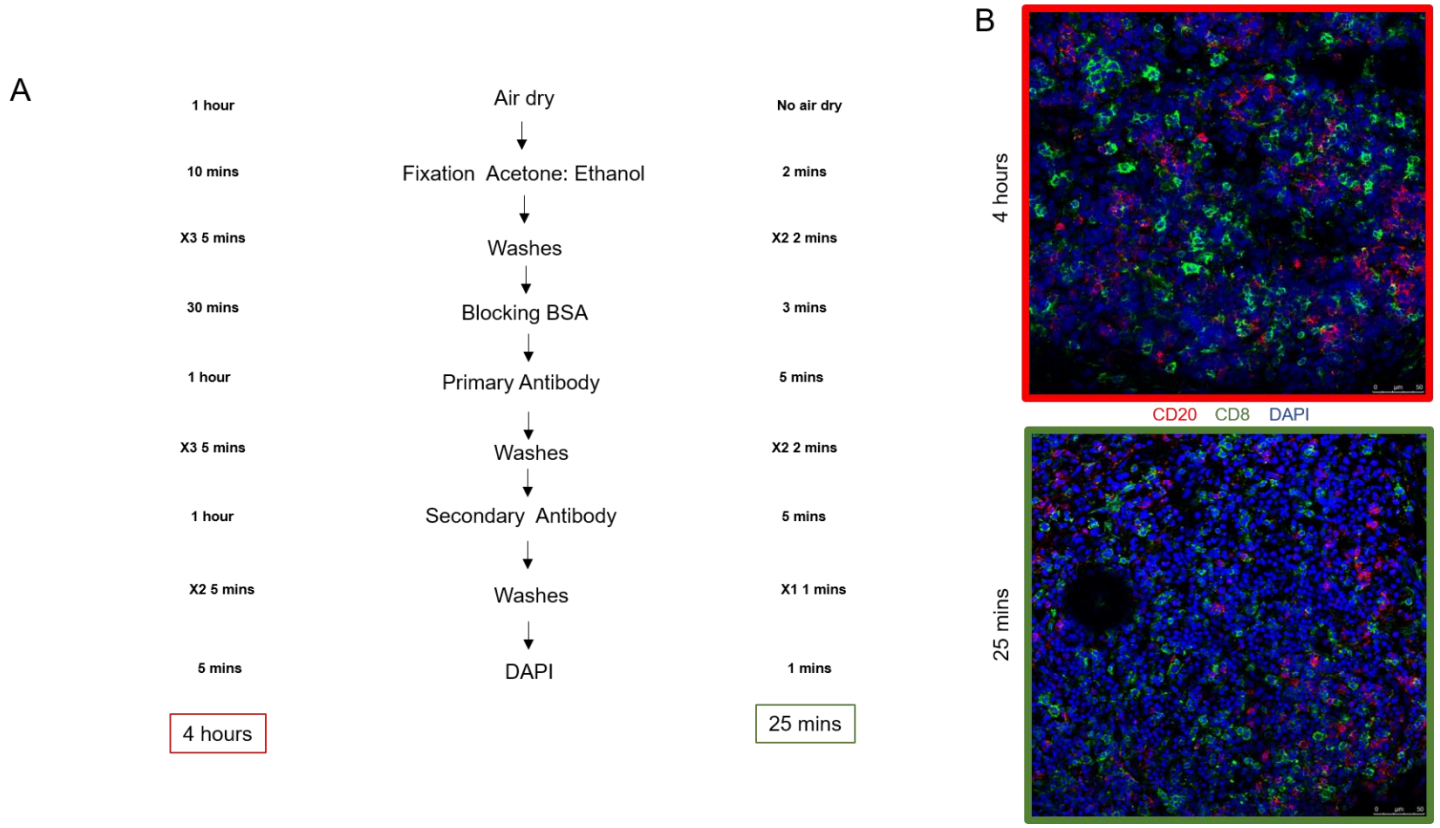

Figure 5-1 Comparable immunofluorescence staining of CD20 B cells and CD8 T cells is achieved in lymph node tissue sections processed through the fast and conventional immuno-staining protocols.

Tissues sections from the lymph node were stained using a slow (4 hour) or fast (25 minute) staining protocol (A). Tissue sections were imaged using confocal microscopy to detect CD20+ B cells and CD8+ T cells. Representative images are shown in (B). Confocal imaging was performed by Guido Sebastiano (University of Siena). Magnification are indicated by the scale bar in each image.

5.3 Detection of CD20 B cells and CD8 T cells in pancreatic tissue

With the detection of CD20 B cells and CD8 T cells in the lymph node tissue sections, the fast staining protocol was applied to tissue sections from the pancreas of a post-mortem sample obtained from an individual with long duration T1D (21 years since diagnosis, age 39 at time of death, donor information in Section 2.25). Pancreatic sections used were serially cut from a tissue block containing a section of the tail portion of the pancreas. As expected, immune cells were observed at a lower frequency as compared to lymph nodes. In particular, considering the age of disease onset of the donor (18 years of age), and the long duration of disease, B cell numbers are likely to be low due to stratification into the CD20lo endotype (Leete *et al.*, 2016). Figure 2A provides an illustrative example of the selective staining of CD20 B cells and CD8 T cells in the pancreatic tissue. Importantly, both cells were successfully visualised by IF and confocal microscopy using the fast staining protocol (Figure 5-2A). Interestingly, in one part of the section, CD8 T cells and CD20 B cells were visualised in close proximity (Figure 5-2B).

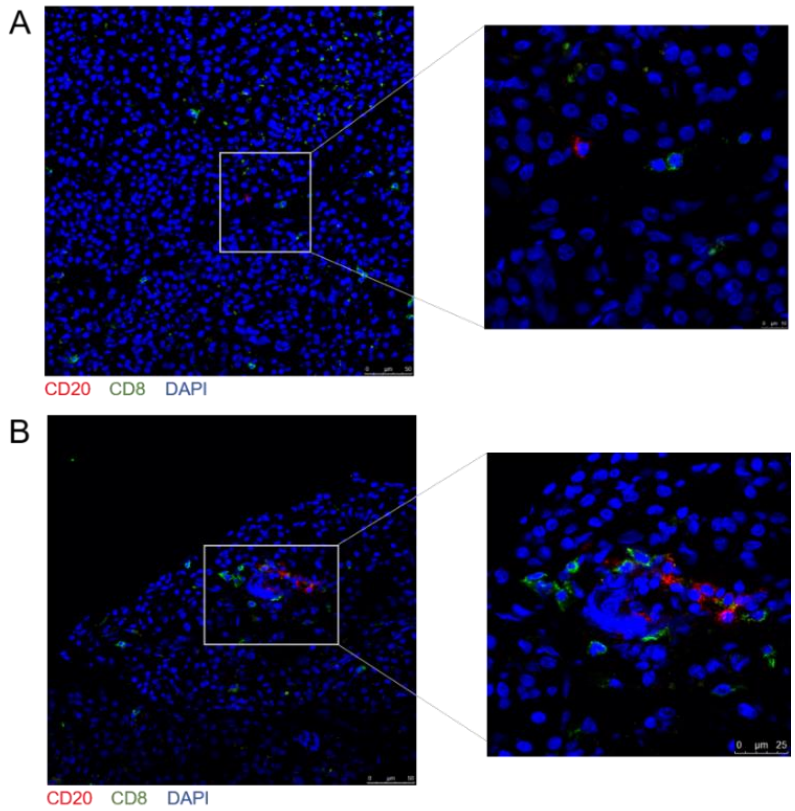

Figure 5-2 B cells are detected in tissue sections from the pancreas using the fast-staining protocol and are observed in proximity with CD8 T cells.
Tissue sections from the pancreas of an individual with T1D were processed for immunofluorescence detection of CD20 B cells and CD8 T cells using the fast-staining protocol and imaged using confocal microscopy for identification of B cells alone (A), and B cells in close proximity with CD8 T cells (B). Magnifications are indicated by the scale bar in each image. Confocal imaging was performed by Guido Sebastiano at (University of Siena).

5.4 Laser capture microdissection of individual B cells from tissue sections

LCM is a technique which allows segregation of single cells from tissue for downstream molecular analysis. The optimisation of a fast staining protocol allowed coupling of this with LCM to isolate single B cells for downstream molecular analysis. For successful LCM, the IF stained tissue needs to be prepared for laser capture through dehydration steps. The section is treated with increasing concentrations of ethanol which replaces the water in the sample, before a 5 minute incubation with xylene, which replaces the alcohol due to its miscibility. Initial attempts to visualise CD20 B cells and CD8 T cells in lymph node tissue sections after dehydration showed that the original staining pattern was lost. This suggests that the dehydration step had interfered with the secondary antibody signal. Despite attempted optimisation of the dehydration protocol in further serial lymph node

sections i.e. reduced concentrations of ethanol, fixation of the secondary antibody staining with 1% PFA, and use of membrane slides that omitted the need for dehydration, efficient staining of the cells in the tissue could not be rescued or preserved (data not shown). From these observations, I concluded that the fluorescence was being quenched with the dehydration step. Therefore, the secondary antibody (for anti-CD20 primary antibody) was replaced with a Cy2 goat anti-mouse antibody, due to cyanine conjugates being more resistant to ethanol. Indeed, sufficient staining of CD20 B cells was achieved after dehydration steps using the cyanine conjugated secondary antibody. Due to time constraints during my lab visit and the lack of an available cyanine conjugated secondary antibody for the anti-CD8 primary antibody, staining for CD8 T cells was omitted from future experiments. With the successful detection of CD20 B cells in the tissue sections after tissue dehydration, LCM of single B cells was carried out (Figure 5-3A). Here, transfer film is present on the LCM tube cap, and a laser pulse (used for cutting a pre-determined area) focally activates this transfer film – securing the single cell of interest and capturing it from the tissue section. Figure 5-3B represents illustrative images of the IF microscope field of view and selection of single B cells. Of note, background autofluorescence was relatively high, particularly in the pancreas sample, and single B cells were selected based on uniform staining around the circumference of the cell. To confirm successful capture of the single cell, the LCM cap was visualised in brightfield and fluorescence, in order to confirm the presence of the cell on the LCM cap (Figure 5-3C). Overall, LCM of single B cells was successful, with 10 single B cells captured from the lymph node tissue section and 10 single B cells from the pancreatic tissue section.

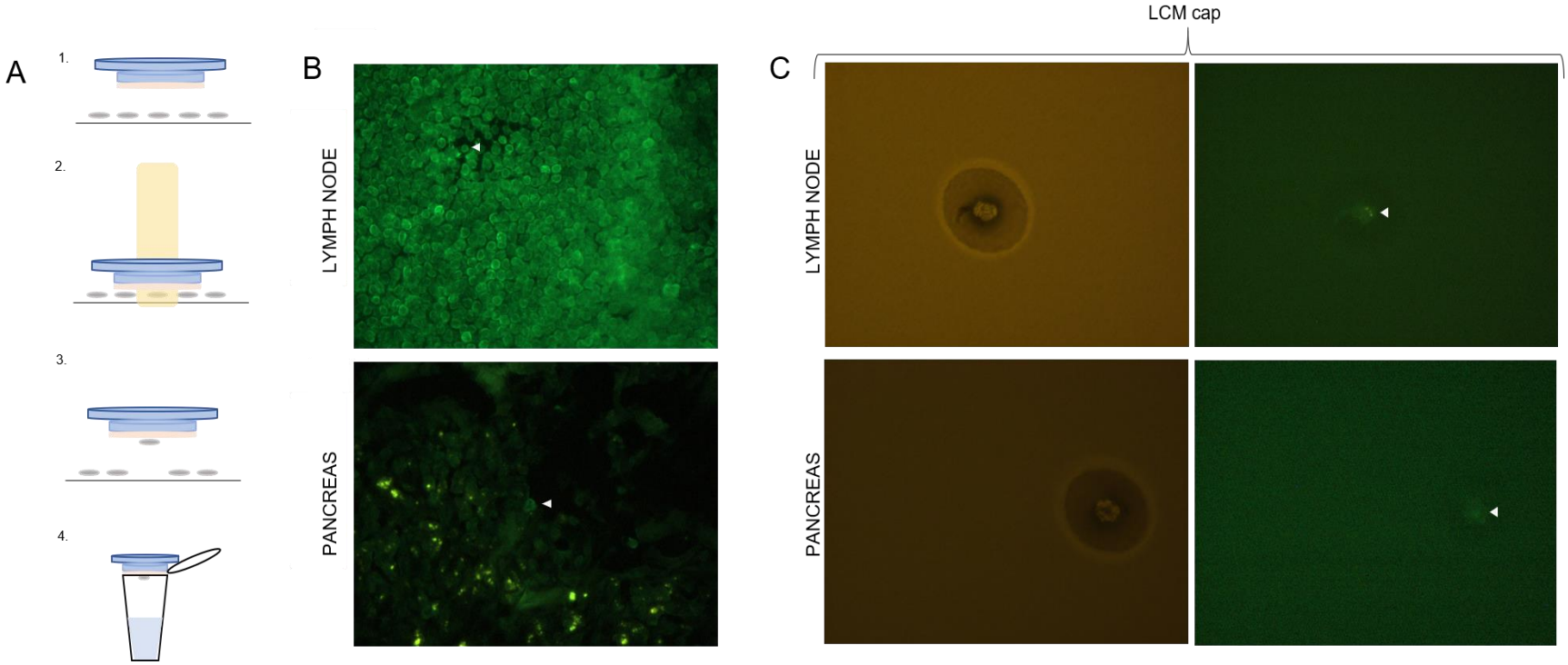

Figure 5-3 Single B cells can be identified and collected from lymph node and pancreatic tissue sections, using laser capture microdissection.
Tissue sections were stained for CD20+ B cells and visualised using an immunofluorescence microscope coupled to an LCM machine (A). Single B cells were selected visually (indicated by white arrowheads) and targeted for dissection (B). Cells were captured into the LCM cap and presence confirmed using brightfield and IF (C).

5.5 Identification of a 'key' ligandome from transcriptomic analysis of B cells and CD8 T cells

The successful isolation of single B cells from tissue sections provided the material required for molecular analysis to validate the role of B cells *in situ*. As data presented throughout this thesis has eluded to, B cells may function in the islets to govern CD8 T cell responses through cross-presentation of antigen, and cell-cell communication through pathways of adhesive and signalling capabilities. Validation of the former function using the LCM single B cells is challenging due to the lack of a tangible molecular signature. The latter however, used RNA-seq analysis to define ligand: receptor pairs that existed between the B cells and CD8 T cells. Therefore, as a natural extension to validate the relevance of these pathways, I assessed the expression of ligands on B cells isolated from the pancreatic tissue. Their expression on pancreas-infiltrating B cells isolated *in situ* would provide evidence for governance of CD8 T cell responses central to β-cell destruction.

As shown in Chapter 4, over 20 ligand: receptor pairs were identified between B cells and CD8 T cells, and over 15 were observed between CD8 T cells and B cells. It was experimentally infeasible to screen LCM single B cells for all ligands and receptors detected in the transcriptomic analysis (due to lack of material and expense of reagents). Therefore, I refined these analyses to identify the key 'ligandome' present between B cells and CD8 T cells. To do this, I applied a stringent TPM expression threshold of 3 for both the ligand and receptor, and interaction scores were calculated as the product of these values. This cut off identified the top expressing ligand: receptor interactions between the two cell subsets, in both directions. Additionally, this threshold prevented ligand: receptor pairs being included that scored highly by the metric but were driven predominantly by high expression of one component of the pair.

Focussing the analysis on the CD40- stimulated, ADS pulsed B cells, 8 ligand: receptor pairs were identified, two of which expressed the ligand on the T cell while the remaining six expressed the ligand on the B cell (Figure 5-4A,B). As expected from the previous analyses, pairs identified were dominated by members of chemokine and cytokine families, as well extra-cellular matrix and integrin families. This further bolstered my previous conclusion (Chapter 4) that B:CD8 interactions

may represent signalling and adhesive pathways that modulate CD8 T cell function. Importantly, the identification of a key ligandome provided target genes to analyse the expression of on the LCM-captured single B cells, in order to validate their function in disease specific tissue.

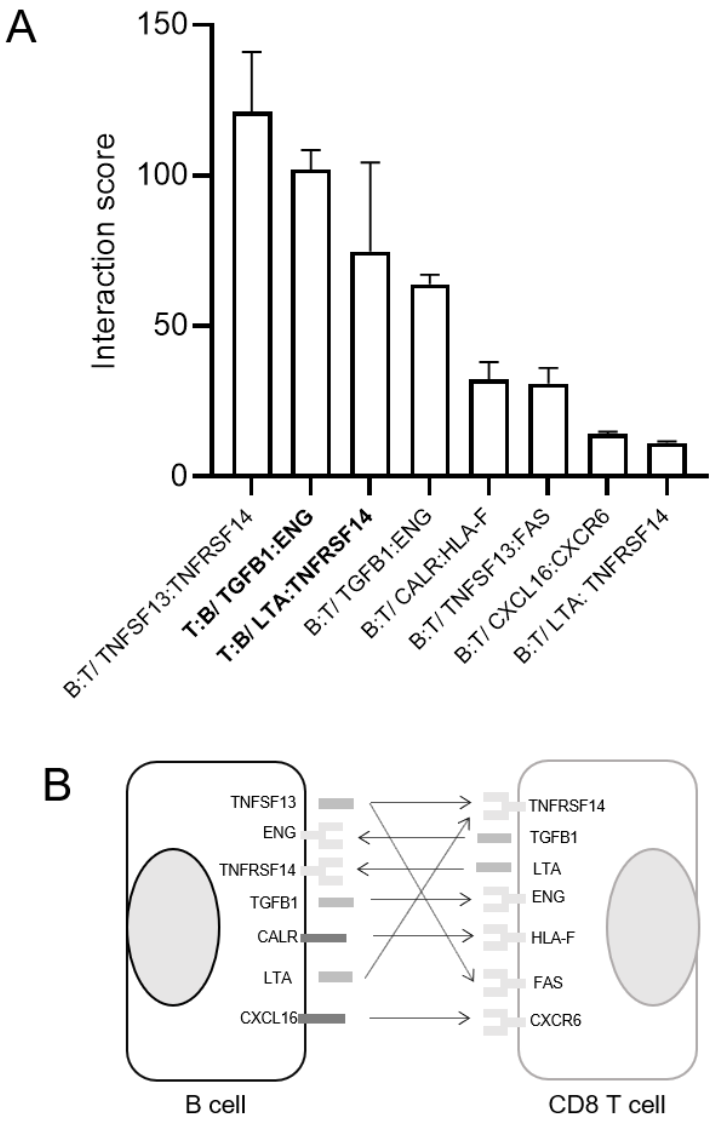

Figure 5-4 A key ligandome of eight ligand: receptor pairs is detected between B cells and CD8 T cells using a stringent analysis of RNA-seq data.

Top expressing pairs were identified between B cells and CD8 T cells, by calculating the interaction score for each ligand: receptor pair as the product of the expression of the ligand and the expression of the receptor, using a TPM threshold of 3 for each ligand and receptor of each pair (A). Data represents the average interaction score for three independent B cell donors, ± SEM. Corresponding ligand: receptor pairs between each cell type are displayed schematically (B).

5.6 Optimisation of single cell qRT-PCR optimisation

5.6.1 Experimental approach

With the successful isolation of single B cells and the identification of target genes that comprise the key ligandome, the next experimental step was to assess the expression of these genes on single cells. To do this, a molecular approach was adopted using a single cell qRT-PCR protocol – utilising Taqman technology for gene expression analysis. Taqman technology was selected over SYBR due to its higher specificity for target, and compatibility with an established protocol for cDNA synthesis, amplification and downstream gene expression analysis (Methods; Single-Cell-to-CT qRT-PCR kit, ThermoFisher). Target genes were selected as the ligands or receptors expressed on the B cell, shown in Figure 5-4 – *TNFSF13, ENG, TNFSFR14, TGFB1, CALR, LTA, CXCL16*. B cell reference genes (*CD79A, CD19*) and housekeeping (HK) genes (*ACTB, YWHAZ*) were also included in the gene expression analysis as positive controls to confirm the presence of at least one B cell in each sample, and to validate success at each stage of the protocol.

For example, if single cells showed expression of at least one HK gene and one reference gene, then it can be concluded that at least a single B cell was successfully acquired, that lysis of the cell was efficient to release RNA and that the RNA integrity and concentration was high enough for successful cDNA synthesis. Taqman gene expression assays were selected from the library of pre-designed assays provided by ThermoFisher; when multiple assays were available for the same target, the assay with the best coverage, and shortest amplicon length was chosen.

5.6.2 Validation of the efficiency of Taqman gene expression assays

The efficiency of the gene expression assays (Taqman probes) for the target genes, and HK and reference genes, was determined by establishing a serial dilution of the cDNA template (converted from bulk RNA extracted from PBMCs) in order to generate a standard curve for each gene. A 1:10 dilution series with 5 points was created for each gene expression assay, and the RT-qPCR reaction performed. The cycle to threshold (Ct) value was then plotted against the dilution factor of the cDNA template in a base 10 semi logarithmic graph, and the data fit to a straight line. As shown in Figure 5-5, R^2 (correlation coefficient) values for all gene expression

assays were over 0.99. The slope of the straight line could then be used for determining the amplification efficiency using the following calculation:

Amplification efficiency = [10(-1/slope)]-1

100% amplification efficiency equals a doubling of message every cycle; the closer the straight line is to - 3.32, the closer the amplification efficiency is to 100% i.e. for every 10-fold dilution of the template, it would take 3.32 more cycles of amplification to reach the threshold. As indicated in Figure 5-5D, the slope for each gene expression assay was close to -3.32, and the efficiency for each was consistently calculated at over 88%. Taken together, these data indicate that the Taqman gene expression assays selected were efficient at amplifying their target gene.

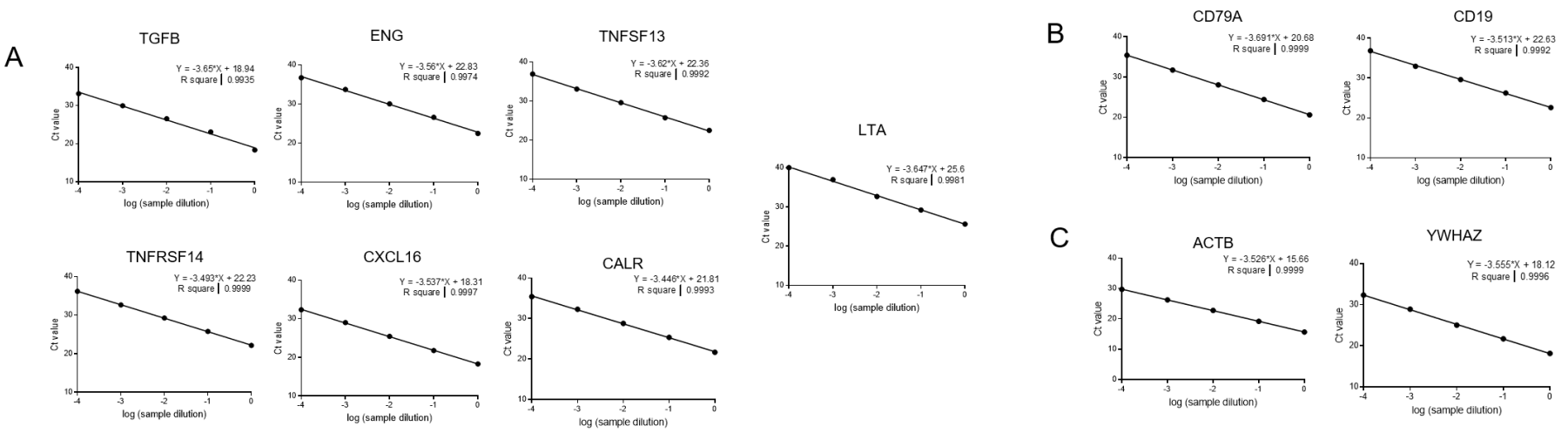

D

	TGFB	ENG	TNFSF13	TNFRSF14	LTA	CXCL16	CALR	CD79	CD19	ACTB	YWHAZ
slope	-3.65	-3.56	-3.62	-3.49	-3.64	-3.53	-3.44	-3.69	-3.51	-3.52	-3.55
efficiency	88	91	89	93	88	92	95	87	93	93	91
R squared	0.9935	0.9974	0.9992	0.9999	0.9981	0.9997	0.9993	0.9999	0.9992	0.9999	0.9996

Figure 5-5 Gene expression assays (Taqman) selected for each target gene showed good primer efficiency.

Results of amplification curves of target genes (A), B cell reference genes (B) and housekeeping genes (C). A standard curve was generated using five serial 10-fold dilutions of total RNA extracted from $1x10^6$ PBMCs from healthy control blood. The efficiency of each primer was evaluated by plotting the cycle threshold value (Ct) at each dilution point against the logarithm of the fold dilution of the sample. The efficiency of the primers were calculated from the standard curve slope, as were the slope value and R squared value (D).

5.7 Validation of key ligandome expression in RNA from bulk B cell

As the key ligandome had been identified from the RNA-seq data, it was necessary to validate and confirm the expression of genes in bulk populations of B cells using qRT-PCR. RNA was extracted from 100,000 class-switched, memory B cells, isolated from PBMCs from a healthy control individual. cDNA was then synthesised, and qPCR reactions performed using the validated gene expression assays. As seen in Figure 5-6, all genes were expressed by the class switched, memory B cell population. This independently confirmed the RNA-seq data, providing evidence that the key ligandome was expressed by the B cells. The reference genes and housekeeping genes were also expressed by the B cells, validating the use of these targets as controls in the gene expression experiments.

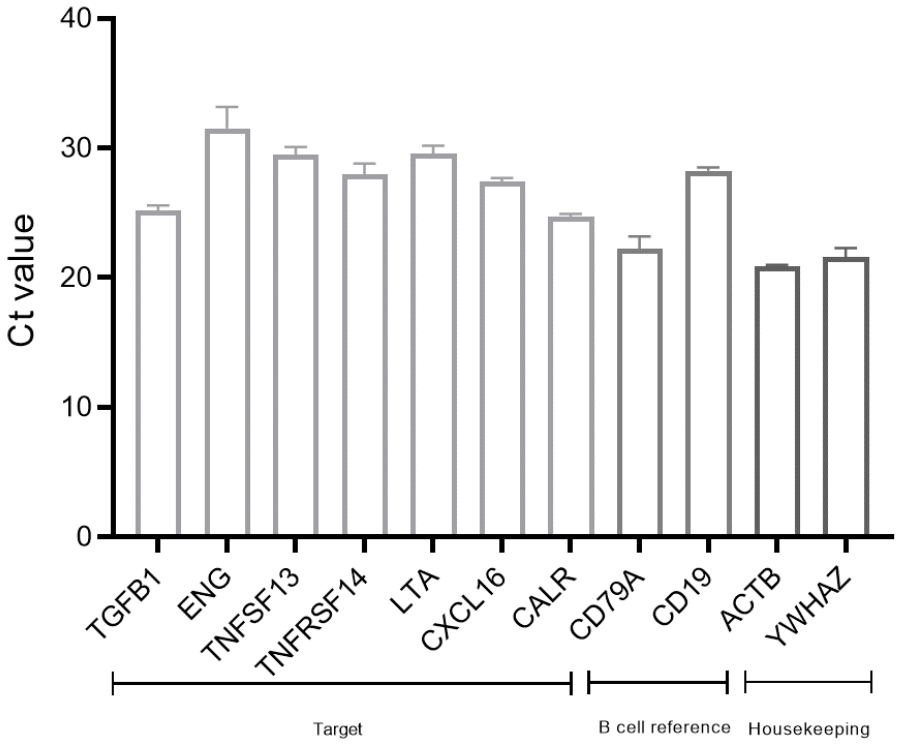

Figure 5-6 Key ligandome genes, and the B cell reference and housekeeping genes, are expressed by class-switched memory, CD40L stimulated B cells isolated from the peripheral blood.

RNA was isolated from 10,000 class-switched memory B cells and cDNA was synthesized. Quantitative RT-PCR reactions were then performed on the cDNA for each target gene. Data represents the average Ct value (mean average ± SD) of two independent experiments (n=2), in which each gene was analysed in technical duplicate. Ct= threshold cycle.

5.8 Optimisation of single cell q RT-PCR experimental strategy

With the confirmation of the gene expression assay efficiency for the target genes, and the validation of their expression in bulk B cell populations, a single cell gene expression experimental strategy could be optimised in order to finally assess the expression of the key ligandome on the LCM single B cells. The protocol used for the single cell gene expression experiments was that of the Single-Cell-to-CT qRT-PCR kit (ThermoFisher). Briefly, after the capture of a single cell into lysis buffer, reverse transcription from RNA to cDNA is performed directly on the lysed sample, followed by a pre amplification step using a pool of the gene expression assays for all the targets of interest. Amplification reactions for each target gene were then performed on the preamplified product, using qRT-PCR.

To initially validate the use of this protocol, RNA was extracted from 500 class-switched memory B cells. Additionally, RNA from a population of CD4 T cells was used, in order to confirm the specificity of target gene amplification. No template controls (NTC) were included, in which the template is omitted from the reaction and replaced with water, to serve as a control for contamination or primer-dimer formation. As seen in Figure 5-7, the protocol was successful in detection of the targets of interest, with Ct values of <35 for all genes; confirming successful cDNA synthesis, pre-amplification and RT-PCR of RNA isolated from a bulk population of B cells. Importantly, the B cell reference genes were not detected in the samples of CD4 T cell RNA, confirming specificity of the gene amplification. Additionally, in the NTC samples there was no expression of any of the genes – providing evidence against any contamination throughout the protocol that would result in false positives, or formation of primer-dimers. Of note, these controls were included in all further experiments to confirm experimental success and validity of test sample results.

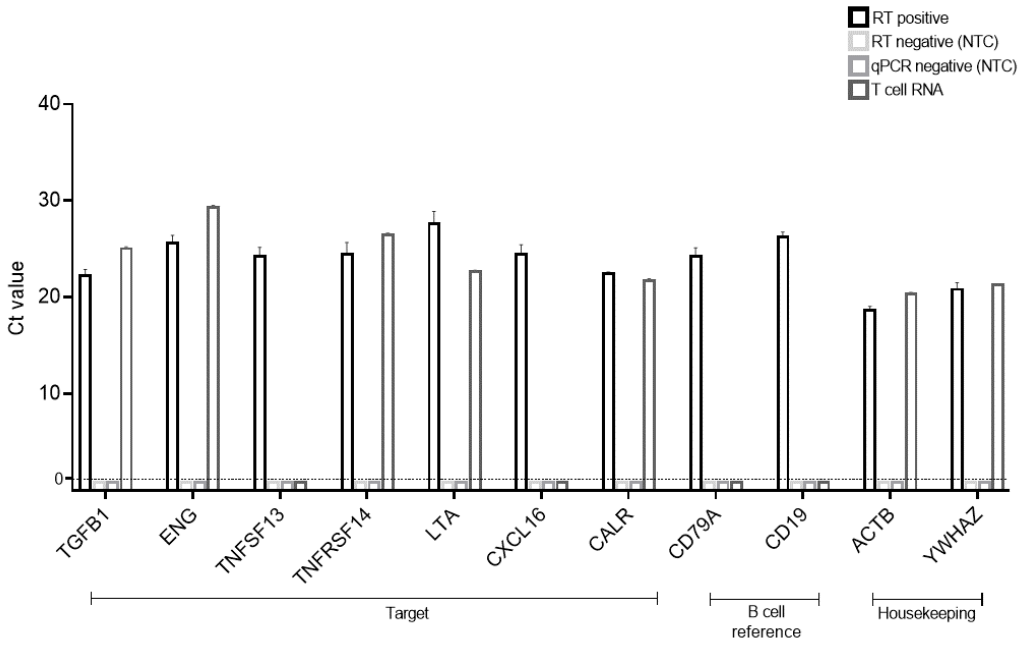

Figure 5-7 The single cell qPCR protocol can specifically, and efficiently detect expression of the target genes, and B cell reference and housekeeping genes, in a bulk population of memory, class-switched B cells.

Following the single cell RT-qPCR protocol (methods) cDNA was synthesized from a bulk population of memory class-switched, CD40L stimulated B cells (500 cells), or a bulk population of CD4+ T cells (500 cells), pre-amplified and processed through the RT-qPCR reaction with separate reactions for each gene expression assay (target gene). No template controls were included in the cDNA synthesis stage and the RT-qPCR reaction stage. RT-qPCR reactions were performed in technical duplicate, and the average Ct value calculated from the duplicates. Data represents the average Ct value from two independent experiments (± SD, n=2).

With the notion that the Single-Cell-to-CT qRT-PCR protocol was efficient and specific in detecting and quantifying expression of the target genes in bulk populations of B cells, the next aim was to validate the use of the same protocol in single B cells. To do this, class switched memory B cells were isolated from PBMCs and stimulated for 24 hours with MEGACD40L. Single cells were then sorted by FACs into cell lysis buffer, in order to mimic the capture and lysis of single B cells from the tissue by LCM. Data presented in Figure 5-8A shows the frequency of cells that expressed each target gene. Data shown is from two independent experiments, in which 5 single cells were analysed per experiment, therefore the frequency of cells expressing each gene correlates to how many cells out of the 10 had a Ct value of

<35. Figure 5-8, shows the average Ct values for the cells that were expressing the genes <35 Ct, i.e. if 100% of cells showed expression, the average mean Ct value for 10 cells is plotted, however if 50% of cells showed expression, the average Ct value was plotted for the 5 positive cells. As seen in Figure 5.8, 100% of the cells expressed the housekeeping genes *ACTB* and *YWHAZ*, 100% of the cells expressed the B cell reference gene *CD79A*, and 70% expressed the B cell reference gene *CD19*. This confirmed the presence of at least a single cell in each sample and indicated that the cell lysis was efficient and that the RNA from the single cell was successfully reverse-transcribed to cDNA. Of the target genes comprising the key ligandome, all of the cells expressed *TGFB1* with an average Ct value of 29.6. 70 % of the B cells expressed *TNFRSF14* (Ct = 31.1 $\pm$ 2.3), half of the B cells expressed *LTA* (Ct = 28.18 $\pm$ 1.3), and 100% of the cells expressed *CALR* (Ct = 29.39 $\pm$ 1.9). *ENG, TNFSF13 AND CXCL16* were not expressed in any of the analysed 10 cells (non-determined Ct value due to no amplification). Although not all the targets were detected, the expression of reference and housekeeping genes, and target expression in the positive controls (Figure 5-7), supported the conclusion that in those cells, the target was either not expressed or was expressed below the level of detection.

Taken together, this data validated the experimental system to assess gene expression in single cells. Efficient detection of housekeeping and B cell reference genes confirmed the presence of (at least) a single B cell in each sample, and indicated successful cDNA synthesis, pre-amplification and specific amplification of the target by the primers. Additionally, the detection of some target genes of the key ligandome further bolstered the robustness of the experimental approach.

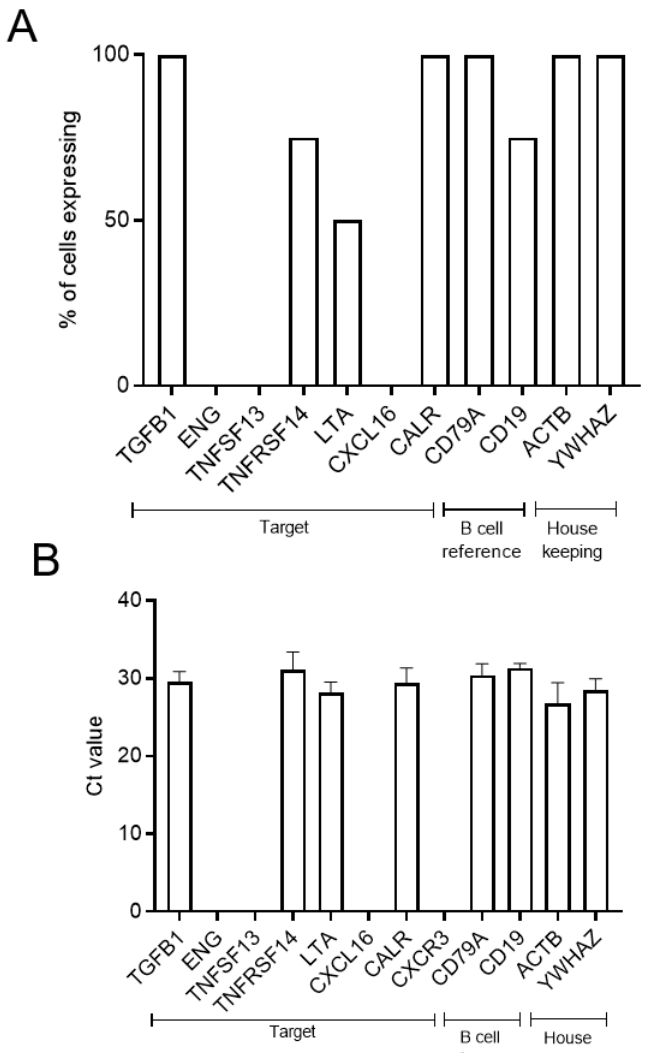

Figure 5-8 Expression of B cell reference genes, housekeeping genes and some target genes from the key ligandome can be detected by the single cell qPCR protocol, in single class-switched memory B cells isolated from PBMCs of healthy individuals and stimulated for 24 hours with MEGACD40L.

Single B cells were sorted using flow cytometry into lysis buffer and cDNA was synthesized prior to a pre-amplification stage. Pre-amplified products were then used in the RT-PCR reaction to determine gene expression. Data represents two independent experiments where each experiment analyzed gene expression in 5 single cells. RT-PCR reactions were performed in technical duplicate, and the average Ct value calculated from the duplicates. Data represents the percentage of cells expressing the gene (Ct value <35, n= 10 single cells), or the average Ct value for the number of cells expressing the target gene (±SD).

5.9 Single cell qRT-PCR of LCM single B cells

The optimisation and validation of a protocol by which gene expression could be assessed in single cells, allowed its use in the assessment of gene expression in the LCM- single B cells from either lymph node tissues or pancreatic tissues. As

aforementioned, analysis of the expression of the key ligandome on single B cells isolated from the pancreas would provide evidence to support their potential pathological role of governing CD8 T cell responses *in situ.* Experimentally, the aim was to first determine the expression of target genes in the single cells in both the lymph node B cells and the pancreatic B cells, before comparing the expression levels between the two locations. The hypothesis of these final experiments was that the pancreatic B cells would preferentially express the target genes from the key ligandome, due to their governing of CD8 T cell responses in order to enhance β-cell destruction in the islets.

For all experiments analysing gene expression in the LCM-single B cells, the positive and negative controls worked as expected (data not shown), confirming success of the experimental procedure. Figure 5-9A shows gene expression results of the single B cells captured from the lymph node tissue, where data is presented as the frequency (of the 10) cells that expressed the gene, as determined by a Ct value of <35. For the housekeeping genes, 100% of the cells expressed *ACTB* and 60% expressed *YWHAZ*. B cell reference genes, *CD19* and *CD79A*, were expressed by 70% and 20% of the cells, respectively. Of the key ligandome cells, 10% expressed *TGFB1*, while 40% expressed *TNFRSF14*. No other target genes appeared to be expressed by the lymph node B cells.

The gene expression data for the single cells isolated from the pancreas is shown in Figure 5-9B. Of note, the location of the B cells relative to the islets was not known due to a lack of additional markers to define the endocrine regions. The only gene I detected expression of was the housekeeping gene *ACTB* in one cell (10%). None of the B cell reference genes were detected, and neither were the target genes of the key ligandome. Due to the lack of housekeeping and reference gene expression in the single cell samples, it is likely that the initial sample was not conducive with successful cDNA synthesis (Discussion). Additionally, it should be considered that the HK and reference genes selected may not be relevant to B cells in different tissues. Therefore, disappointingly, no conclusions can be drawn regarding the expression of the key ligandome on pancreatic single B cells in the current study.

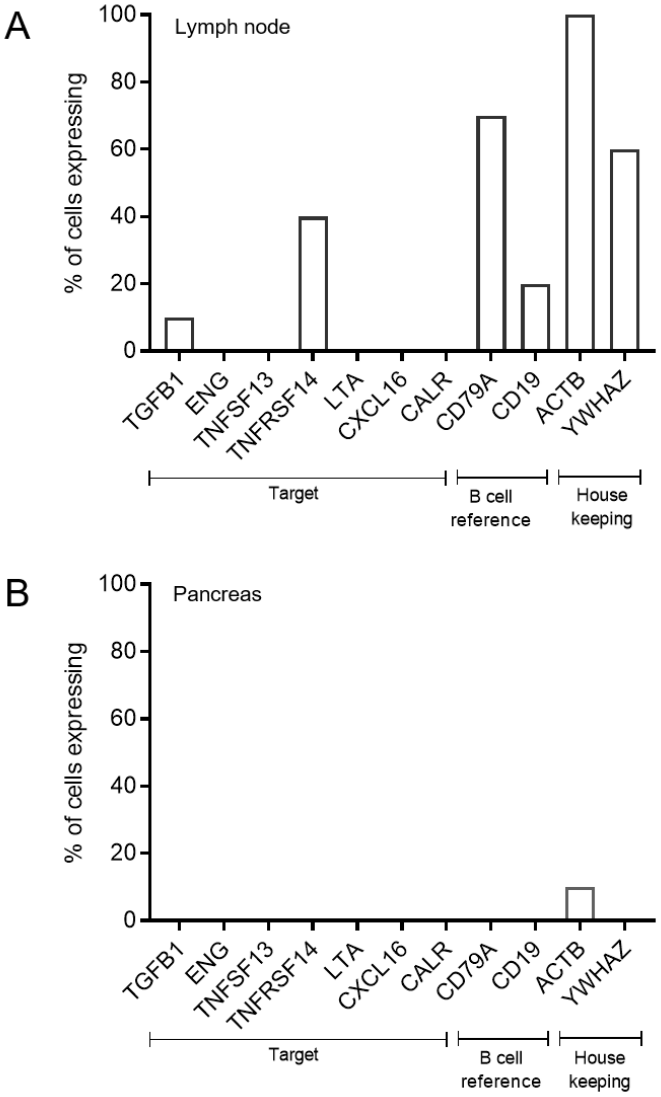

Figure 5-9 Gene expression analysis of LCM-captured single B cells.
Following the single cell qPCR protocol, cDNA was synthesised from the LCM-captured single B cells and pre-amplified. RT-PCR reactions were then performed on the pre-amplified products for each target gene. RT-PCR reactions were performed in technical duplicate, and the average Ct value calculated from the duplicates. Data presented is the percentage of cells (n=10) captured from the lymph node tissue section of a healthy control (A) or the pancreatic tissue section of an individual with T1D (B) that showed expression of the gene (Ct <35) , where 10 single cells were analysed for each.

5.10 CXL16 observation

Despite the failure to experimentally assess the mRNA expression of the key ligandome on **single** B cells isolated from the pancreas, a cluster of B cells was also captured from the pancreatic tissue section (Figure 5-10A). Although no CD8 staining was included in the LCM IF, due to the location of the cluster on the consecutive tissue section and brightfield observations it was presumed that the cluster was the same as the cluster of both CD8 T cells and CD20 B cells identified by confocal microscopy in the optimisation stages (Figure 5-2B). Interestingly, gene expression analysis of this B cell cluster showed expression of the housekeeping gene *ACTB* (Ct = 34.6) and of *CXCL16* (Ct = 34.3), a gene from the key ligandome (Figure 5-10B). While extremely preliminary, and limited to an n of one, this observation presents CXCL16 as a ligand that may be expressed by B cells that cluster and occur in close proximity to CD8 T cells in the pancreas of a T1D individual.

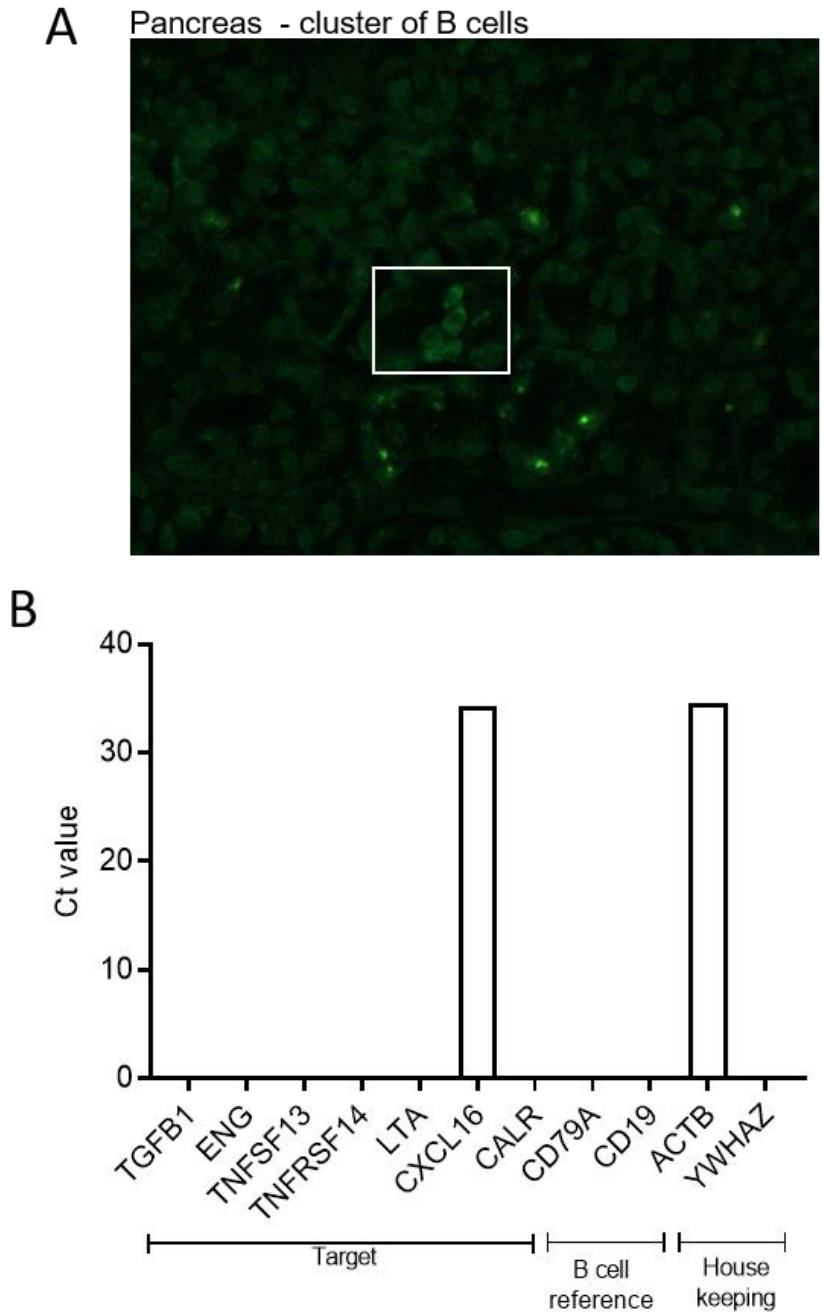

Figure 5-10 CXCL16 gene expression is detected in a cluster of B cells isolated from the pancreas of an individual with T1D.

A B cell cluster was isolated from the tissue using LCM and processed through the single cell q PCR protocol. cDNA was synthesized from the LCM-captured single B cells and pre-amplified. RT-PCR reactions were performed on the pre-amplified products for each target gene. Data represents the Ct value of each target gene in the B cell cluster.

5.11 Discussion

In this chapter, an experimental approach was established that provided an analysis pipeline by which the relevance of B cell interaction with CD8 T cells to T1D tissue pathology could be validated. Specifically, this study focused on a disease relevant, tissue-specific context by utilising pancreatic tissue samples donated to nPOD.

Extending the analysis of the bulk RNA-seq data from Chapter 4, a key ligandome was observed between B cells and CD8 T cells and expression confirmed independently using RT-qPCR in a population of B cells isolated from the peripheral blood of healthy individuals. To contextualise these findings, pancreatic tissue sections from an individual with T1D were utilised. Imaging observations indicated the presence of B cells in the pancreatic tissue of an individual with T1D, and preliminarily identified B cells in close proximity to CD8 T cells. Optimisation of a staining approach compatible with efficient LCM of single B cells, and development of a molecular approach to analyse single cell gene expression, established a methodology to determine the expression of the key ligandome on B cells in the pancreas. Limited by experimental constraints, no conclusive data could be drawn from the single cell gene expression analysis of LCM-captured single cells, however establishment of this approach paves the way for future research. Finally, gene expression analysis from a cluster of B cells isolated from the pancreas provided anecdotal evidence of *CXCL16* expression; postulating this ligand: receptor pair (CXCL16-CXCR6) in a disease relevant setting.

The use of a higher TPM threshold (TPM > 3), refined previous RNA-seq analyses (Chapter 2) to identify the top expressing ligand: receptor pairs between the B cells and CD8 T cells, that may therefore be most relevant to cell-cell communication and B cell governing of T cell responses. Indeed, pairs within the ligandome were enriched for cytokine and chemokine signalling, suggesting positive immune regulation pathways, and further bolstering the concept that B cells may modulate CD8 T cell function through antigen-independent signalling pathways (Chapter 4).

The detection of a key ligandome presented the hypothesis that pancreatic B cells would express these ligands and/or receptors, in order to mediate CD8 T cell cytotoxic responses and contribute to β-cell destruction. The availability of samples from EUnPOD donors allowed this hypothesis to be addressed. These samples were

critical in order to validate B cell function in a disease-relevant, tissue specific context. It is important to note, however, that the key ligandome was identified through RNA-seq of immune cells in the peripheral blood of healthy, non-diabetic individuals, therefore the ligands and receptors identified may be less pertinent to B cell function within the pancreatic tissue of T1D individuals. For example, the expression profile of ligand: receptor pairs may have been different if pancreatic immune cells were analysed in the bulk RNA-seq experiments, particularly in the context of an enriched tissue residency specific gene profile (Weisel *et al.*, 2020) . However, the infeasibility of this approach (lack of tissue availability, experimental requirements for RNA quantity and quality) supports the analysis of immune cells from the blood and the use of the 'key ligandome' in the current study.

To analyse molecular profiles of single cells in tissue, LCM was utilised to isolate cells of interest from the tissue, through combination with IF staining. This experimental approach was adjusted for optimal capture and maintenance of RNA quality by minimising the time required for sufficient IF staining. The staining protocol was reduced from over 4 hours in length to just under 25 minutes. Importantly, visualisation of the B cells (by both IF and confocal microscopy) was comparable between each protocol.

The single cell gene expression protocol was initially optimised on peripheral single B cells sorted by flow cytometry from healthy donor blood. Expression of HK and reference genes was consistent across all single cells. Target gene expression (from the key ligandome) was also identified. Despite this optimisation, molecular profiling of LCM-captured single cells from the tissue was inadequate in efficacy. In particular, detection of gene expression profiles were not conclusive in B cells captured from the pancreatic tissue. The presence of controls at each experimental stage allowed me to reject the possibility that this was due to error in the single cell gene expression protocol. Therefore, the failure to detect gene expression in LCM-captured cells is likely to be due to the sample quality and quantity i.e. RNA integrity and concentration, respectively.

LCM-captured B cells from the lymph node showed some expression of the B cell reference and HK genes. All cells expressed *ACTB* while 70% of cells expressed *CD79A.* Of the key ligandome, 40% of cells expressed *TNFRSF14*. This is in

concordance with previous literature that shows protein expression of TNFRSF14, or HVEM, on B cells in the lymph nodes – occurring as a regulatory mechanism involved in selection (Mintz *et al.*, 2019). In single cells captured from the pancreatic tissue, however, no expression of B cell reference genes or key ligandome genes were detected. As the same staining and LCM protocols were used for lymph node and pancreas tissue sections, this again supports the notion that inconclusive gene expression analysis was due to inadequate sample quantity and quality.

Factors influencing sample quantity and quality are numerous. In the context of tissue versus peripheral blood cell molecular profiling, differences can be attributed to the capture protocol. Isolation of single cells from a peripheral blood sample by FACs is a shorter and less intensive tissue handling and processing procedure as compared to LCM. Therefore, the RNA integrity of the captured and lysed cell from peripheral blood is likely to be higher. Additionally, microfluidic single cell isolation captures the whole cell. LCM captures only a part of the cell, and therefore represents a fraction of the total possible RNA, resulting in a lower starting concentration. Moreover, sample preparation of tissue sections requires surgical dissection. This process is often associated with autolysis of the tissue, due to abundant RNases, DNases and proteases present (Jun *et al.*, 2018). While attempts were made to mitigate this by snap freezing the tissue samples, RNA quality may have been compromised in the initial tissue specimen preparation.

Comparing molecular profiling results of B cells isolated from the lymph node and the pancreas, differences can be attributed to the tissue-specific variances. Endogenous RNase levels are particularly abundant in the pancreas: RNA isolated from the human pancreas is consistently of poor quality due to RNA degradation (Sorrentino, 1998). Therefore, in comparison to lymph node B cells, RNA integrity of pancreatic LCM-captured B cells is likely to be lower. Additionally, B cells in the lymph node are likely to be in a more activated state – increasing the level of cellular RNA and therefore the concentration of starting material.

As well as insufficient sample quality and quantity, the inconclusive gene expression results may also be due to limitations of the single cell RT-qPCR approach. For example, genes of very low transcript level may have been beyond the limit of detection of the assay. To ascertain this, Ct values of the genes of interest can be

compared between experiments analysing single cells, and experiments analysing RNA isolated from a bulk population of the same cell. In the latter, RNA was isolated from 500 cells, representing a 500-fold higher concentration as compared to the single cell. Theoretically, the RT-qPCR reaction will amplify the cDNA exponentially by doubling the target molecules of each cycle. For every 10-fold dilution of sample concentration, the Ct value will therefore increase by 3.3. Accounting for the 500-fold difference between the bulk RNA sample and the single cell, the difference in Ct value would therefore be expected to be ~8 cycles. For example, the Ct value for *TGFB1* in the bulk RNA sample was 22 and 30 in the single cell sample. With this in mind, it is likely that some of the target genes could not be detected at a single cell level, as they were beyond the limit of detection (Ct >35) due to too low a transcript level.

Attempts were made to address this. For example, increasing the concentration of pre-amplified cDNA added into the RT- qPCR reaction and increasing the number of cycles within the RT – qPCR reaction (data not shown). These did not impact the Ct values. Therefore, an extension of the study would be to optimise alternative stages of the protocol, such as the preamplification stage. Here, target specific preamplification is performed by PCR using predesigned primer pools in order to yield sufficient numbers of molecules for the downstream RT- qPCR reactions. For robust detection of a target gene, one study extended their preamplification stage from the recommended 14 cycles to 20 cycles, in order to ensure > 99% probability of detecting one cDNA molecule (Livak *et al.*, 2013) .

A preferable approach to address the research question of this chapter would therefore be one that preserves RNA integrity, has sufficient starting material, and is sensitive to low expressing transcripts. Importantly, spatial information and compatibility with fresh frozen tissue sections should still be retained. Fluorescence *in situ* hybridization (FISH) uses probes - DNA fragments incorporated with fluorophore-coupled nucleotides, to analyse the presence of transcripts in tissues under a fluorescent microscope. Major advantages of this method include high sensitivity and specificity, and resolution at a single cell level. Additionally, the *in situ* nature of the method is significantly less laborious than LCM, potentially reducing the risk of contamination and degradation that may interfere with

experimental success. One of the newest methods using FISH is RNAscope (Advanced Cell Diagnostics), whose proprietary material allows detection of a single molecule of RNA. Studies in the literature have shown that RNAscope can be combined with IF or immunohistochemistry staining in order to examine mRNA profiles in distinct cells. For example, one study combined FISH and IF staining to elucidate the cellular source of cytokine production in brain cortex tissue sections. Sections were immunostained for macrophage markers and a specific probe used to detect *TGFβ* gene expression. This allowed TGFβ cytokine production to be attributed to the macrophages (Lanfranco *et al.*, 2017). Therefore, a similar approach could be applied to assess expression of the key ligandome on B cells in the pancreatic tissue, using the IF staining protocol established in this chapter, and RNAscope probes designed to detect the transcripts of the target genes.

Additionally, transcriptome-wide quantative analysis of a tissue sample can be achieved using a barcoding-based technology and a direct, on-slide cDNA synthesis approach. This results in capture of the transcripts *in situ,* and sequencing *ex situ.* Recently, this has become widely accessible using the 10x genomics visium platform, in which transcriptomic analysis is carried out on intact tissue sections and maps where gene activity is occurring (Ji *et al.*, 2020). This application could be considered in future studies to gain further understanding of the role of B cells in the tissue microenvironment as a whole, or in studies of a higher throughput nature i.e. analysis of multiple tissue sections from multiple donors and patient groups. For the current study, this technology was beyond the experimental scope due to the unbiased analysis of the complete transcriptome. Additionally, the resolution required to examine the immune infiltrate within the tissue samples may not be sufficient with this technology.

It is important to recognise that analysis of B cells in the pancreas in this chapter was primarily a ‘first look/glance’ approach. Only one patient sample was analysed, and only 10 single cells each from the pancreas and lymph node were captured by LCM and analysed for expression of the key ligandome.

In terms of the B cells selected, it is necessary to note that no morphological analysis to identify the islets in the pancreatic tissue sections was undertaken. Therefore, it is not possible to definitively conclude that the B cells captured by LCM are part of the

islet infiltrate, and therefore engaged in β-cell destruction. For future studies, inflamed islets, detected using methodology well established in the field (Willcox *et al.*, 2009; Leete *et al.*, 2016) could be pre-identified in the tissue specimen of interest. Using this spatial information, serial sections of the same tissue specimen could be cut, and B cells isolated from the pre-determined areas of insulitis.

Regarding the patient sample selection, the T1D patient selected was an individual with long standing T1D (21 years since diagnosis at death), who had been diagnosed at age 16. Within the field, it is becoming increasingly clear that T1D presents in two distinct endotypes – one of which is associated with a younger age at diagnosis (<7 years of age) and a more aggressive and rapid destruction of β-cells, while the other is associated with a less destructive phenotype and an older age of diagnosis (>13 years of age) (Leete *et al.*, 2016). Pertinent to my research question, those in the former group displayed a CD20 high islet infiltrate phenotype – suggesting CD20 B cells are more engaged in disease process in this group and contribute to the CD8 T cell mediated destruction of β-cells. In the thesis thus far, I have presented data that supports B cell modulation of CD8 T cell responses through cross-presentation of antigen, and signalling and adhesive pathways (i.e. the key ligandome). Future studies into the expression profiles of B cells within the pancreas would therefore be more relevant if patient samples were selected from individuals diagnosed at a younger age, in which B cells appear to be more central to disease pathogenesis and are present at a higher frequency in the pancreatic tissue. An interesting extension of this would be to compare expression profiles of the key ligandome in B cells isolated via LCM from tissue specimens from individuals from the two distinct disease endotypes.

Although extremely preliminary, the observation of *CXCL16* expression on a cluster of B cells (and CD8 T cells) was interesting. No formal conclusions can be drawn due to the limitations of this analysis; CD8 staining was not included so the notion that the cluster consists of B cells and CD8 T cells is purely speculative. Additionally, while the housekeeping gene *ACTB* was expressed, the B cell reference genes showed no expression.

CXCL16 protein exists in two isoforms, in a membrane anchored form, and as a small, soluble chemokine generated by metalloproteinase cleavage of the membrane-

bound form. Secretion as a soluble chemokine induces a chemo attractive gradient that directs CXCR6 expressing cells - a process critical for homing and persistence of CD8 T cells at sites of inflammation and infection, including inflammatory tissue sites in various autoimmune disorders (Günther *et al.*, 2012; Steel *et al.*, 2020). It is therefore possible that expression of *CXCL16* by the B cell directly impacts the recruitment of the CD8 T cells; in line with the speculative theory that the B cell cluster isolated through LCM also contained CD8 T cells. Interestingly, a two-fold model for the role of CXCL16 was proposed by Shimaoka *et al*., (2004). Authors identified that the soluble form attracted CXCR6 positive CD8 T cells towards the CXCL16 expressing cell, where the membrane-anchored form then mediated direct adhesion of CXCR6 expressing cells. Dendritic cells and macrophages selectively express CXCL16, and the authors proposed that this two-fold model may play an important role in the interaction between DCs and T cells, and contribute to the activation of antigen specific CD8 T cell responses (Shimaoka *et al.*, 2004). Perhaps, with the identification of CXCL16-CXCR6 as a ligand: receptor pair in the key 'ligandome' and the expression of *CXCL16* on B cells isolated from the pancreas of an individual with T1D, B cells may act in a similar manner to govern CD8 T cell responses *in situ.*

The observation that *CXCL16* expression was detected in a cluster of B cells, and not in a single cell, could be due to at least two (not necessarily mutually exclusive) explanations. In line with the concept that the sample (RNA) quantity was lower in the LCM captured cells, and therefore not sufficient for effective gene expression analysis, LCM of a higher number of cells may result in an RNA concentration conducive with detection of low expressing transcripts. Additionally, if the B cells were in fact forming a cluster with CD8 T cells, the physical close proximity could result in increased expression of CXCL16. This presents the consideration of extending the study to compare gene expression profiles between B cells in close proximity to CD8 T cells i.e. doublets, with their single, 'alone' counterparts – something easily addressed using the aforementioned experimental approaches.

Concluding remarks

To conclude, initial studies into the characterisation of B cells within the pancreatic tissue were undertaken in this chapter, in order to validate data presented throughout

the thesis to elucidate the mechanisms by which B cells may govern CD8 mediated β-cell destruction *in situ*. While no conclusions could be definitively drawn, B cells were detected in the pancreatic tissue of an individual with T1D and the experimental methodology established provides a pipeline to guide future experiments: utilising the fast IF staining approach and using the key ligandome as a molecular signature to validate B cell function in pancreatic tissue pathology in T1D. Future study design would require further optimisation of the single cell molecular analysis approach as discussed and adjusting of the study design in terms of patient selection and cell selection within the tissue.

6 FINAL DISCUSSION

This thesis addressed the phenomenon that in T1D, B cell production of autoantibodies is a pivotal disease biomarker, however there is no evidence to support a pathogenic role for autoantibodies in disease. Therefore, it is likely that autoantibodies are a proxy for autoreactive B cells of the same specificity, that are engaged in disease processes in an alternative manner. As discussed throughout, literature presents evidence for a breach in B cell tolerogenic mechanisms in individuals with T1D and indicates distinctive B cell phenotypes in the peripheral circulation. B cells appear to be critical in the islets, correlating with hyper-inflammation and more aggressive β-cell destruction. Additionally, B cells infiltrate islets in a manner that parallels CD8 T cells.

Taken together this suggests a dynamic interplay between the B cells and CD8 T cells that promotes CD8 T cell mediated β-cell destruction. Pre-clinical models in the NOD mouse have eluded to a direct interaction between B cells and CD8 T cells in the islets and pancreatic lymph nodes however studies into the molecular mechanisms governing this interaction are limited. Increasing our understanding of the immune pathways involved in disease progression is important in the design of therapeutic intervention studies, with the aim to preserve residual β-cell function in individuals with T1D. Therefore, with the inclination from clinical and preclinical studies that B cells may interact with CD8 T cells to govern CD8 mediated β-cell destruction, elucidation of the molecular mechanisms involved in the interaction may present a viable node for therapeutic intervention.

The overarching hypothesis addressed was that a cognate interaction occurs between B cells and CD8 T cells within the pancreatic islets of individuals with T1D, that promotes the β-cell directed cytotoxicity of the CD8 T cells.

6.1 Implications for the disease model

In the *in vitro* studies, B cell cross-presentation of a model antigen drives the acquisition of a CD8 T cell cytotoxic function. In these co-cultures, B:CD8 doublets occur - suggestive of a sustained interaction between B cells and CD8 T cells. While cognate antigen is required for a functional T cell output, B:CD8 doublets still arise in the absence of peptide. This is indicative of an antigen-independent interaction,

suggesting additional cell-cell communication pathways of adhesive and signalling capacity which may further contribute to B cell governance of CD8 T cell responses. Identification of B cells in the pancreatic tissue of an individual with T1D provides *in situ* evidence for their pathogenic relevance to disease.

Taken together, data presented in this thesis therefore provides novel evidence to speculate the relationship between B cells, CD8 T cells and enhanced β-cell destruction in individuals with T1D. Evidence infers a functional *in situ* cellular interaction between B cells and CD8 T cells that promotes CD8 T cell effector function and β-cell destruction. This provides a mechanistic explanation for the preservation of β-cell function observed upon B cell depletion (Rituximab) in newly diagnosed individuals (Pescovitz *et al.*, 2009) and the distinct pathobiological mechanism that defines the CD20 high disease endotype (Arif *et al.*, 2014; Leete *et al.*, 2016).

In the context of the disease model, literature suggests that promotion of β-cell directed effector CD8 T cell function is likely to be governed by events in the pancreatic islets, explaining the self-perpetuating nature of CD8 T cell mediated β-cell destruction after disease initiation. B cell depletion in pre-clinical models prevents the conversion of NOD mice from a benign insulitis to overt disease, implicating B cells in control of a late pathogenic event i.e. the amplification of self-reactive CD8 cytotoxic T cells after initiation of disease.

Data presented in this thesis provides mechanistic evidence to support this hypothesis. In the islets, B cells are likely to promote effector development of antigen-experienced CD8 T cells through cognate mechanisms such as antigen cross-presentation, and additional adhesive and signalling communication pathways. Importantly, therapeutic disruption or prevention of this islet resident cellular interaction by targeting these modalities may reduce or prevent β-cell destruction in individuals with T1D or those at-risk.

6.2 Future outlook

6.2.1 Tissue specific studies

In this work, I have presented data that characterises the interaction between B cells and CD8 T cells and eludes towards the potential pathogenic relevance of this to T1D. Preliminary 'first look' studies were established in this thesis utilising the pancreatic tissue of T1D individuals. These experiments are essential to provide a disease specific, tissue context for the relevance of B:CD8 T cell interactions. While *in vitro* experiments were critical to characterise the molecular mechanisms involved in the interaction, the setting fails to encompass the tissue microenvironment and inflammatory state specific to disease. In this thesis, I therefore do not have evidence to directly implicate the molecular mechanisms and functional output of the B:CD8 T cell interaction in disease. Future work should extend the tissue studies and validate the role of B:CD8 interactions in tissue pathology.

6.2.1.1 B cell cross-presentation in the islets

While the use of β-cell autoantigens within the ADS *in vitro* would determine the ability of B cells to cross present disease relevant antigen to CD8 T cells, it would be important to contextualize the cognate interaction in tissue pathology. Using a similar approach to that established in Chapter 5, B:CD8 doublets could be detected in the pancreatic tissue of nPOD samples, and isolated as a cluster using LCM. To circumvent the low levels of RNA isolated from small cell numbers, a larger area of surrounding tissue could be included in the captured tissue.

It would be expected that if the B:CD8 clusters represent a cognate interaction driven by β-cell autoantigen presentation, the TCR and the BCR would carry specific autoreactive sequences responding to the same islet autoantigen. The antigen specificity of the B cell and CD8 T cell in the cluster could be determined using downstream molecular approaches. For the BCR, this technology has been described post-LCM – encompassing expression vector cloning to produce monoclonal antibodies and establish specificity (Obiakor *et al.*, 2002; Tiller *et al.*, 2008). Specifically, this would involve RT-PCR for antibody V(D)J gene segments followed by expression vector cloning in HEK293T cells to produce antibodies and determine specificity using immunoassay approaches such as ELISA. For TCR specificity, paired TCR α- and β-chains can be expressed in a TCR deficient, human CD8 T cell line in order to test responses to known epitopes presented by HLA-matched APCs *in vitro* i.e. K562 cells. Single B cells and single CD8 T cells within

the same tissue could also be captured and their specificity determined, as a control to ascertain that the same specificity in the cluster is driven by a cognate mechanism. Additionally, these experiments would inform the relationship between tissue infiltrating B cells and circulating autoantibodies, providing a direct link between autoantibody specificity and B cell engagement in disease.

6.2.1.2 Molecular cross talk between interacting B:CD8 T cells in the islets

In this thesis, RNA sequencing of bulk populations of B cells and CD8 T cells permitted analysis to identify potential ligand: receptor pairs that existed between the two cells, inferring functional cell-cell communication. The relevance of these ligand: receptor pairs to disease was then preliminarily addressed by assessing their expression on B cells isolated from the pancreatic tissue of an individual with T1D. A limitation of this approach was the profiling of each cell population separately, as opposed to when they are interacting; information on cell-cell interactions can only be assumed. Future work could employ alternative molecular approaches to characterize intercellular interaction specific pathways at a much higher resolution.

Recently, a molecular approach has been presented for sequencing of physically interacting cells (PIC-seq), that combines isolation of physically interacting cells (PICs) with single cell RNA sequencing (Giladi *et al.*, 2020). Specifically, PIC-seq involves the capture of interacting cells, or cell conjugates (in the context of this thesis, B:CD8 doublets). Single cells from non-conjugated populations are also captured in order to generate a background metacell model for transcriptional distribution specific to the interacting cells. In this manner, cross talk between interacting cells can be molecularly interrogated by identifying gene expression patterns specific to the interaction. The functional impact of the interaction can also be determined through characterisation of gene regulation downstream of the cell-cell cross talk. For example, the authors tested PIC-seq on prototypic cross talk between DCs and CD4 T cells. In comparison to single cells, PICs showed an upregulation of genes related to T cell helper differentiation. Importantly, the authors demonstrated the applicability of the technique on interacting cells in *in vitro* co-cultures, as well as for interacting cells in tissue, so long as appropriate tissue dissociation methods are used.

Therefore, PIC-seq could be applied to the current study for direct inference of *in situ* cellular interactions between B cells and CD8 T cells, characterisation of their molecular cross talk and elucidation of the functional outcome of the interaction. The similarities in experimental set up i.e. co-cultures of DCs and CD4 T cells with cognate antigen and cell sorting of double positive conjugates, make it a natural experimental extension. Importantly, PIC-seq could also be applied directly to interacting B:CD8 T cells in the pancreatic tissue of individuals with T1D.

6.2.1.3 Involvement of tertiary lymphoid structures

An important consideration in the context of emerging evidence is also the relevance of tertiary lymphoid structures (TLS) in the inflamed islets. TLSs are 'ectopic' secondary lymphoid organs that develop at sites of chronic inflammation, in response to a series of pro-inflammatory cytokines, TNF receptor family member signalling, and immune cell crosstalk with stromal cells, and serve as sites of immune induction (Carragher, Rangel-Moreno and Randall, 2008). TLS display similar features to SLOs. For example, segregated T and B cell zones, formation of B cell follicles and germinal centres and the presence of follicular dendritic cell networks (Pipi *et al.*, 2018). In cancer immunology, TLSs are associated with increased survival, and improved response to immune checkpoint therapy. Relevant to my research question, localisation of B cells within the TLSs underscored the prognostic role of the TLS (Cabrita *et al.*, 2020; Helmink *et al.*, 2020; Petitprez *et al.*, 2020). In these studies, B cells were critical for sustaining CD8-mediated anti-tumour immunity, and TLS-rich tumours were more infiltrated by CD8 T cells. Although the mechanistic mechanisms were not explored, it is likely that TLSs are sites where anti-tumoral immunity is generated, with B cell cross-presentation of tumour antigen driving this response. A similar phenomenon may be occurring in the pancreatic tissue of individuals with T1D, where TLSs represent a site of persistent immune cell activation. In the pre-clinical NOD mouse model, islet associated TLSs are a frequent occurrence, and are reported to promote autoimmunity and chronic inflammation (Astorri *et al.*, 2010). This is one of the striking differences that exist between the NOD mouse model and patients, as TLSs have rarely been identified in individuals with T1D. Recently, however, the first description of a potential TLS in the endocrine pancreas of a patient with T1D was recorded (Smeets *et al.*, 2020). A

systematic search for TLS in T1D patients, and molecular analysis of the B cells and CD8 T cells within the TLS using the aforementioned experimental approaches, would further support the concept of cognate B:CD8 T cell interactions driving β-cell destruction.

7 Reference list

Achenbach, P. *et al.* (2004) 'Stratification of Type 1 Diabetes Risk on the Basis of Islet Autoantibody Characteristics', *Diabetes*, 53(2), pp. 384–392. doi: 10.2337/diabetes.53.2.384.

Ackerman, A. L. *et al.* (2003) 'Early phagosomes in dendritic cells form a cellular compartment sufficient for cross presentation of exogenous antigens', *Proceedings of the National Academy of Sciences*. National Academy of Sciences, 100(22), pp. 12889–12894. doi: 10.1073/pnas.1735556100.

Ahmadi, T. *et al.* (2008) 'CD40 Ligand-activated, antigen-specific B cells are comparable to mature dendritic cells in presenting protein antigens and major histocompatibility complex class I- and class II-binding peptides', *Immunology*, 124(1), pp. 129–140. doi: 10.1111/j.1365-2567.2007.02749.x.

Akashi, M. *et al.* (1997) 'Direct evidence for the contribution of B cells to the progression of insulitis and the development of diabetes in non-obese diabetic mice', *International Immunology*, 9(8), pp. 1159–1164. doi: 10.1093/intimm/9.8.1159.

Allen, C. D. C. *et al.* (2004) 'Germinal center dark and light zone organization is mediated by CXCR4 and CXCR5', *Nature Immunology*, 5(9), pp. 943–952. doi: 10.1038/ni1100.

Allen, C. D. C. *et al.* (2007) 'Imaging of Germinal Center Selection Events During Affinity Maturation', *Science*. American Association for the Advancement of Science, 315(5811), pp. 528–531. doi: 10.1126/science.1136736.

Almaden, J. V *et al.* (2014) 'A pathway switch directs BAFF signaling to distinct NFκB transcription factors in maturing and proliferating B cells.', *Cell reports*, 9(6), pp. 2098–2111. doi: 10.1016/j.celrep.2014.11.024.

American Diabetes Association (2020) 'Classification and diagnosis of diabetes: Standards of Medical Care in Diabetes-2020', *Diabetes Care*, 43(January), pp. S14–S31. doi: 10.2337/dc20-S002.

Ansel, K. M. *et al.* (2000) 'A chemokine-driven positive feedback loop organizes lymphoid follicles ', *Nature*, 406(6793), pp. 309–314. doi: 10.1038/35018581.

Arif, S. *et al.* (2014) ‘Blood and islet phenotypes indicate immunological heterogeneity in type 1 diabetes’, *Diabetes*, 63(11), pp. 3835–3845. doi: 10.2337/db14-0365.

Arif, S., Pujol-Autonell, I. and Eichmann, M. (2020) ‘Assessing effector T cells in type 1 diabetes’, *Current Opinion in Endocrinology, Diabetes and Obesity*, 27(4). Available at: https://journals.lww.com/co-endocrinology/Fulltext/2020/08000/Assessing_effector_T_cells_in_type_1_diabetes.8.aspx.

Astorri, E. *et al.* (2010) ‘Evolution of ectopic lymphoid neogenesis and in situ autoantibody production in autoimmune nonobese diabetic mice: cellular and molecular characterization of tertiary lymphoid structures in pancreatic islets.’, *Journal of immunology (Baltimore, Md. : 1950)*. United States, 185(6), pp. 3359–3368. doi: 10.4049/jimmunol.1001836.

Babon, J. A. B. *et al.* (2017) ‘Analysis of self-antigen specificity of islet-infiltrating T cells from human donors with type 1 diabetes’, *Nature Medicine*, 22(12). doi: 10.1038/nm.4203.

Baker, R. L. *et al.* (2019) ‘Hybrid Insulin Peptides Are Autoantigens in Type 1 Diabetes’, *Diabetes*, 68(9), pp. 1830 LP – 1840. doi: 10.2337/db19-0128.

Bannard, O. *et al.* (2013) ‘Germinal center centroblasts transition to a centrocyte phenotype according to a timed program and depend on the dark zone for effective selection’, *Immunity*. Elsevier Inc., 39(5), pp. 912–924. doi: 10.1016/j.immuni.2013.08.038.

Batista, F. D. and Neuberger, M. S. (1998) ‘Affinity dependence of the B cell response to antigen: A threshold, a ceiling, and the importance of off-rate’, *Immunity*, 8(6), pp. 751–759. doi: 10.1016/S1074-7613(00)80580-4.

Bell, G. I., Horita, S. and Karam, J. H. (1984) ‘A polymorphic locus near the human insulin gene is associated with insulin-dependent diabetes mellitus.’, *Diabetes*. United States, 33(2), pp. 176–183. doi: 10.2337/diab.33.2.176.

Bender, C. *et al.* (2020) ‘The healthy exocrine pancreas contains preproinsulin-specific CD8 T cells that attack islets in type 1 diabetes’, *Science Advances*, 6(42),

pp. 1–10.

Berberich, I. *et al.* (1996) ‘Cross-linking CD40 on B cells preferentially induces stress-activated protein kinases rather than mitogen-activated protein kinases’, *EMBO Journal*, 15(1), pp. 92–101. doi: 10.1002/j.1460-2075.1996.tb00337.x.

Berberich, I., Shu, G. L. and Clark, E. A. (1994) ‘Cross-linking CD40 on B cells rapidly activates nuclear factor-κB’, *Journal of Immunology*, 153(10), pp. 4357–4366.

Boldison, J. *et al.* (2019) ‘Phenotypically distinct anti-insulin B cells repopulate pancreatic islets after anti-CD20 treatment in NOD mice’, *Diabetologia*. Diabetologia, 62(11), pp. 2052–2065. doi: 10.1007/s00125-019-04974-y.

Bottazzo, G. F., Florin-Christensen, A. and Doniach, D. (1974) ‘Islet-cell antibodies in diabetes mellitus with autoimmune polyendocrine deficiencies.’, *Lancet (London, England)*. England, 2(7892), pp. 1279–1283. doi: 10.1016/s0140-6736(74)90140-8.

Bottini, N. *et al.* (2004) ‘A functional variant of lymphoid tyrosine phosphatase is associated with type I diabetes.’, *Nature genetics*. United States, 36(4), pp. 337–338. doi: 10.1038/ng1323.

Brodie, G. M. *et al.* (2008) ‘B-Cells Promote Intra-Islet CD8ɧ Cytotoxic T-Cell Survival to Enhance Type 1 Diabetes’, *Diabetes*, 57(4), pp. 909–917. doi: 10.2337/db07-1256.G.M.B.

Burel, J. G. *et al.* (2019) ‘Circulating T cell-monocyte complexes are markers of immune perturbations’, *eLife*, 8, pp. 1–21. doi: 10.7554/eLife.46045.001.

Burrack, A. L., Martinov, T. and Fife, B. T. (2017) ‘T cell-mediated beta cell destruction: Autoimmunity and alloimmunity in the context of type 1 diabetes’, *Frontiers in Endocrinology*. doi: 10.3389/fendo.2017.00343.

Butz, E. A. and Bevan, M. J. (1998) ‘Massive expansion of antigen-specific CD8+ T cells during an acute virus infection.’, *Immunity*, 8(2), pp. 167–175. doi: 10.1016/s1074-7613(00)80469-0.

Cabrita, R. *et al.* (2020) ‘Tertiary lymphoid structures improve immunotherapy and survival in melanoma’, *Nature*, 577(7791), pp. 561–565. doi: 10.1038/s41586-019-

1914-8.

Cambier, J. C. *et al.* (2007) ‘B-cell anergy: from transgenic models to naturally occurring anergic B cells?’, *Nature reviews. Immunology*, 7(8), pp. 633–643. doi: 10.1038/nri2133.

Campbell-Thompson, M. *et al.* (2016) ‘Insulitis and β-Cell Mass in the Natural History of Type 1 Diabetes’, *Diabetes*. American Diabetes Association, 65(3), pp. 719–731. doi: 10.2337/db15-0779.

Campbell-Thompson, M. L. *et al.* (2013) ‘The diagnosis of insulitis in human type 1 diabetes’, *Diabetologia*, 56, pp. 2541–2543. doi: 10.1007/s00125-013-3043-5.

Cardwell, C. R. *et al.* (2008) ‘Caesarean section is associated with an increased risk of childhood-onset type 1 diabetes mellitus: a meta-analysis of observational studies.’, *Diabetologia*. Germany, 51(5), pp. 726–735. doi: 10.1007/s00125-008-0941-z.

Carragher, D. M., Rangel-Moreno, J. and Randall, T. D. (2008) ‘Ectopic lymphoid tissues and local immunity’, *Seminars in Immunology*, 20(1), pp. 26–42. doi: https://doi.org/10.1016/j.smim.2007.12.004.

Chamberlain, N. *et al.* (2016) ‘Rituximab does not reset defective early B cell tolerance checkpoints’, *Journal of Clinical Investigation*, 126(1), pp. 1–6. doi: 10.1172/JCI83840DS1.

Chee, J. *et al.* (2014) ‘Effector-Memory T Cells Develop in Islets and Report Islet Pathology in Type 1 Diabetes’, *Journal of Immunology*, 192(2), pp. 572–580. doi: 10.4049/jimmunol.1302100.

Coppieters, K. T. *et al.* (2012) ‘Demonstration of islet-autoreactive CD8 T cells in insulitic lesions from recent onset and long-term type 1 diabetes patients’, *Journal of Experimental Medicine*, 209(1), pp. 51–60. doi: 10.1084/jem.20111187.

Cui, W. and Kaech, S. M. (2010) ‘Generation of effector CD8+ T cells and their conversion to memory T cells.’, *Immunological reviews*, 236, pp. 151–166. doi: 10.1111/j.1600-065X.2010.00926.x.

Culina, S. *et al.* (2018) ‘Islet-reactive CD8+ T-cell frequencies in the pancreas but

not blood distinguish type 1 diabetes from healthy donors', *science immunology*, 3(20). doi: 10.1126/sciimmunol.aao4013.Islet-reactive.

Cursons, J. *et al.* (2019) 'A gene signature predicting natural killer cell infiltration and improved survival in melanoma patients', *Cancer Immunology Research*, 7(7), pp. 1162–1174. doi: 10.1158/2326-6066.CIR-18-0500.

Curtsinger, J. M. *et al.* (1999) 'Inflammatory cytokines provide a third signal for activation of naive CD4+ and CD8+ T cells.', *Journal of immunology (Baltimore, Md. : 1950)*, 162(6), pp. 3256–62. Available at: http://www.ncbi.nlm.nih.gov/pubmed/10092777.

Dasari, V. *et al.* (2016) 'Autophagy and proteasome interconnect to coordinate cross-presentation through MHC class I pathway in B cells', *Immunology and Cell Biology*, 94(10), pp. 964–974. doi: 10.1038/icb.2016.59.

Dauer, M. *et al.* (2003) 'Mature Dendritic Cells Derived from Human Monocytes Within 48 Hours: A Novel Strategy for Dendritic Cell Differentiation from Blood Precursors', *The Journal of Immunology*, 170(8), pp. 4069–4076. doi: 10.4049/jimmunol.170.8.4069.

Delamarre, L. *et al.* (2005) 'Differential Lysosomal Proteolysis in Antigen-Presenting Cells Determines Antigen Fate', *Science*. American Association for the Advancement of Science, 307(5715), pp. 1630–1634. doi: 10.1126/science.1108003.

Delong, T. *et al.* (2016) 'Pathogenic CD4 T cells in type 1 diabetes recognize epitopes formed by peptide fusion', *Science*, 351(6274), pp. 711 LP – 714. doi: 10.1126/science.aad2791.

Deng, C. *et al.* (2016) 'Altered peripheral B-lymphocyte subsets in type 1 diabetes and latent autoimmune diabetes in adults', *Diabetes Care*, 39(3), pp. 434–440. doi: 10.2337/dc15-1765.

Deola, S. *et al.* (2008) 'Helper B Cells Promote Cytotoxic T Cell Survival and Proliferation Independently of Antigen Presentation through CD27/CD70 Interactions', *The Journal of Immunology*, 180(3), pp. 1362–1372. doi: 10.4049/jimmunol.180.3.1362.

Devarajan, P. and Chen, Z. (2013) ‘Autoimmune effector memory T cells: the bad and the good.’, *Immunologic research*, 57(1–3), pp. 12–22. doi: 10.1007/s12026-013-8448-1.

DIAMOND Project Group (2006) ‘Incidence and trends of childhood Type 1 diabetes worldwide 1990-1999.’, *Diabetic medicine : a journal of the British Diabetic Association*. England, 23(8), pp. 857–866. doi: 10.1111/j.1464-5491.2006.01925.x.

Dominguez-Bello, M. G. *et al.* (2010) ‘Delivery mode shapes the acquisition and structure of the initial microbiota across multiple body habitats in newborns’, *Proceedings of the National Academy of Sciences of the United States of America*, 107(26), pp. 11971–11975. doi: 10.1073/pnas.1002601107.

Dufort, M. J. *et al.* (2019) ‘Cell type-specific immune phenotypes predict loss of insulin secretion in new-onset type 1 diabetes’, *JCI insight*, 4(4), pp. 1–16. doi: 10.1172/jci.insight.125556.

Dustin, M. L. (2002) ‘The immunological synapse’, *Arthritis research*, 4, pp. S119–S125. doi: 10.1186/ar559.

Dustin, M. L. (2014) ‘The immunological synapse.’, *Cancer immunology research*, 2(11), pp. 1023–1033. doi: 10.1158/2326-6066.CIR-14-0161.

Efremova, M. *et al.* (2020) ‘CellPhoneDB: inferring cell–cell communication from combined expression of multi-subunit ligand–receptor complexes’, *Nature Protocols*. Springer US, 15(4), pp. 1484–1506. doi: 10.1038/s41596-020-0292-x.

Embgenbroich, M. and Burgdorf, S. (2018) ‘Current concepts of antigen cross-presentation’, *Frontiers in Immunology*, 9(JUL). doi: 10.3389/fimmu.2018.01643.

Endesfelder, D. *et al.* (2019) ‘Time-Resolved Autoantibody Profiling Facilitates Stratification of Preclinical Type 1 Diabetes in Children.’, *Diabetes*, 68(1), pp. 119–130. doi: 10.2337/db18-0594.

Espina, V. *et al.* (2006) ‘Laser-capture microdissection’, *Nature Protocols*, 1(2), pp. 586–603. doi: 10.1038/nprot.2006.85.

EURODIAB ACE Study Group (2000) ‘Variation and trends in incidence of

childhood diabetes in Europe', *The Lancet*. Elsevier, 355(9207), pp. 873–876. doi: 10.1016/S0140-6736(99)07125-1.

Fecteau, J. F., Côté, G. and Néron, S. (2006) ' A New Memory CD27 − IgG + B Cell Population in Peripheral Blood Expressing V H Genes with Low Frequency of Somatic Mutation ', *The Journal of Immunology*, 177(6), pp. 3728–3736. doi: 10.4049/jimmunol.177.6.3728.

Fignani, D. *et al.* (2020) 'SARS-CoV-2 Receptor Angiotensin I-Converting Enzyme Type 2 (ACE2) Is Expressed in Human Pancreatic β-Cells and in the Human Pancreas Microvasculature', *Frontiers in Endocrinology*, 11(November), pp. 1–19. doi: 10.3389/fendo.2020.596898.

Fiorina, P. *et al.* (2008) 'Targeting CD22 reprograms b-cells and reverses autoimmune diabetes', *Diabetes*, 57(11), pp. 3013–3024. doi: 10.2337/db08-0420.

Franco, A. *et al.* (2000) 'Epitope affinity for MHC class I determines helper requirement for CTL priming', *Nature Immunology*, 1(2), pp. 145–150. doi: 10.1038/77827.

Franke, F. *et al.* (2020) 'IL-21 in Conjunction with Anti-CD40 and IL-4 Constitutes a Potent Polyclonal B Cell Stimulator for Monitoring Antigen-Specific Memory B Cells.', *Cells*, 9(2). doi: 10.3390/cells9020433.

Franks, S. E., Getahun, A. and Cambier, J. C. (2019) 'A Precision B Cell–Targeted Therapeutic Approach to Autoimmunity Caused by Phosphatidylinositol 3-Kinase Pathway Dysregulation', *The Journal of Immunology*, 202(12), pp. 3381–3393. doi: 10.4049/jimmunol.1801394.

Frederiksen, B. *et al.* (2013) 'Infant exposures and development of type 1 diabetes mellitus: The Diabetes Autoimmunity Study in the Young (DAISY).', *JAMA pediatrics*, 167(9), pp. 808–815. doi: 10.1001/jamapediatrics.2013.317.

Friedman, R. S. *et al.* (2014) 'An evolving autoimmune microenvironment regulates the quality of effector T cell restimulation and function', *Proceedings of the National Academy of Sciences of the United States of America*, 111(25), pp. 9223–9228. doi: 10.1073/pnas.1322193111.

Fujisawa, T. *et al.* (1995) ‘Class I HLA is associated with age-at-onset of IDDM, while class II HLA confers susceptibility to IDDM.’, *Diabetologia*. Germany, pp. 1493–1495. doi: 10.1007/BF00400620.

Gagnerault, M. C. *et al.* (2002) ‘Pancreatic lymph nodes are required for priming of β cell reactive T cells in NOD mice’, *Journal of Experimental Medicine*, 196(3), pp. 369–377. doi: 10.1084/jem.20011353.

García-Guerrero, E. *et al.* (2018) ‘Selection of tumor-specific cytotoxic T lymphocytes in acute myeloid leukemia patients through the identification of T-cells capable to establish stable interactions with the leukemic cells: “Doublet technology”’, *Frontiers in Immunology*, 9(SEP). doi: 10.3389/fimmu.2018.01971.

Gardner, S. G. *et al.* (1999) ‘Progression to diabetes in relatives with islet autoantibodies. Is it inevitable?’, *Diabetes care*. United States, 22(12), pp. 2049–2054. doi: 10.2337/diacare.22.12.2049.

Garside, P. *et al.* (1998) ‘Visualization of specific B and T lymphocyte interactions in the lymph node.’, *Science (New York, N.Y.)*. United States, 281(5373), pp. 96–99. doi: 10.1126/science.281.5373.96.

Gattinoni, L. *et al.* (2011) ‘A human memory T cell subset with stem cell–like properties’, *Nature Medicine*, 17(10), pp. 1290–1297. doi: 10.1038/nm.2446.

Gebhardt, T. *et al.* (2009) ‘Memory T cells in nonlymphoid tissue that provide enhanced local immunity during infection with herpes simplex virus’, *Nature Immunology*, 10(5), pp. 524–530. doi: 10.1038/ni.1718.

Giladi, A. *et al.* (2020) ‘Dissecting cellular crosstalk by sequencing physically interacting cells’, *Nature Biotechnology*, 38(5), pp. 629–637. doi: 10.1038/s41587-020-0442-2.

Gondre-Lewis, T. A., Moquin, A. E. and Drake, J. R. (2001) ‘Prolonged Antigen Persistence Within Nonterminal Late Endocytic Compartments of Antigen-Specific B Lymphocytes’, *The Journal of Immunology*, 166(11), pp. 6657–6664. doi: 10.4049/jimmunol.166.11.6657.

Gonzalez-Duque, S. *et al.* (2018) ‘Conventional and Neo-antigenic Peptides

Presented by β Cells Are Targeted by Circulating Naïve CD8+ T Cells in Type 1 Diabetic and Healthy Donors', *Cell Metabolism*, 28(6), pp. 946-960.e6. doi: https://doi.org/10.1016/j.cmet.2018.07.007.

Graham, K. L. *et al.* (2011) 'Autoreactive cytotoxic T lymphocytes acquire higher expression of cytotoxic effector markers in the islets of NOD mice after priming in pancreatic lymph nodes', *American Journal of Pathology*. Elsevier Inc., 178(6), pp. 2716–2725. doi: 10.1016/j.ajpath.2011.02.015.

Green, E. A., Eynon, E. E. and Flaveirti, R. A. (1998) 'Local expression of TNFα in neonatal NOD mice promotes diabetes by enhancing presentation of islet antigens', *Immunity*, 9(5), pp. 733–743. doi: 10.1016/S1074-7613(00)80670-6.

Griss, J. *et al.* (2019) 'B cells sustain inflammation and predict response to immune checkpoint blockade in human melanoma', *Journal of Investigative Dermatology*, 139(9), p. S297. doi: 10.1016/j.jid.2019.07.529.

Groettrup, M., Kirk, C. J. and Basler, M. (2010) 'Proteasomes in immune cells: more than peptide producers?', *Nature reviews. Immunology*. England, pp. 73–78. doi: 10.1038/nri2687.

Grubin, C. E. *et al.* (1994) 'A novel radioligand binding assay to determine diagnostic accuracy of isoform-specific glutamic acid decarboxylase antibodies in childhood IDDM', *Diabetologia*, 37(4), pp. 344–350. doi: 10.1007/BF00408469.

Guermonprez, P. *et al.* (2003) 'ER–phagosome fusion defines an MHC class I cross-presentation compartment in dendritic cells', *Nature*, 425(6956), pp. 397–402. doi: 10.1038/nature01911.

Günther, C. *et al.* (2012) 'CXCL16 and CXCR6 are upregulated in psoriasis and mediate cutaneous recruitment of human CD8+ T cells', *Journal of Investigative Dermatology*, 132(3 PART 1), pp. 626–634. doi: 10.1038/jid.2011.371.

Habib, T. *et al.* (2012) 'Altered B Cell Homeostasis Is Associated with Type I Diabetes and Carriers of the PTPN22 Allelic Variant', *The Journal of Immunology*, 188(1), pp. 487–496. doi: 10.4049/jimmunol.1102176.

Hahne, M. *et al.* (1998) 'APRIL, a new ligand of the tumor necrosis factor family,

stimulates tumor cell growth', *Journal of Experimental Medicine*, 188(6), pp. 1185–1190. doi: 10.1084/jem.188.6.1185.

Hanenberg, H. *et al.* (1989) 'Macrophage infiltration precedes and is a prerequisite for lymphocytic insulitis in pancreatic islets of pre-diabetic BB rats.', *Diabetologia*. Germany, 32(2), pp. 126–134. doi: 10.1007/BF00505185.

Hanna, S. J. *et al.* (2020) 'Slow progressors to type 1 diabetes lose islet autoantibodies over time , have few islet antigen-specific CD8 + T cells and exhibit a distinct CD95 hi B cell phenotype', *Diabetologia*. Diabetologia, 63(6), pp. 1174–1185.

Hanninen, A. *et al.* (1992) 'Macrophages, T cell receptor usage, and endothelial cell activation in the pancreas at the onset of insulin-dependent diabetes mellitus', *Journal of Clinical Investigation*, 90(5), pp. 1901–1910. doi: 10.1172/JCI116067.

Hardy, R. R. and Hayakawa, K. (2001) 'B Cell Development Pathways', *Annual Review of Immunology*. Annual Reviews, 19(1), pp. 595–621. doi: 10.1146/annurev.immunol.19.1.595.

Harjutsalo, V., Sjöberg, L. and Tuomilehto, J. (2008) 'Time trends in the incidence of type 1 diabetes in Finnish children: a cohort study', *The Lancet*, 371(9626), pp. 1777–1782. doi: 10.1016/S0140-6736(08)60765-5.

Harms, R. Z. *et al.* (2018) 'Abnormal T Cell Frequencies, Including Cytomegalovirus-Associated Expansions, Distinguish Seroconverted Subjects at Risk for Type 1 Diabetes.', *Frontiers in immunology*, 9, p. 2332. doi: 10.3389/fimmu.2018.02332.

Hassainya, Y. *et al.* (2005) 'Identification of naturally processed HLA-A2 - Restricted proinsulin epitopes by reversed immunology', *Diabetes*, 54(7), pp. 2053–2059. doi: 10.2337/diabetes.54.7.2053.

Hawa, M. I. *et al.* (2013) 'Adult-onset autoimmune diabetes in Europe is prevalent with a broad clinical phenotype: Action LADA 7.', *Diabetes care*, 36(4), pp. 908–913. doi: 10.2337/dc12-0931.

Helmink, B. A. *et al.* (2020) 'B cells and tertiary lymphoid structures promote

immunotherapy response.', *Nature*. Springer US, 577(February 2019). doi: 10.1038/s41586-019-1922-8.

Hu, C. Y. *et al.* (2007) 'Treatment with CD20-specific antibody prevents and reverses autoimmune diabetes in mice', *Journal of Clinical Investigation*, 117(12), pp. 3857–3867. doi: 10.1172/JCI32405.

Hulbert, C *et al.* (2001) 'B cell specificity contributes to the outcome of diabetes in nonobese diabetic mice.', *Journal of immunology (Baltimore, Md. : 1950)*, 167(10), pp. 5535–8. doi: 10.4049/jimmunol.167.10.5535.

Hulbert, Chrys *et al.* (2001) 'Cutting Edge: B Cell Specificity Contributes to the Outcome of Diabetes in Nonobese Diabetic Mice', *The Journal of Immunology*, 167(10), pp. 5535–5538. doi: 10.4049/jimmunol.167.10.5535.

Hussain, S. and Delovitch, T. L. (2005) 'Dysregulated B7-1 and B7-2 Expression on Nonobese Diabetic Mouse B Cells Is Associated with Increased T Cell Costimulation and the Development of Insulitis', *The Journal of Immunology*, 174(2), pp. 680–687. doi: 10.4049/jimmunol.174.2.680.

Hyttinen, V. *et al.* (2003) 'Genetic liability of type 1 diabetes and the onset age among 22, 650 young Finnish twin pairs: A nationwide follow-up study', *Diabetes*, 52(4), pp. 1052–1055. doi: 10.2337/diabetes.52.4.1052.

In't Veld, P. *et al.* (2007) 'Screening for insulitis in adult autoantibody-positive organ donors', *Diabetes*, 56(9), pp. 2400–2404. doi: 10.2337/db07-0416.

In't Veld, P. (2011) 'Insulitis in human type 1 diabetes: The quest for an elusive lesion.', *Islets*, 3(4), pp. 131–138. doi: 10.4161/isl.3.4.15728.

In't Veld, P. (2014a) 'Insulitis in human type 1 diabetes: a comparison between patients and animal models', *Seminars in Immunopathology*, 36(5), pp. 569–579. doi: 10.1007/s00281-014-0438-4.

In't Veld, P. (2014b) 'Insulitis in human type 1 diabetes: A comparison between patients and animal models', *Seminars in Immunopathology*, 36(5), pp. 569–579. doi: 10.1007/s00281-014-0438-4.

Ise, W. *et al.* (2018) 'T Follicular Helper Cell-Germinal Center B Cell Interaction

Strength Regulates Entry into Plasma Cell or Recycling Germinal Center Cell Fate', *Immunity*, 48(4), pp. 702-715.e4. doi: https://doi.org/10.1016/j.immuni.2018.03.027.

Itoh, N. *et al.* (1993) 'Mononuclear cell infiltration and its relation to the expression of major histocompatibility complex antigens and adhesion molecules in pancreas biopsy specimens from newly diagnosed insulin-dependent diabetes mellitus patients', *Journal of Clinical Investigation*, 92(5), pp. 2313–2322. doi: 10.1172/JCI116835.

Jabbari, A. and Harty, J. T. (2006) 'Secondary memory CD8+ T cells are more protective but slower to acquire a central-memory phenotype.', *The Journal of experimental medicine*, 203(4), pp. 919–932. doi: 10.1084/jem.20052237.

Ji, A. L. *et al.* (2020) 'Multimodal Analysis of Composition and Spatial Architecture in Human Squamous Cell Carcinoma', *Cell*, 182, pp. 497–514. doi: 10.1016/j.cell.2020.05.039.

Jun, E. *et al.* (2018) 'Method Optimization for Extracting High-Quality RNA From the Human Pancreas Tissue', *Translational Oncology*. The Authors, 11(3), pp. 800–807. doi: 10.1016/j.tranon.2018.04.004.

Jung, S. *et al.* (2002) 'In vivo depletion of CD11c+ dendritic cells abrogates priming of CD8+ T cells by exogenous cell-associated antigens', *Immunity*, 17(2), pp. 221–220. doi: 10.1016/j.jsbmb.2011.07.002.Identification.

Kägi, D. *et al.* (1994) 'Fas and perforin pathways as major mechanisms of T cell-mediated cytotoxicity.', *Science (New York, N.Y.)*. United States, 265(5171), pp. 528–530. doi: 10.1126/science.7518614.

Kahn, H. S. *et al.* (2009) 'Association of type 1 diabetes with month of birth among U.S. youth: The SEARCH for Diabetes in Youth Study', *Diabetes care*. 2009/08/12. American Diabetes Association, 32(11), pp. 2010–2015. doi: 10.2337/dc09-0891.

Kaprio, J. *et al.* (1992) 'Concordance for Type 1 (insulin-dependent) and Type 2 (non-insulin-dependent) diabetes mellitus in a population-based cohort of twins in Finland', *Diabetologia*, 35(11), pp. 1060–1067. doi: 10.1007/BF02221682.

Karvonen, M. *et al.* (2000) 'Incidence of childhood type 1 diabetes worldwide.

Diabetes Mondiale (DiaMond) Project Group.', *Diabetes care*. United States, 23(10), pp. 1516–1526. doi: 10.2337/diacare.23.10.1516.

Ke, Y. and Kapp, J. A. (1996) 'Exogenous antigens gain access to the major histocompatibility complex class I processing pathway in B cells by receptor-mediated uptake', *Journal of Experimental Medicine*, 184(3), pp. 1179–1184. doi: 10.1084/jem.184.3.1179.

Kendall, P. L. *et al.* (2013) 'Tolerant Anti-Insulin B Cells Are Effective APCs', *The Journal of Immunology*, 190(6), pp. 2519–2526. doi: 10.4049/jimmunol.1202104.

Kimura, K. *et al.* (2001) 'Peptide-specific cytotoxicity of T lymphocytes against glutamic acid decarboxylase and insulin in type 1 diabetes mellitus', *Diabetes Research and Clinical Practice*, 51(3), pp. 173–179. doi: 10.1016/S0168-8227(00)00225-4.

Kleffel, S. *et al.* (2015) 'Interleukin-10+ regulatory b cells arise within antigen-experienced CD40+ B cells to maintain tolerance to islet autoantigens', *Diabetes*, 64(1), pp. 158–171. doi: 10.2337/db13-1639.

Klein, U., Rajewsky, K. and Küppers, R. (1998) 'Human immunoglobulin (Ig)M+IgD+ peripheral blood B cells expressing the CD27 cell surface antigen carry somatically mutated variable region genes: CD27 as a general marker for somatically mutated (memory) B cells.', *The Journal of experimental medicine*, 188(9), pp. 1679–1689. doi: 10.1084/jem.188.9.1679.

Knight, R. R. *et al.* (2013) 'Human β-cell killing by autoreactive preproinsulin-specific CD8 T cells is predominantly granule-mediated with the potency dependent upon T-cell receptor avidity.', *Diabetes*, 62(1), pp. 205–213. doi: 10.2337/db12-0315.

Knight, R. R. *et al.* (2015) 'A distinct immunogenic region of glutamic acid decarboxylase 65 is naturally processed and presented by human islet cells to cytotoxic CD8 T cells', *Clinical and Experimental Immunology*, 179(1), pp. 100–107. doi: 10.1111/cei.12436.

Kracht, M. J. L. *et al.* (2017) 'Autoimmunity against a defective ribosomal insulin gene product in type 1 diabetes.', *Nature medicine*. United States, 23(4), pp. 501–

507. doi: 10.1038/nm.4289.

Krischer, J. P. *et al.* (2015) 'The 6 year incidence of diabetes-associated autoantibodies in genetically at-risk children: the TEDDY study.', *Diabetologia*, 58(5), pp. 980–987. doi: 10.1007/s00125-015-3514-y.

Kronenberg, D. *et al.* (2012) 'Circulating Preproinsulin Signal Peptide–Specific CD8 T Cells Restricted by the Susceptibility Molecule HLA-A24 Are Expanded at Onset of Type 1 Diabetes and Kill Beta Cells', *Diabetes*, 61, pp. 1752–1759. doi: 10.2337/db11-1520.

Krummel, M. F. *et al.* (2000) 'Differential clustering of CD4 and CD3ζ during T cell recognition', *Science*, 289(5483), pp. 1349–1352. doi: 10.1126/science.289.5483.1349.

Kumar, M. P. *et al.* (2018) 'Analysis of Single-Cell RNA-seq Identifies Cell-Cell Communication Associated with Tumor Characteristics', *Cell reports*, 25(6), pp. 1458–1468. doi: 10.1016/j.celrep.2018.10.047.Analysis.

Kyvik, K. O., Green, A. and Beck-Nielsen, H. (1995) 'Concordance rates of insulin dependent diabetes mellitus: a population based study of young Danish twins', *BMJ*. BMJ Publishing Group Ltd, 311(7010), pp. 913–917. doi: 10.1136/bmj.311.7010.913.

Lanfranco, M. F. *et al.* (2017) 'Combination of Fluorescent in situ Hybridization (FISH) and Immunofluorescence Imaging for Detection of Cytokine Expression', *Physiology & behavior*, 176(3), pp. 139–148. doi: 10.21769/BioProtoc.2608.Combination.

Lawand, M. *et al.* (2016) 'TAP-Dependent and -Independent Peptide Import into Dendritic Cell Phagosomes', *The Journal of Immunology*. American Association of Immunologists, 197(9), pp. 3454–3463. doi: 10.4049/jimmunol.1501925.

Lee, B. O. *et al.* (2003) 'CD40, but Not CD154, Expression on B Cells Is Necessary for Optimal Primary B Cell Responses', *The Journal of Immunology*, 171(11), pp. 5707–5717. doi: 10.4049/jimmunol.171.11.5707.

Leete, P. *et al.* (2016) 'Differential insulitic profiles determine the extent of β-cell

destruction and the age at onset of type 1 diabetes', *Diabetes*, 65(5), pp. 1362–1369. doi: 10.2337/db15-1615.

Lendrum, R. *et al.* (1976) 'ISLET-CELL ANTIBODIES IN DIABETES MELLITUS', *The Lancet*, 308(7998), pp. 1273–1276. doi: https://doi.org/10.1016/S0140-6736(76)92033-X.

Lennon-Duménil, A.-M. *et al.* (2002) 'Analysis of Protease Activity in Live Antigen-presenting Cells Shows Regulation of the Phagosomal Proteolytic Contents During Dendritic Cell Activation ', *Journal of Experimental Medicine*, 196(4), pp. 529–540. doi: 10.1084/jem.20020327.

Li, Z. *et al.* (1996) 'The primary structure of p38γ: A new member of p38 group of MAP kinases', *Biochemical and Biophysical Research Communications*, 228(2), pp. 334–340. doi: 10.1006/bbrc.1996.1662.

Linsley, P. S. *et al.* (2019) 'B lymphocyte alterations accompany abatacept resistance in new-onset type 1 diabetes', *JCI insight*, 4(4), pp. 1–15. doi: 10.1172/jci.insight.126136.

Liu, E. H. *et al.* (2009) 'Pancreatic beta cell function persists in many patients with chronic type 1 diabetes, but is not dramatically improved by prolonged immunosuppression and euglycaemia from a beta cell allograft.', *Diabetologia*, 52(7), pp. 1369–1380. doi: 10.1007/s00125-009-1342-7.

Livak, K. J. *et al.* (2013) 'Methods for qPCR gene expression profiling applied to 1440 lymphoblastoid single cells', *Methods*. Elsevier Inc., 59(1), pp. 71–79. doi: 10.1016/j.ymeth.2012.10.004.

Lub, M. *et al.* (1997) 'Dual role of the actin cytoskeleton in regulating cell adhesion mediated by the integrin lymphocyte function-associated molecule-1', *Molecular Biology of the Cell*, 8(2), pp. 341–351. doi: 10.1091/mbc.8.2.341.

Luce, S. *et al.* (2011) 'Single Insulin-Specific CD8 + T Cells Show Characteristic Gene Expression Profiles in Human Type 1 Diabetes', *Diabetes*, 60(12), pp. 3289–3299. doi: 10.2337/db11-0270.

van Lummel, M. *et al.* (2014) 'Posttranslational Modification of HLA-DQ Binding

Islet Autoantigens in Type 1 Diabetes', *Diabetes*, 63(1), pp. 237 LP – 247. doi: 10.2337/db12-1214.

Maahs, D. M. *et al.* (2010) 'Epidemiology of type 1 diabetes.', *Endocrinology and metabolism clinics of North America*, 39(3), pp. 481–497. doi: 10.1016/j.ecl.2010.05.011.

MacLennan, I. C. M. *et al.* (2003) 'Extrafollicular antibody responses.', *Immunological reviews*. England, 194, pp. 8–18. doi: 10.1034/j.1600-065x.2003.00058.x.

Mahnke, Y. D. *et al.* (2013) 'The who's who of T-cell differentiation: Human memory T-cell subsets', *European Journal of Immunology*, 43(11), pp. 2797–2809. doi: 10.1002/eji.201343751.

Manis, J. P., Tian, M. and Alt, F. W. (2002) 'Mechanism and control of class-switch recombination', *Trends in Immunology*, 23(1), pp. 31–39. doi: 10.1016/S1471-4906(01)02111-1.

Mannering, S. I. *et al.* (2005) 'The insulin A-chain epitope recognized by human T cells is posttranslationally modified', *Journal of Experimental Medicine*, 202(9), pp. 1191–1197. doi: 10.1084/jem.20051251.

Marie-Cardine, A. *et al.* (2008) 'Transitional B cells in humans: characterization and insight from B lymphocyte reconstitution after hematopoietic stem cell transplantation.', *Clinical immunology (Orlando, Fla.)*. United States, 127(1), pp. 14–25. doi: 10.1016/j.clim.2007.11.013.

Mariño, E. *et al.* (2009) 'CD4+CD25+ T-cells control autoimmunity in the absence of B-cells', *Diabetes*, 58(7), pp. 1568–1577. doi: 10.2337/db08-1504.

Mariño, E. *et al.* (2012) 'B-cell cross-presentation of autologous antigen precipitates diabetes', *Diabetes*, 61(11), pp. 2893–2905. doi: 10.2337/db12-0006.

Marre, M. L. *et al.* (2018) 'Modifying Enzymes Are Elicited by ER Stress, Generating Epitopes That Are Selectively Recognized by CD4⁺ T Cells in Patients With Type 1 Diabetes', *Diabetes*, 67(7), pp. 1356 LP – 1368. doi: 10.2337/db17-1166.

Marroqui, L. *et al.* (2017) ‘Interferon-α mediates human beta cell HLA class I overexpression, endoplasmic reticulum stress and apoptosis, three hallmarks of early human type 1 diabetes.’, *Diabetologia*. Germany, 60(4), pp. 656–667. doi: 10.1007/s00125-016-4201-3.

Martin, M. D. and Badovinac, V. P. (2018) ‘Defining Memory CD8 T Cell’, 9(November), pp. 1–10. doi: 10.3389/fimmu.2018.02692.

Masopust, D. *et al.* (2006) ‘Stimulation history dictates memory CD8 T cell phenotype: implications for prime-boost vaccination.’, *Journal of immunology (Baltimore, Md. : 1950)*. United States, 177(2), pp. 831–839. doi: 10.4049/jimmunol.177.2.831.

Mayer-Davis, E. J. *et al.* (2017) ‘Incidence Trends of Type 1 and Type 2 Diabetes among Youths, 2002-2012.’, *The New England journal of medicine*, 376(15), pp. 1419–1429. doi: 10.1056/NEJMoa1610187.

Mayer, C. T. *et al.* (2017) ‘The microanatomic segregation of selection by apoptosis in the germinal center’, *Science*. American Association for the Advancement of Science, 358(6360). doi: 10.1126/science.aao2602.

Menard, L. *et al.* (2011) ‘The PTPN22 allele encoding an R620W variant interferes with the removal of developing autoreactive B cells in humans’, *The Journal of clinical investigation*, 121(9), pp. 3635–3644. doi: 10.1172/JCI45790.chronic.

Mintz, M. A. *et al.* (2019) ‘The HVEM-BTLA Axis Restrains T Cell Help to Germinal Center B Cells and Functions as a Cell-Extrinsic Suppressor in Lymphomagenesis’, *Immunity*. The Authors, 51(2), pp. 310-323.e7. doi: 10.1016/j.immuni.2019.05.022.

Mobasseri, M. *et al.* (2020) ‘Prevalence and incidence of type 1 diabetes in the world: A systematic review and meta-analysis’, *Health Promotion Perspectives*, 10(2), pp. 98–115. doi: 10.34172/hpp.2020.18.

Moltchanova, E. V. *et al.* (2009) ‘Seasonal variation of diagnosis of Type 1 diabetes mellitus in children worldwide’, *Diabetic Medicine*, 26(7), pp. 673–678. doi: 10.1111/j.1464-5491.2009.02743.x.

Montecino-Rodriguez, E. and Dorshkind, K. (2012) ‘B-1 B cell development in the fetus and adult.’, *Immunity*, 36(1), pp. 13–21. doi: 10.1016/j.immuni.2011.11.017.

Moran, S. T. *et al.* (2007) ‘Synergism between NF-kappa B1/p50 and Notch2 during the development of marginal zone B lymphocytes.’, *Journal of immunology (Baltimore, Md. : 1950)*. United States, 179(1), pp. 195–200. doi: 10.4049/jimmunol.179.1.195.

Mouquet, H. *et al.* (2008) ‘B-cell depletion immunotherapy in pemphigus: Effects on cellular and humoral immune responses’, *Journal of Investigative Dermatology*, 128(12), pp. 2859–2869. doi: 10.1038/jid.2008.178.

Muehlinghaus, G. *et al.* (2005) ‘Regulation of CXCR3 and CXCR4 expression during terminal differentiation of memory B cells into plasma cells’, *Blood*, 105(10), pp. 3965–3971. doi: 10.1182/blood-2004-08-2992.

Müllbacher, A. *et al.* (2002) ‘Antigen-dependent release of IFN-gamma by cytotoxic T cells up-regulates Fas on target cells and facilitates exocytosis-independent specific target cell lysis.’, *Journal of immunology (Baltimore, Md. : 1950)*. United States, 169(1), pp. 145–150. doi: 10.4049/jimmunol.169.1.145.

Nakanishi, K. *et al.* (1993) ‘Association of HLA-A24 with complete beta-cell destruction in IDDM.’, *Diabetes*. United States, 42(7), pp. 1086–1093. doi: 10.2337/diab.42.7.1086.

Nakanishi, K. *et al.* (1999) ‘Human leukocyte antigen-A24 and -DQA1*0301 in Japanese insulin-dependent diabetes mellitus: independent contributions to susceptibility to the disease and additive contributions to acceleration of beta-cell destruction.’, *The Journal of clinical endocrinology and metabolism*. United States, 84(10), pp. 3721–3725. doi: 10.1210/jcem.84.10.6045.

Nguyen, T. T. T. *et al.* (2016) ‘PLEKHG3 enhances polarized cell migration by activating actin filaments at the cell front’, *Proceedings of the National Academy of Sciences of the United States of America*, 113(36), pp. 10091–10096. doi: 10.1073/pnas.1604720113.

Nigi, L. *et al.* (2020) ‘From immunohistological to anatomical alterations of human pancreas in type 1 diabetes: New concepts on the stage’, *Diabetes/Metabolism*

Research and Reviews, 36(4), pp. 1–18. doi: 10.1002/dmrr.3264.

Nisticò, L. *et al.* (1996) 'The CTLA-4 gene region of chromosome 2q33 is linked to, and associated with, type 1 diabetes. Belgian Diabetes Registry.', *Human molecular genetics*. England, 5(7), pp. 1075–1080. doi: 10.1093/hmg/5.7.1075.

Noble, J. A. *et al.* (1996) 'The role of HLA class II genes in insulin-dependent diabetes mellitus: molecular analysis of 180 Caucasian, multiplex families.', *American journal of human genetics*, 59(5), pp. 1134–1148.

Noorchashm, H. *et al.* (1999) 'I-Ag7-mediated antigen presentation by B lymphocytes is critical in overcoming a checkpoint in T cell tolerance to islet beta cells of nonobese diabetic mice.', *Journal of immunology (Baltimore, Md. : 1950)*, 163(2), pp. 743–50. Available at: http://www.ncbi.nlm.nih.gov/pubmed/10395666.

Obar, J. J. and Lefrançois, L. (2010) 'Early events governing memory CD8+ T-cell differentiation.', *International immunology*, 22(8), pp. 619–625. doi: 10.1093/intimm/dxq053.

Obiakor, H. *et al.* (2002) 'A comparison of hydraulic and laser capture microdissection methods for collection of single B cells, PCR, and sequencing of antibody VDJ', *Analytical Biochemistry*, 306(1), pp. 55–62. doi: 10.1006/abio.2002.5671.

Ogura, H. *et al.* (2018) 'Identification and Analysis of Islet Antigen-Specific CD8(+) T Cells with T Cell Libraries.', *Journal of immunology (Baltimore, Md. : 1950)*, 201(6), pp. 1662–1670. doi: 10.4049/jimmunol.1800267.

Okada, T. *et al.* (2005) 'Antigen-engaged B cells undergo chemotaxis toward the T zone and form motile conjugates with helper T cells.', *PLoS biology*, 3(6), p. e150. doi: 10.1371/journal.pbio.0030150.

Packard, T. *et al.* (2016) 'B Cell Receptor Affinity for Insulin Dictates Autoantigen Acquisition and B Cell Functionality in Autoimmune Diabetes', *Journal of Clinical Medicine*, 5(11), p. 98. doi: 10.3390/jcm5110098.

Palm, A.-K. E. and Henry, C. (2019) 'Remembrance of Things Past: Long-Term B Cell Memory After Infection and Vaccination', *Frontiers in Immunology*, 10, p.

1787. doi: 10.3389/fimmu.2019.01787.

Panagiotopoulos, C. *et al.* (2003) 'Identification of a Beta-Cell–Specific HLA Class I Restricted Epitope in Type 1 Diabetes', *Diabetes*, 52(11), pp. 2647–2651.

Panigrahi, A. K. *et al.* (2008) 'RS rearrangement frequency as a marker of receptor editing in lupus and type 1 diabetes.', *The Journal of experimental medicine*, 205(13), pp. 2985–2994. doi: 10.1084/jem.20082053.

Panina-bordignon, P. *et al.* (1995) 'Cytotoxic T Cells Specific for Glutamic Acid Decarboxylase in Autoimmune Diabetes', *Diabetes*, 181(May), pp. 1–5.

Parikka, V. *et al.* (2012) 'Early seroconversion and rapidly increasing autoantibody concentrations predict prepubertal manifestation of type 1 diabetes in children at genetic risk', *Diabetologia*, 55(7), pp. 1926–1936. doi: 10.1007/s00125-012-2523-3.

Payton, M. A., Hawkes, C. J. and Christie, M. R. (1995) 'Relationship of the 37,000- and 40,000-Mr tryptic fragments of islet antigens in insulin-dependent diabetes to the protein tyrosine phosphatase-like molecule IA-2 (ICA512)', *Journal of Clinical Investigation*, 96(3), pp. 1506–1511. doi: 10.1172/JCI118188.

Pescovitz, M. D. *et al.* (2009) 'Rituximab, B-Lymphocyte Depletion, and Preservation of Beta-Cell Function', *New England Journal of Medicine*, 361(22), pp. 2143–52.

Pescovitz, M. D. *et al.* (2014) 'B-lymphocyte depletion with rituximab and β-cell function: Two-year results', *Diabetes Care*, 37(2), pp. 453–459. doi: 10.2337/dc13-0626.

Petitprez, F. *et al.* (2020) 'B cells are associated with survival and immunotherapy response in sarcoma', *Nature*, 577(7791), pp. 556–560. doi: 10.1038/s41586-019-1906-8.

Pillai, S. and Cariappa, A. (2009) 'The follicular versus marginal zone B lymphocyte cell fate decision.', *Nature Reviews Immunology*, 9(11), pp. 767–777. doi: 10.1038/nri2656.

Pinkse, G. G. M. *et al.* (2005) 'Autoreactive CD8 T cells associated with beta cell destruction in type 1 diabetes', *Proceedings of the National Academy of Sciences*,

102(51), pp. 18425–18430.

Pipi, E. *et al.* (2018) ‘Tertiary Lymphoid Structures: Autoimmunity Goes Local.’, *Frontiers in immunology*, 9, p. 1952. doi: 10.3389/fimmu.2018.01952.

Powell, W. E. *et al.* (2018) ‘Loss of CXCR3 expression on memory B cells in individuals with long-standing type 1 diabetes’, *Diabetologia*. Diabetologia, 61(8), pp. 1794–1803. doi: 10.1007/s00125-018-4651-x.

Powell, W. E. *et al.* (2019) ‘Detecting autoreactive B cells in the peripheral blood of people with type 1 diabetes using ELISpot’, *Journal of Immunological Methods*, 471(April), pp. 61–65. doi: 10.1016/j.jim.2019.05.007.

Pugliese, A. *et al.* (1995) ‘HLA-DQB1*0602 is associated with dominant protection from diabetes even among islet cell antibody-positive first-degree relatives of patients with IDDM.’, *Diabetes*. United States, 44(6), pp. 608–613. doi: 10.2337/diab.44.6.608.

Qu, H.-Q. *et al.* (2009) ‘The type I diabetes association of the IL2RA locus.’, *Genes and immunity*, 10 Suppl 1(Suppl 1), pp. S42-8. doi: 10.1038/gene.2009.90.

Ramilowski, J. A. *et al.* (2015) ‘A draft network of ligand-receptor-mediated multicellular signalling in human’, *Nature Communications*, 6. doi: 10.1038/ncomms8866.

Ren, B. C. L. *et al.* (1994) ‘Signal Transduction via CD40 Involves Activation of lyn kinase and Phosphatidylinositol-3-klnase, and Phosphorylation of PhosphoHpase C3r2’, *J. Exp. Med*, 179(February), pp. 673–680.

Richardson, S. J. *et al.* (2009) ‘The prevalence of enteroviral capsid protein vp1 immunostaining in pancreatic islets in human type 1 diabetes.’, *Diabetologia*. Germany, 52(6), pp. 1143–1151. doi: 10.1007/s00125-009-1276-0.

Richardson, S. J. *et al.* (2016) ‘Islet cell hyperexpression of HLA class I antigens: a defining feature in type 1 diabetes’, *Diabetologia*. Diabetologia, 59(11), pp. 2448–2458. doi: 10.1007/s00125-016-4067-4.

Robson, N. C., Donachie, A. M. and Mowat, A. M. I. (2008) ‘Simultaneous presentation and cross-presentation of immune-stimulating complex-associated

cognate antigen by antigen-specific B cells', *European Journal of Immunology*, 38(5), pp. 1238–1246. doi: 10.1002/eji.200737758.

Roche, P. and Furuta, K. (2015) 'The ins and outs of MHC class II-mediated antigen processing and presentation', *Nature Reviews Immunology*, 15, pp. 203–216.

Rodriguez, A. *et al.* (1999) 'Selective transport of internalized antigens to the cytosol for MHC class I presentation in dendritic cells.', *Nature cell biology*. England, 1(6), pp. 362–368. doi: 10.1038/14058.

Roep, B. O. (2003) 'The role of T-cells in the pathogenesis of Type 1 diabetes: From cause to cure', *Diabetologia*, 46(3), pp. 305–321. doi: 10.1007/s00125-003-1089-5.

Roncarolo, M. G. and Battaglia, M. (2007) 'Regulatory T-cell immunotherapy for tolerance to self antigens and alloantigens in humans', *Nature Reviews Immunology*, pp. 585–598. doi: 10.1038/nri2138.

da Rosa, L. C. *et al.* (2018) 'B cell depletion reduces T cell activation in pancreatic islets in a murine autoimmune diabetes model', *Diabetologia*, pp. 1–14. doi: 10.1007/s00125-018-4597-z.

Da Rosa, L. C. *et al.* (2018) 'B cell depletion reduces T cell activation in pancreatic islets in a murine autoimmune diabetes model', *Diabetologia*. Diabetologia, 61(6), pp. 1397–1410. doi: 10.1007/s00125-018-4597-z.

Rosmalen, J. G. M. *et al.* (2000) 'Islet abnormalities associated with an early influx of dendritic cells and macrophages in NOD and NODscid mice', *Laboratory Investigation*, 80(5), pp. 769–777. doi: 10.1038/labinvest.3780080.

Sallusto, F., Geginat, J. and Lanzavecchia, A. (2004) 'Central memory and effector memory T cell subsets: Function, generation, and maintenance', *Annual Review of Immunology*, 22, pp. 745–763. doi: 10.1146/annurev.immunol.22.012703.104702.

Sater, R. A., Sandel, P. C. and Monroe, J. G. (1998) 'B cell receptor-induced apoptosis in primary transitional murine B cells: signaling requirements and modulation by T cell help.', *International immunology*. England, 10(11), pp. 1673–1682. doi: 10.1093/intimm/10.11.1673.

Schultze, J. L. *et al.* (1997) 'CD40-activated human B cells: An alternative source of

highly efficient antigen presenting cells to generate autologous antigen-specific T cells for adoptive immunotherapy', *Journal of Clinical Investigation*, 100(11), pp. 2757–2765. doi: 10.1172/JCI119822.

Schweitzer, S. *et al.* (2000) 'Flow cytometric analysis of peptide binding to major histocampatibility complex class I for hepatitis C virus core T-cell epitopes', *Cytometry*, 41(4), pp. 271–278. doi: 10.1002/1097-0320(20001201)41:4<271::AID-CYTO5>3.0.CO;2-M.

Seifert, M. and Küppers, R. (2016) 'Human memory B cells', *Leukemia*, 30(12), pp. 2283–2292. doi: 10.1038/leu.2016.226.

Serr, I. and Daniel, C. (2018) 'Regulation of T Follicular Helper Cells in Islet Autoimmunity.', *Frontiers in immunology*, 9, p. 1729. doi: 10.3389/fimmu.2018.01729.

Serreze, D. V. *et al.* (1994) 'Major histocompatibility complex class I - Deficient NOD-B2mnull mice are diabetes and insulitis resistant', *Diabetes*, 43(3), pp. 505–509.

Serreze, D. V. *et al.* (1996) 'B lymphocytes are essential for the initiation of T cell-mediated autoimmune diabetes: Analysis of a new "speed congenic" stock of NOD.Igμ(null) mice', *Journal of Experimental Medicine*, 184(5), pp. 2049–2053. doi: 10.1084/jem.184.5.2049.

Serreze, D. V *et al.* (1996) 'B lymphocytes are essential for the initiation of T cell-mediated autoimmune diabetes: analysis of a new "speed congenic" stock of NOD.Ig mu null mice.', *The Journal of experimental medicine*, 184(5), pp. 2049–2053. doi: 10.1084/jem.184.5.2049.

Serwold, T. *et al.* (2002) 'ERAAP customizes peptides for MHC class I molecules in the endoplasmic reticulum.', *Nature*. England, 419(6906), pp. 480–483. doi: 10.1038/nature01074.

Shaw, S. *et al.* (1986) 'Two antigen-independent adhesion pathways used by human cytotoxic T-cell clones', *Nature*, 323(6085), pp. 262–264. doi: 10.1038/323262a0.

Shaw, S. and Luce, G. (1987) 'The lymphocyte function-associated antigen (LFA) -

1 and CD2 / LFA-3 pathways of antigen-independent human T cell adhesion.', *Journal of Immunology*, 139(4).

Shimaoka, T. *et al.* (2004) 'Cell surface-anchored SR-PSOX/CXC chemokine ligand 16 mediates firm adhesion of CXC chemokine receptor 6-expressing cells', *Journal of Leukocyte Biology*, 75(2), pp. 267–274. doi: 10.1189/jlb.1003465.

Siemasko, K. *et al.* (1998) 'Cutting Edge: Signals from the B Lymphocyte Antigen Receptor Regulate MHC Class II Containing Late Endosomes', *The Journal of Immunology*. American Association of Immunologists, 160(11), pp. 5203–5208. Available at: https://www.jimmunol.org/content/160/11/5203.

Siemasko, K. *et al.* (1999) 'Igα and Igβ Are Required for Efficient Trafficking to Late Endosomes and to Enhance Antigen Presentation', *The Journal of Immunology*. American Association of Immunologists, 162(11), pp. 6518–6525. Available at: https://www.jimmunol.org/content/162/11/6518.

Signore, A. *et al.* (1989) 'The natural history of lymphocyte subsets infiltrating the pancreas of NOD mice.', *Diabetologia*. Germany, 32(5), pp. 282–289. doi: 10.1007/BF00265543.

Silveira, P. A. *et al.* (2002) 'The preferential ability of B lymphocytes to act as diabetogenic APC in NOD mice depends on expression of self-antigen-specific immunoglobulin receptors', *European Journal of Immunology*, 32(12), pp. 3657–3666. doi: 10.1002/1521-4141(200212)32:12<3657::AID-IMMU3657>3.0.CO;2-E.

Skowera, A. *et al.* (2008) 'CTLs are targeted to kill β cells in patients with type 1 diabetes through recognition of a glucose-regulated preproinsulin epitope', *Journal of Clinical Investigation*, 118(10), pp. 3390–3402. doi: 10.1172/JCI35449DS1.

Skowera, A., Ladell, K., Mclaren, J. E., *et al.* (2015) 'Europe PMC Funders Group β -cell-specific CD8 T cell phenotype in type 1 diabetes reflects chronic autoantigen exposure', 64(December 2013), pp. 916–925. doi: 10.2337/db14-0332.

Skowera, A., Ladell, K., McLaren, J. E., *et al.* (2015) 'β-Cell-specific CD8 T cell phenotype in type 1 diabetes reflects chronic autoantigen exposure', *Diabetes*, 64(3), pp. 916–925. doi: 10.2337/db14-0332.

Smeets, S. *et al.* (2020) ‘Insulitis and lymphoid structures in the islets of Langerhans of a 66-year-old patient with long-standing type 1 diabetes’, *Virchows Archiv*. doi: 10.1007/s00428-020-02915-4.

Smith, M. J. *et al.* (2015) ‘Loss of anergic B cells in prediabetic and new-onset type 1 diabetic patients’, *Diabetes*, 64(5), pp. 1703–1712. doi: 10.2337/db13-1798.

Smith, M. J. *et al.* (2018) ‘Silencing of high-affinity insulin-reactive B lymphocytes by anergy and impact of the NOD genetic background in mice’, *Diabetologia*, 61(12), pp. 2621–2632. doi: 10.1007/s00125-018-4730-z.Silencing.

Smyth, M. J. *et al.* (1994) ‘HYPOTHESIS: CYTOTOXIC LYMPHOCYTE GRANULE SERINE PROTEASES ACTIVATE TARGET CELL ENDONUCLEASES TO TRIGGER APOPTOSIS’, *Clinical and Experimental Pharmacology and Physiology*, 21(1), pp. 67–70. doi: https://doi.org/10.1111/j.1440-1681.1994.tb02438.x.

Song, W. *et al.* (1995) ‘Entry of B cell antigen receptor and antigen into class II peptide-loading compartment is independent of receptor cross-linking.’, *Journal of immunology (Baltimore, Md. : 1950)*, 155(9), pp. 4255–63. Available at: http://www.ncbi.nlm.nih.gov/pubmed/7594583.

Sorrentino, S. (1998) ‘Human extracellular ribonucleases: Multiplicity, molecular diversity and catalytic properties of the major RNase types’, *Cellular and Molecular Life Sciences*, 54(8), pp. 785–794. doi: 10.1007/s000180050207.

Spadaro, F. *et al.* (2012) ‘IFN-α enhances cross-presentation in human dendritic cells by modulating antigen survival, endocytic routing, and processing.’, *Blood*. United States, 119(6), pp. 1407–1417. doi: 10.1182/blood-2011-06-363564.

Speake, C. *et al.* (2019) ‘A composite immune signature parallels disease progression across T1D subjects’, *JCI Insight*, 4(23), pp. 1–15. doi: 10.1172/jci.insight.126917.

Spielman, R. S., Baker, L. and Zmijewski, C. M. (1980) ‘Gene dosage and suceptibility to insulin-dependent diabetes.’, *Annals of human genetics*. England, 44(2), pp. 135–150. doi: 10.1111/j.1469-1809.1980.tb00954.x.

Stavnezer, J., Guikema, J. E. J. and Schrader, C. E. (2008) ‘Mechanism and regulation of class switch recombination’, *Annual Review of Immunology*, 26, pp. 261–292. doi: 10.1146/annurev.immunol.26.021607.090248.

Stebegg, M. *et al.* (2018) ‘Regulation of the Germinal Center Response.’, *Frontiers in immunology*, 9, p. 2469. doi: 10.3389/fimmu.2018.02469.

Steck, A. K. *et al.* (2015) ‘Predictors of Progression From the Appearance of Islet Autoantibodies to Early Childhood Diabetes: The Environmental Determinants of Diabetes in the Young (TEDDY).’, *Diabetes care*, 38(5), pp. 808–813. doi: 10.2337/dc14-2426.

Steel, K. J. A. *et al.* (2020) ‘Polyfunctional, Proinflammatory, Tissue-Resident Memory Phenotype and Function of Synovial Interleukin-17A+CD8+ T Cells in Psoriatic Arthritis’, *Arthritis and Rheumatology*, 72(3), pp. 435–447. doi: 10.1002/art.41156.

Steinberg, M. W., Cheung, T. C. and Ware, C. F. (2011) ‘The signaling networks of the herpesvirus entry mediator (TNFRSF14) in immune regulation’, *Immunological Reviews*, 244(1), pp. 169–187. doi: 10.1111/j.1600-065X.2011.01064.x.

Stene, L. C. *et al.* (2004) ‘Perinatal factors and development of islet autoimmunity in early childhood: the diabetes autoimmunity study in the young.’, *American journal of epidemiology*. United States, 160(1), pp. 3–10. doi: 10.1093/aje/kwh159.

Sutherland, C. L. *et al.* (1996) ‘Differential Activation of the ERK, JNK, and p38 Mitogen-Activated Protein Kinases by CD40 and the B Cell Antigen Receptor’, *Journal of immunology (Baltimore, Md. : 1950)*, 157(8), pp. 3381–33890.

Takahashi, K., Honeyman, M. C. and Harrison, L. C. (2001) ‘Cytotoxic T cells to an epitope in the islet autoantigen IA-2 are not disease-specific’, *Clinical Immunology*, 99(3), pp. 360–364. doi: 10.1006/clim.2001.5031.

Takaki, T. *et al.* (2006) ‘HLA-A*0201-Restricted T Cells from Humanized NOD Mice Recognize Autoantigens of Potential Clinical Relevance to Type 1 Diabetes’, *The Journal of Immunology*, 176(5), pp. 3257–3265. doi: 10.4049/jimmunol.176.5.3257.

Tangye, S. G. *et al.* (1998) 'Identification of functional human splenic memory B cells by expression of CD148 and CD27', *Journal of Experimental Medicine*, 188(9), pp. 1691–1703. doi: 10.1084/jem.188.9.1691.

Theofilopoulos, A. N., Kono, D. H. and Baccala, R. (2017) 'The multiple pathways to autoimmunity.', *Nature immunology*, 18(7), pp. 716–724. doi: 10.1038/ni.3731.

Thomas, N. J. M. *et al.* (2016) 'Classifying diabetes by type 1 genetic risk shows autoimmune diabetes cases are evenly distributed above and below 30 years of age', in *Diabetologia*. SPRINGER 233 SPRING ST, NEW YORK, NY 10013 USA, pp. S135–S135.

Thompson, W. S. *et al.* (2014) 'Multi-parametric flow cytometric and genetic investigation of the peripheral B cell compartment in human type 1 diabetes', *Clinical and Experimental Immunology*, 177(3), pp. 571–585. doi: 10.1111/cei.12362.

Tibaldi, E. V., Salgia, R. and Reinherz, E. L. (2002) 'CD2 molecules redistribute to the uropod during T cell scanning: Implications for cellular activation and immune surveillance', *Proceedings of the National Academy of Sciences of the United States of America*, 99(11), pp. 7582–7587. doi: 10.1073/pnas.112212699.

Tiller, T. *et al.* (2007) 'Autoreactivity in human IgG+ memory B cells', *Immunity*, 26(2), pp. 205–213. doi: 10.1038/jid.2014.371.

Tiller, T. *et al.* (2008) 'Efficient generation of monoclonal antibodies from single human B cells by single cell RT-PCR and expression vector cloning.', *Journal of immunological methods*, 329(1–2), pp. 112–124. doi: 10.1016/j.jim.2007.09.017.

Toma, A. *et al.* (2005) 'Recognition of a subregion of human proinsulin by class I-restricted T cells in type 1 diabetic patients', *Proceedings of the National Academy of Sciences of the United States of America*, 102(30), pp. 10581–10586. doi: 10.1073/pnas.0504230102.

Tomiyama, H., Matsuda, T. and Takiguchi, M. (2002) ' Differentiation of Human CD8 + T Cells from a Memory to Memory/Effector Phenotype ', *The Journal of Immunology*, 168(11), pp. 5538–5550. doi: 10.4049/jimmunol.168.11.5538.

Trombetta, E. S. *et al.* (2003) ‘Activation of Lysosomal Function During Dendritic Cell Maturation’, *Science*. American Association for the Advancement of Science, 299(5611), pp. 1400–1403. doi: 10.1126/science.1080106.

Urban, S. *et al.* (2012) ‘ The Efficiency of Human Cytomegalovirus pp65 495–503 CD8 + T Cell Epitope Generation Is Determined by the Balanced Activities of Cytosolic and Endoplasmic Reticulum-Resident Peptidases ’, *The Journal of Immunology*, 189(2), pp. 529–538. doi: 10.4049/jimmunol.1101886.

Velthuis, J. H. *et al.* (2010) ‘Simultaneous Detection of Circulating Autoreactive CD8ɧ T-Cells Specific for Different Islet Cell–Associated Epitopes Using Combinatorial MHC Multimers’, *Diabetes*, 59(July), pp. 1721–1730. doi: 10.2337/db09-1486.J.H.V.

Vettermann, C. and Schlissel, M. S. (2010) ‘Allelic exclusion of immunoglobulin genes: models and mechanisms.’, *Immunological reviews*, 237(1), pp. 22–42. doi: 10.1111/j.1600-065X.2010.00935.x.

Victora, G. D. *et al.* (2012) ‘Identification of human germinal center light and dark zone cells and their relationship to human B-cell lymphomas.’, *Blood*, 120(11), pp. 2240–2248. doi: 10.1182/blood-2012-03-415380.

Viisanen, T. *et al.* (2017) ‘Circulating CXCR5+PD-1+ICOS+ Follicular T Helper Cells Are Increased Close to the Diagnosis of Type 1 Diabetes in Children With Multiple Autoantibodies.’, *Diabetes*. United States, 66(2), pp. 437–447. doi: 10.2337/db16-0714.

Voss, C. Y. *et al.* (2009) ‘Increased effector-target cell conjugate formation due to HLA restricted specific antigen recognition’, *Immunol Res*, 23(1), pp. 1–7. doi: 10.1007/s12026-008-8041-1.Increased.

Wang, J. H. *et al.* (1999) ‘Structure of a heterophilic adhesion complex between the human CD2 and CD58 (LFA-3) counterreceptors’, *Cell*, 97(6), pp. 791–803. doi: 10.1016/S0092-8674(00)80790-4.

Wang, X. *et al.* (2011) ‘Follicular dendritic cells help establish follicle identity and promote B cell retention in germinal centers’, *Journal of Experimental Medicine*, 208(12), pp. 2497–2510. doi: 10.1084/jem.20111449.

Wang, Y. *et al.* (2020) ‘Decrease in the proportion of CD24hiCD38hi B cells and impairment of their regulatory capacity in type 1 diabetes patients’, *Clinical and Experimental Immunology*, 200(1), pp. 22–32. doi: 10.1111/cei.13408.

Wasserfall, C. *et al.* (2017) ‘Persistence of Pancreatic Insulin mRNA Expression and Proinsulin Protein in Type 1 Diabetes Pancreata.’, *Cell metabolism*, 26(3), pp. 568-575.e3. doi: 10.1016/j.cmet.2017.08.013.

Weisel, N. M. *et al.* (2020) ‘Comprehensive analyses of B-cell compartments across the human body reveal novel subsets and a gut-resident memory phenotype.’, *Blood*, 136(24), pp. 2774–2785. doi: 10.1182/blood.2019002782.

Wenzlau, J. M. *et al.* (2007) ‘The cation efflux transporter ZnT8 (Slc30A8) is a major autoantigen in human type 1 diabetes’, *Proceedings of the National Academy of Sciences of the United States of America*, 104(43), pp. 17040–17045. doi: 10.1073/pnas.0705894104.

Wiedeman, A. E. *et al.* (2020) ‘Autoreactive CD8+ T cell exhaustion distinguishes subjects with slow type 1 diabetes progression’, *Journal of Clinical Investigation*, 130(1), pp. 480–490. doi: 10.1172/JCI126595.

Willcox, A. *et al.* (2009) ‘Analysis of islet inflammation in human type 1 diabetes’, *Clinical and Experimental Immunology*, 155(2), pp. 173–181. doi: 10.1111/j.1365-2249.2008.03860.x.

Wills, M. R. *et al.* (1996) ‘The human cytotoxic T-lymphocyte (CTL) response to cytomegalovirus is dominated by structural protein pp65: frequency, specificity, and T-cell receptor usage of pp65-specific CTL.’, *Journal of virology*, 70(11), pp. 7569–7579. doi: 10.1128/jvi.70.11.7569-7579.1996.

Wirth, T. C. *et al.* (2010) ‘Repetitive antigen stimulation induces stepwise transcriptome diversification but preserves a core signature of memory CD8+ T cell differentiation’, *Immunity*. Elsevier Ltd, 33(1), pp. 128–140. doi: 10.1016/j.immuni.2010.06.014.

de Wit, J. *et al.* (2010) ‘Antigen-specific B cells reactivate an effective cytotoxic T Cell response against phagocytosed Salmonella through cross-presentation’, *PLoS ONE*, 5(9), pp. 2–11. doi: 10.1371/journal.pone.0013016.

Wither, J. E., Roy, V. and Brennan, L. A. (2000) 'Activated B cells express increased levels of costimulatory molecules in young autoimmune NZB and (NZB x NZW)F1 mice', *Clinical Immunology*, 94(1), pp. 51–63. doi: 10.1006/clim.1999.4806.

Woittiez, N. J. C. and Roep, B. O. (2015) 'Impact of disease heterogeneity on treatment efficacy of immunotherapy in Type 1 diabetes: different shades of gray.', *Immunotherapy*. England, 7(2), pp. 163–174. doi: 10.2217/imt.14.104.

Wong, F. S. *et al.* (2004) 'Investigation of the role of B-cells in type 1 diabetes in the NOD mouse', *Diabetes*, 53(10), pp. 2581–2587. doi: 10.2337/diabetes.53.10.2581.

Worzfeld, T. *et al.* (2018) 'Proteotranscriptomics Reveal Signaling Networks in the Ovarian Cancer Microenvironment', *Molecular and Cellular Proteomics*, 17(2), pp. 270–289. doi: 10.1074/mcp.RA117.000400.

Wu, L. C. *et al.* (2002) 'Competing interests statement Two-step binding mechanism for T-cell receptor recognition of peptide–MHC', *Nature*, 418(August), pp. 552–556. Available at: www.nature.com/nature.

Wu, N. *et al.* (2013) 'The role of annexin A3 playing in cancers', *Clinical and Translational Oncology*, 15(2), pp. 106–110. doi: 10.1007/s12094-012-0928-6.

Xing, Y. and Hogquist, K. A. (2012) 'T-cell tolerance: central and peripheral.', *Cold Spring Harbor perspectives in biology*, 4(6). doi: 10.1101/cshperspect.a006957.

Xiu, Y. *et al.* (2008) 'B Lymphocyte Depletion by CD20 Monoclonal Antibody Prevents Diabetes in Nonobese Diabetic Mice despite Isotype-Specific Differences in FcγR Effector Functions', *The Journal of Immunology*, 180(5), pp. 2863–2875. doi: 10.4049/jimmunol.180.5.2863.

Yeo, L. *et al.* (2018) 'Autoreactive T effector memory differentiation mirrors β cell function in type 1 diabetes', *Journal of Clinical Investigation*, 128(8), pp. 3460–3474. doi: 10.1172/JCI120555.

Yeo, L. *et al.* (2019) 'Circulating β cell-specific CD8 + T cells restricted by high-risk HLA class I molecules show antigen experience in children with and at risk of type 1 diabetes', *Clinical and Experimental Immunology*, 199, pp. 263–277. doi:

10.1111/cei.13391.

Yu, L. *et al.* (2000) ‘Early expression of antiinsulin autoantibodies of humans and the NOD mouse: Evidence for early determination of subsequent diabetes’, *Proceedings of the National Academy of Sciences of the United States of America*, 97(4), pp. 1701–1706. doi: 10.1073/pnas.040556697.

Yuan, D. *et al.* (2019) ‘Systematic expression analysis of ligand-receptor pairs reveals important cell-to-cell interactions inside glioma’, *Cell Communication and Signaling*. Cell Communication and Signaling, 17(1), pp. 1–10. doi: 10.1186/s12964-019-0363-1.

Zheng, P., Li, Z. and Zhou, Z. (2018) ‘Gut microbiome in type 1 diabetes: A comprehensive review’, *Diabetes/Metabolism Research and Reviews*, 34(7), pp. 1–9. doi: 10.1002/dmrr.3043.

Ziegler, A. G. *et al.* (2013) ‘Seroconversion to multiple islet autoantibodies and risk of progression to diabetes in children.’, *JAMA*, 309(23), pp. 2473–2479. doi: 10.1001/jama.2013.6285.

Zimmermann, V. S. *et al.* (1999) ‘Engagement of B Cell Receptor Regulates the Invariant Chain-Dependent MHC Class II Presentation Pathway’, *The Journal of Immunology*. American Association of Immunologists, 162(5), pp. 2495–2502. Available at: https://www.jimmunol.org/content/162/5/2495.

Zinkernagel, R. M. and Hengartner, H. (2001) ‘Regulation of the Immune Response by Antigen’, *Science*. American Association for the Advancement of Science, 293(5528), pp. 251–253. doi: 10.1126/science.1063005.

Zipitis, C. S. and Akobeng, A. K. (2008) ‘Vitamin D supplementation in early childhood and risk of type 1 diabetes: a systematic review and meta-analysis.’, *Archives of disease in childhood*. England, 93(6), pp. 512–517. doi: 10.1136/adc.2007.128579.

Zirpel, H. and Roep, B. O. (2021) ‘Islet-Resident Dendritic Cells and Macrophages in Type 1 Diabetes: In Search of Bigfoot’s Print.’, *Frontiers in endocrinology*, 12, p. 666795. doi: 10.3389/fendo.2021.666795.